Molecular and Developmental Analysis of Non-Coding RNA Metabolism in *C. elegans*: the Exoribonuclease XRN2 and the RNA-Binding Proteins SART-3 and USIP-1

Inauguraldissertation
zur
Erlangung der Würde eines Doktors der Philosophie
vorgelegt der
Philosophisch-Naturwissenschaftlichen Fakultät
der Universität Basel

von

Stefan Rüegger
Aus Maur, Schweiz

Basel, 2014

Originaldokument gespeichert auf dem Dokumentenserver der Universität Basel
edoc.unibas.ch

Dieses Werk ist unter dem Vertrag „Creative Commons Namensnennung-Keine kommerzielle Nutzung-Keine Bearbeitung 3.0 Schweiz“ (CC BY-NC-ND 3.0 CH) lizenziert. Die vollständige Lizenz kann unter
creativecommons.org/licenses/by-nc-nd/3.0/ch/
eingesehen werden.

Genehmigt von der Philosophisch-Naturwissenschaftlichen Fakultät

auf Antrag von Prof. Dr. Nancy Hynes, Dr. Helge Grosshans, Dr. Javier Martinez

Basel, den 18.02.2014

Prof. Dr. Jörg Schibler

(Dekan)

Namensnennung-Keine kommerzielle Nutzung-Keine Bearbeitung 3.0 Schweiz
(CC BY-NC-ND 3.0 CH)

Sie dürfen: **Teilen** — den Inhalt kopieren, verbreiten und zugänglich machen

Unter den folgenden Bedingungen:

Namensnennung — Sie müssen den Namen des Autors/Rechteinhabers in der von ihm festgelegten Weise nennen.

Keine kommerzielle Nutzung — Sie dürfen diesen Inhalt nicht für kommerzielle Zwecke nutzen.

Keine Bearbeitung erlaubt — Sie dürfen diesen Inhalt nicht bearbeiten, abwandeln oder in anderer Weise verändern.

Wobei gilt:

- **Verzichtserklärung —** Jede der vorgenannten Bedingungen kann **aufgehoben** werden, sofern Sie die ausdrückliche Einwilligung des Rechteinhabers dazu erhalten.
- **Public Domain (gemeinfreie oder nicht-schützbare Inhalte) —** Soweit das Werk, der Inhalt oder irgendein Teil davon zur Public Domain der jeweiligen Rechtsordnung gehört, wird dieser Status von der Lizenz in keiner Weise berührt.
- **Sonstige Rechte —** Die Lizenz hat keinerlei Einfluss auf die folgenden Rechte:
    - Die Rechte, die jedermann wegen der Schranken des Urheberrechts oder aufgrund gesetzlicher Erlaubnisse zustehen (in einigen Ländern als grundsätzliche Doktrin des **fair use** bekannt);
    - Die **Persönlichkeitsrechte** des Urhebers;
    - Rechte anderer Personen, entweder am Lizenzgegenstand selber oder bezüglich seiner Verwendung, zum Beispiel für **Werbung** oder Privatsphärenschutz.
- **Hinweis —** Bei jeder Nutzung oder Verbreitung müssen Sie anderen alle Lizenzbedingungen mitteilen, die für diesen Inhalt gelten. Am einfachsten ist es, an entsprechender Stelle einen Link auf diese Seite einzubinden.

Quelle: http://creativecommons.org/licenses/by-nc-nd/3.0/ch/ Datum: 12.11.2013

Acknowledgments

I would like to express my deepest gratitude to my PhD advisor, Helge Großhans, for his patient, caring, and motivating guidance.

I would like to express my sincere gratitude to Iskra Katic for always being willing to share her immense knowledge of *C. elegans*, for providing cutting-edge worm tools, and for invaluable hands-on help with worm injections.

I wish to thank Daniel Hess for performing mass spectrometry experiments, which crucially contribute to the work at hand.

I am thankful for the scientific support from my thesis committee, Nancy Hynes and Javier Martinez.

I wish to express my gratitude to Boehringer Ingelheim Fonds for financial support but particularly also for personal support and for organizing many enjoyable events.

Contents

Acknowledgments 2

1 Summary 4

2 RNA metabolism in eukaryotes 6

3 The exoribonuclease XRN2 in *C. elegans*: Its role in development and its interplay with the novel protein PAXT-1 11

- 3.1 Abstract and contributions 12
- 3.2 Introduction 13
  - 3.2.1 XRN 5’-to-3’ exoribonucleases 13
  - 3.2.2 The nuclear exoribonuclease XRN2 14
  - 3.2.3 The cytoplasmic exoribonuclease XRN1 17
  - 3.2.4 Publication: “MicroRNA turnover: when, how, and why” 19
- 3.3 Results and Discussion 31
  - 3.3.1 Publication: “Engineering of a Conditional Allele Reveals Multiple Roles of XRN2 in *Caenorhabditis elegans* Development and Substrate Specificity in MicroRNA Turnover” 32
  - 3.3.2 Additional results 55
- 3.4 Outlook 60

4 USIP-1 is a terminal transferase acting upstream of SART-3 in spliceosome assembly 61

- 4.1 Abstract 62
- 4.2 Introduction 63
- 4.3 Results 72
- 4.4 Discussion 83
- 4.5 Supplementary figures 87
- 4.6 Methods 91

5 Conclusion 95

6 Publication: “PAXT-1 promotes XRN2 activity by stabilizing it through a conserved domain” 96

7 Publication: “The Decapping Scavenger Enzyme DCS-1 Controls MicroRNA Levels in *Caenorhabditis elegans*” 107

8 References 115

9 Curriculum vitae 126

1 Summary

About three quarters of a eukaryotic genome are transcribed into RNA. However, only <2% of these transcripts are translated into protein while the bulk of transcripts execute their biological function as RNA. Non-protein coding RNAs (ncRNAs) associate with proteins in ribonucleoprotein particles (RNPs) to regulate gene expression at various stages thereby greatly increasing the functional complexity of the genome. Nonetheless, the function and mode of action of the vast majority of ncRNAs is unknown and even in well studied examples little is known about the post-transcriptional regulation of ncRNAs themselves. In the thesis at hand, I explored the molecular and developmental functions of proteins implicated in the metabolism of ncRNAs, namely the miRNA-degrading enzyme XRN2 and the U6 snRNA-interacting proteins SART-3 and USIP-1. The XRN2 project was a collaboration with Takashi Miki and Hannes Richter.

XRN2 project

XRN2 is a conserved 5’-to-3’ exoribonuclease involved in various pathways including transcription termination and processing of precursor forms of rRNAs and snoRNAs. Our lab had established a function of XRN2 in the turnover of mature miRNAs, however, whether XRN2 targets all or specific miRNAs *in vivo* remained unclear. Although XRN2 substrates have extensively been characterized, the developmental function of XRN2 is essentially unexplored. Moreover, knowledge of co-factors regulating XRN2 function beyond transcription termination is scarce in multicellular organisms. In order to elucidate the developmental role of XRN2, we characterized an *xrn-2* null and *xrn-2* temperature-sensitive mutant. We found that XRN2 is essential during several stages of *C. elegans* development, including embryogenesis, and that only specific miRNAs are affected by XRN2 *in vivo*. Co-immunoprecipitations identified PAXT-1 (PArtner of XRN-Two 1) as a tight interaction partner of XRN2. *paxt-1* depletion enhanced the *xrn-2ts* mutant phenotype and a *paxt-1* null mutant slowed-down miRNA degradation *in vivo*, similar to XRN2 inactivation. These observations, as we showed, are due to a stabilizing effect of PAXT-1 on XRN2. Truncation mutants of PAXT-1 revealed a conserved N-terminal domain of unknown function, DUF3469, sufficient for XRN2 binding. We were excited to discover that human proteins containing DUF3469 were also able to bind to XRN2. Hence, we renamed DUF3469 to XRN2-binding domain (XTBD). Collectively, we identified PAXT-1 as an essential interaction partner of XRN2 in *C. elegans* and established a protein domain (XTBD) that serves as a binding platform for XRN2 beyond *C. elegans*.

Finally, the laboratory of Dr. Martin Simard found that the scavenger decapping enzyme DCS-1 interacts with the exonuclease XRN1, a paralogue of XRN2, to promote miRNA degradation in *C. elegans*. Collaborating on their project, I evaluated the subcellular localization of XRN1 and XRN2 in *C. elegans* and provided tools useful to their experiments such as an XRN1 antibody. This collaborative work has been published and can be found in section 7.

SART-3 project

The human protein SART3 and its yeast homolog Prp24 have previously been implicated in spliceosome assembly, namely the association of the U4 and U6 snRNP into the U4/U6 di-snRNP complex. Additionally, a physical interaction of SART3 with the Argonaute proteins AGO1 and AGO2 had been reported, suggesting an involvement of SART3 in the miRNA pathway. However, a putative function of SART3 in the miRNA pathway remained to be established. In order uncover such a function and to shed light on the so far largely neglected systemic role of SART3 in a multicellular context, I investigated its *C. elegans* homolog SART-3. Co-immunoprecipitations of SART-3 revealed an interaction with a previously uncharacterized putative terminal uridylyl transferase (TUTase), whereas I could not verify an interaction between SART-3 and AGO1/AGO2. It is known that SART3 binds specifically to the U6 snRNA which contains a post-transcriptionally elongated uridine (U)-tail essential for spliceosome assembly. Therefore it was appealing to assume that this U-tail is polymerized by the identified TUTase. Subsequent analyses unveiled an interaction between the TUTase and U6 snRNA, which hence was renamed to U Six snRNA Interacting Protein 1 (USIP-1). It appeared that USIP-1 binds to a U6 snRNA species that is devoid of Lsm proteins suggesting a role for USIP-1 early in spliceosome assembly. Moreover, knock-down of *sart-3* in a *usip-1* null mutant background led to a synthetic, embryonic lethal phenotype. This phenotype was rescued by transgenic expression of wild-type USIP-1. Although formal demonstration of TUTase-activity for USIP-1 is lacking, the synthetic lethality was not rescued by a supposedly catalytically inactive version of USIP-1. In sum, I established a physical and functional interaction between two previously uncharacterized proteins in *C. elegans*, SART-3 and USIP-1, and explored their developmental phenotypes.

2 RNA metabolism in eukaryotes

RNA metabolism is defined as the collectivity of cellular chemical reactions and pathways involving RNA. RNAs can be broadly classified into protein-coding messenger RNAs (mRNAs) and non-coding RNAs (ncRNAs), the latter representing transcripts that execute their biological function as RNAs itself without being translated into protein. These two classes are highly interconnected in that ncRNAs play a role in transcription, maturation, translation, and stability of mRNAs.

The life cycle of an mRNA – wedded to RNPs

The life cycle of an mRNA can be divided into five stages: transcription, RNA processing, mRNA export, translation, and finally degradation. All these steps are controlled by survey mechanisms that ensure proper handling of the mRNA at a given stage and, if required, eliminate wrongly processed or mutant RNAs. Each of the steps during an mRNA's life is carried out by large multi-protein complexes that often are associated with ncRNAs forming so called ribonucleoproteins (RNPs).

The life of an RNA starts with its transcription, which is divided into four phases, pre-initiation, initiation, elongation and termination. In eukaryotes, all protein-coding genes are transcribed by RNA polymerase II (RNA pol II), which is recruited to transcription start sites (TSSs) by general transcription factors and activators recognizing specific sequence elements in promoter regions (Hahn, 2004). This initial complex forming at promoters is called pre-initiation complex and exhibits a conformation that prohibits transcription. The largest subunit of RNA pol II contains a carboxyl-terminal domain (CTD), which, in humans, consists of 52 tandem repeats of a seven-amino-acid sequence (Dahmus, 1996). During transcription initiation, phosphorylation of serine 5 of each repeat in CTD releases RNA pol II from promoter regions and allows it to synthesize an immature precursor mRNA (pre-mRNA) (Cho et al., 2001). The cyclin-dependent kinase P-TEFb is crucial in mediating the transition from transcription initiation to elongation by phosphorylating CTD as well as negative elongation factors such as NELF (Fujinaga et al., 2004; Marshall et al., 1996). P-TEFb is regulated itself by the 7SK snRNP, a multi-protein complex containing the scaffolding 7SK ncRNA. 7SK snRNP-bound P-TEFb is kept in an inactive state (Yik et al., 2003). Its release and thus activation is mediated by the HIV transactivator Tat or the bromodomain containing protein BRD4 (Krueger et al., 2010; Sedore et al., 2007).

The nascent pre-mRNA is processed co-transcriptionally in several ways and the CTD serves as a landing platform for the different sets of proteins involved, depending on its phosphorylation state (Buratowski, 2009). The first step in pre-mRNA processing, taking place as soon as its 5' end emerges from the RNA exit channel of RNA pol II, is addition of a 5' cap consisting of a methylated GMP (Shatkin and Manley, 2000). The 5' cap protects the mRNA from degradation and facilitates translation initiation. Most mammalian protein-coding genes contain intervening, non-coding sequences (introns), which need to be removed from the primary transcript before it can be used for translation into protein (Chorev and Carmel, 2012). The process through which introns are removed and the coding sequences of a primary transcript, the exons, are joined is referred to as splicing (Sharp, 2005). The nasent pre-mRNA is spliced as it emerges from the polymerase. Tight coupling of transcription and splicing is thought to make sure that exons are joined in a correct 5'-to-3' order (Maniatis and Reed, 2002). Splicing is carried out by the spliceosome, a large complex composed of several ncRNAs and numerous proteins (Wahl et al., 2009). The RNA components of the spliceosome comprise five, uridine (U)-rich, small nuclear RNAs (snRNAs) called U1, U2, U4, U5, U6 (Valadkhan and Gunawardane, 2013). Spliceosomal U snRNAs recognize short consensus sequences within the pre-mRNA that is to be spliced, act as scaffolds for associated proteins, and, in the case of U6 snRNA, might even participate in splicing catalysis (Valadkhan, 2010). A detailed introduction on splicing can be found in section 4.2. In a last processing step, the nascent transcript is cleaved and polyadenylated once the RNA pol II complex has passed the poly(A) signal, a sequence motif that initiates 3' end processing (Proudfoot, 2011). Similar to the 5' cap, the 3' poly(A) tail of mRNAs protects them from unspecific degradation and is required for efficient translation (Shatkin and Manley, 2000). The cleavage and polyadenylation specificity factor (CPSF-73) is the endonuclease that mediates 3ʻ cleavage and polyadenylation is catalyzed by polyadenylate polymerase (PAP) (Mandel et al., 2006; Shatkin and Manley, 2000). The two enzymes are integrated into a large complex comprising >80 accessory factors (Shi et al., 2009). These cleavage and polyadenylation factors are also involved in transcription termination, the process whereby the ternary complex of RNA pol II, template DNA, and mRNA is disrupted (Guo and Price, 2013). The details of transcription termination remain unclear put it has been suggested that the 5'-to-3' exoribonuclease XRN2 plays a role in this process by degrading the 3' product of the CPSF-73 cleavage and by recruiting cleavage and polyadenylation factors (see section 3.2.2).

Following transcription termination, the mature mRNA is exported into the cytoplasm where it is translated into protein. Translation is carried out by a large RNP, the ribosome, which contains ribosomal RNAs (rRNAs) and transfer RNAs (tRNAs) (Jackson et al., 2010). rRNAs provide a structural framework to the ribosome but at the same time catalyze peptidyl transferase activity, which links amino acids (Cech, 2000). The amino acids linked by the ribosome are provided by the tRNAs (Schimmel et al., 1993). Each tRNA contains a triplet sequence, called anticodon, which is associated with a specific amino acid. Thus, tRNAs serve as adapter molecules providing a physical link between genetic information and protein sequence. rRNAs and tRNAs, together with the above mentioned snRNAs, are methylated and pseudouridylated by small nucelolar RNPs (snoRNPs), which are guided sequence-specifically to their targets by their ncRNA component, the small nucleolar RNAs (snoRNAs) (Dieci et al., 2009).

Together, gene expression requires many ncRNAs involved in transcription (7SK RNA), processing (snRNA, snoRNA), and translation (rRNA, tRNA). In fact, in recent years, it became evident that only <2% of the human genome encode for transcripts that are translated into proteins (Frith et al., 2005). In contrast, ~75% of the human genome is transcribed into RNA that is never translated into protein (Djebali et al., 2012). The dimensions of the ncRNA world have been underestimated for so long due to the fact that transcriptome analyses have traditionally focused on cytoplasmic polyA + RNA. RNA-seq on total rather than polyA + RNA brought to light diverse novel classes of ncRNAs, the function of most of which, however, is not yet or only little understood (Aalto and Pasquinelli, 2012; Fatica and Bozzoni, 2014).

RNA decay mechanisms

The level at which an RNA is expressed is determined by its rate of transcription but similarly by its rate of degradation. The importance of RNA decay mechanisms is reflected by the enormous diversity of enzymes that are capable of degrading RNA, called ribonucleases (RNases) (Aravind and Koonin, 2001; Arraiano et al., 2013). RNases can be grouped into two main classes: endoribonucleases, which cleave RNA molecules internally and exoribonucleases, which degrade RNA molecules from either the 5’ or 3’ end (Arraiano et al., 2013). The cleavage products generated by endoribonucleases serve as substrates for 5’-to-3’ or 3’-to-5’ exonucleolytic degradation, thus the two systems are closely linked. During its life cycle, an mRNA, and similarly ncRNAs processing/regulating the mRNA, are targeted by several RNases, some of which we will come across repeatedly. Below, human names are used for conserved proteins.

The major players in RNA turnover are the 3’-to-5’ exosome complex and the 5’-to-3’ exonucleases XRN1 and XRN2. The exosome consists of a core of nine proteins which associates with the actual catalytic subunits, RRP6 and DIS3/DIS3L, with DIS3/DIS3L possessing endonuclease activity in addition to exonuclease activity (Chlebowski et al., 2013). A nuclear and a cytoplasmic form of the exosome exist, which differ in their co-factors. The nuclear exosome interacts with the TRAMP complex, whereas the cytoplasmic exosome interacts with the SKI complex (Chlebowski et al., 2013). XRN1 and XRN2 have also been found in several complexes. A detailed discussion of substrates, interacting proteins, and developmental functions of XRN1 and XRN2 is given in sections 3.2.1-3.2.3.

Regular turnover of mature mRNAs is the prototype to illustrate how multiple ribonucleases act cooperatively in a tightly regulated pathway (Nagarajan et al., 2013). Degradation of the majority of mRNAs is initiated by exonucleases, called deadenylases, that trim the 3’ poly(A) tail (Wahle and Winkler, 2013). Subsequent to deadenylation, the mRNA can be degraded 3’-to-5’ by the exosome and the SKI complex or, following hydrolytic removal of the 5’ cap through decapping enzymes (Arribas-Layton et al., 2013), by XRN1. The degradation of a minority of mRNAs is triggered by endonucleolytic cleavage, which creates newly available 5’ and 3’ ends that are degraded by XRN1 and the exosome, respectively (Nagarajan et al., 2013). One RNase that triggers endonucleolytic cleavage of mRNAs is the argonaute protein AGO2 (Krol et al., 2010). It is guided to target mRNAs in a sequence-specific manner by small interfering RNAs (siRNAs) and certain microRNAs (miRNAs), originating from exogenous and endogenous double-stranded RNA substrates, respectively. Today, thousands of miRNAs are known in humans and present a critical layer of gene expression regulation (Djuranovic et al., 2011). Moreover, miRNAs do not only regulate the stability of target mRNAs but are themselves subject to active degradation. The nucleases and cellular conditions that promote miRNA turnover are reviewed in section 3.2.4. The exosome and XRN1 are not only involved in constitutive turnover of mRNAs but also, and these functions are shared with XRN2, in the processing of pre-rRNAs and pre-snoRNAs into their mature form and degradation of maturation byproducts (Chlebowski et al., 2013; Nagarajan et al., 2013). The exosome is also involved in snRNA processing (Chlebowski et al., 2013).

Quality control systems are put in place at various stages during gene expression to dispose spurious or defective RNAs. The executors of these surveillance mechanisms are RNases. In the nucleus, quality control mechanisms involve the exosome, XRN1, and XRN2. The exosome and XRN1 were shown to degrade specific classes of antisense transcripts, cryptic unstable transcripts (CUTs) and XRN1-sensitive unstable transcripts (XUTs), respectively (van Dijk et al., 2011; Wyers et al., 2005). Antisense transcripts emerge for instance from bidirectional promoters and usually lack protein-coding potential (Pelechano and Steinmetz, 2013). Although certain antisense transcripts clearly have a biological function, most of them might present spurious transcripts whose extent needs to be limited. In yeast, the 5’ end cap added to the nascent pre-mRNA shortly after transcription initiation is endonucleolytically cut off by the decapping protein Rai1p, when inappropriately modified, and the resulting 3’ end cleavage product containing a 5’ end monophosphate is degraded by XRN2, which physically interacts with Rai1p (Jiao et al., 2010). In humans, DOM3Z/DXO was found to perform an analogous function although its 5’-to-3’ exoribonuclease activity may allow it to perform degradation of decapped pre-mRNAs XRN2-independently (Jiao et al., 2013). As RNA pol II elongates the nascent pre-mRNA, splicing is taking place co-transcriptionally. Splice-defective pre-mRNAs are cleared by the exosome, XRN1, and XRN2 (Nagarajan et al., 2013; Porrua and Libri, 2013). Moreover, future accurate translation in the cytoplasm is also ensured by degradation of erroneously processed rRNAs and tRNAs in the nucleus by the exosome and XRN2 (Nagarajan et al., 2013; Porrua and Libri, 2013). XRN1 has also been implicated in the degradation of aberrant tRNAs (Chernyakov et al., 2008). Of note, in yeast, it was recently identified that the exosome degrades >50% of intron-containing pre-mRNAs (that represent roughly 5% of yeast genes) as well as ~50% of tRNAs, which do not show a splicing or processing defect, respectively (Gudipati et al., 2012). It is currently unclear why a substantial fraction of apparently functional RNAs undergoes degradation.

A mature mRNA that has reached the cytoplasm might contain genomically encoded mutations that remained unnoticed by nuclear quality control mechanisms. Several types of mutations can affect proper protein synthesis including mutations that lead to a premature termination codon (PTC), to the absence of a termination codon, or to strong secondary structures. mRNAs containing these deleterious mutations are degraded through nonsense-mediated decay (NMD), nonstop mRNA decay (NSD), and no-go mRNA decay (NGD), respectively (Isken and Maquat, 2007). The enzymes that mediate constitutive mRNA turnover, i.e. the exosome and XRN1, also function in NMD, NSD, and NGD. Notably, different eukaryotes, despite the fact that all use the exosome and XRN1 as executors, differ substantially in the upstream part of the NMD and NSD pathway (Isken and Maquat, 2007). NGD has only been studied in yeast.

Despite these intricate quality control mechanisms, mutations are inevitable. In particular, silent mutations in mRNAs are challenging to be tackled by surveillance systems. These mutations, although not changing the amino acid sequence, might still affect splicing. In fact, ~10% of genetic diseases that are caused by point mutations arise from mutations within the three consensus sequences recognized by the spliceosome, the 5’ and 3’ splice-site, respectively, and the branch point (Cooper et al., 2009). Many more exonic and intronic regions exist that are relevant to splicing, called splicing enhancers or silencers, whose consensus sequences, however, are less well established (see section 4.2). A striking example of a single point mutation with a deleterious effect is the C-to-T change at position 6 in exon 7 of the SMN2 (survival of motor neuron 2) gene (Cartegni and Krainer, 2002). It was found that this mutation lies within a splicing enhancer region and causes skipping of exon 7 by preventing binding of the SF2/ASF splicing factor. Skipping of exon 7 leads to an inactive and unstable SMN2 protein. Mutant SMN2 is not able to maintain its function in snRNP biogenesis and thus triggers a detrimental cascade that results in spinal muscular atrophy (SMA) (Cartegni and Krainer, 2002).

3 The exoribonuclease XRN2 in *C. elegans*: Its role in development and its interplay with the novel protein PAXT-1

3.1 Abstract and contributions

XRN2 is an evolutionarily conserved 5’-to-3’ exoribonuclease in eukaryotes. Although various substrates for XRN2 have been established, including pre-mRNAs, pre-rRNAs, pre-snoRNAs, abberant tRNAs and miRNAs, its developmental function remains largely unexplored. In section 3.3.1, we assess the biological role of XRN2 in *C. elegans*. We show that XRN2 is expressed constitutively and ubiquitously across developmental stages and tissues, respectively. Further, we observe a molting defect and early larval arrest in *xrn-2* null mutant worms or worms expressing a catalytically inactive version of *xrn-2*. A *de novo*-generated temperature-sensitive allele allows us to investigate the developmental function of XRN2 beyond an early larval stage revealing an involvement of XRN2 in embryogenesis and fertility. Furthermore, a time-course experiment following α-amanitin-induced transcriptional shut-off uncovers rapidly decaying miRNAs. Interestingly, only a subset of these short-lived miRNAs is stabilized by conditional inactivation of XRN2 indicating specificity of XRN2 towards particular miRNAs *in vivo*. Finally, the time-course experiment reveals that miRNA* strands are markedly less stable compared to miRNA guide strands in agreement with the view that the vast majority of miRNA* strands are processing byproducts rather than having a biological function. Of note, half-lives of miRNA* strands are not affected by XRN2.

Whereas constitutive interaction partners for XRN2 affecting its stability and catalytic activity have been identified in yeast (Rai1p) and the ciliate *Tetrahymena thermophila* (Twi12), such factors await elucidation in metazoans. In section 3.3.2 and 6, we identify PAXT-1 as a novel subunit of an XRN2 complex in *C. elegans*. We show a direct interaction between XRN2 and PAXT-1, which leads to mutual stabilization of the binding partners. Knock-down of *paxt-1* enhances the phenotype of an *xrn-2ts* mutant whereas a *paxt-1* null mutant causes larval arrest at elevated temperature. This larval arrest is rescued by an additional copy of *xrn-2* suggesting that PAXT-1 mainly acts by increasing the stability of XRN2. Indeed, an *in vitro* assay fails to show a modulatory effect of PAXT-1 on XRN2 kinetics. Moreover, a PAXT-1 fragment comprising a previously uncharacterized domain, DUF3469, is able to rescue the larval arrest of the *paxt-1* null mutant and suffices to bind to XRN2. Finally, we find that human proteins that contain DUF3469 (CDKN2AIP/CARF and NKRF/NRF) bind to XRN2 and that, at least in the case of CDKN2AIP/CARF, DUF3469 is sufficient for interaction. In sum, DUF3469 presents a conserved domain that connects different proteins to XRN2, which we therefore renamed to XRN2-binding domain (XTBD).

My contributions to section 3.3.1 include the characterization of the *xrn-2* null and *xrn-2* catalytically-dead mutant as well as the determination of the spatio-temporal expression pattern of XRN2. Takashi Miki generated and characterized the *xrn-2ts* mutant and performed the global decay analysis of miRNAs. My contributions to section 6 include the co-immunoprecipitations (co-IPs) of transgenic and endogenous XRN2 and PAXT-1 in *C. elegans* as well as the generation of transgenic worms expressing different fragments of PAXT-1, which I later used in co-IPs in order to reveal domain requirements of PAXT-1 for binding to XRN2. My data is presented separately in section 3.3.2. Hannes Richter purified recombinant proteins and performed enzymatic assays. Takashi Miki did all the other experiments.

3.2 Introduction

3.2.1 XRN 5'-to-3' exoribonucleases

Yeast and metazoans contain two members of the XRN family of 5'-to-3' exoribonucleases, the cytoplasmic XRN1 (Xrn1p in yeast) and the nuclear XRN2 (Rat1p in yeast) (Nagarajan et al., 2013). Henceforth, the denotations 'XRN1' and 'XRN2' will also be used for the yeast proteins for the sake of clarity. In *A. thaliana,* three XRN2 orthologs are present (AtXRN2, AtXRN3, AtXRN4) but no XRN1 ortholog (Kastenmayer and Green, 2000). However, whereas AtXRN2 and AtXRN3 are nuclear, AtXRN4 is cytoplasmic and exhibits XRN1-functionality such as mRNA turnover (Souret et al., 2004). XRN1 and XRN2 possess two highly conserved regions (CR1 and CR2) in their N-terminal part but show only little conservation outside these regions (Fig. 1). The sequence of CR1 and CR2 among XRN2 homologs is 50-60% identical while that between XRN1 and XRN2 homologs is 40-50% identical. Of note, in *S. cerevisiae*, XRN1 artificially targeted to the nucleus by an NLS complements the temperature sensitivity of an *xrn2* mutant strain (Johnson, 1997). Conversely, mutations within the NLS of XRN2 mislocalize it to the cytoplasm and are able to rescue the lethality of an *xrn1 ski2* double mutant strain (Johnson, 1997). Thus, XRN1 and XRN2 and possibly XRN1/2 from higher eukaryotes are functionally interchangeable exoribonucleases. The catalytically active site of XRNs comprises seven conserved acidic residues within CR1 that coordinate two Mg2+ ions (Chang et al., 2011b; Jinek et al., 2011). Two of these residues (Asp206 and Asp208 in XRN1 from *S. cerevisiae* and Asp207 in *D. melanogaster*) have been shown to abolish catalytic activity of XRN1 *in vitro* and *in vivo* when mutated (Jinek et al., 2011; Solinger et al., 1999). XRN1 contains an extended C-terminal tail that is absent from XRN2 harboring a PAZ/Tudor and an SH3-like domain (Jinek et al., 2011). The far C-terminal end of XRN1 in *S. cerevisiae* (residues 1206-1528) is dispensable for its catalytic activity *in vitro* and for rescue of the growth defect of an *xrn1* null mutant (Page et al., 1998).

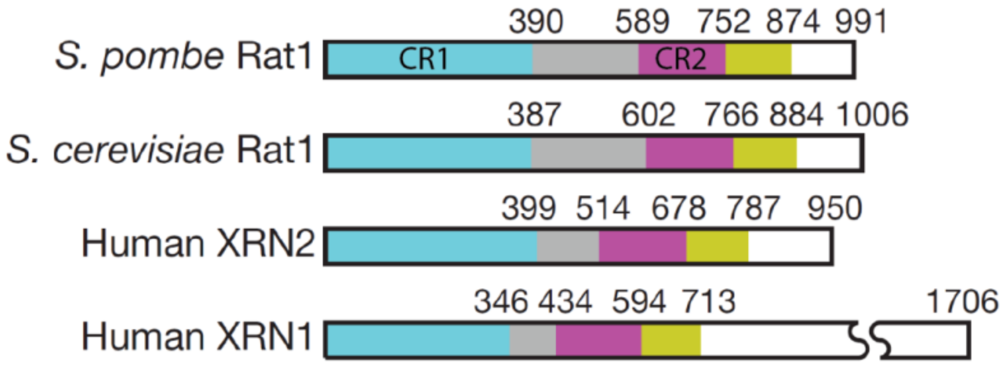

Fig. 1. Sequence conservation of XRNs. Conserved regions (CR1 and CR2) are shown in cyan and magenta, a weakly conserved region is shown in yellow, and unconserved regions are shown in grey and white. Modified with permission from doi: 10.1038/nature07731.

3.2.2 The nuclear exoribonuclease XRN2

Substrates of XRN2

XRN2 is a promiscuous nuclease targeting a wide range of nuclear RNAs whose maturation, levels or quality it controls (Miki and Grosshans, 2013). Some of its substrates are also targeted by XRN1 (see section 3.2.3). A separate section (3.2.4) discusses an involvement of XRN1 and XRN2 in miRNA turnover.

XRN2 participates in the maturation of rRNAs (Amberg et al., 1992; Fang et al., 2005; Petfalski et al., 1998; Wang and Pestov, 2011). A single pre-rRNA molecule is transcribed by RNA polymerase I comprising the 18S, 5.8S and 25S/28S (yeast/mammals) sequences. Additionally, the pre-rRNA transcript contains an external transcribed spacer (ETS) at the 5' and 3' end (5' ETS and 3' ETS, respectively) as well as two internal transcribed spacers (ITS) separating the prospective mature rRNA sequences. Following endonucleolytic cleavage within the ITS's, XRN2 degrades the remaining ITS sequence at the 5' end of the 5.8S and 25S rRNA (Geerlings et al., 2000; Henry et al., 1994). XRN2 also degrades excised fragments of the pre-rRNA spacer regions (Petfalski et al., 1998). Through a conceptually similar process, XRN2 produces 5' ends of snoRNAs (Petfalski et al., 1998; Qu et al., 1999).

XRN2 plays a role in the quality control of several classes of RNAs (Miki and Grosshans, 2013). Defects in rRNA processing lead to polyadenylated pre-rRNAs in yeast (Fang et al., 2004). Polyadenylated pre-rRNAs also accumulate in strains deleted for the exosome subunit Rrp6p indicating that polyadenylation targets pre-rRNAs for degradation by the exosome (Kuai et al., 2004). Deletion of XRN2 was found to enhance the accumulation of polyadenylated pre-rRNAs in strains mutant for Rrp6p (Fang et al., 2005). However, deletion of XRN2 alone did not result in significant accumulation of polyadenylated pre-rRNAs suggesting that the exosome is the main surveillance factor for pre-rRNAs in yeast. In contrast, in mouse cells, knock-down of XRN2 stabilized aberrant pre-rRNA species, highlighting a more prominent role of mammalian XRN2 in the clearance of defective pre-rRNAs (Wang and Pestov, 2011). XRN2 has also been implicated in the degradation of unspliced pre-mRNAs (Bousquet-Antonelli et al., 2000; Davidson et al., 2012). Whereas in yeast the exosome constitutes the major pathway by which deficient pre-mRNAs are removed with only little contribution by XRN2, the latter appears to be more important in mammalian cells. Of note, in yeast, Bousquet-Antonelli and colleagues observed that inhibition of pre-mRNA degradation was accompanied by increased levels of spliced mRNAs arguing for a competition between splicing and degradation of pre-mRNAs independent of splice defects (Bousquet-Antonelli et al., 2000). Lastly, XRN2 mediates turnover of improperly modified mature tRNAs which might impede translation (Chernyakov et al., 2008).

XRN2 has been shown to degrade Telomeric Repeat-containing RNA (TERRA) (Luke et al., 2008). The repetitive nucleotide sequences at the end of linear chromosomes are called telomeres and function in protecting chromosomes from nucleolytic degradation and DNA repair activities at their extremes (O'Sullivan and Karlseder, 2010). In most somatic cells in humans, telomeres get shortened with every cell division due the inability of conventional polymerases to fully replicate the parent DNA (Hug and Lingner, 2006). In *S. cerevisiae* and certain human cells, an enzyme called telomerase provides reverse transcriptase activity to counteract this shortening (Hug and Lingner, 2006). Telomeres are transcribed by RNA polymerase II (RNA pol II) into TERRA, which bind to telomeres and prohibit telomerease action (Azzalin et al., 2007; Luke et al., 2008). An XRN2-mutant yeast strain showed accumulation of TERRA and shortened telomeres (Luke et al., 2008). This suggests a role of XRN2 in the regulation of telomerase activity through degradation of TERRA.

Finally, XRN2 also functions during termination of RNA polymerase II (RNA pol II) transcription in yeast and mammals (Kim et al., 2004b; West et al., 2004) and, at least in yeast, also during termination of RNA pol I transcription (El Hage et al., 2008). For RNA pol II transcription termination, the current model suggests that, following endonucleolytic cleavage of a nascent RNA transcript at the poly(A) site, the 5' cleavage product is polyadenylated whereas the 3' cleavage product is degraded by XRN2. Eventually XRN2 catches up with the elongation complex leading to its release (Tollervey, 2004). However, degradation of the 3' product of the endonucleolytic cleavage is not sufficient, though necessary, to induce transcription termination as XRN1, upon mislocalization to the nucleus, is able to degrade the nascent RNA but does not cause polymerase release (Luo et al., 2006). Of note, XRN2 is also involved in 3' end processing by enhancing recruitment of cleavage and polyadenylation factors such as Pcf11 and Rna15 in yeast (Luo et al., 2006).

Interaction partners of XRN2

Given the diverse pathways XRN2 is involved in, it comes as little surprise that it has been reported on multiple interacting proteins for this enzyme. In yeast, XRN2 has been shown to interact with Rai1p (Rat1p interacting protein 1) (Xiang et al., 2009; Xue et al., 2000). Rai1p deletion leads to a slow-growth phenotype that is rescued by an additional copy of XRN2 as well as nucleus-targeted XRN1 suggesting that Rai1p mainly acts by enhancing the activity of XRN2 (Xue et al., 2000). It has also been shown that Rai1p increases the processivity of XRN2-mediated RNA decay (Xiang et al., 2009). More recently, it was found that Rai1p does not only stabilize XRN2 activity but possesses enzymatic activity on its own. Rai1p is a 5' pyrophosphoydrolase converting 5' triphosphate on RNA substrates to monophosphate (Xiang et al., 2009) and also has non-canonical 5' decapping activity removing 5' unmethylated caps of RNAs (Jiao et al., 2010). Whereas RNAs with 5' triphosphates and cap-structures are not amenable to XRN2 exoribonucleolytic activity (Stevens and Poole, 1995), 5' monophosphorylated RNA products generated by Rai1p through both pyrophosphohydrolase and decapping activity, are (Jiao et al., 2010; Xiang et al., 2009). An appealing model therefore suggests that Rai1p provides XRN2 with targetable substrates. Rai1p has homologs in most eukaryotes, however, its sequence is only weakly conserved. The human and *Drosophila* homolog of Rai1p, DOM3Z and Cuff, respectively, appear not to interact with XRN2 (Chen et al., 2007; Xiang et al., 2009). Nevertheless, the catalytic residues in Rai1p are conserved in DOM3Z (Xiang et al., 2009) as is the pyrophosphohydrolase and decapping enzymatic function (Jiao et al., 2013).

Several interacting factors have been described to cooperate with XRN2 in transcription termination. In yeast, the XRN2/Rai1p complex co-purifies with Rtt103p which contains an RNA pol II carboxy-terminal domain (CTD)-interacting domain (CID) (Kim et al., 2004b). Furthermore, Rtt103p and XRN2/Rai1p co-localize near 3’ ends of genes in chromatin immunoprecipitations (ChIPs). However, the role of Rtt103p in XRN2-mediated transcription termination awaits elucidation as XRN2 recruitment to the 3’ end of genes is not affected in a strain deleted for Rtt103p (Kim et al., 2004b). In mammals, the multifunctional protein p54nrb/PSF appears to recruit XRN2 to the cleavage/polyadenylation machinery (Kaneko et al., 2007). Kim and colleagues noticed in their ChIP data that XRN2 and Rai1p not only crosslink to 3’ ends but also to promoter regions (Kim et al., 2004b). XRN2 in human cells has also been observed to localize near transcription start sites (TTSs) by ChIP-seq (Brannan et al., 2012). Moreover, XRN2 was found to physically interact with a termination factor, TTF2, but also with decapping factors such as DCP1, DCP2, and EDC3 with whom it co-localizes at promoter-proximal regions. Knock-down of XRN2, TTF2 or any of the decapping factors led to a redistribution of RNA pol II occupancy away from TTSs toward upstream and downstream distal positions (Brannan et al., 2012). In HeLa cells, the microprossecor complex consisting of Drosha and DGCR8 has been implicated in the control of premature termination of transcription of a subset of genes by recruiting the transcription termination factor SETX and the ribonucleases XRN2 and RRP6 to promoter-proximal regions (Wagschal et al., 2012). A model was derived whereby promoter-proximal pausing of RNA pol II, facilitated by negative elongation factors such as NELF and DSIF (Chiba et al., 2010), allows quality control mechanisms to assess the status of transcripts. Co-transcriptional decapping by DCP2 or Rai1p and premature termination of transcription by XRN2 is thought to prohibit elongation of defective or undesired transcripts (Brannan et al., 2012; Jiao et al., 2010). In particular, XRN2-mediated premature termination of transcription is thought to limit bidirectional transcription from promoters.

Finally, in the ciliate *Tetrahymena thermophila*, co-immunoprecipitations revealed a trimeric complex consisting of XRN2, the Ago/Piwi protein Twi12, and Tan1 (Twi-associated novel 1) (Couvillion et al., 2012). Twi12 binds to small RNAs (18–22 nt) derived from the 3’ end of mature tRNAs. The Twi12-bound tRNA fragments contain a base modification that most likely precludes their interaction with target RNAs in a similar way to miRNA and siRNAs. Rather, binding of tRNA fragments is required for nuclear import of Twi12. Twi12 localizes XRN2 to the nucleus, stabilizes it, and stimulates its exonuclease activity without possessing nuclease activity on its own (Couvillion et al., 2012). Additionally, depletion of Twi12 or XRN2 leads to an accumulation of rRNA processing intermediates, known substrates of XRN2 (Geerlings et al., 2000; Henry et al., 1994). The functional contribution of Tan1 to the complex is unknown. No homologs for Tan1 exist and in contrast to Twi12 and XRN2, Tan1 is not essential for *Tetrahymena* growth (Couvillion et al., 2012).

Developmental functions of XRN2

Knowledge on the developmental functions of XRN2 is scare (Nagarajan et al., 2013). In yeast, XRN2 has been shown to be essential for viability (Amberg et al., 1992; Sugano et al., 1994). In *C. elegans*, XRN2 has been found in a genome-wide RNAi screen for factors involved in molting (Frand et al., 2005). Besides, knock-down of XRN2 by RNAi causes slow grow and sterility (Chatterjee and Grosshans, 2009). Finally, a genome-wide association study correlates elevated XRN2 levels with an increased risk for spontaneous lung cancer (Lu et al., 2010). The diversity of RNA substrates for XRN2 complicates phenotypical analyses of mutants of this enzyme set out to understand its biological functions. Thus, although some phenotypes upon loss or knock-down of XRN2 have been described, the substrates responsible for the observed phenotypes are largely obscure.

3.2.3 The cytoplasmic exoribonuclease XRN1

Substrates of XRN1

XRN1 mediates turnover of mRNAs and thus, together with the 3’-to-5’-degrading exosome, constitutes the major determinant of an mRNA’s half-life (Chang et al., 2011a). Degradation of mRNAs occurs either through a deadenylation-dependent or deadenylation-independent pathway.

Deadenylation-dependent mRNA decay, as the name implies, is initiated by the recruitment of nucleases, called deadenylases, that trim the poly(A) tail at the 3’ end of mature mRNAs (Parker and Song, 2004). Deadenylase activity is brought about by three different multimeric complexes, CCR4-NOT, PAN2-PAN3, and PARN (Parker and Song, 2004). Following deadenylation, the Lsm1-7 proteins bind to mRNAs and recruit the decapping machinery with its catalytic subunit DCP2 (Coller and Parker, 2004). NUDT16 is another decapping enzyme in mammalian cells, however, whether it is recruited by Lsm1-7 is currently unclear (Song et al., 2010). The deadenylated and decapped mRNA is then degraded by XRN1 (Chang et al., 2011a).

Deadenylation-independent decay constitutes an additional pathway by which the stability of an mRNA is regulated (Nagarajan et al., 2013). This pathway is triggered by endonucleolytic cleavage of the mRNA and subsequent attack of newly available 5’ and 3’ ends by XRN1 and the exosome, respectively (Dodson and Shapiro, 2002; Nagarajan et al., 2013). Furthermore, a pathway referred to as nonsense-mediated decay (NMD) exists that ensures rapid degradation of mRNAs with premature termination codons (PTCs) that could lead to truncated and potentially harmful proteins (Conti and Izaurralde, 2005). In yeast and mammals this pathway involves deadenylation-independent decapping followed by XRN1 degradation as well as deadenylation-dependent exosome degradation (Conti and Izaurralde, 2005). Of note, in *Drosophila*, NMD is initiated by endo- rather than exonucleolytic cleavage followed by degradation of the cleavage products by XRN1 and the exosome (Gatfield and Izaurralde, 2004).

Furthermore, XRN1 is responsible for the turnover of miRNA-targeted mRNAs either by degrading the 3’ cleavage product arising from AGO2-mediated endonucleolytic slicing of the mRNA (Orban and Izaurralde, 2005; Souret et al., 2004) or by degrading translationally inhibited mRNAs in a deadenylation-dependent manner (Carthew and Sontheimer, 2009). Not only mRNA is targeted by XRN1 but also non-coding RNA such a class of long non-coding RNAs (lncRNAs) termed XUTs (Xrn1-sensitive unstable transcripts) (van Dijk et al., 2011).

Finally, it is intriguing that, despite their different subcellular localization, XRN1 and XRN2 have several substrates in common. XRN1, similar to XRN2, is involved in 5’ end processing of precursor forms of rRNAs (Geerlings et al., 2000; Henry et al., 1994) and snoRNAs (Lee et al., 2003; Petfalski et al., 1998), as well as degradation of hypomodified mature tRNAs (Chernyakov et al., 2008) and unspliced pre-mRNAs and intron lariats (Bousquet-Antonelli et al., 2000; Danin-Kreiselman et al., 2003; Hilleren and Parker, 2003). Finally, XRN1 and XRN2 both mediate turnover of certain lncRNAs (Geisler et al., 2012) as well as mature miRNAs (Ruegger and Grosshans, 2012).

Interaction partners of XRN1

Factors that have been found to interact with XRN1 reflect its prominent function in mRNA turnover and include proteins involved in decapping such as DCP1/EDC4 (Braun et al., 2012), Lsm1-7 (Bouveret et al., 2000) and PAT1 (Nissan et al., 2010) as well as proteins involved in the NMD pathway such UPF1, UPF2, and UPF3X (Lejeune et al., 2003). Furthermore, XRN1 forms a complex with the scavenger-decapping enzyme DCS1 in yeast and *C. elegans* and stimulates its activity *in vitro* and *in vivo* (Bosse et al., 2013; Sinturel et al., 2009). Interestingly, in both systems the decapping activity of DCS1 is not required to promote XRN1 exonucleolytic activity.

Developmental functions of XRN1

In unicellular organisms, XRN1 is not essential. Nonetheless, deletion of *xrn1* in yeast (i.e. *S. cerevisiae* and *C. albicans*) and knock-down of *xrn1* in the protozoan parasite *T. brucei* markedly reduces the growth rate (An et al., 2004; Kim and Kim, 2002; Larimer and Stevens, 1990; Li et al., 2006). Additional phenotypes observed in *S. cerevisiae* upon *xrn1* deletion include a defect in nuclear fusion, hypersensitivity to nitrogen starvation and to a microtubule-destabilizing drug (benomyl), increased rate of chromosome loss, and inability of diploids to sporulate (Kim et al., 1990).

In multicellular organisms, XRN1 is essential. In *C. elegans*, knock-down of *xrn1* by RNAi leads to embryos that fail to complete ventral closure due to impaired epithelial movement (Newbury and Woollard, 2004). An analogous morphological defect is observed in *D. melanogaster*, where hypomorphic alleles of *xrn1* (also called Pacman) show impeded dorsal closure in the embryo and thorax closure during metamorphosis (Grima et al., 2008). Furthermore, these reduction-of-function mutants of XRN1 result in significantly decreased fertility of male as well as female flies due to a diminished number of sperm and eggs, respectively (Lin et al., 2008; Zabolotskaya et al., 2008). In *A. thaliana*, mutations in AtXRN4 result in insensitivity to the plant hormone ethylene (Potuschak et al., 2006), serrated leaf edges (Gregory et al., 2008), and late flowering (Geraldo et al., 2009). Late flowering is likely caused by reduced turnover of the floral repressor FLC in an XRN1 mutant background (Geraldo et al., 2009). In human primary osteogenic sarcoma cell lines, missense mutations have been found in conserved regions of XRN1 correlating with reduced levels of XRN1 mRNA levels in these cell lines. Moreover, XRN1 mRNA levels were reduced in patient-derived tissue samples indicating that XRN1 might act as a tumor suppressor gene in osteosarcoma (Zhang et al., 2002). However, a causal link between the mutations in XRN1, its reduced mRNA levels, and the osteosarcoma remains to be proven.

3.2.4 Publication: “MicroRNA turnover: when, how, and why”

Review

MicroRNA turnover: when, how, and why

Stefan Rüegger[1,2] and Helge Großhans[1]

[1] Friedrich Miescher Institute for Biomedical Research, Novartis Research Foundation, Maulbeerstrasse 66, CH-4058 Basel, Switzerland
[2] University of Basel, Petersplatz 1, CH-4003 Basel, Switzerland

MicroRNAs (miRNAs) are short (~22 nucleotide) RNAs that are important for the regulation of numerous biological processes. Accordingly, the expression of miRNAs is itself tightly controlled by mechanisms acting at the level of transcription as well as processing of miRNA precursors. Recently, active degradation of mature miRNAs has been identified as another mechanism that is important for miRNA homeostasis. Here we review the molecular factors and cellular conditions that promote miRNA turnover. We also discuss what is known about the physiological relevance of miRNA decay.

Degradation facilitates dynamic miRNA expression patterns

MicroRNAs are a large class of small regulatory RNAs, ~22 nucleotides long. They bind to partially complementary sequences in target mRNAs and silence them translationally or by inducing mRNA degradation [1]. miRNAs are important for gene regulation in numerous cellular and developmental processes [2], therefore it is perhaps of little surprise that miRNAs themselves are subject to extensive regulation. Indeed, a large body of literature connects dysregulation of miRNAs with disease [3], highlighting a need for robust regulation of miRNA activity. Several such regulatory mechanisms have been shown to affect miRNA biogenesis, a well-understood process (Box 1), and miRNA activity [4]. By contrast, regulation of miRNA levels through degradation of the mature, functional miRNA has received less attention. This may be owed in part to the perception of miRNAs as inherently stable molecules, consistent with the finding that mature miRNAs persist for many hours or even days after their production is arrested (e.g., by transcriptional shut-down through chemical inhibitors or depletion of miRNA processing enzymes) [5–8].

Nonetheless, many miRNAs show a dynamic expression pattern during development, including rapid downregulation in some instances [9–12]. Moreover, specific mature miRNAs have been found to be expressed in a tissue- or stage-specific manner without variation in the expression pattern of the precursor forms (pri- and pre-miRNAs), supporting the notion of regulatory mechanisms acting on the mature miRNA [13,14]. These findings suggest that steady-state levels of miRNAs can be regulated through both biosynthetic and decay processes. Here, we summarize how turnover of mature miRNAs contributes to their homeostasis and permits their dynamic regulation. We focus in particular on reviewing the cellular states that affect miRNA stability as well as molecular mechanisms of miRNA degradation. However, we do note that currently, studies consolidating physiological triggers of miRNA destabilization with molecular mechanisms remain largely elusive. Furthermore, insights into the physiological relevance of mature miRNA degradation are just beginning to emerge.

Cellular conditions affecting miRNA stability

In contrast to the view of miRNAs as generically stable molecules, recent studies have shown that individual miRNAs, or miRNAs in specific environments, are subject to accelerated decay (Table 1), altering miRNA levels and hence activity. This section focuses on discussing cellular conditions and extracellular cues that influence miRNA stability.

The cell cycle

Several miRNA families function in cell cycle regulation; for example, by targeting components of cyclin/CDK complexes [15]. Intriguingly, the reverse is also true; that is, cell cycle stage affects accumulation of certain miRNAs [16–18]. miR-29b is the first example of these [16]. In HeLa cells, miR-29b is polycistronically transcribed together with its 'sister' miR-29a, from which it differs by a nucleotide at position 10 as well as its six 3′-terminal nucleotides. However, whereas miR-29a levels change little during progression through the cell cycle, miR-29b is enriched in mitotic cells. When mature synthetic miR-29b was transfected into cells as an miR:miR*-like duplex siRNA, it was similarly found to accumulate preferentially in mitotically arrested cells, indicating that regulation of miR-29b takes place after it has been processed into the mature form. 'Pulse-chase'-like experiments using transfection revealed a half-life of miR-29b of 4 h in cycling cells, compared to >12 h in mitotically arrested cells, whereas miR-29a has a half-life of >12 h in either case [16]. Mutational analysis suggested that the uracils at nucleotide positions 9–11 are necessary, although not sufficient, for the fast degradation of miR-29b [16,19]. Factors recognizing this element and mediating degradation remain to be discovered. Additionally, because these experiments [19] relied mostly on transfection of synthetic miRNA duplexes at rather high levels (40 nM), it is unclear what fraction of these RNAs is indeed loaded into Argonaute (AGO; Box 1),

---

Corresponding author: Großhans, H. (helge.grosshans@fmi.ch).

0968-0004/$ – see front matter © 2012 Elsevier Ltd. All rights reserved. http://dx.doi.org/10.1016/j.tibs.2012.07.002 Trends in Biochemical Sciences, October 2012, Vol. 37, No. 10

Box 1. miRNA biogenesis and function

MicroRNAs (miRNAs) are typically transcribed by RNA polymerase II as primary transcripts (pri-miRNAs) that are subsequently matured in a multi-step biogenesis process to generate the mature, functional form [4] (Figure I). Pri-miRNAs are capped and polyadenylated and are usually several kilobases long. They possess hairpin structures that comprise the future mature sequence (red) in their stem. Alternatively, the pre-miRNA may reside in introns of mRNAs or other non-coding RNAs. In either case, the nuclear RNase III-type enzyme Drosha, in a complex with its co-factor DGCR8 (DiGeorge syndrome critical region 8 homolog), cleaves near the base of the stem, releasing an approximately 70 nucleotide-long stem-loop precursor miRNA (pre-miRNA) [4]. The pre-miRNA is exported from the nucleus by Exportin 5. In the cytoplasm, another RNase III-type enzyme, Dicer, with its co-factors TRBP (TAR RNA-binding protein 2, also known as TARBP2), cleaves off the terminal loop, resulting in an RNA duplex of ~22 nucleotides [4]. Following Dicer cleavage, the short RNA duplex is bound by an AGO (Argonaute) protein, a component of a multisubunit complex termed miRISC (miRNA-induced silencing complex) [4]. Subsequently, one of the two strands, the so called passenger strand (also referred to as miR*), is released and degraded whereas the other strand, termed guide strand or miR, is retained within miRISC. This strand selection follows a 'thermodynamic asymmetry rule' in that the strand whose 5′-terminus is less stably base-paired is destined to become the guide strand. The guide strand targets miRISC to mRNAs with partially complementary sequences and silences them [1]. The so-called 'seed' region, nucleotides 2–8 from the 5′-end of an miRNA, is particularly important for target recognition; hence, miRNAs that share the seed region but differ outside are frequently considered to form a 'family' of miRNAs with largely overlapping sets of targets [54]. miRISC-bound mRNAs are subjected to translational repression, mainly inhibition of translation initiation, and/or degradation following deadenylation by the CCR4-NOT (carbon catabolite repressor protein 4–General negative regulator of transcription) complex and decapping (not shown) [68]. Irrespective of the mechanism, members of the GW182 (glycine-tryptophane protein of 182 kDa) protein family are essential components of RISC for mRNA silencing [68].

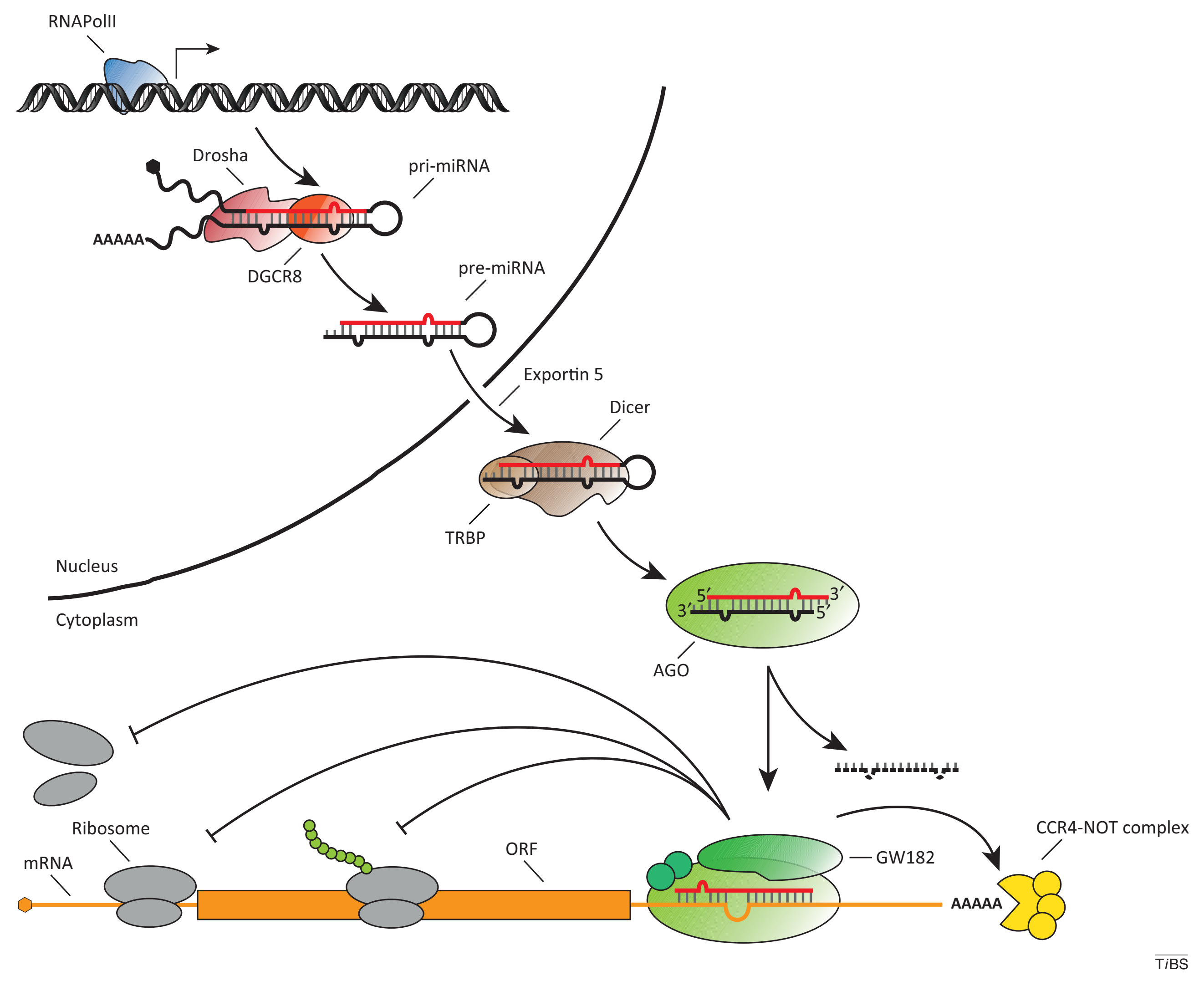

Figure I. Schematic view of miRNA biogenesis and mechanism of action.

and whether loading, which would presumably promote stability [20,21], is equal for all miR-29b mutant variants.

Several other endogenous miRNAs display a cell cycle-dependent expression pattern in HeLa cells [22]. HeLa cells complete a cell cycle in less than 1 day; therefore, this suggests a relatively rapid turnover of these miRNAs, although exact half-lives were not determined. It is also unknown whether stability of these miRNAs, similar to miR-29b, is regulated in a cell cycle-dependent manner. Alternatively, continuously low stability across all cell cycle phases might permit rapid decreases of miRNA levels upon slowed biogenesis. Indeed, Rissland and colleagues observed that this is true for the rapid downregulation of miR-16 family members in mouse NIH 3T3 cells during transition from G0 to G1 phase [17]. Levels of several members of this family rapidly decreased at the G0–G1-transition. Among these, miR-503, an extended miR-16 family member that differs from other family members at nucleotide eight of the seed region (Box 1), decreased most strongly and with an apparent half-life of 3.6 h. Strikingly, a similarly short half-life was observed for miR-503 that was ectopically expressed from a repressible

Table 1. miRNAs that exhibit accelerated decay

miRNA	Half-life[a] (h)	Destabilizing element	Organism/cells	Nuclease	Condition	Refs
miR-29b	4±1.4 ([16]), 7.3±1.8 ([19])	uagcaccauuu gaaaucaguguu	human HeLa, mouse NIH 3T3 cells	ND	Destabilized in cycling cells, stable in mitotic cells	[16,19]
miR-503, miR-15a/b, miR-322, miR-16	3.6 (miR-503), 5.8 (miR-322)	uagcagcg ggaacag uacugcag (miR-503)	Mouse NIH 3T3 cells	ND	Inherently unstable; Decreased at G0–G1 transition due to transcriptional shut-off	[17]
miR-134, miR-155, miR-188, miR-191, miR-198, miR-202, miR-212, miR-320, miR-370, miR-452, miR-498, miR-564, miR-572, miR-575, miR-601, miR-629, miR-630, miR-638, miR-662, miR-663, miR-765, miR-654, miR-671	~1	ND	Human MCF10A immortalized breast and HeLa cervical cancer cells	ND	Destabilized by EGF exposure	[18]
(miR-183/96/182, miR-204, miR-211)*, let-7b, miR-29c, miR-15a, miR-16, miR-124, miR-128, miR-134, miR-138	~1.5 (for light-regulated ones*)	ND	Retinal mouse neurons (*in vivo*), cultured rodent cortical and hippocampal neurons, ES cell-derived neurons	ND	Unstable in neurons; stabilized when neuronal activity is blocked	[23]
miR-125b, miR-132, miR-146a, mir-183, miR-9	0.7 (miR-9) – 3.5 (miR-125b)	ND	Primary human neuron cultures, postmortem human brain tissues	ND	ND	[24]
miR-124, miR-184	ND	ND	Cultured *Aplysia* neurons	ND	Levels reduced upon serotonin exposure	[25]
miR156, miR159, miR163, miR167, miR172, miR173, siR1003 (endo-siRNA),	ND	ND	*A. thaliana*	Combined depletion of SDN1/2/3 and At3g50090	ND	[31]
miR912, miR909.1, miR1157, siRNAs	ND	ND	*Ch. reinhardtii*	RRP6	Quality control mechanism (loss of 2′-*O*-methylation)	[39]
(let-7, miR-48, miR-84, miR-241, miR-237, miR-34, miR-85, miR-240, miR-234, miR-245, miR-77)$^{\circ}$ (let-7, miR-241, miR-77, lin-4)$^{+}$	ND	ND	*C. elegans*	XRN-1^{+}/XRN-2°	ND	[41,42]
miR-382	1.2	gaaguugu ucguggu ggauucg	HEK 293 cells	RRP41/XRN1?	ND	[47]
miR-221, miR-222, miR-106, miR-103, miR-107, miR-183, miR-193a-3p, miR-210, miR-214, miR-29b, miR-320, miR-518a-5p-527, miR-572, miR-612, miR-617, miR-628-3p, miR-630, +12 not yet annotated miRs	ND	ND	Human melanoma cells	PNPase$^{\text{old-35}}$	Destabilized by interferon-β exposure	[48]

Table 1 (***Continued***)

miRNA	Half-life^{a} (h)	Destabilizing element	Organism/cells	Nuclease	Condition	Refs
miR-20a	3–6	ND	Human glioma cells, human and murine astrocytes, HEK 293T cells	ND	Stabilized by binding to QKI	[53]
miR-27	ND	Partial complementarity to HSUR1 from HVS and m169 from MCMV	HVS-infected primate T cells, MCMV infected mouse NIH 3T3 cells	ND	Destabilized by binding to viral non-coding transcript (HSUR1 in HVS, m169 in MCMV)	[60–62]
let-7	3.53	Partial complementarity to miR-107	Several human cancer cell lines and mouse mammary tumor cells/tissues	ND	Destabilized by binding to miR-107	[64]

[a] Only the shortest measured half-life is given for those examples where decay rate was shown to increase by a given stimulus/context.
ND, no data.

transgene within G0. Moreover, whereas its precursor, pre-miR-503, was observed by northern blot in G0-arrested cells, it became undetectable upon cell cycle re-entry, suggesting cell cycle-regulated transcription or processing. Thus, it is not miR-503 stability that is altered during transition into G1. Instead, constitutively low stability of miR-503 permits rapid changes in its levels in response to altered transcription or processing.

Expression of variant pre-miRNA from transgenes revealed that residues in the seed region and at the 3′-end coordinately destabilize miR-503 [17]. The nuclease that rapidly turns over miR-503 awaits identification, and the physiological relevance of fast miR-16 family regulation is currently not clear. However, given that the known and predicted miR-16 target genes include several genes that function in the G1-S transition (e.g., Cyclin D1/2/3, Cyclin E1, and CDK6) and that repression of miR-503 target reporters was reduced in G1- compared to G0-phase [17], a role in modulating cell cycle progression appears likely.

Growth factors

In human MCF10A immortalized breast epithelial cells, the levels of several miRNAs rapidly decreased upon epidermal growth factor (EGF) stimulation [18]. After MCF10A cells had been starved of serum to arrest their proliferation, stimulation by addition of EGF caused a reduction by $\geq$50% of 23 miRNAs within 1 h. Similar observations were made for human HeLa cervical cancer cells, although there was only minor overlap in the set of miRNAs that was affected. Known or predicted targets of the miRNAs downregulated in MCF10A cells include several ‘immediate early genes’; that is, genes that are rapidly upregulated in response to EGF [18]. This suggests that rapid miRNA downregulation contributes to the physiological responses (i.e., proliferation or migration) of a cell to EGF. Conversely, prior to their degradation, the miRNAs might prevent inappropriate activation of these targets in the absence of serum or EGF. However, it remains unclear whether EGF acts by inducing miRNA degradation or, analogously to the situation of miR-503, alters transcription or processing of inherently unstable miRNAs.

Neuronal activity

Strikingly, although rapid degradation affects only subsets of miRNAs in the examples discussed so far, it appears to be a prevailing feature of neurons [23]. Krol and colleagues found that the miRNA-cluster miR-183/96/182, as well as miR-204 and miR-211, are light-regulated in the mouse retina: when mice were shifted from light to dark, levels of these miRNAs fell to roughly 50% of the starting level within ~90 min, and then remained constant. However, like miR-503, the miRNA decay rate was not altered but invariably fast, and rapid decreases in miRNA levels upon dark adaptation were induced by transcriptional repression. Moreover, even miRNAs whose accumulation was not light-regulated (let-7b, miR-29c, miR-15, and miR-16) displayed fast turnover in retinas. However, they were not transcriptionally regulated and so their steady-state levels were unaffected by dark adaptation. Thus, fast miRNA turnover might be a general property of neurons. In support of this notion, non-differentiated mouse ES cells did not exhibit rapid turnover, whereas pyramidal neurons differentiated thereof did [23]. That turnover of miRNAs is generally fast in neurons is also in accordance with the earlier observations in primary human neuron cultures and postmortem human brain tissues that miRNA half-lives were not longer than 3.5 h for all of five tested miRNAs [24].

Notably, fast turnover of neuronal miRNAs is dependent on neuronal activity. Blocking action potentials by using tetrodotoxin or by blocking glutamate receptors prevented fast turnover [23]. However, miR-132, another miRNA that is enriched in neurons, showed the opposite behavior: blocking glutamate receptors activated its decay, whereas addition of glutamate slowed its decay [23].

Rapid downregulation of neuronal miRNAs was also observed in the sea slug *Aplysia californica*, for which treatment with the neurotransmitter serotonin resulted in a decrease of miR-124 and miR-184 levels with an apparent half-life of <3 h [25]. At this point, it is not known whether this finding reflects accelerated decay or decreased miRNA biogenesis rates for miRNAs displaying constitutively rapid decay. The serotonin-induced reduction of miR-124 levels was shown to contribute to learning-related synaptic plasticity, enhancing the switch from short- to long-term facilitation through derepression of the miR-124 target cAMP response element-binding protein 1 (CREB1).

Taken together, cell cycle progression, growth factor signaling, and neuronal activity were identified as physiological triggers affecting miRNA stability. A small set of miRNAs, including miR-141, was additionally reported to be rapidly downregulated upon seeding cells at low density, but recent work has now established that this as an artifact caused by differences in miR-141 extraction efficiency when Trizol reagent was used with different amounts of starting material [26].

In these different instances of rapid miRNA degradation, cis-acting elements have been mapped along the entire length of miRNAs: the seed region, central part, and the 3′-end (Table 1). As none of these motifs sufficed for rapid turnover, there appears to be a complex interplay between miRNA decay factors and different parts of a miRNA. It remains enigmatic how trans-acting turnover factors would access particular sequence motifs. Structural and chemical probing data suggest an unequal accessibility for trans-acting factors to different parts of an AGO-loaded miRNA [27,28]. Because both ends of an miRNA are anchored in specific binding pockets within AGO [29], they are likely to require release from AGO in order to become accessible for exonucleases. Interestingly, structural studies of bacterial AGO show that the 3′-end of a DNA guide strand is dislodged from its binding pocket upon binding to target RNA exhibiting extensive complementarity to the guide 3′-half [30]. The freed 3′-end might then become sensitive to nucleotidyl-transferases and 3′-to-5′ exonucleases, underpinning the emerging role of target RNAs as trans-acting regulators of miRNAs, a fact we discuss later.

We note that in the instances of rapid miRNA downregulation discussed thus far, several examples illustrate the use of constitutive miRNA destabilization to predispose some or all miRNAs of a cell to rapid expression level changes through modulation of their transcription or maturation [17,23]. However, there does not appear to be an inherent constraint against modulating miRNA decay rates [16], and we highlight additional examples in later sections.

Finally, in most of the examples we have discussed, determining the physiological relevance of rapid miRNA decay awaits further study. This is particularly true for the intriguing observation of globally accelerated miRNA decay in neurons. Similarly, identification of trans-acting factors that mediate constitutive or induced miRNA turnover in the studies discussed in this section remains a future challenge. However, different ribonucleases (RNases) have already been implicated in miRNA degradation, and we discuss these next.

miRNA-degrading enzymes

Several miRNA-degrading enzymes have been identified, including both 3′-to-5′ and 5′-to-3′ exoribonucleases, but so far no endoribonucleases (Figure 1). Distinct RNases were found to function in turnover of different sets of miRNAs

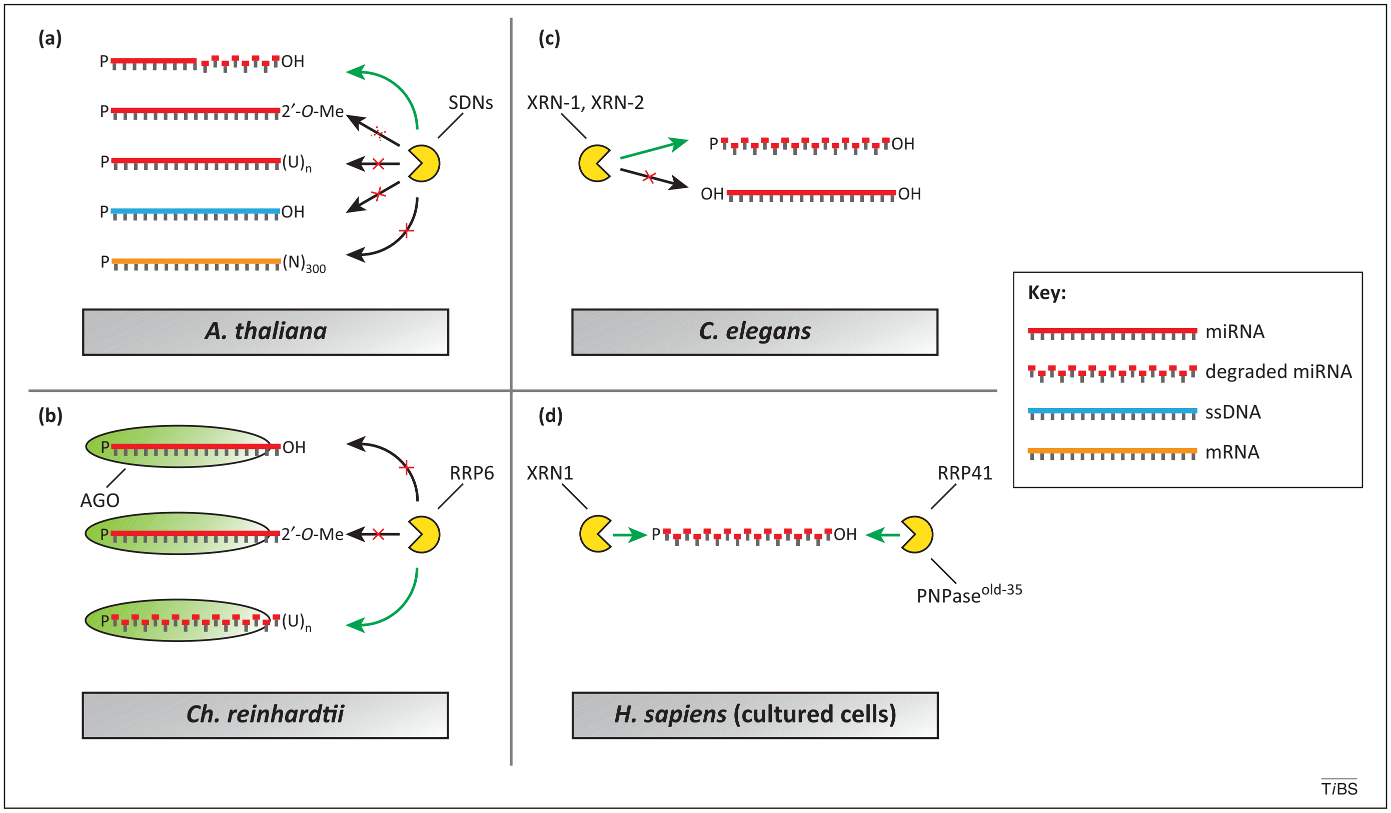

Figure 1. microRNA-degrading enzymes. Distinct enzymes have been implicated in miRNA turnover in various organisms. (**a**) In *Arabidopsis thaliana*, small RNA degrading nucleases (SDNs) degrade miRNAs containing a 3′-OH group yielding a product of 8–9 nt [31]. A 2′-*O*-Me group delays degradation kinetics and oligo-uridine tails render miRNAs degradation-insensitive. Single-stranded DNA (ssDNA; blue) or longer RNAs (orange) are also not targeted by SDNs. (**b**) In the green alga *Chlamydomonas reinhardtii*, ribosomal RNA processing protein 6 (RRP6) degrades Argonaute- (AGO-) loaded miRNAs containing oligo-uridine tails but not miRNAs containing an OH or 2′-*O*-Me group at the 3′-end [39]. RRP6 is proposed to function in a quality control mechanism, eliminating subfunctional small RNAs from AGO. (**c**) In *Caenorhabditis elegans*, exoribonuclease 2 (XRN-2) degrades miRNAs containing a 5′-monophosphate but not an OH group [42] and this is presumably also true for XRN-1 [41]. (**d**) In cultured human cells, ribosomal RNA processing protein 41 (RRP41) [47] and polynucleotide phosphorylase (PNPase^{old-35}) [48] degrade specific miRNAs in the 3′-to-5′ direction, whereas XRN1 [47] acts in the 5′-to-3′ direction. Green arrow: degradation permitted, black arrow with red cross: degradation inhibited.

and/or different organisms, but because these results are only from a small number of studies, substrate specificity and phylogenetic conservation of individual miRNA turnover enzymes remains largely unknown. For convenience, we will refer to miRNA degrading enzymes as 'miRNases', but we emphasize that the substrate spectrum of many or all of these RNases is likely, or in cases even known, to extend beyond miRNAs.

Arabidopsis thaliana*: the small RNA degrading nucleases (SDNs)*

Active degradation of miRNAs was initially reported in *Arabidopsis thaliana*, where it is mediated by the small RNA degrading nucleases (SDNs). The simultaneous depletion of all five SDN family members increased the levels of various miRNAs two- to threefold *in vivo*, and caused pleiotropic developmental phenotypes [31] (Figure 1a). SDNs are homologous to yeast Rex1/2/3/4p, which are involved in the 3′-end processing of rRNAs (yeast does not have miRNA) [32,33]. However, there is no evidence to support a function of plant SDNs in rRNA processing [31], and it is currently not known whether SDN-homologs in other eukaryotes, including animals, function in miRNA degradation.

Experiments with recombinant SDN1 and synthetic miRNAs have revealed that SDN1 uses a 3′-to-5′ exonucleolytic mechanism, yielding a final degradation product of 8–9 nt. SDN1 can degrade single-stranded RNA in the range of 17–27 nt with comparable efficiency, but not pre-miRNAs, longer RNAs, double-stranded RNA or single-stranded DNA. *In vivo*, plant miRNAs are 2′-*O*-methylated at their 3′-ends [34,35]; this feature slowed down but did not prevent miRNA degradation by SDN1 *in vitro* [31]. 2′-*O*-methylation by the methyltransferase HEN1 (HUA ENHANCER1) also stabilizes miRNAs *in vivo* by preventing 3′-end oligouridylation by HESO1 (HEN1 SUPPRESSOR1), a terminal nucleotidyl transferase [36,37]. However, because uridylation, at least *in vitro*, failed to promote and in fact attenuated SDN1-mediated degradation [31], it appears that uridylation influences miRNA degradation through distinct enzymes that remain to be identified. Interestingly, HEN1-mediated 2′-*O*-methylation also prevents uridylation and degradation of other classes of small RNAs, namely piRNAs in various animals and siRNAs in plants and *Drosophila* [38]. Nevertheless, it remains to be shown whether HEN1 is used as a physiological regulator of miRNA degradation.

Chlamydomonas reinhardtii*: MUT68 and RRP6*

Uridylation of miRNAs and siRNAs also contributes to their decay in the green alga *Chlamydomonas reinhardtii* [39]. The terminal nucleotidyl transferase MUT68 was found to uridylate the 3′-ends of these small RNAs *in vivo* and to stimulate their degradation by RRP6 (ribosomal RNA-processing protein 6), a component of the 3′-to-5′ exosome RNase complex, *in vitro* (Figure 1b). Furthermore, depletion of RRP6 elevated miRNA and siRNA levels *in vivo* [39]. The 2′-*O*-methyl group present on endogenous *C. reinhardtii* miRNAs prevented both uridylation and degradation *in vitro.*

Although *MUT68* mutation caused an accumulation of small RNAs, paradoxically, it also resulted in accumulation of an mRNA targeted by siRNA expressed from an inverted repeat transgene [39,40]. The interpretation of this finding is not straightforward, because MUT68 also adenylated the 5′ terminal product that resulted from siRNA-directed cleavage of this mRNA [40]. Hence, it has not been ruled out that stabilization of the full-length mRNA might be an indirect consequence of impaired clearance of its cleavage product. Nonetheless, a reasonable scenario proposed by Cerutti and colleagues [39] is that MUT68 and RRP6 define a quality control pathway that eliminates non-functional miRNAs, which might otherwise compete with functional miRNAs for access to AGO or other components of the miRNA machinery. Instead of contributing to general control of miRNA stability, HEN1 and HESO1 might then be part of an analogous quality control system in *Arabidopsis*.

Caenorhabditis elegans*: XRN-1 and XRN-2*

In the nematode *Caenorhabditis elegans*, the 5′-to-3′ exoribonucleases XRN-1/XRN1 and XRN-2/XRN2/Rat1p were shown to modulate miRNA activity through degradation [41,42] (Figure 1c). XRN1 and XRN2 are conserved across eukaryotes and have been implicated in exonucleolytic degradation and/or processing of various RNA substrates including rRNA, tRNA, small nucleolar (sno)RNA, pre-mRNA, and mRNA [43]. In *C. elegans*, RNAi-mediated depletion of *xrn-1* or *xrn-2* led to an accumulation of several mature miRNAs, whereas levels of pri- and pre-miRNA remained unchanged [41,42]. Depletion of *xrn-1* or *xrn-2* also suppressed mutant phenotypes, such as bursting through the vulva, that are associated with a point mutation in the seed sequence of the *let-7* miRNA. This mutation leads to a reduction of mature *let-7* miRNA levels by affecting its biogenesis [44] and/or stability [41], but *let-7* levels were restored by depletion of *xrn-1* or *xrn-2*. Diminished mRNA levels of the *let-7* targets *daf-12* and *lin-41* provide a molecular basis for the rescue of *let-7* mutant phenotypes by *xrn-2* depletion, and further demonstrate that XRN-2 targets actively repressing rather than scavenging non-functional miRNAs.

RNAi against *xrn-2* led to a $\geq$2-fold increase of nine out of 12 endogenous miRNAs tested *in vivo* [42]. Whether the lack of an effect on the remaining miRNAs reflects a true substrate specificity of XRN-2 or its inefficient depletion at specific times or in specific tissues remains to be determined. *In vitro*, each of four synthetic miRNAs that were tested was degraded irrespective of its sequence.

A few XRN co-factors involved in RNA degradation have been described. In yeast, processive RNA decay by Rat1p/Xrn2p requires binding of its co-factor Rai1p (RAT1 interacting protein). However, the metazoan Rai1p homolog Dom3Z (Downstream of MES-3 homolog Z) does not interact with XRN2 [45], leaving it unclear if metazoan XRN2 requires a processivity-stimulating co-factor. In mouse embryonic fibroblasts, XRN2 degrades 'non-targeting' siRNAs in complex with the endoplasmatic reticulum-resident protein NPGPx (non-selenocysteine containing phospholipid hydroperoxide glutathione peroxidase; or glutathione peroxidase GPX7) [46]. NPGPx expression was induced by stress from accumulation of siRNAs lacking cognate targets. Degradation of the siRNA by the

NPGPx/XRN2 complex appeared to release this stress. However, because the authors did not investigate miRNA levels and used high concentrations of non-targeting siRNAs in their experiments (20–160 nM), the relevance of murine NPGPx and XRN2 for physiological miRNA turnover remains unclear.

Humans: XRN1, RRP41, and PNPase$^{\text{old-35}}$

In human embryonic kidney (HEK293T) cells, Bail *et al.* implicated XRN1 and the exosome in miRNA turnover. Using microarrays to determine the levels of miRNAs following transcriptional shutoff by actinomycin D treatment, they found that 95% of miRNAs remained stable for at least 8 h [47]. Among the miRNAs with a half-life $<$8 h, miR-382 was verified by RT-qPCR (reverse transcription-quantitative polymerase chain reaction) to be unstable. Knock-down of RRP41 (ribosomal RNA-processing protein 41), a core component of the exosome complex, yielded a modest 1.5-fold increase in miR-382 levels (Figure 1d); a 1.3-fold increase was observed upon XRN1 knockdown. XRN2 depletion had no effect. A HEK293T cytoplasmic lysate was found to recapitulate rapid miR-382 turnover relative to a more stable miR-378 control miRNA, but only if the mature miRNA was derived from processing a pre-miRNA with Dicer-overexpressing lysate. By contrast, synthetic mature miR-378 and miR-382 decayed at equal rates. How *in vitro* processing contributes to destabilization of miR-382 remains unclear, but the coupled processing-degradation system permitted demonstration that the 3′-terminus, positions 16–22, was required for rapid decay of miR-382. How this element leads to accelerated decay and the functional relevance of miR-382 destabilization remain to be elucidated.

Finally, the human polynucleotide phosphorylase (PNPase$^{\text{old-35}}$; aka PNPT1 or polyribonucleotide nucleotidyltransferase 1, mitochondrial) degrades certain mature miRNAs in human melanoma cells without affecting pri- or pre-miRNA levels [48] (Figure 1d). PNPase$^{\text{old-35}}$ is an interferon (IFN)-inducible 3′-to-5′ exoribonuclease that has been implicated in the degradation of bacterial small non-coding RNAs [49] and IFN-induced growth arrest of human melanoma cells [50]. Microarray profiling of human melanoma cells highlighted the downregulation of several mature miRNAs (including miR-221, miR-222, and miR-106b) upon ectopic expression of PNPase$^{\text{old-35}}$. RT-qPCR and northern blotting further confirmed the downregulation of miR-221, miR-222, and miR-106b by ectopic or interferon-beta- (IFN-β-) induced expression of PNPase$^{\text{old-35}}$. The reduction in miR-221 and miR-222 levels was accompanied by an upregulation of p27$^{\text{kip1}}$, a validated target of these miRNAs [51]. Interestingly, miR-221 overexpression rendered human melanoma cells insensitive to IFN-β, supporting the notion that IFN-β-mediated growth arrest depends, at least partially, on miR-221 degradation. Of note, several miRNAs (including let-7a, miR-184, and miR-25) did not decrease upon ectopic expression of PNPase$^{\text{old-35}}$. When total RNA from HO-1 cells was incubated with *in vitro* translated PNPase$^{\text{old-35}}$, these same miRNAs were also refractory to degradation, whereas miR-221, miR-222, and miR-106b were sensitive. PNPase$^{\text{old-35}}$ might thus have inherent substrate specificity. PNPase $^{\text{old-35}}$ seems to be preferentially, and possibly exclusively, localized in the mitochondrial inner membrane space [52], therefore, an interesting question is where it degrades miRNAs.

In summary, several 5′-to-3′ and 3′-to-5′ miRNA-degrading enzymes have been identified (Figure 1). Although the miRNases described thus far are widely conserved proteins among eukaryotes, evidence for evolutionary conservation of miRNA turnover pathways has, in fact, not yet been produced. Difficulties in pinpointing orthologous miRNases might arise from (partially) redundant degradation pathways, as illustrated by the need to co-deplete several SDNs in *A. thaliana* to elicit a phenotype *in vivo* [31]. Individual studies also tended to focus on changes in the levels of one or only a few miRNAs, therefore, it is further conceivable that miRNase activity might have been missed due to substrate or tissue specificity. Lastly, several of these studies investigated phenotypes upon depletion of candidate RNases by RNAi rather than gene knockout. Residual RNase activity might thus hamper detection of miRNA turnover defects.

Although miRNases have now been shown to function in maintaining miRNA homeostasis in several organisms, it remains to be identified whether and how these enzymes are regulated. The human RNA-binding protein Quaking (QKI) has recently been shown to bind to and stabilize miR-20a, a function that appears to contribute to the tumor suppressive function of QKI in glioblastoma multiforme [53]. However, it remains unknown which RNase normally degrades miR-20a and how QKI mechanistically prevents degradation. More generally, we have little knowledge of factors that possibly convey processivity, substrate- or tissue-specificity to miRNases. However, recent work has revealed an important role of target RNAs in determining the stability of their cognate miRNAs.

Reversing a relation: regulatory functions of target RNAs on miRNAs

At the heart of miRNA-mediated mRNA regulation lies the sequence-specific interaction of the miRNA and the mRNA [54]. The extent of sequence complementarity between miRNA and mRNA determines the mode of mRNA silencing. Extensive complementarity, reminiscent of the siRNA–mRNA interaction, can result in endonucleolytic cleavage of the target mRNA, and constitutes a major means by which miRNAs regulate mRNAs in plants [55]. In metazoans, miRNAs base-pair with mRNAs mainly through partial complementarity, resulting in translational repression or exonucleolytic degradation [1]. Recent studies now provide evidence for reciprocal regulation, such that target RNAs can modulate miRNA stability (Figure 2). The degree of sequence complementarity appears be fateful for the miRNA as well.

Highly complementary targets can induce miRNA degradation in animals

In flies, mice, and human HeLa and HEK293T cells, miRNAs are destabilized if they are supplied with an artificial target exhibiting extensive complementarity [6,56,57] (Figure 2a). The decline of a miRNA in the presence of a highly complementary target is accompanied by the emergence of longer (‘tailed’; typically multiple [56] or individual

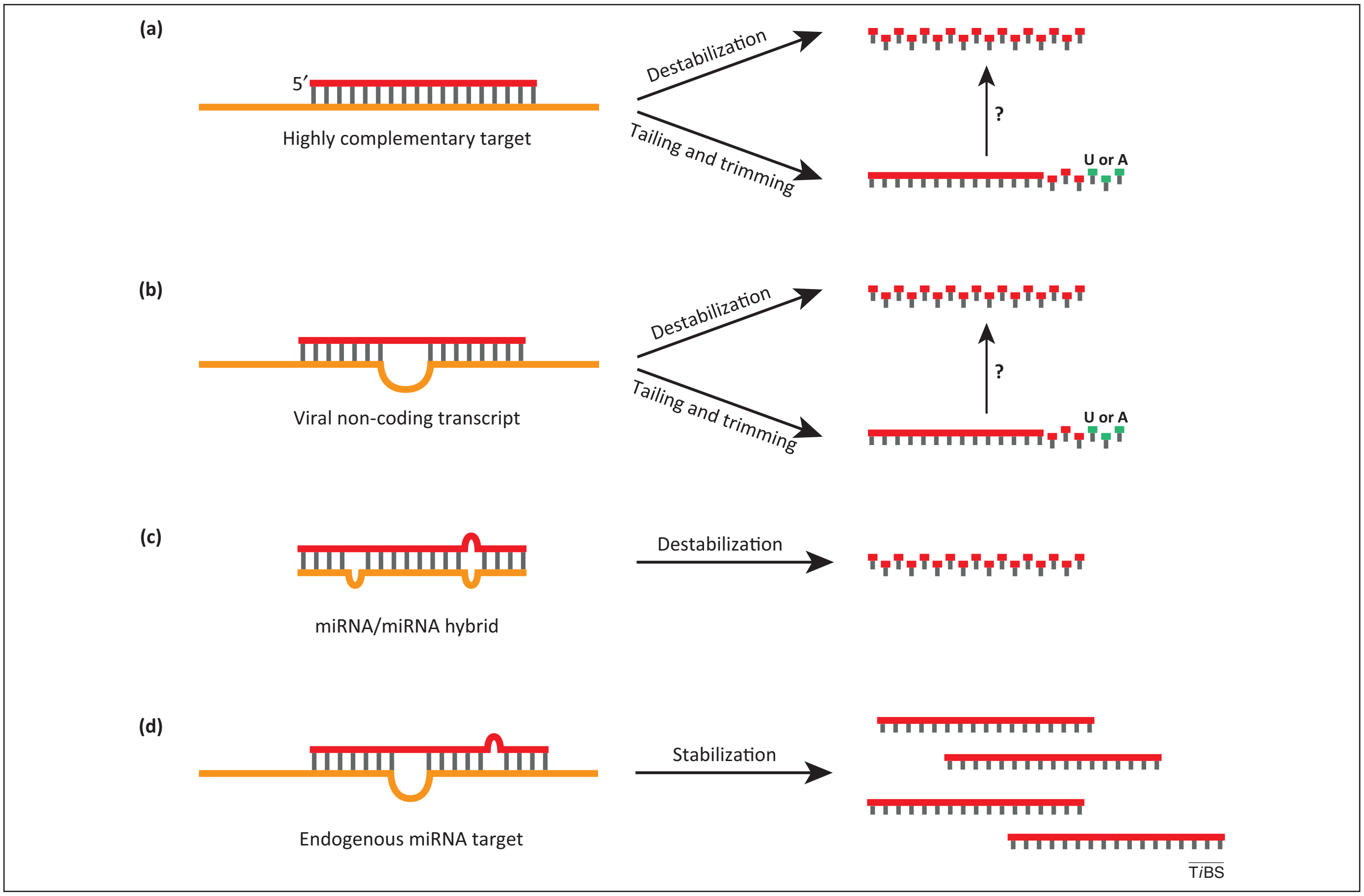

Figure 2. Effects of target RNAs on miRNAs. Target RNAs can stabilize or destabilize cognate miRNAs. (**a**,**b**) Highly complementary targets and viral non-coding transcripts lead to destabilization as well as tailing and trimming of miRNAs [6,56,57,60–62]. The tails (in green) consist predominantly of uridines and adenines. It is currently unknown if and how target-dependent tailing and trimming stimulates miRNA degradation. (**c**) A miRNA/miRNA hybrid has been shown to lead to destabilization of one of the two interacting strands (miR-107/let-7 in [64]). (**d**) Artificial and endogenous miRNA targets stabilize *Caenorhabditis elegans* miRNAs in a trimeric complex consisting of AGO, target, and miRNA [41].

[6,57] added uridines or adenosines) and shorter (‘trimmed’; [56,57]) species of the original miRNA. At this point, it is not known whether tailing precedes trimming, or rather defines a separate miRNA fate upon binding highly complementary targets. For instance, when Baccarini and colleagues turned off miR-223 transcription using a ‘tet-off’ system, levels of mono-uridylated species of miR-223 increased over time, relative to those of the unmodified miRNA [6]. This could mean that uridylation occurs prior to, and promotes, miR-223 degradation. Alternatively, uridylation might stabilize miR-223 so that it decays less rapidly than the unmodified species. Solving this issue will require the identification of the enzymes mediating tailing and trimming in a target-dependent manner. Although *Drosophila* Nibbler, a member of the DEDD family of exonucleases, trims the 3′-ends of some miRNAs by a few nucleotides [58,59], it does not appear to function in miRNA turnover.

Some degree of mismatching between miRNA and target RNA does not abolish tailing and trimming, and in particular base-pairing of the eight 3′ terminal nucleotides is dispensable [56]. However, miRNA ‘seed’ binding sites, that is, those with complementarity to nucleotides 2–8 of the miRNA only, do not induce tailing and trimming. Hence, because miRNA complementarity is limited to the seed for most endogenous targets [54], these targets will not usually induce miRNA degradation [56].

Viruses employ targets to destabilize host miRNAs

No endogenous cellular mRNA has been found to induce tailing and trimming in flies or mammals. By contrast, viruses exploit target-dependent miRNA destabilization to affect gene expression of host cells [60–62] (Figure 2b). In *Herpesvirus saimiri* (HVS) infected primate T cells, small non-coding HSUR RNAs (*H. saimiri* U-rich RNAs) bound to the partially complementary miR-142-3p, miR-27 (comprising miR-27a and miR-27b, which differ by one nucleotide), and miR-16 [60]. However, only miR-27, which base-pairs with HSUR 1, was destabilized by this interaction, causing an increase of FOXO1, a validated miR-27 target. By contrast, binding of HSURs to miR-142-3p or miR-16 did not alter their levels, perhaps due to less extensive base-pairing. How the virus benefits from miR-27 degradation remains unclear.

Similar to HVS, infection of mouse cells with murine cytomegalovirus (MCMV) induces the rapid downregulation of cellular miR-27 through an HSUR-unrelated viral mRNA, m169, which contains a miR-27 binding site in its 3′-UTR [61,62]. Despite hundreds of predicted miR-27-binding sites in the MCMV transcriptome, m169 is solely responsible for miR-27 degradation [61]. Moreover, expression of m169 3′-UTR in uninfected NIH 3T3 cells sufficed for miR-27 degradation, suggesting that no other viral factors are required for this process [62]. Marcinowski and colleagues found that miR-27 degradation was preceded by tailing and trimming, and that degradation and tailing and trimming alike were dependent on an intact miR-27 binding site in m169 [62]. However, 3′-end heterogeneity was observed for several miRNAs even in uninfected mouse cells, possibly suggesting that tailing and trimming also occurred in uninfected cells and that MCMV infection enhances this process specifically for miR-27 [62]. Although the mechanism by which miR-27 degradation facilitates viral infection is unknown, m169-mutant viruses that were unable to degrade miR-27 exhibited attenuated titers in various organs, strongly implying that degradation of miR-27 is important for efficient virus replication *in vivo* [62].

In *Drosophila* embryo lysates, tailing and trimming requires a high degree of complementarity between miRNA and target, such that a central loop of more than 3 nt impaired trimming [56]. By contrast, base-pairing between miR-27 and m169 involves a larger loop, and miR-27 degradation occurred, to a low extent, even with an m169 version carrying a point mutation in the 'seed-match' sequence [62]. It thus appears possible that the requirements for target-induced tailing and trimming might differ for different miRNAs or in different systems. For instance, depending on the thermodynamics of miRNA-target interaction, high expression levels of targets could be permissive for a lower degree of complementarity.

Target-induced miRNA degradation in plants

Unlike in animals, plant target mRNAs are frequently highly complementary to their cognate miRNAs. Moreover, there is precedence for the idea of tailing and trimming, which occurs in *A. thaliana* when 2′-*O*-methylation of small RNA 3′-termini is lost through mutation of *hen1* [34,35]. The tails almost exclusively consist of uridines and also occur on trimmed small RNAs [35]. Although it remains to be shown that endogenous targets can indeed induce plant miRNA degradation, artificial, highly complementary target RNAs containing two target sites were found to cause a severe reduction of cognate miRNA levels [63]. That primary miRNA levels did not decrease confirmed that the effect was post-transcriptional, and partial restoration of mature miRNA levels in *sdn1 sdn2* double mutant plants provided further evidence that targets acted by inducing miRNA degradation. However, as discussed earlier, SDNs are thought to be specific for single-stranded RNA, therefore, it is unclear how target binding could promote SDN-dependent miRNA degradation. It also remains possible that SDNs function in a parallel pathway; that is, their mutation restores miRNA levels by bypassing rather than reversing the miRNA-reducing effect of targets.

Destabilization of one miRNA by another

In human cancer cell lines, miR-107 can reduce the stability of mature let-7 miRNA, but not pri- or pre-let-7, via base-pairing interactions [64] (Figure 2c). Whereas ectopic expression of miR-107 decreased let-7 levels and enhanced the levels of the let-7 targets HMGA2 and RAS, depletion of endogenous miR-107 stabilized let-7 levels and reduced let-7 targets. In a mouse tumor model, let-7-dependent tumor suppression was abolished by transfection of miR-107 but not mutant versions thereof. Examination of mutant variants of let-7 and miR-107 suggested that miR-107-induced let-7 destabilization involved formation of a miR-107/let-7 duplex, but a mechanism remains to be determined. In this regard, it will be of particular interest to determine whether miR-107 is AGO-bound when interacting with let-7. It will also be interesting to determine whether other regulatory miRNA–miRNA interactions exist [65].

Stabilization of a miRNA through its targets

Contrasting with target-induced degradation of miRNAs, target mRNAs in *C. elegans* have been found to stabilize miRNAs *in vivo* by preventing their release from AGO proteins [41] (Figure 2d). Chatterjee *et al*. found that reduced availability of endogenous targets decreased accumulation of the cognate miRNAs, whereas miRNA levels increased in the presence of artificial target RNAs. This process, termed target-mediated miRNA protection (TMMP) counteracts miRNA decay mediated by XRN-1 and XRN-2. Together, miRNA decay and TMMP could thus serve as a proofreading mechanism that ensures preferential occupation of AGO with functional, that is, target-engaged miRNA.

Although miRNA* (also known as passenger; Box 1) strands are not normally loaded onto AGO proteins, miR-241* was stabilized when an artificial target RNA was provided *in vitro* or *in vivo* [41]. This effect may be limited to a subset of miRNA duplexes that, like miR-241:miR-241*, do not conform to the thermodynamic asymmetry rule for selection of the miRNA guide strand (Box 1). Nonetheless, it offers the possibility that TMMP might provide a way to drive evolution of new miRNAs by stabilizing previously unused miRNA* strands once targets, and thus potential biological functions, have been acquired. Such a mechanism might explain how the ratios of miR and miR* levels can vary in different tissues of an organism or during development [9,66,67].

In sum, target RNAs have been found to affect partially complementary miRNAs in various systems, causing either miRNA stabilization or destabilization. At this point, it remains unclear whether targets can mediate miRNA stabilization as well as destabilization in the same system, or whether these are distinct miRNA regulatory systems occurring in different organisms. Interestingly, Kuchen and colleagues observed that in mouse A70 proB and human HEK293T cells, expression of RNAs with eight or 16 highly complementary target sites, containing a four nucleotide central bulge, resulted in reduced accumulation for five out of six targeted miRNA passenger strands, and increased accumulation of one [66]. Although it was not investigated in these experiments whether the effects were related to mature miRNA turnover, the results emphasize a need for a detailed investigation of how target architecture, including the extent of complementarity, and expression levels of the target and/or its cognate miRNA determine the outcome of miRNA binding by target mRNA.

Box 2. Outstanding questions

- What are the (patho-)physiological functions of miRNA turnover processes? For instance, are there developmental processes or responses to environmental cues that rely on rapid miRNA turnover?
- Is there a 'major', widely conserved miRNA turnover pathway or do different miRNAs, cells, organisms, etc. rely on distinct miRNA degrading enzymes?
- Is miRNA turnover regulated and if so, how? How is specificity provided in situations where individual miRNAs are selectively degraded?
- To what extent and to what end do endogenous targets modulate miRNA levels? Are there specific 'regulatory' targets? Which factors decide the outcome of miRNA binding by targets, that is, stablization or destabilization? In particular, what is the contribution of target site architecture, target expression levels, and cell type or experimental system?
- Where does miRNA turnover occur within the cell? Is localization of the turnover machinery important for regulation of miRNA degradation, for example, by restricting access to specific substrates?

Concluding remarks

Although miRNAs were initially considered to be highly stable molecules, rapid and active miRNA degradation has now been demonstrated in many different organisms and experimental systems. Somewhat surprisingly, there appears to be a great diversity of miRNA degrading enzymes and, thus far, little evidence for conserved usage of individual enzymes across phylogeny. However, given that this field is still in its early days, further studies may force us to revise this view by revealing pathways that are used more broadly.

Degradation can be specific or affect large sets of miRNAs; however, it is currently largely unclear how specificity is achieved (Box 2). The use of target RNAs to modulate miRNA stability, positively or negatively, would provide an elegant solution, but it remains to be shown how widely this approach is used. For now, endogenous targets that alter miRNA levels are largely unknown. However, if targets were shown to broadly modulate miRNA levels, this would also challenge our current concept of miRNAs; rather than thinking of miRNA regulation as a one-way street leading to target mRNA silencing, we might need to consider a more complex network of mutual regulation of miRNAs and their targets.

Finally, miRNA turnover occurs widely in various organisms and systems, implying that it represents an important aspect of miRNA regulation. Indeed, the striking observation that miRNA turnover is generally accelerated in neurons strongly suggests a major role for this pathway in neuronal development, homeostasis, and/or function. Nonetheless, identification of the precise physiological function of miRNA turnover remains a major challenge in this as well as most other instances (Box 2).

Note added in proof

Eri1 (3′-to-5′ exoribonuclease 1) has recently been implicated in miRNA turnover in murine immune cells [69]. Previously, *C. elegans* mutant for *eri-1* had been found to accumulate siRNAs derived from exogenously supplied double-stranded RNA [70], although this may be a consequence of enhanced biogenesis rather than, or in addition to, impaired turnover of the siRNAs [71,72]. Thomas *et al.* now found that loss of Eri1 impaired mouse natural killer cell development, maturation and function. It also increased the levels of many miRNAs by approximately twofold in these, and to a lower extent in T-cells [69]. It remains to be determined if Eri1 alters mature miRNA levels directly, by degradation, and whether it is miRNA overexpression or some other consequence of Eri1 deficiency that causes the observed immune cell phenotypes.

Acknowledgments

We thank Stefan Ameres, Xuemei Chen, Bin Yu, and V. Narry Kim for sharing pre-prints. We are grateful to Nicolas Antih, Witold Filipowicz, Manuel de la Mata, Takashi Miki, and Hannes Richter for comments on the manuscript. S.R. was supported by a Boehringer Ingelheim Fonds PhD Fellowship. Work in the Großhans lab is funded by the Novartis Research Foundation, the Swiss National Science Foundation, and the European Research Council.

References

1 Djuranovic, S. *et al.* (2011) A parsimonious model for gene regulation by miRNAs. *Science* 331, 550–553
2 Bushati, N. and Cohen, S.M. (2007) microRNA functions. *Annu. Rev. Cell Dev. Biol.* 23, 175–205
3 Chang, T.C. and Mendell, J.T. (2007) microRNAs in vertebrate physiology and human disease. *Annu. Rev. Genomics Hum. Genet.* 8, 215–239
4 Krol, J. *et al.* (2010) The widespread regulation of microRNA biogenesis, function and decay. *Nat. Rev. Genet.* 11, 597–610
5 van Rooij, E. *et al.* (2007) Control of stress-dependent cardiac growth and gene expression by a microRNA. *Science* 316, 575–579
6 Baccarini, A. *et al.* (2011) Kinetic analysis reveals the fate of a microRNA following target regulation in mammalian cells. *Curr. Biol.* 21, 369–376
7 Lee, Y. *et al.* (2003) The nuclear RNase III Drosha initiates microRNA processing. *Nature* 425, 415–419
8 Gantier, M.P. *et al.* (2011) Analysis of microRNA turnover in mammalian cells following Dicer1 ablation. *Nucleic Acids Res.* 39, 5692–5703
9 Okamura, K. *et al.* (2008) The regulatory activity of microRNA* species has substantial influence on microRNA and 3′ UTR evolution. *Nat. Struct. Mol. Biol.* 15, 354–363
10 Kato, M. *et al.* (2009) Dynamic expression of small non-coding RNAs, including novel microRNAs and piRNAs/21U-RNAs, during *Caenorhabditis elegans* development. *Genome Biol.* 10, R54
11 Avril-Sassen, S. *et al.* (2009) Characterisation of microRNA expression in post-natal mouse mammary gland development. *BMC Genomics* 10, 548
12 Wang, J. *et al.* (2011) Deep small RNA sequencing from the nematode *Ascaris* reveals conservation, functional diversification, and novel developmental profiles. *Genome Res.* 21, 1462–1477
13 Martinez, N.J. *et al.* (2008) Genome-scale spatiotemporal analysis of *Caenorhabditis elegans* microRNA promoter activity. *Genome Res.* 18, 2005–2015
14 Lee, E.J. *et al.* (2008) Systematic evaluation of microRNA processing patterns in tissues, cell lines, and tumors. *RNA* 14, 35–42
15 Chen, D. *et al.* (2010) MicroRNA as a new player in the cell cycle. *J. Cell Physiol.* 225, 296–301
16 Hwang, H.W. *et al.* (2007) A hexanucleotide element directs microRNA nuclear import. *Science* 315, 97–100
17 Rissland, O.S. *et al.* (2011) MicroRNA destabilization enables dynamic regulation of the miR-16 family in response to cell-cycle changes. *Mol. Cell* 43, 993–1004
18 Avraham, R. *et al.* (2010) EGF decreases the abundance of microRNAs that restrain oncogenic transcription factors. *Sci. Signal* 3, ra43
19 Zhang, Z. *et al.* (2011) Uracils at nucleotide position 9-11 are required for the rapid turnover of miR-29 family. *Nucleic Acids Res.* 39, 4387–4395
20 Diederichs, S. and Haber, D.A. (2007) Dual role for argonautes in microRNA processing and posttranscriptional regulation of microRNA expression. *Cell* 131, 1097–1108

21 O'Carroll, D. *et al.* (2007) A Slicer-independent role for Argonaute 2 in hematopoiesis and the microRNA pathway. *Genes Dev.* 21, 1999–2004
22 Zhou, J.Y. *et al.* (2009) Analysis of microRNA expression profiles during the cell cycle in synchronized HeLa cells. *BMB Rep.* 42, 593–598
23 Krol, J. *et al.* (2010) Characterizing light-regulated retinal microRNAs reveals rapid turnover as a common property of neuronal microRNAs. *Cell* 141, 618–631
24 Sethi, P. and Lukiw, W.J. (2009) Micro-RNA abundance and stability in human brain: specific alterations in Alzheimer's disease temporal lobe neocortex. *Neurosci. Lett.* 459, 100–104
25 Rajasethupathy, P. *et al.* (2009) Characterization of small RNAs in Aplysia reveals a role for miR-124 in constraining synaptic plasticity through CREB. *Neuron* 63, 803–817
26 Kim, Y.K. *et al.* (2012) Short structured RNAs with low GC content are selectively lost during extraction from a small number of cells. *Mol. Cell* 46, 893–895
27 Wang, Y. *et al.* (2008) Structure of the guide-strand-containing argonaute silencing complex. *Nature* 456, 209–213
28 Lambert, N.J. *et al.* (2011) The conformation of microRNA seed regions in native microRNPs is prearranged for presentation to mRNA targets. *Nucleic Acids Res.* 39, 4827–4835
29 Sasaki, H.M. and Tomari, Y. (2012) The true core of RNA silencing revealed. *Nat. Struct. Mol. Biol.* 19, 657–660
30 Wang, Y. *et al.* (2009) Nucleation, propagation and cleavage of target RNAs in Ago silencing complexes. *Nature* 461, 754–761
31 Ramachandran, V. and Chen, X. (2008) Degradation of microRNAs by a family of exoribonucleases in *Arabidopsis*. *Science* 321, 1490–1492
32 van Hoof, A. *et al.* (2000) Three conserved members of the RNase D family have unique and overlapping functions in the processing of 5S, 5.8S, U4, U5, RNase MRP and RNase P RNAs in yeast. *EMBO J.* 19, 1357–1365
33 Faber, A.W. *et al.* (2004) The RNA catabolic enzymes Rex4p, Rnt1p, and Dbr1p show genetic interaction with trans-acting factors involved in processing of ITS1 in Saccharomyces cerevisiae pre-rRNA. *RNA* 10, 1946–1956
34 Yu, B. *et al.* (2005) Methylation as a crucial step in plant microRNA biogenesis. *Science* 307, 932–935
35 Li, J. *et al.* (2005) Methylation protects miRNAs and siRNAs from a 3′-end uridylation activity in *Arabidopsis*. *Curr. Biol.* 15, 1501–1507
36 Zhao, Y. *et al.* (2012) The *Arabidopsis* nucleotidyl transferase HESO1 uridylates unmethylated small RNAs to trigger their degradation. *Curr. Biol.* 22, 689–694
37 Ren, G. *et al.* (2012) Uridylation of miRNAs by *hen1 suppressor 1* in *Arabidopsis*. *Curr. Biol.* 22, 695–700
38 Ji, L. and Chen, X. (2012) Regulation of small RNA stability: methylation and beyond. *Cell Res.* 22, 624–636
39 Ibrahim, F. *et al.* (2010) Uridylation of mature miRNAs and siRNAs by the MUT68 nucleotidyltransferase promotes their degradation in Chlamydomonas. *Proc. Natl. Acad. Sci. U.S.A.* 107, 3906–3911
40 Ibrahim, F. *et al.* (2006) Untemplated oligoadenylation promotes degradation of RISC-cleaved transcripts. *Science* 314, 1893
41 Chatterjee, S. *et al.* (2011) Target-mediated protection of endogenous microRNAs in *C. elegans*. *Dev. Cell* 20, 388–396
42 Chatterjee, S. and Grosshans, H. (2009) Active turnover modulates mature microRNA activity in *Caenorhabditis elegans*. *Nature* 461, 546–549
43 Chang, J.H. *et al.* (2011) 5′-3′-Exoribonucleases. In *Ribonucleases* (Nicholson, A., ed.), pp. 167–192, Springer
44 Zisoulis, D.G. *et al.* (2012) Autoregulation of microRNA biogenesis by let-7 and Argonaute. *Nature* 486, 541–544
45 Xiang, S. *et al.* (2009) Structure and function of the 5′→3′ exoribonuclease Rat1 and its activating partner Rai1. *Nature* 458, 784–788
46 Wei, P.C. *et al.* (2012) Non-targeting siRNA induces NPGPx expression to cooperate with exoribonuclease XRN2 for releasing the stress. *Nucleic Acids Res.* 40, 323–332
47 Bail, S. *et al.* (2010) Differential regulation of microRNA stability. *RNA* 16, 1032–1039
48 Das, S.K. *et al.* (2010) Human polynucleotide phosphorylase selectively and preferentially degrades microRNA-221 in human melanoma cells. *Proc. Natl. Acad. Sci. U.S.A.* 107, 11948–11953
49 Andrade, J.M. and Arraiano, C.M. (2008) PNPase is a key player in the regulation of small RNAs that control the expression of outer membrane proteins. *RNA* 14, 543–551
50 Sarkar, D. *et al.* (2006) Defining the mechanism by which IFN-beta dowregulates c-myc expression in human melanoma cells: pivotal role for human polynucleotide phosphorylase (hPNPaseold-35). *Cell Death Differ.* 13, 1541–1553
51 Galardi, S. *et al.* (2007) miR-221 and miR-222 expression affects the proliferation potential of human prostate carcinoma cell lines by targeting p27Kip1. *J. Biol. Chem.* 282, 23716–23724
52 Chen, H.W. *et al.* (2007) Human polynucleotide phosphorylase: location matters. *Trends Cell Biol.* 17, 600–608
53 Chen, A.J. *et al.* (2012) STAR RNA-binding protein Quaking suppresses cancer via stabilization of specific miRNA. *Genes Dev.* 26, 1459–1472
54 Bartel, D.P. (2009) MicroRNAs: target recognition and regulatory functions. *Cell* 136, 215–233
55 Jones-Rhoades, M.W. *et al.* (2006) MicroRNAS and their regulatory roles in plants. *Annu. Rev. Plant Biol.* 57, 19–53
56 Ameres, S.L. *et al.* (2010) Target RNA-directed trimming and tailing of small silencing RNAs. *Science* 328, 1534–1539
57 Xie, J. *et al.* (2012) Long-term, efficient inhibition of microRNA function in mice using rAAV vectors. *Nat. Methods* 9, 403–409
58 Han, B.W. *et al.* (2011) The 3′-to-5′ exoribonuclease Nibbler shapes the 3′ ends of microRNAs bound to *Drosophila* Argonaute1. *Curr. Biol.* 21, 1878–1887
59 Liu, N. *et al.* (2011) The exoribonuclease Nibbler controls 3′ end processing of microRNAs in Drosophila. *Curr. Biol.* 21, 1888–1893
60 Cazalla, D. *et al.* (2010) Down-regulation of a host microRNA by a Herpesvirus saimiri noncoding RNA. *Science* 328, 1563–1566
61 Libri, V. *et al.* (2012) Murine cytomegalovirus encodes a miR-27 inhibitor disguised as a target. *Proc. Natl. Acad. Sci. U.S.A.* 109, 279–284
62 Marcinowski, L. *et al.* (2012) Degradation of cellular mir-27 by a novel, highly abundant viral transcript is important for efficient virus replication in vivo. *PLoS Pathog.* 8, e1002510
63 Yan, J. *et al.* (2012) Effective small RNA destruction by the expression of a short tandem target mimic in *Arabidopsis*. *Plant Cell* 24, 415–427
64 Chen, P.S. *et al.* (2011) miR-107 promotes tumor progression by targeting the let-7 microRNA in mice and humans. *J. Clin. Invest.* 121, 3442–3455
65 Lai, E.C. *et al.* (2004) Complementary miRNA pairs suggest a regulatory role for miRNA:miRNA duplexes. *RNA* 10, 171–175
66 Kuchen, S. *et al.* (2010) Regulation of microRNA expression and abundance during lymphopoiesis. *Immunity* 32, 828–839
67 Chiang, H.R. *et al.* (2010) Mammalian microRNAs: experimental evaluation of novel and previously annotated genes. *Genes Dev.* 24, 992–1009
68 Fabian, M.R. and Sonenberg, N. (2012) The mechanics of miRNA-mediated gene silencing: a look under the hood of miRISC. *Nat. Struct. Mol. Biol.* 19, 586–593
69 Thomas, M.F. *et al.* (2012) Eri1 regulates microRNA homeostasis and mouse lymphocyte development and antiviral function. *Blood* 120, 130–142
70 Kennedy, S. *et al.* (2004) A conserved siRNA-degrading RNase negatively regulates RNA interference in *C. elegans*. *Nature* 427, 645–649
71 Duchaine, T.F. *et al.* (2006) Functional proteomics reveals the biochemical niche of *C. elegans* DCR-1 in multiple small-RNA-mediated pathways. *Cell* 124, 343–354
72 Lee, R.C. *et al.* (2006) Interacting endogenous and exogenous RNAi pathways in *Caenorhabditis elegans*. *RNA* 12, 589–597

3.3 Results and Discussion

3.3.1 Publication: “Engineering of a Conditional Allele Reveals Multiple Roles of XRN2 in *Caenorhabditis elegans* Development and Substrate Specificity in MicroRNA Turnover”

Nucleic Acids Research Advance Access published January 20, 2014

Nucleic Acids Research, 2014, ***1–12***
doi:10.1093/nar/gkt1418

Engineering of a conditional allele reveals multiple roles of XRN2 in *Caenorhabditis elegans* development and substrate specificity in microRNA turnover

Takashi S. Miki[1], Stefan Rüegger[1,2], Dimos Gaidatzis[1,3], Michael B. Stadler[1,3] and Helge Großhans[1,*]

[1]Friedrich Miescher Institute for Biomedical Research, Maulbeerstrasse 66, CH-4058 Basel, Switzerland, [2]University of Basel, Petersplatz 1, CH-4003 Basel, Switzerland and [3]Swiss Institute of Bioinformatics, Maulbeerstrasse 66, CH-4058 Basel, Switzerland

Received October 28, 2013; Revised December 20, 2013; Accepted December 24, 2013

ABSTRACT

Although XRN2 proteins are highly conserved eukaryotic 5′→3′ exonucleases, little is known about their function in animals. Here, we characterize *Caenorhabditis elegans* XRN2, which we find to be a broadly and constitutively expressed nuclear protein. An *xrn-2* null mutation or loss of XRN2 catalytic activity causes a molting defect and early larval arrest. However, by generating a conditionally mutant *xrn-2ts* strain *de novo* through an approach that may be also applicable to other genes of interest, we reveal further functions in fertility, during embryogenesis and during additional larval stages. Consistent with the known role of XRN2 in controlling microRNA (miRNA) levels, we can demonstrate that loss of XRN2 activity stabilizes some rapidly decaying miRNAs. Surprisingly, however, other miRNAs continue to decay rapidly in *xrn-2ts* animals. Thus, XRN2 has unanticipated miRNA specificity *in vivo*, and its diverse developmental functions may relate to distinct substrates. Finally, our global analysis of miRNA stability during larval stage 1 reveals that miRNA passenger strands (miR*s) are substantially less stable than guide strands (miRs), supporting the notion that the former are mostly byproducts of biogenesis rather than a less abundant functional species.

INTRODUCTION

XRN2 proteins constitute a family of eukaryotic 5′→3′ exoribonucleases that have various RNA substrates (1). For instance, in yeast, where XRN2 has been particularly well studied and is commonly known as Rat1p, it is involved in processing of ribosomal RNAs and small nucleolar RNAs (2–6), transcriptional termination (7) and degradation of aberrant transfer RNAs (8), among other functions. The diversity of substrates *in vivo* is reflected by relaxed substrate specificity *in vitro* where Rat1p processively degrades 5′ monophosphorylated RNAs that lack strong secondary structures to mononucleotides (9,10). The catalytic site of XRN2/Rat1p contains seven acidic amino acids, which form a pocket for a divalent cation (Mg^{2+} or Mn^{2+}) required for the exoribonuclease activity (11).

A paralogous enzyme, Xrn1p, exists in the yeast cytoplasm (12), where it is involved in degradation of decapped mRNAs (13). Single orthologues of XRN1 and XRN2, respectively, are also found in animals, and it is assumed that distinct localization and the resulting division of labor that characterize yeast Xrn1p and Rat1p (14) also apply to their orthologues in other organisms, although this has not yet been investigated systematically. A nuclear localization signal present in Rat1p is not conserved in XRN2 orthologues of other species (14), but nuclear RNAs such as pre-mRNAs and 5.8S and 18S ribosomal RNAs have been reported as common substrates of XRN2 in yeast and other species [reviewed in (15)]

Downloaded from http://nar.oxfordjournals.org/ at Novartis Forschungsstiftung / Friedrich Miescher Institute on January 20, 2014

---

[*] To whom correspondence should be addressed. Tel: +41 61 697 6580; Fax: +41 61 697 3976; Email: helge.grosshans@fmi.ch

The authors wish it to be known that, in their opinion, the first two authors should be regarded as Joint First Authors.

© The Author(s) 2014. Published by Oxford University Press.
This is an Open Access article distributed under the terms of the Creative Commons Attribution Non-Commercial License (http://creativecommons.org/licenses/by-nc/3.0/), which permits non-commercial re-use, distribution, and reproduction in any medium, provided the original work is properly cited. For commercial re-use, please contact journals.permissions@oup.com

In *Caenorhabditis elegans*, the single XRN2-type protein was found to function in degradation of mature microRNAs (miRNAs) (16). These short (~22 nt) non-coding RNAs are derived from longer precursor transcripts, from which two successive processing steps release a ~22 nt duplex RNA consisting of an miRNA guide (miR) bound to an miRNA passenger (miR*) strand (17). This duplex is loaded onto an Argonaute protein and the guide strand retained, whereas the passenger strand is released and presumably discarded. The designation of miR and miR* was initially based on their relative abundance, with the more abundant strand assumed functional and thus designated miR. However, individual miR*s have also been shown to be functional [reviewed in (18)], so that in recent times the use of two suffixes indicating the 'arm' of the precursor transcript from which an miRNA is derived, i.e. −3p or −5p, has become more common. At any rate, miRNA-Argonaute complexes can bind to partially complementary sequences in 3′-untranslated regions (3′-UTRs) of mRNAs to repress their translation and induce their degradation (19). They thus regulate a large number of genes, affording them, as a class, important roles in animal development and pathology (20).

Two lines of evidence support a function of XRN2 in the degradation of mature miRNAs (16). First, *C. elegans* lysates containing wild-type levels of XRN2 were more active in decay of naked synthetic and Argonaute-associated miRNAs than XRN2-depleted lysates. Second, depletion of XRN2 by RNA interference (RNAi) yielded increased steady-state levels of a number of endogenous miRNAs. In these latter experiments, however, the levels of some miRNAs were unchanged. Because RNAi may be inefficient in certain tissues or at certain times, it remained unknown whether this reflected true substrate specificity or a technical limitation of the experiment.

Despite prominent molecular functions, the roles of XRN2 in animal development largely remain to be explored (15). In mice and humans, over-expression of XRN2 has been implicated as a risk factor for a specific type of lung cancer (21), but a molecular basis remains to be established. In *C. elegans*, XRN2, encoded by the *xrn-2* gene, was found in a genome-wide RNAi screen for factors involved in molting (22), the process in which worms synthesize a new and shed their old cuticle. Molting occurs once at the end of each of the four larval stages, L1 through L4, (23) and Frand *et al.* (22) found that *xrn-2* depleted animals were unable to shed the cuticle from the pharynx at the final (L4) molt. Consistent with this phenotype, a putative *xrn-2* promoter, with only limited spatial activity as assayed by a Green Fluorescent Protein (GFP) reporter, was active in myoepithelial cells that secrete the pharyngeal cuticle (22). Promoter activity also occurred in other cells implicated in molting, including a particular pharyngeal neuron and intestinal cells. How XRN2 affects molting is unknown, although this function may involve regulation of expression of MoLTing Defective 10 (MLT-10), another molting factor, in a direct or indirect manner, through an unknown mechanism. RNAi against *xrn-2* also causes slow growth and sterility (16), but again the basis of these phenotypes remains unknown.

To obtain a better understanding of the developmental functions of XRN2 and its role in miRNA turnover, we have characterized *xrn-2* null mutant *C. elegans*. We find that these animals arrest at the L2 stage, following a failed molt from the L1 to the L2 stage. The unanticipated ability to complete embryogenesis was not due to the absence of an essential embryonic function of XRN2, but reflected masking of the null phenotype due to maternal contribution. We demonstrate this through an *xrn-2ts* allele, which we generated by transplanting conditional mutations from yeast to *C. elegans*. We can thus show that XRN2 is essential during several stages of *C. elegans* development, including embryogenesis. These broader functions are consistent with a revised picture of *xrn-2* expression that we obtained using a rescuing transgene and detection of the endogenous protein by western blotting. Using small RNA deep sequencing to determine miRNA decay rates, we find that miR*s are generally less stable than miRs. Strikingly, among the small group of unstable miRs, only some become stabilized by inactivation of XRN2. We conclude that XRN2 has unanticipated miRNA substrate specificity *in vivo* and diverse developmental functions.

MATERIALS AND METHODS

Strains

Caenorhabditis elegans strains were cultured by standard methods described previously (24). The Bristol N2 strain was used as wild-type. Animals heterozygous for *xrn-2(tm3473)* were obtained from Dr Shohei Mitani, backcrossed three times and balanced. Strains used are shown in Supplementary Table S1.

Cloning and site-directed mutagenesis

Cloning and site-directed mutagenesis were performed by PfuUltra II Fusion HS DNA Polymerase (Agilent Technologies, Santa Clara, CA, USA) according to the supplier's protocol using specific primers (Supplementary Table S2). The codon-optimized *xrn-2* with three artificial introns (Supplementary Table S3) was designed according to a previous report (25) and synthesized using a commercial service (GenScript, Piscataway, NJ, USA).

Single-copy transgene insertion

DNA fragments were inserted into pCFJ210 (for chromosome I) or pCFJ201 (for chromosome IV) vectors by Multisite Gateway Technology (Life Technologies, Carlsbad, CA, USA) according to the supplier's protocol. Mos1-mediated single-copy transgene insertion was performed according to previous reports (26,27). Following confirmation of correct insertion by polymerase chain reaction (PCR), transgenic strains were backcrossed at least three times to the N2 strain.

Multicopy transgene arrays

The multisite gateway cloning system (Invitrogen) was used to insert transgenes into the pCG150 destination vector (containing *unc-119* rescuing fragment), which

Downloaded from http://nar.oxfordjournals.org/ at Novartis Forschungsstiftung / Friedrich Miescher Institute on January 20, 2014

was transformed into young adult *unc-119(ed3)* worms by microparticle bombardment using the Biolistic PDS-1000/He particle delivery system (BioRad) (28). For each bombardment, 16 µl of 0.5 µg/µl pCG150 and 4 µl of 0.8 µg/µl pCFJ90 (co-injection marker containing Pmyo-2::mCherry) were coupled to 1-µm microcarrier gold beads (BioRad, Cat#165-2263). Worms were allowed to recover for 1 h at 15°C after bombardment and were then grown at 25°C on NG 2% plates seeded with OP50 bacteria for ca. 2 weeks before screening for wild-type moving worms and mCherry-fluorescence from the co-injection marker. Transgenes containing wild-type or D234A-D236A double mutant *xrn-2* sequences were stably transmitted and expressed in the germline, suggesting integration into the genome.

Antibodies and western blotting

Recombinant full-length *C. elegans* XRN2 was prepared as described (16) and used to immunize rats (Charles River Laboratories, Kisslegg, Germany), to obtain an anti-XRN2 antibody. A mouse monoclonal anti-actin antibody (clone C4) was purchased from Millipore (Billerica, MA, USA). The anti-XRN2 antibody and anti-actin antibody were used with 1000- and 3000-fold dilutions, respectively, followed by horseradish peroxidase-conjugated secondary antibody (GE Healthcare, Little Chalfont, UK) reaction. The membranes were treated with ECL Western Blotting Detection Reagents, and protein bands were detected using Amersham Hyperfilm ECL (Figure 3C) or by an ImageQuant LAS 4000 hemiluminescence imager (all GE Healthcare) (Figure 4C). Band intensities were quantified using the ImageJ software (NIH, Bethesda, MD, USA).

Microscopy

Differential Interference Contrast (DIC) and fluorescent images were obtained using an Axio Observer Z1 microscope and AxioVision SE64 (release 4.8) software (Carl Zeiss, Oberkochen, Germany). Stereoscopic images were obtained by M205 A stereo microscope (Leica, Solms, Germany).

RNA preparation, sequencing and RT-qPCR

Gravid N2 or *xrn-2ts* worms were treated with bleaching solution [30% sodium hypochlorite (5% chlorine) reagent (Thermo Fisher Scientific, Waltham, MA, USA), 750 mM potassium hydroxide] to extract eggs, which were then incubated in M9 medium overnight to hatch. The resulting synchronized L1 larvae were cultured with *Escherichia coli* OP50 in S-medium supplemented with trace metal solution (29) at a concentration of 1×10^4 worms/ml with shaking (180 rpm) at 25°C for 2 h. Subsequently, α-amanitin (Sigma-Aldrich, St. Louis, MO, USA) was added to a final concentration of 50 µg/ml, which blocks transcription and stalls larval development (Supplementary Figure S2). A total of 1.5×10^4 worms were harvested at each sampling time point during the next 8 h, washed three times with M9 medium, resuspended in 700 µl of TRIzol reagent (Life Technologies) and frozen in liquid nitrogen. Worms were broken open by five repeats of freeze and thaw using liquid nitrogen and a 42°C heating block, before RNA was extracted and purified according to the supplier's protocol with the modification that RNA was incubated with 50% 2-propanol at −80°C overnight for efficient precipitation of small RNA.

Small RNA (15–30 nt) libraries were prepared from extracted total RNA using TruSeq Small RNA Sample Prep Kit (Illumina, San Diego, CA, USA) according to the supplier's protocol. All samples were multiplexed and 13 pM of the multiplexed libraries sequenced on two lanes of an Illumina HiSeq 2000 instrument using RTA 1.13.48. Individual reads were assigned to their sample based on the TruSeq barcode using the Illumina software Casava v1.8.0.

Quantification of individual miRNAs by reverse transcription-quantitative polymerase chain reaction (RT-qPCR) was done using TaqMan MicroRNA Assays (Life Technologies) and StepOnePlus Real-time PCR Systems (Applied Biosystems, Foster City, CA, USA) according to the suppliers' protocols. Forty nanogram of total RNA was used as a template for reverse transcription reaction (15 µl), and 1.3 µl of the reaction was used for qPCR reaction (25 µl). The miRNA levels were normalized to the small nucleolar RNA sn2841 levels.

For mRNA quantification, complementary DNA (cDNA) was generated from total RNA by ImProm-II Reverse Transcription System (Promega, Fitchburg, WI, USA) using oligo(dT)$_{15}$ primers (for Figure 4D) or random primers (for Supplementary Figure S2B, C) according to the supplier's protocol. RT-qPCR was performed with specific primers (Supplementary Table S2), a SYBR Green PCR Master Mix (Applied Biosystems) and a StepOnePlus Real-time PCR System. Primer sequences for pre-eft-3 mRNA and 18S ribosomal RNA were taken from (30) and (31), respectively.

Analysis of the miRNA sequencing data

For each read, the 3′ adaptor TGGAATTCTCGGGTGCCAAGG was removed by aligning it to the read allowing one or two mismatches in prefix alignments of at least 7 or 10 bases, respectively. Reads with low complexity were filtered out based on their dinucleotide entropy (removing <1% of the reads). Only reads with a minimum length of 14 nt were retained. Alignments to the miRNA database miRBase release 18 (http://www.mirbase.org/) were performed by the software bowtie (version 0.9.9.1) (32) with parameters -v 2 -a -m 100, tracking up to 100 best alignment positions per query and allowing at most two mismatches. Reads that mapped to a miRNA but at the same time also mapped with fewer mismatches to the genome (ce6) were filtered out. The expression of each miRNA was determined by counting the number of associated reads. To compensate for differences in the read depths of the individual libraries, each sample was divided by its total number of counts and multiplied by the average sample size. The resulting values were $\log_2$ transformed using a pseudo-count of 1 ($y = \log_2(x+1)$). To obtain relative decay rates for the time window $t = 1$ h to $t = 8$ h, the change in expression of

Downloaded from http://nar.oxfordjournals.org/ at Novartis Forschungsstiftung / Friedrich Miescher Institute on January 20, 2014

each miRNA over time was determined by the slope of a linear fit performed in R (www.r-project.org). Slopes for the two replicates were calculated separately and then averaged for further use.

Release 18 of miRBase does no longer provide identifiers that label a miRNA as a mature or a star form. We thus identified the star forms by firstly pairing the 5p and 3p forms using the miRNA name (without the −5p and −3p extensions) and then assigning the star label to the form with the lower expression level in the untreated sample.

Determination of miRNA half-life

We assumed miRNAs to decay exponentially according to the following equation:

$$N(t) = N_0 \cdot 2^{-t/\tau}$$

where t is the time, $N(t)$ is the concentration of the miRNA at time point t, N_0 is the starting concentration and τ is the half-life of the miRNA.

From this follows a linear relationship between the logarithmic concentration (measured as delta-Ct values) and the half-time τ:

$$log_2(N(t)) = (-1/\tau) \cdot t + log_2(N_0)$$

τ can be obtained from the slope of a linear regression by the following equation:

$$\tau = -1/slope$$

The intercept term captures differences in the starting concentration; for visualization, the term was subtracted from delta-Ct values.

The miRNA half-lives were calculated for individual replicate experiments. The half-life of stable miRNAs that decreased <20% (the detection limit) over the course of the 8-h experiment was set to 30 h, which is the τ resulting from a 20% decrease in 8 h and corresponds to a lower limit estimate for the half-life of such miRNAs.

The significance of differences in half-lives between worm strains was calculated using a two sample *t*-test assuming equal variances.

RESULTS

tm3473 is a *bona fide* null allele of *xrn-2*

Previous studies on *xrn-2* mutant phenotypes relied on its depletion by RNAi (16,22). However, knock-down of genes by RNAi is usually incomplete and may vary across tissues. Therefore, we set out to characterize the *xrn-2* mutant *xrn-2(tm3473)*, provided by Dr Shohei Mitani. The *tm3473*-allele is a deletion of 278 bases in exon 3 leading to a frame shift at amino acid position 278 and a premature stop codon at position 308 (Figure 1A). Western blotting using an antibody against XRN2 confirmed absence of full-length XRN2 protein in the *xrn-2(tm3473)* background (Figure 1B). This strain, and a wild-type strain included for comparison, contains a transgene to express full-length GFP-tagged XRN2 to achieve wild-type development (see later in the text). We also failed to detect a band corresponding to the predicted size of a potential truncated translation product (data not shown). Although we cannot formally exclude that the polyclonal antiserum that we used would fail to

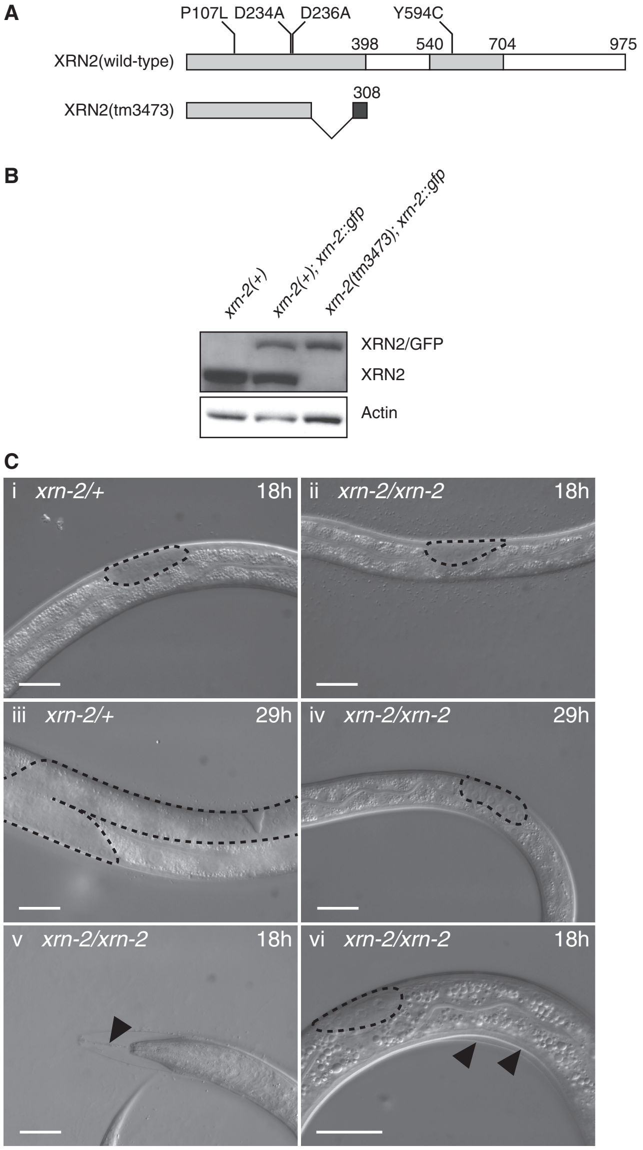

Figure 1. *xrn-2(tm3473)* is a *bona fide* null allele that causes molting defects and developmental arrest. (**A**) Schematic representation of wild-type and mutant XRN2. Conserved regions are shown in light grey. Dark grey indicates sequence unique to the *xrn-2(tm3473)* mutant due to a frame shift. Point mutations investigated in this study are indicated. (**B**) Western blotting confirms absence of endogenous XRN2 in the *xrn-2(tm3473)* background (lane 3). *xrn-2(+)* denotes the N2 wild-type strain. Note the presence of an XRN2/GFP-encoding transgene in the strains shown in lane 2 and 3, used to restore development of the *xrn-2(tm3473)* mutant strain. (**C**) DIC micrographs of worms grown at 25°C; gonads are outlined to facilitate staging. (i, ii) After 18 h, both *xrn-2/+* (*tm3473* heterozygous) and *xrn-2/xrn-2* (*tm3473* homozygous) worms are at the L2 stage. (iii, iv) After 29 h, *xrn-2/xrn-2* worms remain arrested at the L2 stage (iv), whereas the heterozygous siblings have reached the L4 stage (iii). (v, vi) Larval arrest is accompanied by molting defects. *xrn-2/xrn-2* worms are unable to shed the pharyngeal cuticle (v, arrow head), which leads to superposition of the old and newly synthesized cuticle (vi, arrow heads). Scale bar, 20 µm.

Downloaded from http://nar.oxfordjournals.org/ at Novartis Forschungsstiftung / Friedrich Miescher Institute on January 20, 2014

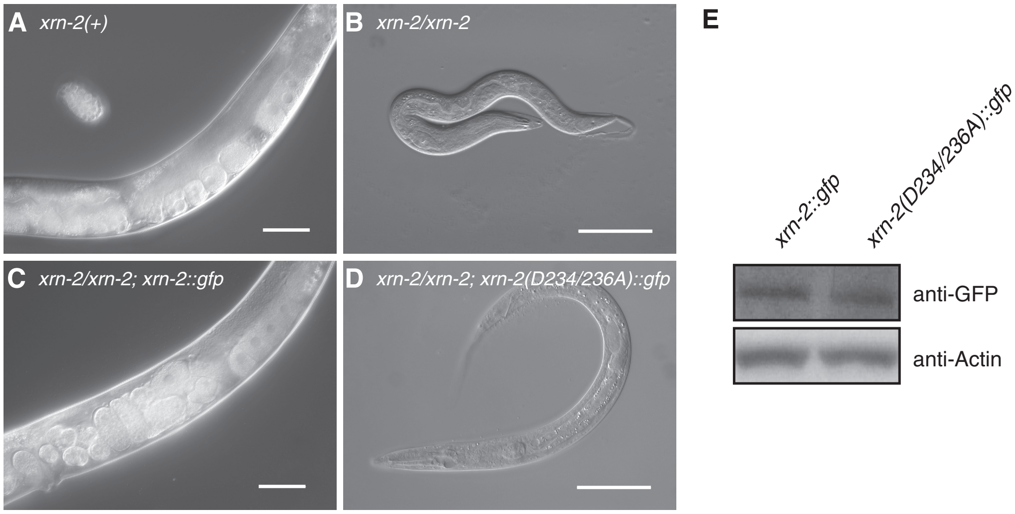

Figure 2. XRN2 catalytic activity is required for molting and growth beyond the L2 stage. (**A**) Wild-type worms develop into gravid adults, whereas (**B**) *xrn-2(tm3473)* homozygous worms arrest development. (**C**) Transgenic extrachromosomal *xrn-2* expressed under the control of the *xrn-2* 1413-bp promoter and *xrn-2* 3′-UTR rescues *xrn-2(tm3473)* mutant animals, whereas (**D**) a catalytically inactive version of *xrn-2* with two point mutations (D234A and D236A) does not. Both transgenes contain a C-terminal GFP tag, permitting their detection with an anti-GFP antibody. (E) Western blotting reveals equivalent accumulation of wild-type (lane 1) and mutant (lane 2) protein *in vivo*. Scale bar, 50 µm. *xrn-2(+)* denotes the N2 wild-type strain.

cross-react with such a truncated product despite the fact that it was raised against recombinant full-length protein, the data suggest that the mutant mRNA may be degraded through nonsense-mediated decay. We conclude that *xrn-2(tm3473)* is a bona fide null allele.

xrn-2(0) mutant animals fail to molt and arrest during L2

Worms exposed to *xrn-2(RNAi)* from L1 stage arrest as L4 larvae that are unable to ecdyse, i.e. shed the cuticle (22). By contrast, *xrn-2(tm3473)* animals already displayed penetrant defects in the L1-to-L2 molt (Figure 1C), the first molt during development. Ecdysis starts with loosening of the cuticle at the pharynx followed by rotations around the longitudinal axis that loosen the body cuticle (33). XRN2 appears to be involved in the early shedding of the cuticle taking place at the pharynx as the mouth of worms homozygous for *tm3473* remained attached to the old cuticle through a string-like structure [Figure 1C(v)]. The rest of the cuticle around the head and the body was at least partially detached [Figure 1C(v and vi)], and a new cuticle was already visible beneath the old one, indicating that XRN2 is predominantly involved in ecdysis rather than cuticle synthesis. Finally, following failure to shed the L1 cuticle, and possibly as a direct consequence (33), the mutant worms arrested during the L2 stage [Figure 1C(iv and iii)].

XRN-2 catalytic activity is required for molting

Although XRN2 is an RNase, it was not evident that the RNase activity was actually required for the developmental functions of this protein. XRN1 and XRN2 proteins share a conserved three amino acid motif, DXD, that is essential for exonuclease activity *in vivo* (11,34). The aspartic acids (D) in this motif are important for coordination of Mg^{2+} ions that are required for RNA hydrolysis. We thus constructed cDNA-based transgenes that encoded either the wild-type XRN2 or the catalytic dead D234A-D236A double mutant protein, where A stands for alanine. Both transgenes were driven from a promoter region covering 1.4 kb of upstream sequence and carried the *xrn-2* 3′-UTR as well as a C-terminal triple GFP/His_6/Flag-tag (Figure 2). As expected, the wild-type transgene efficiently rescued both the molting defect and larval arrest when introduced as a stable multicopy array (Figure 2C). By contrast, the mutant transgene was incapable of rescuing molting defect and larval arrest (Figure 2D), although mutant and wild-type protein accumulated at equivalent levels *in vivo* (Figure 2E). We conclude that the RNase activity of XRN2 is essential for its function in early larval development.

xrn-2 is expressed broadly and constitutively

Frand *et al.* (22) previously analysed the ability of a 132 bp sequence upstream from the *xrn-2* start codon to drive expression of *gfp* when present in a multicopy extrachromosomal array, and concluded that *xrn-2* expression was limited, occurring mostly in the pharyngeal myoepithelium, the intestine and certain neurons. This seemed surprising given that, based on our understanding of yeast and human Rat1p/XRN2 proteins, *C. elegans* XRN2 would be expected to be broadly involved in RNA processing and decay processes. Moreover, the Wormbase database annotates *xrn-2* as the second gene in a two-gene operon where rpl-43 is the upstream gene, 132 bp away (Figure 3A). In generating the rescuing transgene described earlier in the text, we had therefore used an extended sequence of 1413 bp upstream of the *xrn-2* start codon, reaching the 5’-end of the Y48B6A.1 ORF (Figure 3A). This construct revealed widespread, possibly ubiquitous expression, with XRN2/GFP signal

Downloaded from http://nar.oxfordjournals.org/ at Novartis Forschungsstiftung / Friedrich Miescher Institute on January 20, 2014

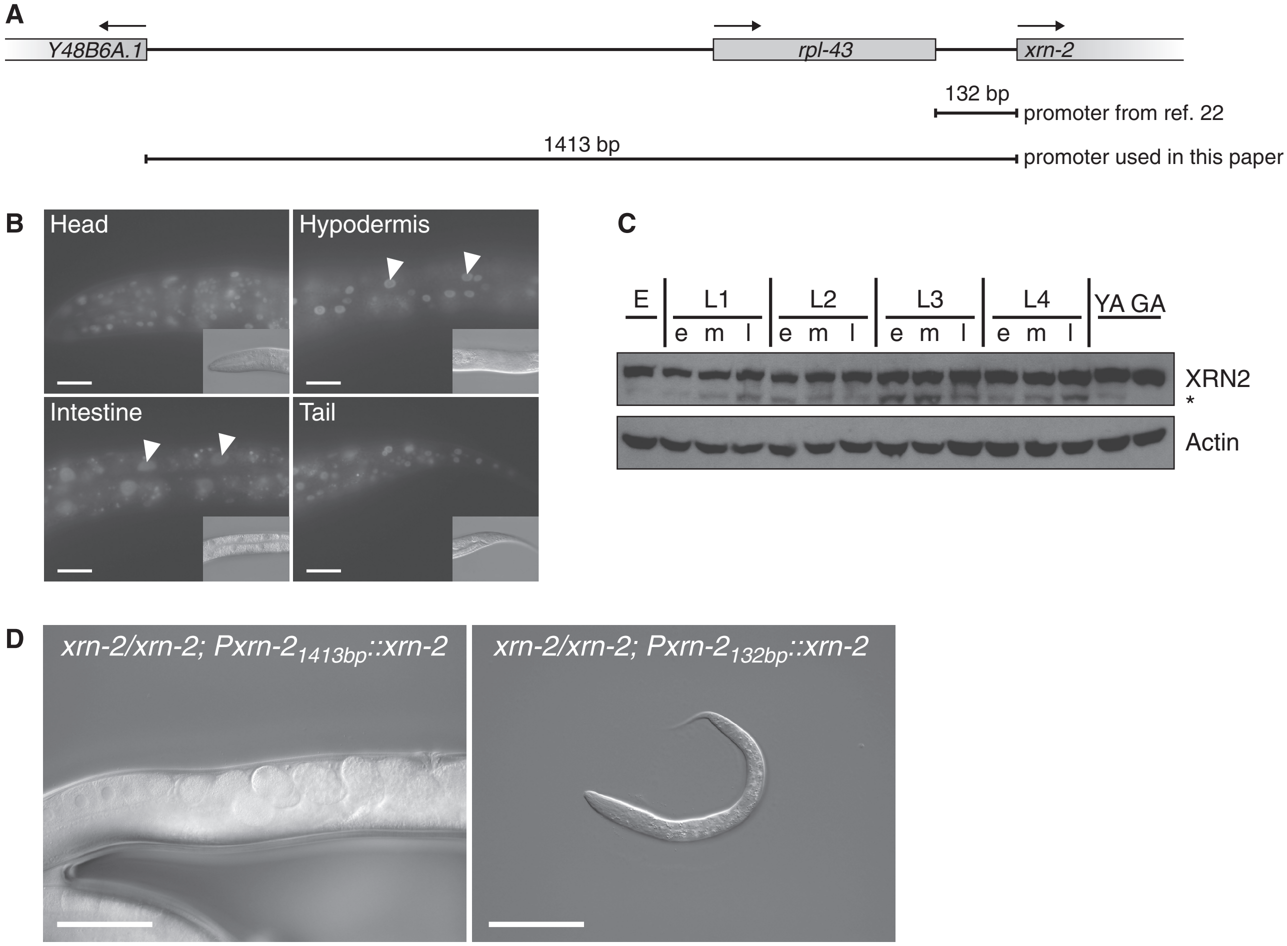

Figure 3. XRN2 is ubiquitously and constitutively expressed. (**A**) Schematic depiction of the *xrn-2* genomic locus and promoters used. The arrows indicate the direction of transcription. (**B**) Micrographs showing GFP signal of single-copy-integrated, codon-optimized and *gfp*-tagged *xrn-2* expressed under the control of the 1413-bp long promoter region. The GFP signal is ubiquitously detected. Examples of hypodermal and intestinal cells are marked with arrowheads. Insets: DIC images of the same worms. (**C**) Western blot showing a time-course for endogenous XRN2. 'e', 'm' and 'l' stands for early, mid and late, respectively; 'YA' and 'GA' for young and gravid adult, respectively. An asterisk indicates an apparent proteolytic fragment of XRN2, which did not occur consistently in other western blots. (**D**) Single-copy-integrated, codon-optimized and *gfp*-tagged *xrn-2* expressed under the control of the 1413-bp long *xrn-2* promoter region rescues the phenotypes of *xrn-2(tm3473)*, but the 132-bp long *xrn-2* promoter region does not. Scale bar, 20 µm (B) and 50 µm (D).

being detectable from early embryo through adulthood (Figure 3B). This expression was further validated through a time course that followed endogenous XRN2 protein by western blotting, and equally revealed continuous *xrn-2* expression throughout the *C. elegans* life cycle (Figure 3C).

Complementation of mutant phenotypes can provide a functional test for the authenticity of a putative promoter, and we found that *xrn-2* transgenes driven by the *xrn-2* 'long' promoter could rescue the *xrn-2(tm3473)* strain. This was true both when *xrn-2* cDNA was used (Figure 2C), which resulted in protein levels that were reduced relative to the endogenous protein (Figure 1B), and when a codon-optimized variant with synthetic introns was used (Figure 3D), which generated protein levels more similar to endogenous levels (see later in the text). By contrast, the *xrn-2* 'short' promoter failed to rescue the *xrn-2(tm3473)* mutation, although the optimized transgene was used (Figure 3D). Taken together, our results demonstrate that *xrn-2* is expressed broadly, perhaps ubiquitously, across tissues and developmental stages, and that expression beyond previously reported tissues is important for its role in molting.

A *xrn-2* temperature-sensitive allele generated *de novo* reveals additional XRN2 functions

Our finding of a molting defect as the predominant phenotype of *xrn-2* null mutant animals was consistent with a previously reported molting defect in *xrn-2(RNAi)* animals (22). However, given the broad expression of XRN2, which extends to the embryo, we wondered whether earlier phenotypes were obscured due to maternal contribution of mRNA or protein from *xrn-2*/+ heterozygous mothers to their *xrn-2*/*xrn-2* homozygous daughters. Rapidly inactivatable, conditional alleles would permit addressing this issue, but such alleles can currently not be generated in a targeted manner, for a specific gene of interest, in *C. elegans*. However, temperature-sensitive (ts) alleles have been described in *Saccharomyces cerevisiae* for Rat1p (35) and the Rat1p/XRN2 paralogue Xrn1p

Downloaded from http://nar.oxfordjournals.org/ at Novartis Forschungsstiftung / Friedrich Miescher Institute on January 20, 2014

(36). Individual mutation of either aspartate of the DXD motif mentioned earlier in the text to alanine (A) may further impair but not abrogate Mg^{2+} binding and render the protein function ts (34). We thus went to test whether the corresponding mutations in *C. elegans* *xrn-2*-elicited temperature sensitivity within the worm's physiological temperature window, ~10°C below that of yeast. We introduced single-copy integrated *xrn-2* transgenes with appropriate mutations into strains that were homozygous for *xrn-2(tm3473)*, i.e. lacked endogenous XRN2. Among three distinct mutations that we tested (Figure 1A), P107L, corresponding to *S. cerevisiae* *xrn1-10(P90L)* (36), conferred temperature sensitivity, supporting viability at 15°C but not at 25°C. By contrast, a Y594C-mutant transgene supported viability at either temperature, whereas the D234A mutant transgene rescued at neither temperature. In the following, we will refer to the mutant strain that expresses *xrn-2P107L* as $xrn\text{-}2ts_{cDNA}$ to distinguish it from an optimized version described later in the text. An analysis of different temperature regimens revealed numerous phenotypes of $xrn\text{-}2ts_{cDNA}$ animals beyond the molting defect observed with the *xrn-2* null strain, including arrest in embryonic development and sterility (Supplementary Figure S1). These mutant strains thus revealed multiple functions of XRN2 beyond molting, which had been obscured in the null mutant animals.

Although the $xrn\text{-}2ts_{cDNA}$ transgene permitted rapid and tight inactivation of *xrn-2* (Supplementary Figure S1), it failed to provide full XRN2 activity at the permissive temperature as illustrated by slow growth and small brood sizes small (~25 relative to ~250 for wild-type animals) relative to wild-type animals. This reduced the strain's utility for molecular or biochemical studies or genetic screens. Because low-protein levels relative to the endogenous protein (Figure 1B) might account for the reduced functionality, we introduced artificial introns into the *xrn-2* cDNA and optimized its codon composition (25). For the wild-type protein, these nucleotide changes increased XRN2/GFP levels as determined by epifluorescence microscopy (data not shown). Moreover, *xrn-2(tm3473)* animals expressing the sequence-optimized xrn-2P107L::*gfp* single-copy transgene, which we will henceforth call *xrn-2ts*, grew better (although still more slowly than wild-type animals) and had an increased brood size. At the same time, we could still rapidly and efficiently inactivate the optimized transgene by raising the temperature (Figure 4A, B), although a fully penetrant embryonic or L1 arrest now necessitated incubation at 26°C, rather than 25°C. Viability and development of N2 wild-type animals remained unimpaired at this temperature (Figure 4B) (37).

The P107L mutation induces temperature sensitivity by reducing XRN2 stability

To test whether destabilization of the protein by elevated temperature contributed to the ts behavior of *xrn-2P107L*, we examined steady-state levels of XRN2 at 15 and 26°C. We observed that XRN2 levels were substantially lower in the *xrn-2ts* mutant strain than either N2 or a strain carrying the wild-type transgene (Figure 4C). We note that wild-type XRN2/GFP levels were also reduced relative to endogenous XRN2 concentration in N2, particularly at 26°C, but the decrease was less than that seen with XRN2P107L/GFP. Hence, it seems likely that the P107L mutation renders XRN2 ts by destabilizing it, consistent also with its location directly adjacent to an unusually long α-helix, previously termed 'tower domain' (11). To test this possibility further, we quantified *xrn-2* mRNA levels in the two *xrn-2* transgenic strains. Unlike XRN2 protein levels, the *xrn-2* mRNA levels were not reduced in the mutant strain. In fact, *xrn-2ts* mRNA accumulated at increased concentrations relative to the wild-type mRNA, particularly at 26°C (Figure 4D). Hence, these results not only confirm that the P107L mutation causes temperature sensitivity by reducing XRN2 protein stability but also indicate the existence of an auto-regulatory mechanism that promotes transcription or stabilization of *xrn-2* mRNA when XRN2 activity is low.

The miR* strands decay more rapidly than guide strands

Our previous studies (16,38) had implicated *C. elegans* XRN2 in miRNA turnover by revealing increased steady-state levels of certain endogenous miRNAs in *xrn-2(RNAi)* worms and XRN2-dependent degradation of naked or Argonaute-loaded miRNAs in worm lysates. However, a formal demonstration that XRN2 depletion slowed miRNA degradation *in vivo* was missing. Moreover, certain endogenous miRNAs appeared unchanged on XRN2 depletion, but whether due to substrate specificity, or technical limitations, e.g. in the kinetics or tissue distribution of RNAi-mediated XRN2 depletion, remained unknown. To address these two issues, we examined miRNA decay globally *in vivo* in wild-type N2 animals. We performed a time-course experiment in which we inhibited transcription in L1 stage larvae by addition of α-amanitin (Supplementary Figure S2) and surveyed miRNAs at several subsequent time points over the next 8 h by deep sequencing (Figure 5A). We chose the L1 stage because these larvae had previously been reported to be sensitive to treatment with α-amanitin (39), and we confirmed that this treatment efficiently blocked transcription by assaying eft-3 pre-mRNA levels (Supplementary Figure S2B, C). For each time point, we calculated the levels of each miRNA as reads normalized to average library size ('Materials and Methods' section), which means that these numbers can go up or down or stay unchanged for a given miRNA depending on whether it decays less rapidly, more rapidly or just as rapidly as the average miRNA in this pool. Accordingly, the fold changes per hour in $\log_2$ can be positive, negative or 0, with negative values indicating less stable miRNAs. However, these values cannot be translated into absolute decay rates.

The fold changes per hour thus calculated for two independent biological replicates correlated well (Supplementary Figure S3) and their averages were used for subsequent analysis. A scatter plot displaying fold changes versus read numbers revealed that decay rates were broadly distributed with a subset of miRNAs displaying a strikingly faster decay than average (Figure

Downloaded from http://nar.oxfordjournals.org/ at Novartis Forschungsstiftung / Friedrich Miescher Institute on January 20, 2014

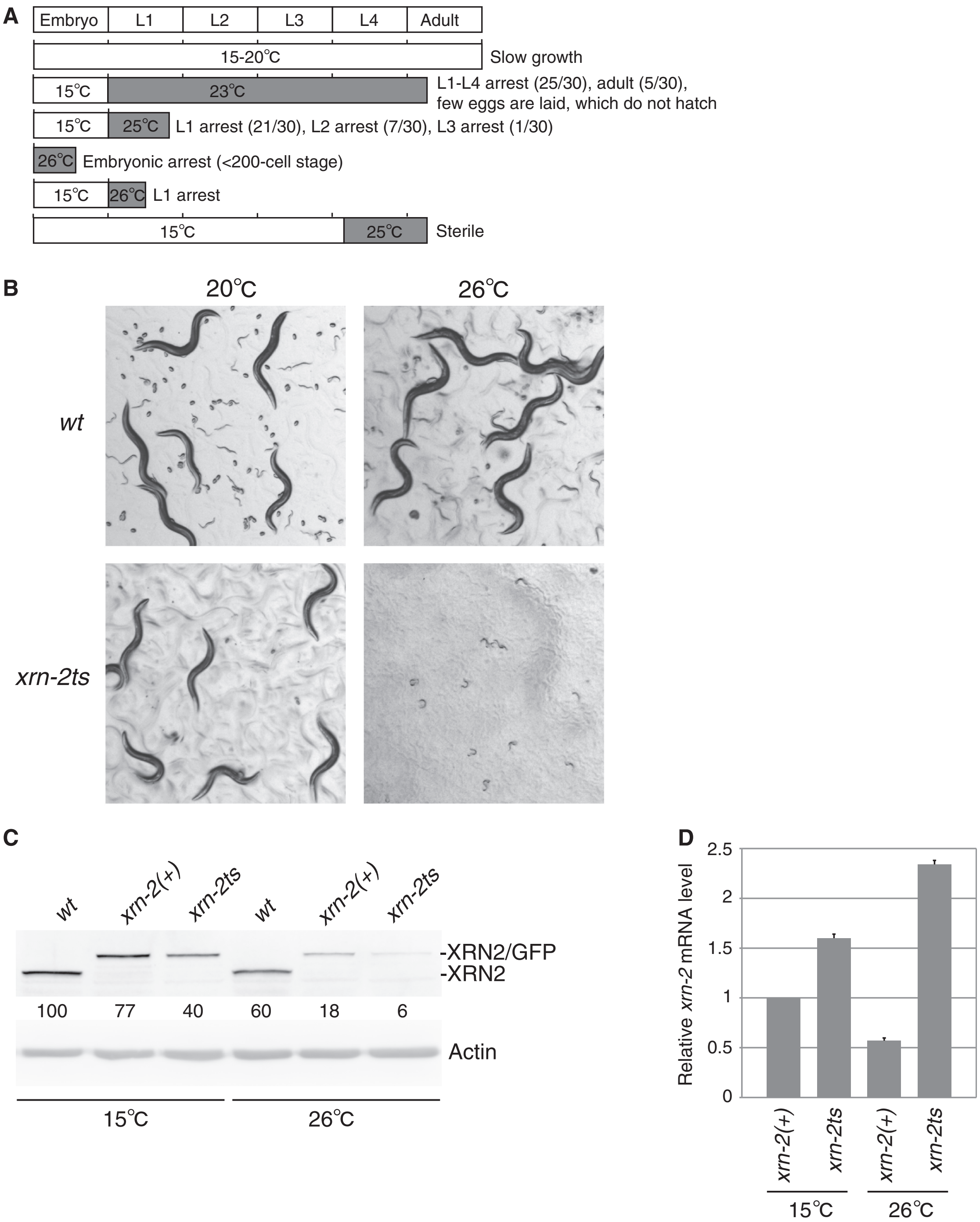

Figure 4. Characterization of an improved *xrn-2ts* strain reveals reduced XRN2 levels at restrictive temperature. (**A**) Schematic representation of *xrn-2ts* phenotypes at different temperature. *xrn-2ts* embryos or worms were cultured under the indicated conditions. Phenotypes observed are described on the right. For less-penetrant phenotypes, a number indicating worms affected/worms scored is shown in brackets. (**B**) The wild-type ('wt'; N2) and *xrn-2ts* worms were cultured from L1-stage at 20 or 26°C as indicated for 72 h (wt) and 93 h (*xrn-2ts*), respectively. The worms were observed by stereo microscopy at the same magnification. (**C, D**) The wt, *xrn-2(+)* and *xrn-2ts* worms were cultured from mid L3- to late L4-stage at 15°C or 26°C and harvested. (C) XRN2, XRN2/GFP and actin protein levels were examined by western blotting. XRN2 and XRN2/GFP levels were normalized to actin levels and shown with values of wt at 15°C defined as 100. (D) The mRNA levels of the *xrn-2::gfp* transgenes in *xrn-2(+)* and *xrn-2ts* worms were quantified by RT-qPCR, normalized to actin mRNA levels and shown with values of *xrn-2(+)* at 15°C as 1 ($n = 2$, means + SEM). '*xrn-2(+)*' denotes *xrn-2(tm3473)* homozygous animals expressing a wild-type *xrn-2* transgene.

5B). The effect was particularly pronounced for miRNAs of lower abundance. Strikingly, when we coloured miR*s, operationally defined as the one of two miRNA strands derived from a pre-miRNA that is less abundant, in red, and miRs in black, a clear separation of colours became apparent (Figure 5B). Hence, highly unstable RNAs were almost exclusively miR*s (Figure 5B). This result makes immediate and intuitive sense when considering miR*s as

Downloaded from http://nar.oxfordjournals.org/ at Novartis Forschungsstiftung / Friedrich Miescher Institute on January 20, 2014

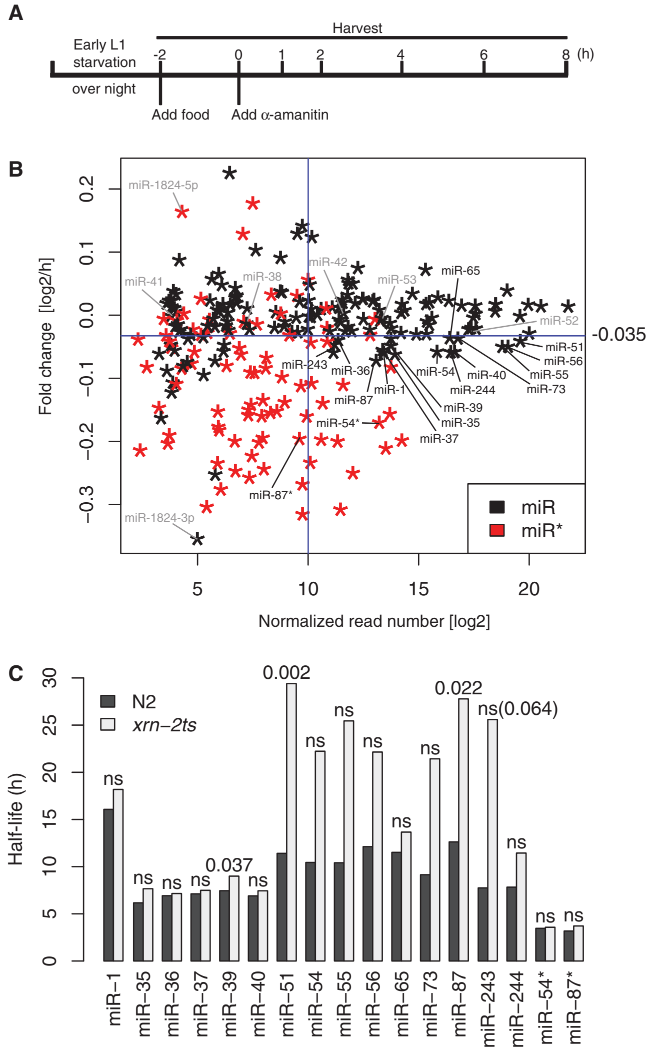

Figure 5. Specific miRNAs are stabilized on XRN2 depletion. (**A**) Experimental design for miRNA decay analysis. RNA was extracted for (**B**) deep sequencing and (**C**) RT-qPCR analyses. (B) Relative decay rates of miRNAs are plotted against normalized reads for miRNAs with sufficient expression ('Materials and Methods' section). Black stars, miRs; red stars, miR*s. Fifteen miRs that showed high-read numbers and fast relative decay as indicated by the blue cut-off lines. (Because the plot shows fold changes per hour, not decay constants, unstable miRNAs are those below the cut-off line.) These and two miR*s, indicated in black, were further examined by RT-qPCR. Other miRs discussed in the main text are shown in grey. (C) The miRNA levels at each time point in wt and *xrn-2ts* worms were quantified by RT-qPCR, and their half-lives were

biogenesis byproducts. It is also consistent with generally long miRNA half-lives observed in a microarray-based study that was confined to a survey of annotated miRs (40).

Specific miRNAs are stabilized on XRN2 inactivation

Although the fast decay rates were preferentially seen for miR*s, some miRs exhibited unusually low stability, most notably several members, though not all, of each of the miR-35 (miR-35 through miR-42) and the miR-51 (miR-51 through miR-56) families. To test whether this was due to decay by XRN2, we repeated the α-amanitin time-course experiment for wild-type and *xrn-2ts* worms. Under the conditions that we use, α-amanitin completely blocks development at the early L1 stage (Supplementary Figure S2; Supplementary Materials and Methods), so that wild-type and *xrn-2ts* animals are equally arrested in development.

For this analysis, we focused on miRNAs with low stability (apparent $\log_2$ fold change of less than −0.035/h and thus below the blue cut-off line in Figure 5B) and moderately high, to high, expression levels ($>2^{10}$ normalized reads, to the right of the cut-off line). We determined the levels of individual miRNAs by RT-qPCR and normalized them to sn2841, a small nucleolar RNA whose level is stable during the time course (data not shown). When testing the five rapidly decaying members of the miR-35 family, all of them displayed comparable half-lives in wild-type and *xrn-2ts* animals (Figure 5C and Supplementary Figure S4). Similarly, *xrn-2* inactivation had little effect on the decay of miR-1, miR-65 and miR-244. By contrast, the decay of miR-51 and miR-87 was substantially and significantly delayed in *xrn-2ts* animals. The miR-54, miR-55, miR-56, miR-73 and miR-243 showed a similar trend, although differences failed to reach statistical significance (Supplementary Figure S4). We also examined decay of the highly expressed and unstable miR-54* and found it to be unaffected by XRN2 inactivation. Similarly, miR-87*, unlike miR-87, continued to decay rapidly when XRN2 was inactive. As the passenger and guide strand derive from the same precursor, this directly confirms that the decreased apparent half-lives of the guide strands truly reflects stabilization of this guide strand and not a secondary effect of altered processing of residual pre-miRNAs. Taken together, our data reveal that XRN2 is essential for rapid decay of a subset of miRNAs during the first larval stage.

DISCUSSION

xrn-2 is broadly expressed and functions in processes beyond molting

Although molecular functions of XRN2 proteins have been studied extensively, particularly in yeast and cultured human cells, their developmental functions have remained virtually unexplored (15). An RNAi-based screen had implicated XRN2 in molting in *C. elegans*, consistent also with its expression in tissues important for cuticle generation or shedding (22), and in agreement with this idea, we find that an *xrn-2* null mutation causes a penetrant L1 molting defect and subsequent L2 stage arrest. However, by generating a conditional allele, we could demonstrate that this only represents the tip of the iceberg; XRN2 in *C. elegans* is required for numerous events during embryonic and post-embryonic development as demonstrated for instance by embryonic lethality and sterility under appropriate regimens.

In yeast, where Rat1p/XRN2 is essential for viability, mutations cause a diverse array of defects in various RNA

Downloaded from http://nar.oxfordjournals.org/ at Novartis Forschungsstiftung / Friedrich Miescher Institute on January 20, 2014

metabolic processes, such as transcriptional termination, ribosomal RNA processing, intron degradation and aberrant transfer RNA degradation (15). However, it remains to be determined which of these processes constitutes the essential function of Rat1p or whether it is any one process. Similarly, it remains to be established for *C. elegans* whether the requirements for functional XRN2 in different tissues and developmental stages reflect a core underlying theme, or whether the respective targets and processes that become dysregulated on XRN2 depletion vary. We also note that although we have focused here on miRNAs as the only currently known substrate of *C. elegans* XRN2, it is highly likely that numerous additional substrates exist, and any of these, individually or in combination, may be relevant for the *xrn-2* mutant phenotypes. Nonetheless, our demonstration that mutations inactivating the XRN2 catalytic site also abrogate its ability to complement an *xrn-2* null mutation argue that it is processing or degradation of one or several RNA substrates that are important for the function of XRN2 in molting. Modulator, i.e. enhancer and suppressor, screens may offer a way forward to identify specific targets and pathways affected by *xrn-2* deficiency and have been initiated in our laboratory.

XRN2 substrate preferences

In vitro, XRN2 proteins can degrade various RNA sequences, provided they are 5′-monophosphorylated and devoid of stable structures (9,10). However, we find here that in the L1 stage, only a subset of miRNAs is stabilized on XRN2 inactivation. We cannot formally rule out that XRN2 activity at the restrictive temperature is not fully eliminated in the *xrn-2ts* strain and that complete loss of activity would stabilize all miRNAs. Nonetheless, the available data demonstrate that, minimally, some miRNAs are more dependent on XRN2 for degradation than others.

The mechanisms that provide specificity remain to be elucidated. On the XRN2 side, the enzyme may either contain previously unrecognized intrinsic specificity, or its substrate range may be restricted specifically *in vivo* through the action of protein binding partners, such as the newly identified PAXT-1 (41). Similarly, features of the miRNA that render them sensitive or insensitive to XRN2 remain to be identified. Although we lack enough examples of miRNAs that are stabilized by mutation of *xrn-2* to confidently comment on the involvement of sequence features, we note that there is almost no overlap in sequence between miR-51 and miR-87, and they even differ in their 5’ ends, with miR-51 sporting the miRNA-characteristic U and miR-87 and miR-243 a more unusual G and C, respectively. Hence, it seems possible that instead of, or in addition to, sequence, the site of expression of an miRNA might affect its sensitivity to degradation by XRN2. Because our expression analysis of XRN2 indicates widespread, possibly ubiquitous expression of *xrn-2*, such a model would imply the existence of additional factors that either promote degradation of specific miRNAs by XRN2 in some tissues or prevent it in others. Targets of miRNAs might be one such factor. We previously reported that target RNAs protected their cognate miRNAs from degradation (16,38). At this point, it is not known whether any target can do this, for any miRNA, or if specific miRNA-target duplex architectures are required. Nonetheless, differences in the levels of either the entire group of target RNAs, or only individual targets, might thus alter XRN2 activity towards miRNAs in a tissue-specific manner.

Finally, intracellular localization of miRNAs may affect their susceptibility to degradation by XRN2. This notion is based on our finding that XRN2 accumulates preferentially, perhaps exclusively in the nucleus [this study and (42)]. By contrast, miRNAs are thought to function in the cytoplasm, where they would thus be shielded from XRN2 activity. At the same time, a number of mature *C. elegans* miRNAs have recently been detected in both nucleus and cytoplasm, with individual miRNAs apparently differing in their nucleocytoplasmic distribution (43). However, because we have so far been unable to achieve sufficiently clean fractionation of nuclei versus cytoplasm, it remains to be determined whether XRN2-sensitive miRNAs partition more extensively to the nucleus than those that are XRN2-insensitive.

miRs and miR*s differ in their stabilities

Initially, it was assumed that miRNA precursors give rise to only one functional molecule, the mature miRNA or guide strand/miR. A second partially complementary molecule derived from the opposite strand of the pre-miRNA, the passenger strand/miR*, might be visible at much lower levels and constitute merely a biogenesis intermediate. More recently, however, several examples of functional miR*s have been described, and it has emerged that in some cases the ratio of miR to miR* may be variable and change with site of expression or development (18). Accordingly, a different nomenclature that identifies miRNA molecules based on their provenance from either the 5′ or the 3′ arm of the pre-miRNA has been adopted. Although there can be little doubt on the functionality of certain miR*s, our decay data strongly suggest that at least in our system most of them accumulate only transiently, supporting their designation as processing intermediates. Although ours is the first demonstration of this phenomenon on a global scale, Winter and Diederichs previously examined the half-lives of a small number of miRs and miR*s in human cells and equally observed reduced half-lives of the latter (44). Moreover, they noted that over-expression of Argonaute proteins could stabilize two miR*s that were investigated, suggesting that it is lack of Argonaute loading that renders miR*s unstable, which would also deprive them of a functional miRNA status.

We note that the least stable of all miRNAs that we observe is annotated as miR, miR-1824-3p, rather than miR*. However, deep sequencing is subject to sequence-dependent biases that prevent exact quantification of distinct small RNAs [(45) and our unpublished data]. The miR-1824-3p displays only marginally (~1.6-fold) more reads than its presumed miR*, miR-1824-5p,

Downloaded from http://nar.oxfordjournals.org/ at Novartis Forschungsstiftung / Friedrich Miescher Institute on January 20, 2014

which is much more stable ($\log_2$ fold change of 0.16/h versus −0.35/h for 5p versus 3p). Hence, we predict that absolute quantification would reveal that miR-1824-5p is more abundant than miR-1824-3p and thus the true miR by our criterion.

De novo generation of a conditional *xrn-2* allele

Genetic mutations are invaluable tools in assigning function to genes. However, if a gene has multiple consecutive functions in development, it can be difficult or impossible to study all of them with 'constitutive' mutations especially when an early function is essential during development. At the same time, for essential genes, homozygously mutant animals by necessity need to be derived from heterozygous parents, which may contribute mRNA or protein to their offspring so that early phenotypes can be masked (46). RNAi may be used to deplete such maternal mRNAs, but usually results in only partial depletion of transcripts and protein products. Similarly, although RNAi may be applied such that an early terminal phenotype in development is bypassed (47,48), it can usually not be timed precisely. Although *xrn-2(RNAi)* phenocopies the sterile phenotype of *xrn-2ts* animals, none of the conditions we tried so far were able to elicit embryonic lethality.

Conditional alleles, encoding rapidly inactivatable gene products, would permit addressing both of the aforementioned issues. The ts alleles are widely used for instance in yeast, and screens have been conducted in *C. elegans* to identify ts alleles for specific processes. However, because it has not been possible to predict a priori which mutations will generate a ts allele, targeted approaches for generation of conditional alleles of specific genes have been lacking.

We provide here proof of principle that a *C. elegans* ts mutation can be generated *de novo* by exploiting information from a different organism, yeast, despite major differences in their physiological temperature ranges. We note that our approach is not easily scalable and its generality remains to be established. However, many yeast ts alleles exist, and new ones can easily be generated, e.g. by complementing yeast deletion mutant cells with randomly mutagenized transgenes expressing the genes of interests. Hence, ours may be a fertile approach for other researchers interested in generating conditionally mutant *C. elegans* strains, complementing transcriptional (49,50), co-transcriptional (51) or post-transcriptional (52) approaches that modulate mRNA levels and thus, indirectly, protein activity.

ACCESSION NUMBERS

The small RNA sequencing data discussed in this study have been deposited at GEO and can be accessed at http://www.ncbi.nlm.nih.gov/geo/query/acc.cgi?token=xdwvjqcwsguaozo&acc=GSE46753.

SUPPLEMENTARY DATA

Supplementary Data are available at NAR Online.

ACKNOWLEDGEMENTS

The authors are grateful to Dr Iskra Katic, Dr Rafal Ciosk and Matyas Ecsedi for helpful comments on the manuscript. The authors thank Kirsten Jacobeit and Sophie Dessus-Babus of the FMI Functional Genomics Facility for library preparation and sequencing, which was performed at the Basel Deep Sequencing Facility, Dr Iskra Katic for help with *C. elegans* transgenesis and Dr David T. Harris and Dr Robert H. Horvitz for strain MT16418. The authors are particularly grateful to Dr Shohei Mitani and the National Bioresource Project for *C. elegans* (Japan) for the *tm3473* allele, and to Dr Saibal Chatterjee for generating XRN2 protein used to raise the anti-XRN2 antibody.

FUNDING

European Union Seventh Framework Programme (FP7/2007-2013) under grant agreement number [241985] (European Research Council 'miRTurn'). Novartis Research Foundation through the FMI and the Swiss National Science Foundation [SNF 31003A_127052 and SNF 31003A_143313]. Boehringer Ingelheim Fonds PhD fellowship (to S.R.). Funding for open access charge: European Union Seventh Framework Programme.

Conflict of interest statement. None declared.

REFERENCES

1. Miki,T.S. and Großhans,H. (2013) The multifunctional RNase XRN2. *Biochem. Soc. Trans.*, **41**, 825–830.
2. Henry,Y., Wood,H., Morrissey,J.P., Petfalski,E., Kearsey,S. and Tollervey,D. (1994) The 5′ end of yeast 5.8S rRNA is generated by exonucleases from an upstream cleavage site. *EMBO J.*, **13**, 2452–2463.
3. Petfalski,E., Dandekar,T., Henry,Y. and Tollervey,D. (1998) Processing of the precursors to small nucleolar RNAs and rRNAs requires common components. *Mol. Cell. Biol.*, **18**, 1181–1189.
4. Villa,T., Ceradini,F., Presutti,C. and Bozzoni,I. (1998) Processing of the intron-encoded U18 small nucleolar RNA in the yeast *Saccharomyces cerevisiae* relies on both exo- and endonucleolytic activities. *Mol. Cell. Biol.*, **18**, 3376–3383.
5. Qu,L.H., Henras,A., Lu,Y.J., Zhou,H., Zhou,W.X., Zhu,Y.Q., Zhao,J., Henry,Y., Caizergues-Ferrer,M. and Bachellerie,J.P. (1999) Seven novel methylation guide small nucleolar RNAs are processed from a common polycistronic transcript by Rat1p and RNase III in yeast. *Mol. Cell. Biol.*, **19**, 1144–1158.
6. Geerlings,T.H., Vos,J.C. and Raue,H.A. (2000) The final step in the formation of 25S rRNA in *Saccharomyces cerevisiae* is performed by 5′–>3′ exonucleases. *RNA*, **6**, 1698–1703.
7. Kim,M., Krogan,N.J., Vasiljeva,L., Rando,O.J., Nedea,E., Greenblatt,J.F. and Buratowski,S. (2004) The yeast Rat1 exonuclease promotes transcription termination by RNA polymerase II. *Nature*, **432**, 517–522.
8. Chernyakov,I., Whipple,J.M., Kotelawala,L., Grayhack,E.J. and Phizicky,E.M. (2008) Degradation of several hypomodified mature tRNA species in *Saccharomyces cerevisiae* is mediated by Met22 and the 5′-3′ exonucleases Rat1 and Xrn1. *Genes Dev.*, **22**, 1369–1380.
9. Kenna,M., Stevens,A., McCammon,M. and Douglas,M.G. (1993) An essential yeast gene with homology to the exonuclease-encoding XRN1/KEM1 gene also encodes a protein with exoribonuclease activity. *Mol. Cell. Biol.*, **13**, 341–350.
10. Stevens,A. and Poole,T.L. (1995) 5′-exonuclease-2 of *Saccharomyces cerevisiae*. Purification and features of ribonuclease

Downloaded from http://nar.oxfordjournals.org/ at Novartis Forschungsstiftung / Friedrich Miescher Institute on January 20, 2014

activity with comparison to 5′-exonuclease-1. *J. Biol. Chem.*, **270**, 16063–16069.
11. Xiang,S., Cooper-Morgan,A., Jiao,X., Kiledjian,M., Manley,J.L. and Tong,L. (2009) Structure and function of the 5′–>3′ exoribonuclease Rat1 and its activating partner Rai1. *Nature*, **458**, 784–788.
12. Heyer,W.D., Johnson,A.W., Reinhart,U. and Kolodner,R.D. (1995) Regulation and intracellular localization of *Saccharomyces cerevisiae* strand exchange protein 1 (Sep1/Xrn1/Kem1), a multifunctional exonuclease. *Mol. Cell. Biol.*, **15**, 2728–2736.
13. Hsu,C.L. and Stevens,A. (1993) Yeast cells lacking 5′–>3′ exoribonuclease 1 contain mRNA species that are poly(A) deficient and partially lack the 5' cap structure. *Mol. Cell. Biol.*, **13**, 4826–4835.
14. Johnson,A.W. (1997) Rat1p and Xrn1p are functionally interchangeable exoribonucleases that are restricted to and required in the nucleus and cytoplasm, respectively. *Mol. Cell. Biol.*, **17**, 6122–6130.
15. Nagarajan,V.K., Jones,C.I., Newbury,S.F. and Green,P.J. (2013) XRN 5'–>3' exoribonucleases: Structure, mechanisms and functions. *Biochim. Biophys. Acta*, **1829**, 590–603.
16. Chatterjee,S. and Großhans,H. (2009) Active turnover modulates mature microRNA activity in *Caenorhabditis elegans*. *Nature*, **461**, 546–549.
17. Krol,J., Loedige,I. and Filipowicz,W. (2010) The widespread regulation of microRNA biogenesis, function and decay. *Nat. Rev. Genet.*, **11**, 597–610.
18. Mah,S.M., Buske,C., Humphries,R.K. and Kuchenbauer,F. (2010) miRNA*: a passenger stranded in RNA-induced silencing complex? *Crit. Rev. Eukaryot. Gene Expr.*, **20**, 141–148.
19. Fabian,M.R. and Sonenberg,N. (2012) The mechanics of miRNA-mediated gene silencing: a look under the hood of miRISC. *Nat. Struct. Mol. Biol.*, **19**, 586–593.
20. Mendell,J.T. and Olson,E.N. (2012) MicroRNAs in stress signaling and human disease. *Cell*, **148**, 1172–1187.
21. Lu,Y., Liu,P., James,M., Vikis,H.G., Liu,H., Wen,W., Franklin,A. and You,M. (2010) Genetic variants cis-regulating Xrn2 expression contribute to the risk of spontaneous lung tumor. *Oncogene*, **29**, 1041–1049.
22. Frand,A.R., Russel,S. and Ruvkun,G. (2005) Functional genomic analysis of *C. elegans* molting. *PLoS Biol.*, **3**, e312.
23. Johnstone,I.L. (2000) Cuticle collagen genes. Expression in *Caenorhabditis elegans*. *Trends Genet.*, **16**, 21–27.
24. Brenner,S. (1974) The genetics of *Caenorhabditis elegans*. *Genetics*, **77**, 71–94.
25. Redemann,S., Schloissnig,S., Ernst,S., Pozniakowsky,A., Ayloo,S., Hyman,A.A. and Bringmann,H. (2011) Codon adaptation-based control of protein expression in *C. elegans*. *Nat. Methods*, **8**, 250–252.
26. Frokjaer-Jensen,C., Davis,M.W., Hopkins,C.E., Newman,B.J., Thummel,J.M., Olesen,S.P., Grunnet,M. and Jorgensen,E.M. (2008) Single-copy insertion of transgenes in *Caenorhabditis elegans*. *Nat. Genet.*, **40**, 1375–1383.
27. Frokjaer-Jensen,C., Davis,M.W., Hollopeter,G., Taylor,J., Harris,T.W., Nix,P., Lofgren,R., Prestgard-Duke,M., Bastiani,M., Moerman,D.G. *et al.* (2010) Targeted gene deletions in *C. elegans* using transposon excision. *Nat. Methods*, **7**, 451–453.
28. Praitis,V., Casey,E., Collar,D. and Austin,J. (2001) Creation of low-copy integrated transgenic lines in *Caenorhabditis elegans*. *Genetics*, **157**, 1217–1226.
29. Lewis,J.A. and Fleming,J.T. (1995) Basic culture methods. *Methods Cell Biol.*, **48**, 3–29.
30. Guang,S., Bochner,A.F., Burkhart,K.B., Burton,N., Pavelec,D.M. and Kennedy,S. (2010) Small regulatory RNAs inhibit RNA polymerase II during the elongation phase of transcription. *Nature*, **465**, 1097–1101.
31. Sumitani,M., Kasashima,K., Matsugi,J. and Endo,H. (2011) Biochemical properties of *Caenorhabditis elegans* HMG-5, a regulator of mitochondrial DNA. *J. Biochem.*, **149**, 581–589.
32. Langmead,B., Trapnell,C., Pop,M. and Salzberg,S.L. (2009) Ultrafast and memory-efficient alignment of short DNA sequences to the human genome. *Genome Biol.*, **10**, R25.
33. Singh,R.N. and Sulston,J.E. (1978) Some observations on molting in *Caenorhabditis elegans*. *Nematologica*, **24**, 63–71.
34. Solinger,J.A., Pascolini,D. and Heyer,W.D. (1999) Active-site mutations in the Xrn1p exoribonuclease of *Saccharomyces cerevisiae* reveal a specific role in meiosis. *Mol. Cell. Biol.*, **19**, 5930–5942.
35. Amberg,D.C., Goldstein,A.L. and Cole,C.N. (1992) Isolation and characterization of RAT1: an essential gene of *Saccharomyces cerevisiae* required for the efficient nucleocytoplasmic trafficking of mRNA. *Genes Dev.*, **6**, 1173–1189.
36. Page,A.M., Davis,K., Molineux,C., Kolodner,R.D. and Johnson,A.W. (1998) Mutational analysis of exoribonuclease I from *Saccharomyces cerevisiae*. *Nucleic Acids Res.*, **26**, 3707–3716.
37. Alvarez-Saavedra,E. and Horvitz,H.R. (2010) Many families of *C. elegans* microRNAs are not essential for development or viability. *Curr. Biol.*, **20**, 367–373.
38. Chatterjee,S., Fasler,M., Bussing,I. and Großhans,H. (2011) Target-mediated protection of endogenous microRNAs in *C. elegans*. *Dev. Cell*, **20**, 388–396.
39. Sanford,T., Golomb,M. and Riddle,D.L. (1983) RNA polymerase II from wild type and alpha-amanitin-resistant strains of *Caenorhabditis elegans*. *J. Biol. Chem.*, **258**, 12804–12809.
40. Lehrbach,N.J., Castro,C., Murfitt,K.J., Abreu-Goodger,C., Griffin,J.L. and Miska,E.A. (2012) Post-developmental microRNA expression is required for normal physiology, and regulates aging in parallel to insulin/IGF-1 signaling in *C. elegans*. *RNA*, **18**, 2220–2235.
41. Miki,T.S., Richter,H., Rüegger,S. and Großhans,H. (2014) PAXT-1 promotes XRN2 activity by stabilizing it through a conserved domain. *Mol. Cell*, doi:10.1016/j.molcel.2014/01.001.
42. Bosse,G.D., Ruegger,S., Ow,M.C., Vasquez-Rifo,A., Rondeau,E.L., Ambros,V.R., Großhans,H. and Simard,M.J. (2013) The decapping scavenger enzyme DCS-1 controls microRNA levels in *Caenorhabditis elegans*. *Mol. Cell*, **50**, 281–287.
43. Zisoulis,D.G., Kai,Z.S., Chang,R.K. and Pasquinelli,A.E. (2012) Autoregulation of microRNA biogenesis by let-7 and Argonaute. *Nature*, **486**, 541–544.
44. Winter,J. and Diederichs,S. (2011) Argonaute proteins regulate microRNA stability: Increased microRNA abundance by Argonaute proteins is due to microRNA stabilization. *RNA Biol.*, **8**, 1149–1157.
45. Hafner,M., Renwick,N., Brown,M., Mihailovic,A., Holoch,D., Lin,C., Pena,J.T., Nusbaum,J.D., Morozov,P., Ludwig,J. *et al.* (2011) RNA-ligase-dependent biases in miRNA representation in deep-sequenced small RNA cDNA libraries. *RNA*, **17**, 1697–1712.
46. Jorgensen,E.M. and Mango,S.E. (2002) The art and design of genetic screens: *Caenorhabditis elegans*. *Nat. Rev. Genet.*, **3**, 356–369.
47. Kamath,R.S., Martinez-Campos,M., Zipperlen,P., Fraser,A.G. and Ahringer,J. (2001) Effectiveness of specific RNA-mediated interference through ingested double-stranded RNA in *Caenorhabditis elegans*. *Genome Biol.*, **2**, RESEARCH0002.
48. Ding,X.C., Slack,F.J. and Großhans,H. (2008) The let-7 microRNA interfaces extensively with the translation machinery to regulate cell differentiation. *Cell Cycle*, **7**, 3083–3090.
49. Wei,X., Potter,C.J., Luo,L. and Shen,K. (2012) Controlling gene expression with the Q repressible binary expression system in *Caenorhabditis elegans*. *Nat. Methods*, **9**, 391–395.
50. Bacaj,T. and Shaham,S. (2007) Temporal control of cell-specific transgene expression in *Caenorhabditis elegans*. *Genetics*, **176**, 2651–2655.
51. Calixto,A., Ma,C. and Chalfie,M. (2010) Conditional gene expression and RNAi using MEC-8-dependent splicing in *C. elegans*. *Nat Methods*, **7**, 407–411.
52. Gaudet,J. and Mango,S.E. (2002) Regulation of organogenesis by the *Caenorhabditis elegans* FoxA protein PHA-4. *Science*, **295**, 821–825.

Downloaded from http://nar.oxfordjournals.org/ at Novartis Forschungsstiftung / Friedrich Miescher Institute on January 20, 2014

SUPPLEMENTARY FIGURES AND TABLES

for Miki & Rüegger et al. (2014). Engineering of a Conditional Allele Reveals Multiple Roles of XRN2 in *Caenorhabditis elegans* Development and Substrate Specificity in MicroRNA Turnover.

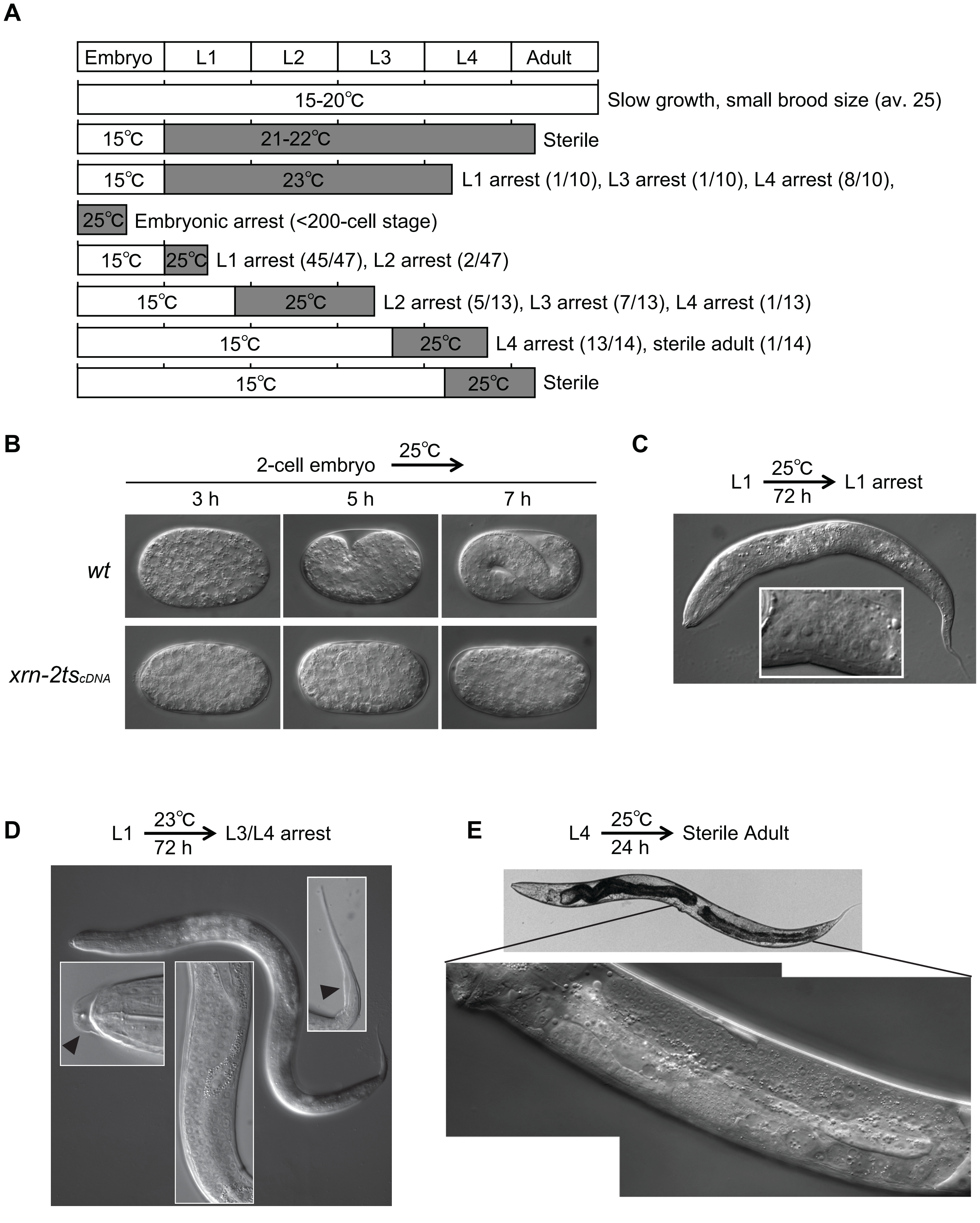
A
Embryo
L1
L2
L3
L4
Adult
15-20°C
Slow growth, small brood size (av. 25)
15°C
21-22°C
Sterile
15°C
23°C
L1 arrest (1/10), L3 arrest (1/10), L4 arrest (8/10),
25°C
Embryonic arrest (<200-cell stage)
15°C
25°C
L1 arrest (45/47), L2 arrest (2/47)
15°C
25°C
L2 arrest (5/13), L3 arrest (7/13), L4 arrest (1/13)
15°C
25°C
L4 arrest (13/14), sterile adult (1/14)
15°C
25°C
Sterile
B
2-cell embryo
25°C
3 h
5 h
7 h
wt
xrn-2tscDNA
C
L1
25°C
72 h
L1 arrest
D
L1
23°C
72 h
L3/L4 arrest
E
L4
25°C
24 h
Sterile Adult

Figure S1. XRN2 is required during several events throughout development.
(A) Schematic representation of *xrn-2ts*$_{cDNA}$ phenotypes at different temperature. *xrn-2ts*$_{cDNA}$ embryos or worms were cultured under the indicated conditions yielding the phenotypes described on the right. For less-penetrant phenotypes, a number indicating worms affected/worms scored is shown in brackets. **(B)-(E)** Micrographs showing examples of the phenotypes scored in (A). **(B)** An xrn-2tscDNA embryos shifted to 25°C at the two-cell stage fails to complete embryogenesis and arrested at a <200 cell stage. **(C)** Following hatching at permissive temperature, placement of early L1 larvae on food at 25°C causes development arrest, observed here after 72h at 25°C. **(D)** When the temperature is reduced to 23°C in this procedure, most animals develop up to the L3 or L4 stage, with a partially penetrant molting defect, observed in (D) after 72h at 23°C using DIC microscopy. **(E)** When animals are grown at 15°C until L4 stage and then shifted to 25°C, they develop into adults, but these are sterile, as illustrated here after growth for 24h at 25°C. Similarly, sterility ensues when L1 larvae are shifted to 21°C or 22°C for development into adults (cp. panel (A)). (C),(E) Insets magnify gonads to illustrate developmental stage and sterility, respectively. (D) Insets show unshed cuticles (arrowheads).

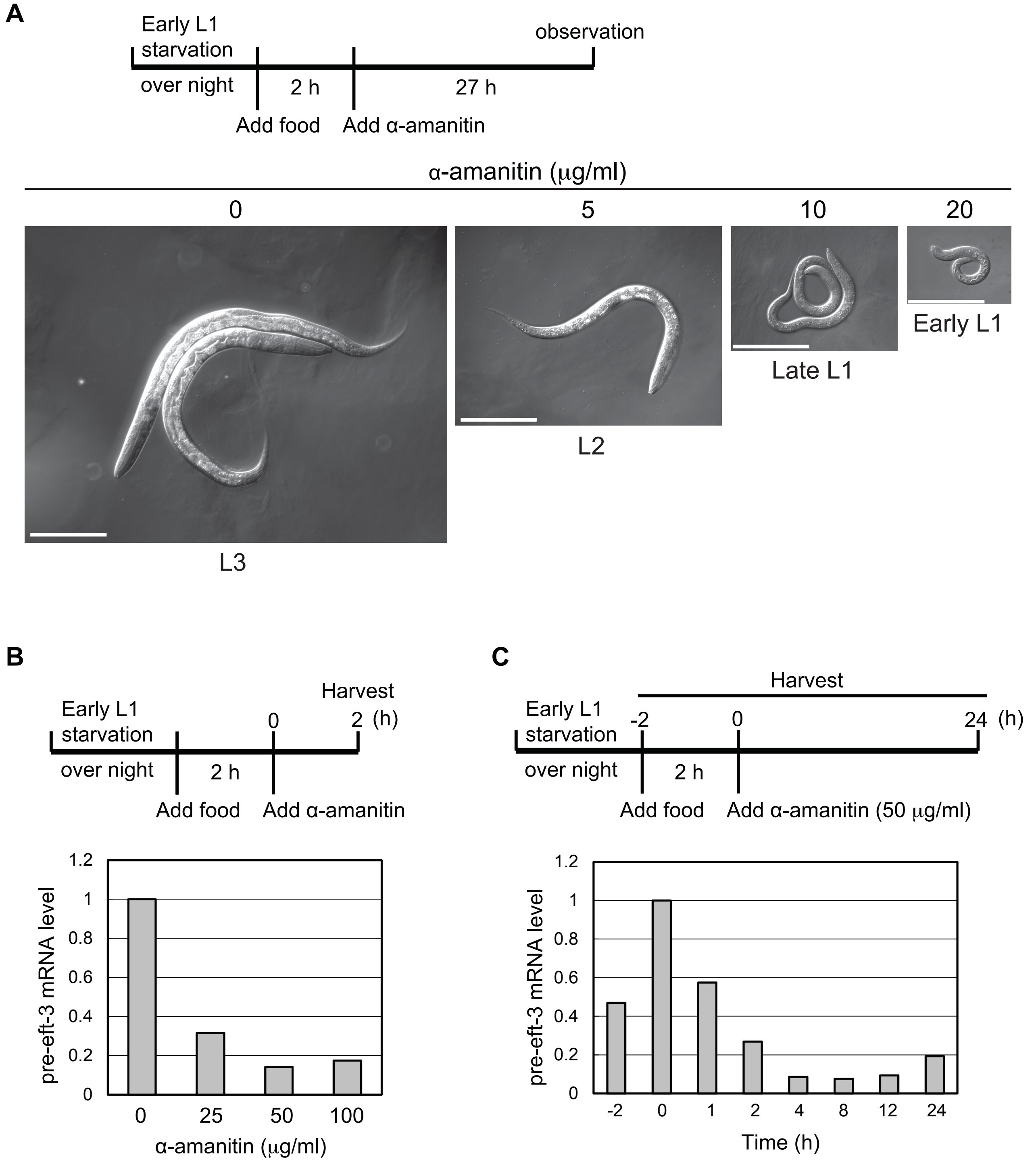

Figure S2. 50 μg/ml α-amanitin efficiently blocks Pol II-mediated transcription in, and development of, L1-stage worms.
(A) Synchronized early L1-stage N2 worms were liquid-cultured with food for 2 hours, and α-amanitin was added to the indicated final concentrations. The worms were observed after 27 hours by stereo-microscopy. Scale bar, 100 μm. **(B)** Worms were treated as in (A) and harvested after 2 hours. Following RNA extraction, pre-eft-3 mRNA levels were examined by RT-qPCR and normalized to 18S rRNA levels with the value at 0 μg/ml α-amanitin defined as 1. **(C)** Synchronized early L1-stage N2 worms were liquid-cultured with food for 2 hours, and α-amanitin was added to 50 μg/ml final concentration. The worms were harvested at indicated time points, and RNA was extracted. pre-eft-3 mRNA levels were examined by RT-qPCR and normalized to 18S rRNA levels with the value at 0 h defined as 1.

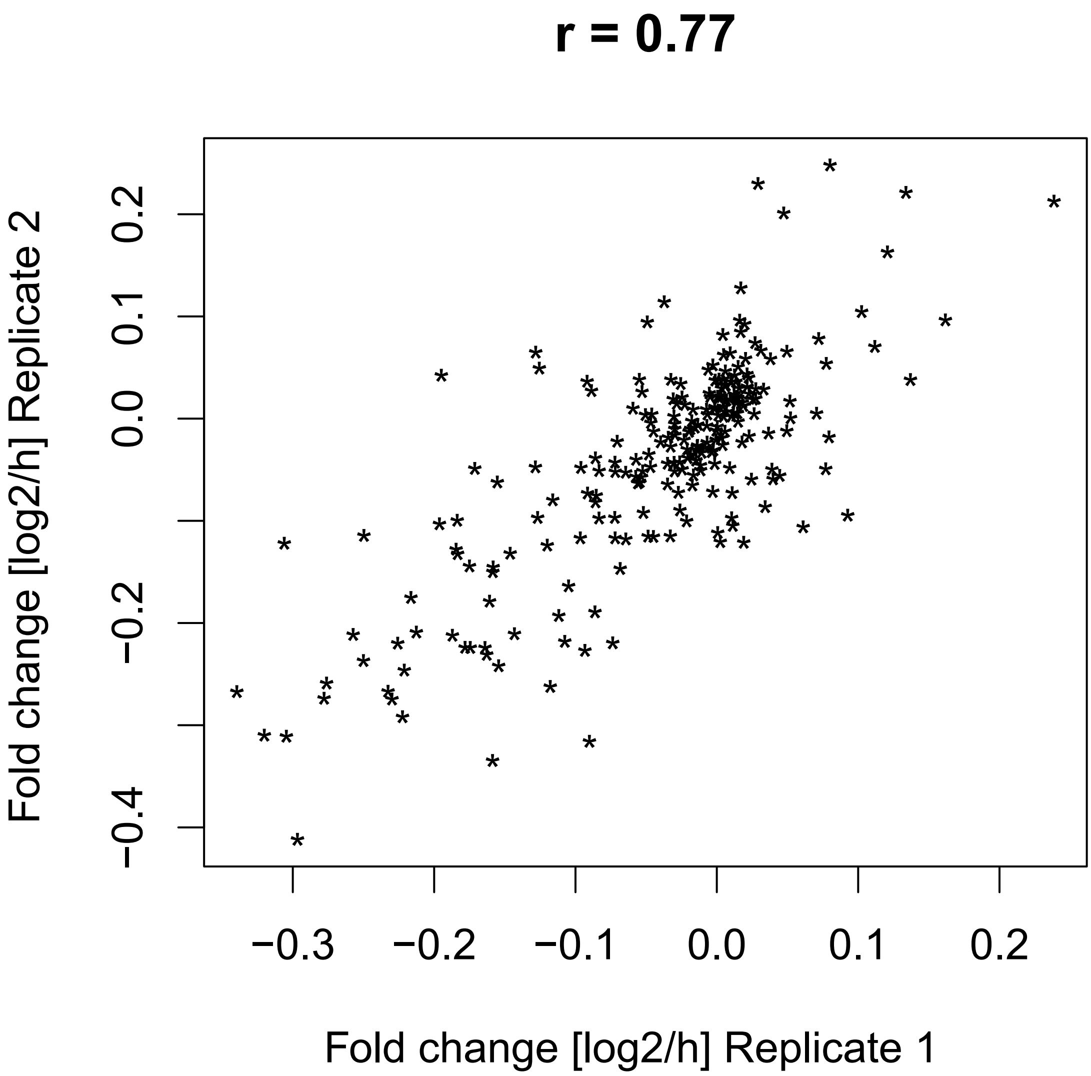

Figure S3. Correlation of relative decay rates calculated from two biological replicates.
Relative fold changes per hour were calculated as described in Materials and Methods independently for two biological replicates and found to correlate well (r=0.77).

Figure S4

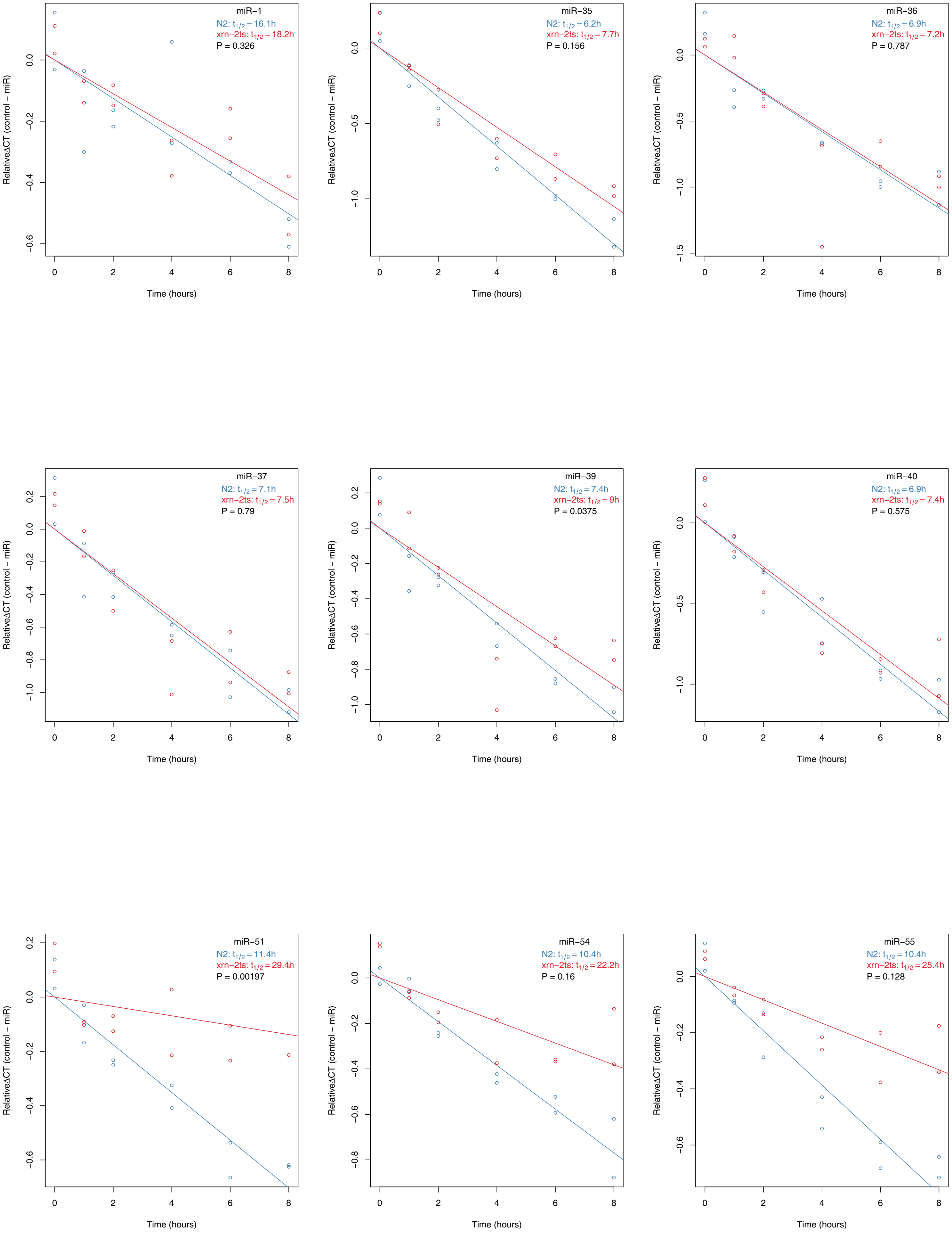
miR−1
N2: $t_{1/2} = 16.1$h
xrn−2ts: $t_{1/2} = 18.2$h
P = 0.326
miR−35
N2: $t_{1/2} = 6.2$h
xrn−2ts: $t_{1/2} = 7.7$h
P = 0.156
miR−36
N2: $t_{1/2} = 6.9$h
xrn−2ts: $t_{1/2} = 7.2$h
P = 0.787
miR−37
N2: $t_{1/2} = 7.1$h
xrn−2ts: $t_{1/2} = 7.5$h
P = 0.79
miR−39
N2: $t_{1/2} = 7.4$h
xrn−2ts: $t_{1/2} = 9$h
P = 0.0375
miR−40
N2: $t_{1/2} = 6.9$h
xrn−2ts: $t_{1/2} = 7.4$h
P = 0.575
miR−51
N2: $t_{1/2} = 11.4$h
xrn−2ts: $t_{1/2} = 29.4$h
P = 0.00197
miR−54
N2: $t_{1/2} = 10.4$h
xrn−2ts: $t_{1/2} = 22.2$h
P = 0.16
miR−55
N2: $t_{1/2} = 10.4$h
xrn−2ts: $t_{1/2} = 25.4$h
P = 0.128
Relative∆CT (control − miR)
Time (hours)
0
2
4
6
8
0.0
−0.2
−0.4
−0.6
−0.5
−1.0
−1.5
0.2
−0.8

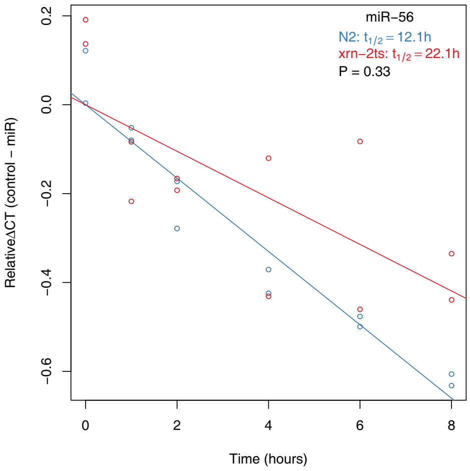
miR−56
N2: $t_{1/2} = 12.1$h
xrn−2ts: $t_{1/2} = 22.1$h
P = 0.33
RelativeΔCT (control − miR)
0.2
0.0
−0.2
−0.4
−0.6
Time (hours)
0
2
4
6
8

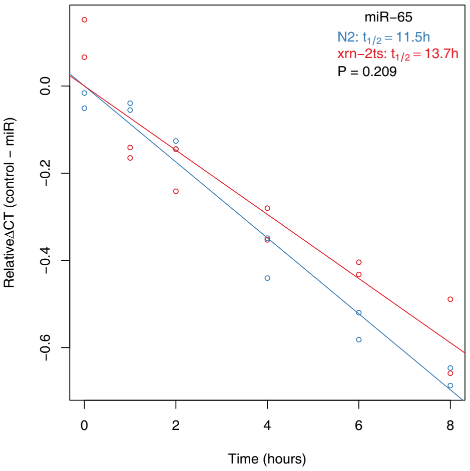
miR−65
N2: $t_{1/2} = 11.5$h
xrn−2ts: $t_{1/2} = 13.7$h
P = 0.209
RelativeΔCT (control − miR)
0.0
−0.2
−0.4
−0.6
Time (hours)
0
2
4
6
8

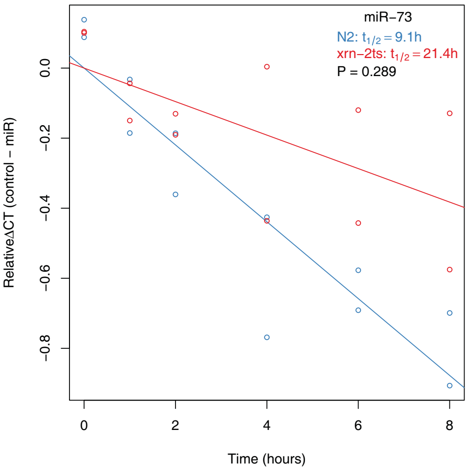
miR−73
N2: $t_{1/2} = 9.1$h
xrn−2ts: $t_{1/2} = 21.4$h
P = 0.289
RelativeΔCT (control − miR)
0.0
−0.2
−0.4
−0.6
−0.8
Time (hours)
0
2
4
6
8

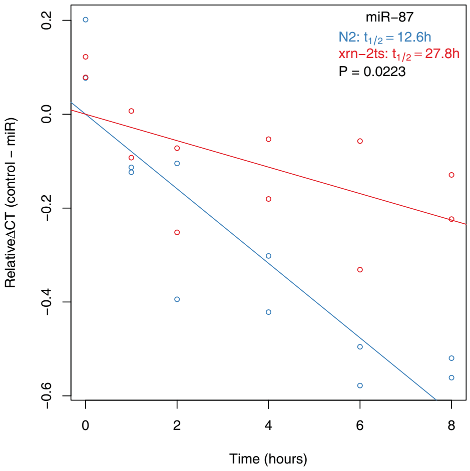
miR−87
N2: $t_{1/2} = 12.6$h
xrn−2ts: $t_{1/2} = 27.8$h
P = 0.0223
RelativeΔCT (control − miR)
0.2
0.0
−0.2
−0.4
−0.6
Time (hours)
0
2
4
6
8

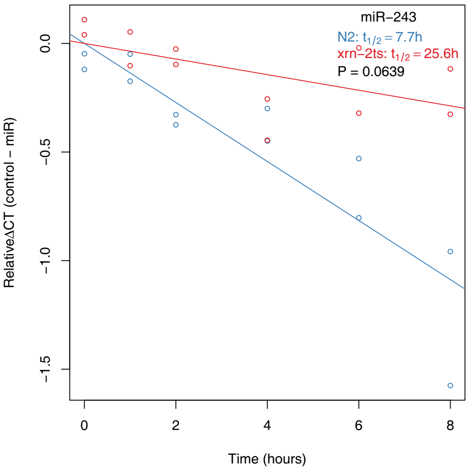
miR−243
N2: $t_{1/2} = 7.7$h
xrn−2ts: $t_{1/2} = 25.6$h
P = 0.0639
RelativeΔCT (control − miR)
0.0
−0.5
−1.0
−1.5
Time (hours)
0
2
4
6
8

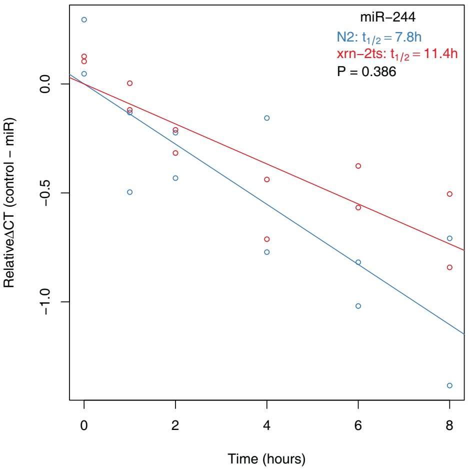
miR−244
N2: $t_{1/2} = 7.8$h
xrn−2ts: $t_{1/2} = 11.4$h
P = 0.386
RelativeΔCT (control − miR)
0.0
−0.5
−1.0
Time (hours)
0
2
4
6
8

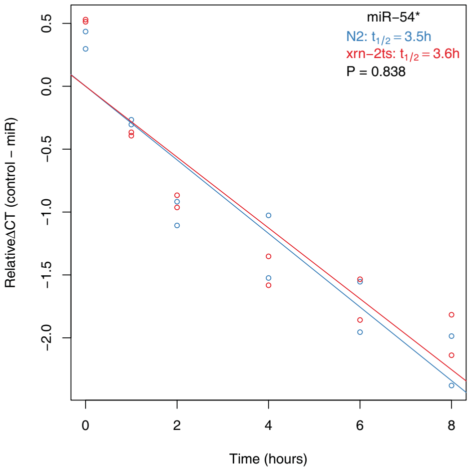
miR−54*
N2: $t_{1/2} = 3.5$h
xrn−2ts: $t_{1/2} = 3.6$h
P = 0.838
RelativeΔCT (control − miR)
0.5
0.0
−0.5
−1.0
−1.5
−2.0
Time (hours)
0
2
4
6
8

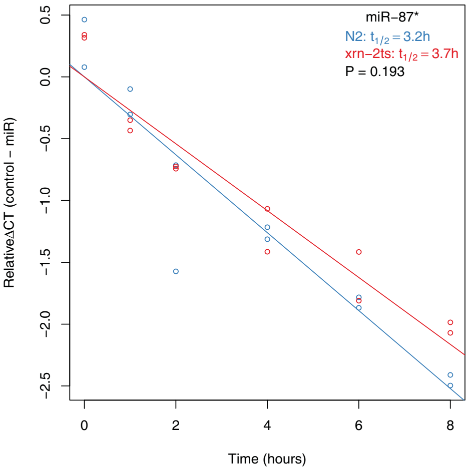
miR−87*
N2: $t_{1/2} = 3.2$h
xrn−2ts: $t_{1/2} = 3.7$h
P = 0.193
RelativeΔCT (control − miR)
0.5
0.0
−0.5
−1.0
−1.5
−2.0
−2.5
Time (hours)
0
2
4
6
8

Figure S4. Decay of miRNAs in L1-stage wt and *xrn-2ts* worms.

miRNA levels at each time point in L1-stage wt and *xrn-2ts* worms were quantified by RT-qPCR and normalized to sn2841 levels. Values (circles) and trend lines for each miRNA in wt and *xrn-2ts* worms are shown in blue and red, respectively. Half-lives ($t_{1/2}$) and P-values are also shown (see Materials and Methods).

Supplementary Tables.

Table S1. Strain information

Strain name	Alias	Genotype	Locus of single copy insertion
HW426		*xrn-2(tm3473)/+ II*	
HW666		*xrn-2(tm3473) II ; unc-119(ed3) III; xeEx267[Pxrn-2:xrn-2(D234/236A)::gfp::his::flag::xrn-2 3'utr, unc-119(+)]*	
HW737		*xrn-2(tm3473) II ; unc-119(ed3) III; xeEx234[Pxrn-2::xrn-2(cDNA)::gfp::his::flag::xrn-2 3'utr, unc-119(+)]*	
HW777		*xeSi15[Pxrn-2::xrn-2(cDNA)::gfp::his::flag::xrn-2 3'utr] IV*	*cxTi10882*
HW844*		*xrn-2(tm3473) II/mnC1[dpy-10(e128) unc-52(e444) nIs190] II*	
HW851		*xrn-2(tm3473) II ; xeSi15[Pxrn-2::xrn-2(cDNA)::gfp::his::flag::xrn-2 3'utr] IV*	*cxTi10882*
HW1011	*xrn-2ts*$_{cDNA}$	*xeSi56[Pxrn-2::xrn-2(P107L)::GFP::his::flag::xrn-2 3'utr;unc-119(+)] I; xrn-2(tm3473) II*	*ttTi4348*
HW1021		*xeSi60[Pxrn-2::xrn-2(codon-optimized)::gfp::his::flag::xrn-2 3'utr;unc-119(+)] I*	*ttTi4348*
HW1023	*xrn-2(+)*	*xeSi60[Pxrn-2::xrn-2(codon-optimized)::gfp::his::flag::xrn-2 3'utr;unc-119(+)] I; xrn-2(tm3473) II*	*ttTi4348*
HW1026	*xrn-2ts*	*xeSi57[Pxrn-2::xrn-2(codon-optimized/P107L)::GFP::his::flag::xrn-2 3'utr;unc-119(+)] I; xrn-2(tm3473) II*	*ttTi4348*
HW1094		*xeSi74[Pxrn-2*$_{132bp}$*::xrn-2(codon-optimized)::gfp::his::flag::xrn-2 3'utr, unc-119(+)] I ; xrn-2(tm3473) II/mnC1[dpy-10(e128) unc-52(e444) nIs190] II**	*ttTi4348*

*The *xrn-2(tm3473)* mutation was balanced in this strain using a gfp-tagged mnC1 balancer introduced by crossing with strain MT16418, kindly provided by R. Horvitz and D.T. Harris

Table S2. Primer information

Cloning		
	Forward (5'-->3')	**Reverse (5'-->3')**
Pxrn-2$_{1413bp}$	ctgatggaaatatattaa	tctcggagttttattttctc
Pxrn-2$_{132bp}$	acatattaatcccccgaacggggcctcc	tctcggagttttattttctctaaat
xrn-2(cds)	atgggagttcccgcattc	tctccatgatgaatttcc
xrn-2_3'utr	catcagcattcagtcgat	gcgctccatggacaatcgcct
Site-directed mutagenesis		
	Forward (5'-->3')	**Reverse (5'-->3')**
P107L for xrn-2cts	atcgatggagttgctctgcgagccaagatgaacc	ggttcatcttggctcgcagagcaactccatcgat
P107L for xrn-2ts	catcgacggagtcgccctacgtgccaagatgaac	gttcatcttggcacgtagggcgactccgtcgatg
D234A	gcctctgcggagccgccgccgaccttattatgctcgg	
D236A	gcggagccgacgccgcccttattatgctcgg	ccgagcataataagggcggcgtcggctccgc
Y594C	ggtatttcccgtatcattgtgcaccgtttgccagcg	
RT-qPCR		
	Forward (5'-->3')	**Reverse (5'-->3')**
pre-eft-3 mRNA	acttgatctacaagtgcggagga	cgggtgagaaaatctttcaaacta
18S rRNA	cagaccaaacgttttcggacgttg	ttggacgtggtagccgtttctaag
codon-optimized xrn-2 mRNA	ggacacgagctcaagggagtg	gctccttctcgaggtactcacg
actin mRNA	gttgcccagaggctatgttc	caagagcggtgatttccttc
Genotyping		
	Forward (5'-->3')	**Reverse (5'-->3')**
tm3473 genotyping	gagacttaaatccctaaaattcacc	ctttgtcagataacctttcatctgg

Table S3. The sequence of codon-optimized *xrn-2* with three introns

```
ATGGGAGTCCCAGCCTTCTTCCGTTGGCTCACCAAGAAGTACCCAGCCACCGTCGTCAACGCCAACGA
GGACCGTCAACGTGACCAAGACGGAAACCGTGTCCCAGTCGACTGCACCCAACCAAACCCAAACTTCC
AAGAGTTCGACAACCTCTACCTCGACATGAACGGAATCATCCACCCATGCACCCACCCAGAGGACCGT
CCAGCCCCAAAGAACGAGGACGAGATGTTCGCCCTCATCTTCGAGTACATCGACCGTATCTACTCCAT
CGTCCGTCCACGTCGTCTCCTCTACATGGCCATCGACGGAGTCGCCCCACGTGCCAAGATGAACCAAC
AACGTTCCCGTCGTTTCCGTGCCTCCAAGGAGATGGCCGAGAAGGAGGCCTCCATCGAGGAGCAACG
TAACCGTCTCATGGCCGAGGGAATCGCCGTCCCACCAAAGAAGAAGGAGGAGGCCCACTTCGACTCC
AACTGCATCACCCCAGGAACCCCATTCATGGCCCGTCTCGCCGACGCCCTCCGTTACTACATCCACGA
CCGTGTCACCAACGACGCCTCCTGGGCCAACATCGAGATCATCCTCTCCGACGCCAACGTCCCAGGA
GAGGGAGAGCACAAGATCATGGACTACGTCCGTAAGCAACGTGGAAACCCAGCCCACGACCCAAACA
CCGTCCACTGCCTCTGCGGAGCCGACGCCGACCTCATCATGCTCGGAATCGCCACCCACGAGGCCAA
CTTCAACATCATCCGTGAGGAGTTCGTCCCAAACCAACCACGTGCCTGCGACCTCTGCGGACAATACG
GACACGAGCTCAAGgtaagtttaaacatatatatactaactaaccctgattatttaaattttcagGAGTGCCGTGGAGCCGAGAAC
GAGACCGACCTCGGAGACGACTACTGCAAGCCAGAGCAACGTGAGAAGAACTTCATCTTCCTCCGTAT
CCCAGTCCTCCGTGAGTACCTCGAGAAGGAGCTCTCCATGCCAAACCTCCCATTCAAGTTCGACGTCG
AGCGTGCCCTCGACGACTGGGTCTTCCTCTGCTTCTTCGTCGGAAACGACTTCCTCCCACACCTCCCAT
CCCTCGAGATCCGTGAGGGAGCCATCGACCGTCTCATCAAGCTCTACAAGGAGATGGTCTACCAAATG
AAGGGATACCTCACCAAGGACGGAATCCCAGAGCTCGACCGTGTCGAGATGATCATGAAGGGACTCG
GACGTGTCGAGGACGAGATCTTCAAGCGTCGTCAACAAGACGAGGAGCGTTTCCAAGAGAACCAACGT
AACAAGAAGGCCCGTATGCAAATGTACGGAGGAGGAGGACGTGGAGGACGTGGACGTGGACGTGGAC
GTGGACAACAACCAGCCTTCGTCCCAACCCACGGAATCCTCGCCCCAATGGCCGCCCCAATGCACCAC
TCCGGAGAGTCCACCCGTCAAATGGCCTCCGAGGCCCGTCAAACCGCCATGAAGTTCACCAACGACG
CCAACGAGACCGCCGCCGCCAACCTCAAGgtaagtttaaacagttcggtactaactaaccatacatatttaaattttcagGCCCTC
CTCAACGTCAAGGGAGAGGAGTCCCCAGCCGACATCGCCTCCCGTAAGCGTAAGGCCGAGCAACCAC
TCATCAAGCCAGAGGAGGAGGAGGACGAGGGACCAAAGGACGACATCCGTCTCTACGAGTCCGGATG
GAAGGACCGTTACTACCGTGCCAAGTTCGACGTCGGATCCGACGACATCGAGTTCCGTCACCGTGTCG
CCTGGGCCTACGTCGAGGGACTCTGCTGGGTCCTCCGTTACTACTACCAAGGATGCGCCTCCTGGGAC
TGGTACTTCCCATACCACTACGCCCCATTCGCCTCCGACTTCGAGACCGTCGGAGAGTTCCAACCAGA
CTTCACCCGTCCAACCAAGCCATTCAACCCACTCGAGCAACTCATGTCCGTCTTCCCAGCCGCCTCCAA
GCAACACCTCCCAGTCGAGTGGCAAAAGCTCATGATCCAAGACGACTCCCCAATCATCGACCTCTACC
CAGCCGACTTCCGTATCGACCTCAACGGAAAGAAGTACGCCTGGCAAGGAGTCGCCCTCCTCCCATTC
GTCGACGAGACCCGTCTCCTCGCCACCCTCCAATCCGTCTACCCAACCCTCACCGCCGAGGAGAAGC
AACGTAACACCCGTGGACCAAACCGTATCTTCATCGGACGTAACCACAAGTCCTTCGAGTTCTTCCAAC
AAGTCGCCGAGTCCAAGTCCGACGACCTCGTCCCACTCGACCCAACCCTCCTCAACGGAGTCTCCGGA
AAGgtaagtttaaacatgattttactaactaactaatctgatttaaattttcagATCGCCTACGACTCCACCGCCACCGCCCCAGGA
CTCCCATTCGTCTCCCCAGTCAACCACGACGAGTGCCAAGACCTCCCAACCAACTGCGGAATCTGCGT
CCTCTACGAGGACCCAGAGTACCCACAAGACTACATCTTCCCAGCCCTCCGTCTCGACGGAGCCAAGG
AGCCAGAGAAGACCCTCAAGCCAGACGACTGGAACGACCGTCGTGACGGACGTTACCAACCACAAGT
CGGATTCAACCGTAACGCCCCACGTGGATCCCTCGACCAATCCGGACACCGTCAAGTCCACCACTACG
TCCGTGGAGGAGGAGGAGGAGGAGGAGGATACCGTGGAAACTCCTACGACGACCGTCGTGGAGGAG
GAGGAGGAGGAGGAGGATACAACGACCGTCAAGACTTCGGACGTAACTACGGAGGACGTGACGGAGG
AGGACCACAACGTTACCACGACCAACAACAACAACGTCAAGGAGGATACCAAGGAGGAGGATACGGA
GGAGGATACGGAGGAGGAGGAGGAGGAGGAGGAGGAGGAGGAGGAGGATCCTACCACCAACCATAC
AACCAAGACCAACGTCGTGGAGGACGTGGAGGAGGAGGAGGACCACCAGGATACCAACGTCCACCAT
ACCGTGGAGGAGGAGGAGGAGGATACCACGGAAACTCCTCCTGGCGT
```

Lower case: intron

3.3.2 Additional results

XRN2 and PAXT-1 form a complex

Figure 1 and 2 summarize my main contributions to section 6. For an integral view please refer to section 6. Through co-immunoprecipitations, I identified the previously uncharacterized protein PAXT-1 as an interaction partner of XRN2 (Fig. 1). PAXT-1 does not bind to the XRN2 paralogue XRN1. Additionally, I found that a domain of unknown function (DUF3469) within PAXT-1 is sufficient to bind to XRN2 (Fig. 2). Subsequent experiments carried out by Takashi Miki and Hannes Richter showed that the interaction between XRN2 and PAXT-1 is direct and leads to mutual stabilization of the binding partners (see section 6).

(A)

		XRN2/GFP/FLAG		GFP/FLAG	
		XRN2	PAXT-1	XRN2	PAXT-1
Replicate 1	Assigned spectra	188	27	1	0
	% coverage	47	65	2	0
Replicate 2	Assigned spectra	157	19	0	0
	% coverage	37	45	0	0

(B)

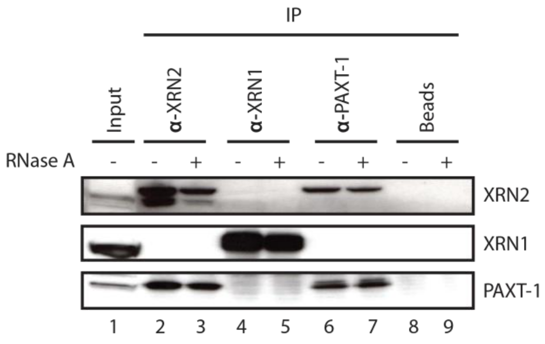

Figure 1. XRN2 and PAXT-1 interact *in vivo*.

(**A**) Two replicates of mass spectrometry following IP of transgenic, FLAG-tagged XRN2 detect R05D11.6/PAXT-1 above the background (i.e. GFP/FLAG control) in total eluates. (**B**) Western blot analysis of IPs against endogenous XRN1, XRN2, and R05D11.6/PAXT-1. R05D11.6/PAXT-1 is detected in the XRN2 IP (lane 2 and 3) and vice versa (lane 6 and 7). R05D11.6/PAXT-1 does not interact with XRN1 (lanes 4-7). RNase A treatment does not abolish the R05D11.6-XRN2 interaction. 10% of input and 100% of eluate was loaded. Note that in this and similar figures below, differences in salt concentrations cause high molecular weight proteins (XRN1, XRN2) to migrate slightly differently in input vs. eluate samples.

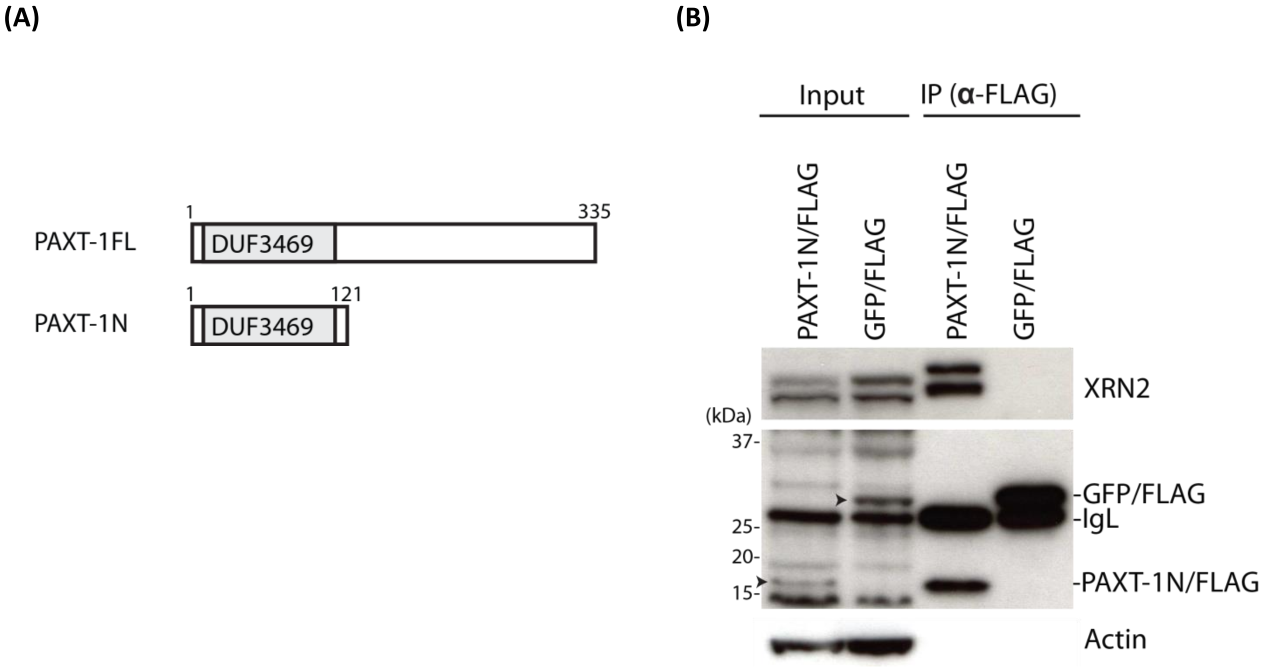
(A)
(B)
PAXT-1FL
1
DUF3469
335
PAXT-1N
1
DUF3469
121
Input
IP (α-FLAG)
PAXT-1N/FLAG
GFP/FLAG
PAXT-1N/FLAG
GFP/FLAG
XRN2
(kDa)
37-
25-
20-
15-
-GFP/FLAG
-IgL
-PAXT-1N/FLAG
Actin

Figure 2. DUF3469 is a *bona fide* XRN2-binding domain.

(**A**) Schematic drawings of full-length (PAXT-1FL) and a truncation muntant (PAXT-1N) of PAXT-1. Amino acid numbers relative to the first methionine of PAXT-1 are indicated. (**B**) PAXT-1N/FLAG co-immunoprecipitates XRN2 whereas GFP/FLAG does not. 5% of input and 15% of eluate was loaded. Note that GFP/FLAG is overloaded. Arrowheads indicate PAXT-1N/GFP and GFP/FLAG. IgL, immunoglobulin light chain.

Towards identification of the nuclear localization signal of XRN2

XRN2 is a nuclear exoribonuclease that targets specific mature miRNAs (section 3.3.1). As mature miRNAs occur in the cytoplasm as well as in the nucleus (Jeffries et al., 2011; Liao et al., 2010) an appealing model suggests that certain miRNAs are shielded from XRN2 degradation by their cytoplasmic localization. In order to test this model, I aimed to mislocalize XRN2 to the cytoplasm. Mutating a putative bipartite nuclear localization signal (NLS) (Fig. 3A) failed to redirect XRN2 to the cytoplasm (data not shown). Subsequently, I tested different truncation mutants for their subcellular localization. The shortest of these mutants, which lacks an unconserved linker between two conserved regions and the C-terminal 154 amino acids, still resided in the nucleus (Fig. 3). The NLS within XRN2 thus remains to be discovered.

(A)

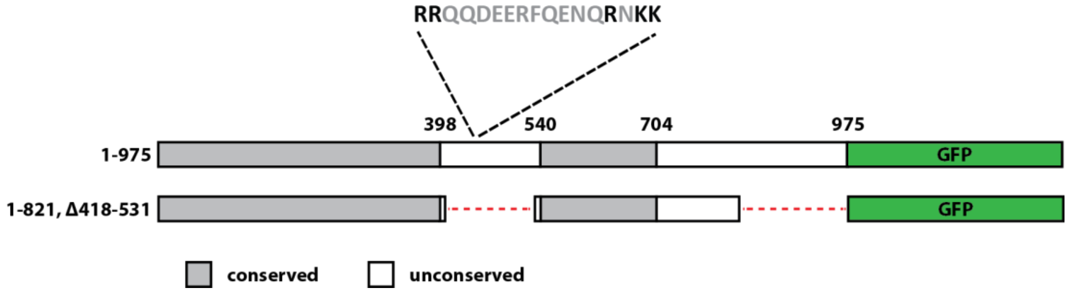

(B)

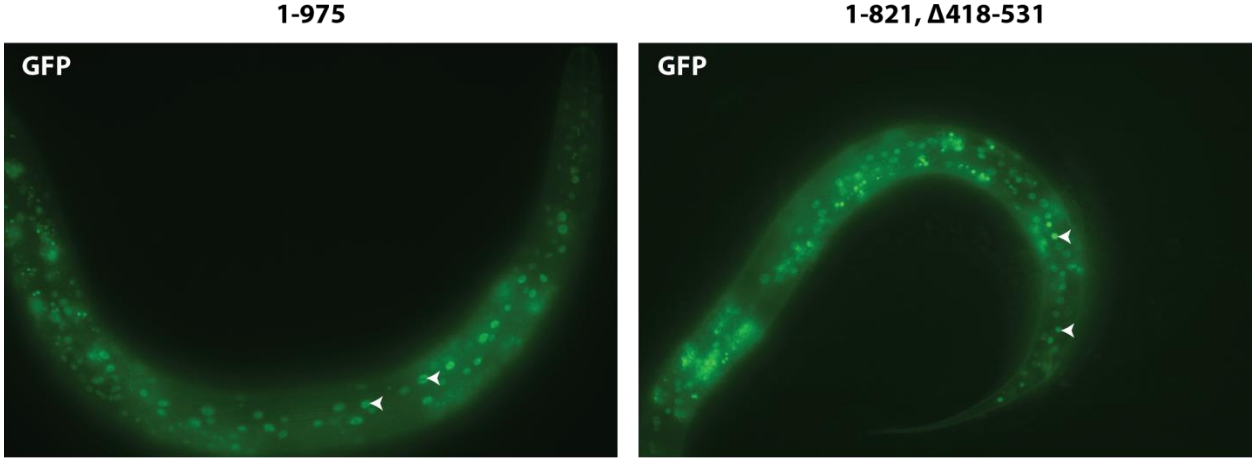

Figure 3. Deletion of a putative NLS does not result in cytoplasmic expression of XRN2.

(**A**) Schematic representation of wild-type XRN2 (1-975) and a truncated version of XRN2 (1-821, Δ418-531). Dashed lines indicate deleted parts. A putative bipartite NLS is highlighted. The five basic residues that define the NLS are shown in black. (**B**) Micrographs showing GFP signal of single-copy-integrated transgenes shown in (A) expressed under the endogenous *xrn-2* promoter and 3' UTR. Both the wild-type and the truncated transgene show an exclusive nuclear localization (arrow heads point to nuclei).

Worms deleted for xrn-1 exhibit strong morphological defects

My work investigated the developmental and molecular function of XRN2 and did largely exclude its cytoplasmic paralogue XRN1. The developmental functions of XRN1 have been investigated to a larger extent compared to XRN2 with the caveat that studies have been relying on *xrn-1* knock-down or hypomorphic alleles (Jones et al., 2012). Loss-of-function mutations of XRN1 might reveal additional phenotypes not detected by reduction-of-function mutations. I created a null allele of *xrn-1* through TALE nuclease-mediated genome editing (SR and HG, unpublished). The allele was called *xe4* and is characterized by a premature termination codon most likely leading to NMD (Fig. 4A). A western blot with lysate from worms homozygous for *xe4* failed to detect full-length XRN1 (Fig. 4B). Surprisingly, worms deficient for *xrn-1*, despite showing multiple morphological defects and greatly reduced brood size, are viable (Fig. 4C and data not shown). Note that I failed to rescue these phenotypes by expressing transgenic, codon-optimized *xrn-1* (Fig. 4B and data not shown). Hence, phenotypes observed in worms homozygous for the *xe4* allele cannot definitely be attributed to XRN1. A thorough analysis of phenotypes arising upon complete loss of XRN1 awaits realization.

(A)

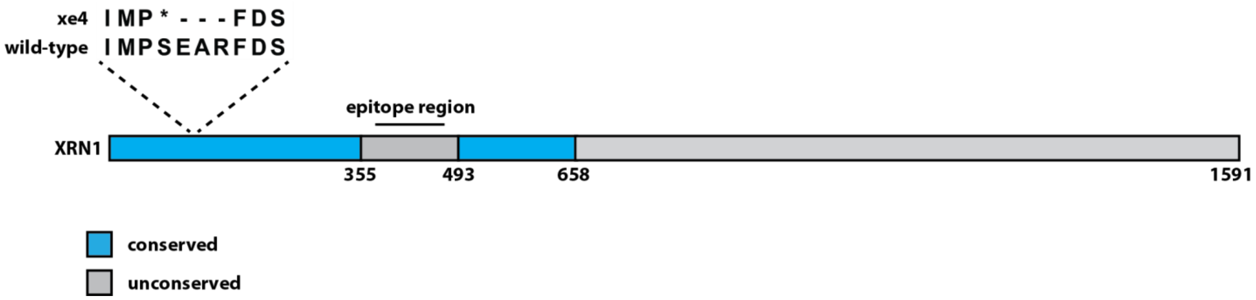
xe4 IMP*---FDS
wild-type IMPSEARFDS
epitope region
XRN1
355
493
658
1591
conserved
unconserved

(B)

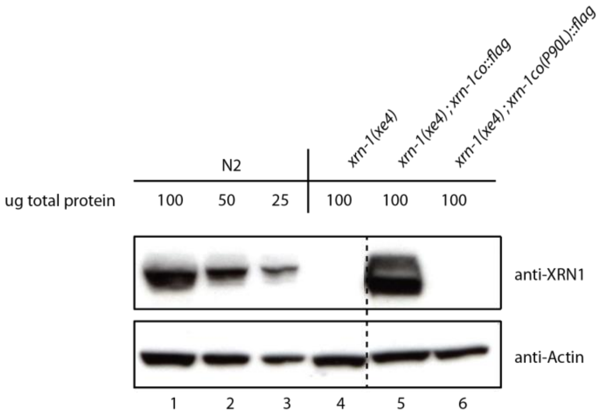
xrn-1(xe4)
xrn-1(xe4); xrn-1co::flag
xrn-1(xe4); xrn-1co(P90L)::flag
N2
ug total protein
100
50
25
100
100
100
anti-XRN1
anti-Actin
1
2
3
4
5
6

(C)

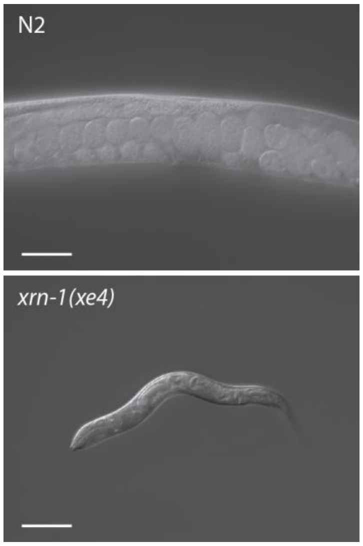

Figure 4. *xrn-1*(*xe4*) is a null allele.

(A) Schematic representation of XRN1 protein. The *xe4* allele of XRN1 is characterized by a stop codon at amino acid position 124 (serine in wild-type XRN1) followed by a deletion of three amino acids. The epitope region for a polyclonal antibody from rabbit (spanning amino acids 375-474) is indicated. **(B)** Western blot showing XRN1 levels in different worm lines. Lane 1-3: wild-type worms, lane 4: worms homozygous for the *x4* allele, lane 5-6: worms expressing transgenic, flag-tagged and codon-optimized (co) wild-type *xrn-1* (lane 5) or mutant *xrn-1* in which leucine (L) at position 90 was changed to proline (P) (lane 6). *xrn-1co* shows a double band whose nature is unknown. Initially, I conceived the possibility that *xrn-1co*(*P90L*) results in a temperature sensitive version of XRN1 similar to the P107L mutation in XRN2 but it appears that XRN1(P90L) is unstable and degraded. The dashed line indicates a region where lanes have been removed. Detection of XRN1 was achieved by a polyclonal antibody produced in rabbit (nr. Q4886). Its epitope region is shown under (A). **(C)** DIC micrograph of a wild-type worm (N2) and a worm homozygous for the *xe4* allele (*xrn-1*(*xe4*)) after 48 h at 25°C. *xrn-1*(*xe4*) animals are greatly developmentally retarded. Scale bar, 50 µm.

3.4 Outlook

A detailed discussion of the results is included in section 3.3.1 and 6. Here, I emphasize some open questions that require our attention in the future.

We find that XRN2 is essential for *C. elegans* at every developmental stage from the embryo to the adult worm. This raises the question of what the pathways are that ultimately cause lethality upon inactivation of XRN2 , a question not easily answered considering the various coding and non-coding RNA substrates reported for XRN2 (Nagarajan et al., 2013). The subset of miRNAs targeted by XRN2 is unlikely to elicit a terminal phenotype as most miRNAs play only a subtle role during development and lack a strong phenotype when deleted individually or as whole families (Alvarez-Saavedra and Horvitz, 2010). Although it cannot be excluded that overexpression of miRNAs, as observed in an *xrn-2* null mutant situation, has actually more detrimental consequences for the worm than their deletion, it is most likely that lethality of *xrn-2* null worms results from abolished processing/degradation of multiple substrates. It remains a future challenge to assign phenotypes to specific XRN2 substrates.

XRN2 is localized in the nucleoplasm (sections 3.3.1 and 7). On the other hand, mature miRNAs have long been assumed to regulate expression of protein-coding genes in the cytoplasm (Krol et al., 2010). This raises the question how XRN2 may gain access to its miRNA targets. This issue is largely resolved by many recent studies revising our view of an exclusive cytoplasmic localization of mature miRNAs. High-throughput approaches, such as deep sequencing and miRNA TaqMan arrays, have been used to compare levels of mature miRNAs in nuclear and cytoplasmic fractions in human cells revealing that most miRNAs are present in both compartments and that a roughly similar fraction is specifically localized in one or the other compartment (Jeffries et al., 2011; Liao et al., 2010). Importantly, Argonaute proteins, the effector components of the miRISC complex, have been shown to reside in the nucleus (Weinmann et al., 2009; Zisoulis et al., 2012). This suggests that the nuclear miRNAs have biological relevance. In fact, it was found that nuclear miRNAs can promote (Zisoulis et al., 2012) or repress (Tang et al., 2012) the processing of primary miRNA transcripts and can direct cleavage of lncRNAs (Hansen et al., 2011). Subcellular localization might be one aspect underlying the specificity of XRN2 towards particular miRNAs. However, whether the specific miRNAs targeted by XRN2 in our study indeed exhibit a predominant nuclear localization remains to be tested. Redirecting XRN2 to the cytoplasm and likewise XRN1 to the nucleus will reveal the contribution of localization to miRNA turnover. Target-specificity might also be brought about by XRN2-binding proteins. We identified PAXT-1 as an essential interaction partner of XRN2. Nonetheless, it remains to be shown whether or not PAXT-1 conveys target-specificity to XRN2.

4 USIP-1 is a terminal transferase acting upstream of SART-3 in spliceosome assembly

4.1 Abstract

The primary transcripts of most eukaryotic genes requires the removal of intervening sequences (introns) through a process referred to as splicing in order to become mature mRNAs. Given the essential role of U6 snRNA in the splicing catalysis it is of great interest to identify *trans*-acting factors that mediate the extensive conformational changes that U6 undergoes during the splicing cycle. The RNA-binding protein Prp24 and SART3 have been reported in yeast and human cell culture, respectively, to interact with the U6 snRNA and to promote its association with the U4 snRNA. Here, we describe the molecular and developmental function of the previously uncharacterized *C. elegans* ortholog of SART3, SART-3. Co-immunoprecipitations of transgenic and endogenous SART-3 from *C. elegans* lysates revealed an interaction with the U4/U6 snRNP complex analogous to human SART3. Furthermore, we identified a U6 snRNA-mediated interaction between SART-3 and USIP-1, a terminal uridylyl transferase (TUTase). Through fluorescence microscopy, we found both SART-3 and USIP-1 to localize in the nucleoplasm and to be constitutively and ubiquitously expressed across developmental stages and tissues, respectively. Whereas SART-3 was found in complex with the U4/U6 di-snRNP, USIP-1 associated with the 'naked', that is Lsm/Sm-unbound, U6 snRNA suggesting a participation of USIP-1 in U6 snRNA processing rather than spliceosome recycling. Knock-down of *sart-3* in a *usip-1* null mutant background caused a synergistic, embryonic lethal phenotype further supporting an involvement of USIP-1 in the U6 snRNA life cycle. The embryonic lethality was rescued by transgenic expression of wild-type USIP-1 but not by a catalytically inactive version of USIP-1. Finally, through MosDEL genome editing we obtained a loss-of-function allele for *sart-3* whose phenotype is characterized by lack of oocytes and vulval bursting. Together, our data demonstrate that SART-3 associates with the U4/U6 snRNP and genetically interacts with the upstream acting terminal transferase USIP-1.

4.2 Introduction

RNA splicing

Alternative splicing increases the coding potential of a genome

During transcription particular segments of DNA are copied into RNA. The primary transcript of almost all protein-coding genes in multicellular organisms, the precursor messenger RNA (pre-mRNA), contains introns and exons. Introns are excised from the pre-mRNA and exons are joined in a process termed splicing in order to establish the mature mRNA with a translatable open reading frame (ORF) (Sharp, 2005). Splicing is found in species from bacteria to humans but whereas splicing is ubiquitous in eukaryotes there are only a few examples in bacteria (Edgell et al., 2000) and archaea (Watanabe et al., 2002; Yokobori et al., 2009). Through alternative splicing (AS) the coding capacity of a genome can be expanded manifold by producing different isoforms from a single transcript (Keren et al., 2010; Kornblihtt et al., 2013). AS events can be categorized into four main groups (Fig. 1): 1) Exon skipping denotes an AS event whereby an exon gets spliced out together with its flanking introns. 2-3) Alternative 3’ and 5’ splice sites can occur within exons resulting in only partial inclusion of a particular exon in the mature mRNA transcript. 4) Lastly, introns can be retained in the mature mRNA (Keren et al., 2010). It is probably of little surprise that it was found that the extent by which an organism uses AS correlates with its complexity, i.e. position within the phylogenetic tree. Higher eukaryotes have a stronger preference for AS than lower eukaryotes (Alekseyenko et al., 2007; Artamonova and Gelfand, 2007; Kim et al., 2004a). Thus, AS might provide an explanation for the difference in complexity between humans and worms despite the fact that both organisms have roughly the same number of genes (worms ~19’000, humans ~22’000). Furthermore, AS, with contribution of alternative initiation of transcription and alternative mRNA cleavage/polyadenylation, illustrates how the discrepancy between the predicted 22’000 protein-coding genes in the human genome and the proteome with estimated 100’000 entities emerges (Modrek and Lee, 2002). Impressively, >90% of human genes were found to undergo AS (Wang et al., 2008). The physiological importance of AS becomes evident by the observation that aberrant alternative splicing plays a causal role in various diseases including cancer (Srebrow and Kornblihtt, 2006; Tazi et al., 2009).

Depending on how much a splice site diverges from the consensus sequence it is considered a weak or a strong splice site. Strong splice sites lead to constitutive splicing whereas the decision whether to use a weak splice site or not requires input from additional *cis* and *trans*-acting factors (Singh and Valcarcel, 2005). *Cis*-regulatory sequences are named according to their position (exonic/intronic) and effect on a particular splice site (enhancer/silencer): exonic splicing enhancer (ESE), exonic splicing silencer (ESS), intronic splicing enhancer (ISE) and intronic splicing silencer (ISS). *Trans*-acting factors, that can be either enhancers, silencers, or both, act by binding to the *cis*-regulatory sequences and include the serine-arginine-rich (SR) and heterogeneous nuclear ribonucleoprotein (hnRNP) protein families (Singh and Valcarcel, 2005). A yet additional layer of splicing regulation was established when it was found that splicing and transcription are functionally coupled. Although splicing is known for quite a while to occur in most cases co-transcriptionally (Beyer and Osheim, 1988), there is now increasing evidence that promoters, transcription factors, and transcriptional co-activators are not only in close proximity to but participate in the regulation of splicing (Kornblihtt et al., 2013).

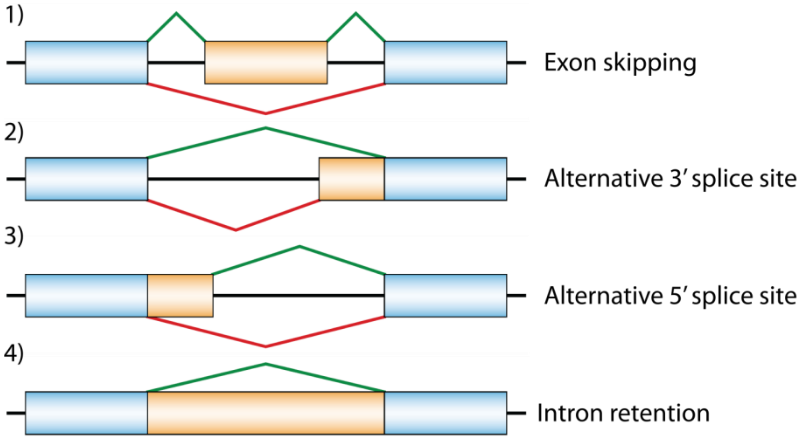

Fig. 1. Modes of alternative splicing. Blue: constitutive exon, orange: alternatively spliced exon, black line: intron. Alternative splicing paths are indicated in green and red, respectively. Modified with permission from doi: 10.1038/nrg775.

The spliceosome

Constitutive and alternative splicing are catalyzed by the same core machinery, the spliceosome, a multisubunit ribonucleoprotein (RNP) (Wahl et al., 2009). The spliceosome binds to short consensus sequences within the intron that lie at the very 5’ end (5’ splice site, 5’SS), at the very 3’ end (3’ splice site, 3’SS), and 20-50 nucleotides upstream of the 3’SS (branch point, BP). Also, there is a pyrimidine-rich sequence found between the branch point and the 3’SS (called polypyrimidine tract) that is recognized by splicing factors. The challenge for the spliceosome is to reliably recognize these rather relaxed consensus elements and precisely align them within the catalytic center in order for splicing to take place. On the other hand the spliceosome should feature a high degree of flexibility to enable AS. In order to cope with these opposed demands of great precision and high flexibility, the spliceosome integrates a multitude of proteins that interact in a highly dynamic manner. Precision of the splicing reaction is achieved by the fact that a particular consensus sequence on the pre-mRNA is recognized several times by consecutive splicing factors. Redundant readout of target sequences ensures that a splicing reaction only takes place at an approved position. Conversely, many binary interactions within the spliceosome are weak but are reinforced upon context-dependent joining of auxiliary splicing factors. This approach allows the spliceosome to respond dynamically to regulatory signals (Wahl et al., 2009).

The major subunits of the spliceosome are five small nuclear RNPs (snRNPs) U1, U2, U4, U5, U6. Each snRNP consists of a uridine-rich (U) snRNA, hence the name. The sequences of the snRNAs are surprisingly little conserved from yeast to mammals with U6 being the exception showing 75% identity between yeast and human (Brow and Guthrie, 1988). Moreover, U6 snRNA differs in several features from the other U snRNAs (reviewd in (Guthrie and Patterson, 1988)). Its unique properties include 1) transcription by RNA polymerase III (RNA pol III) instead of RNA pol II (Reddy et al., 1987), 2) the presence of a γ-monomethyl cap instead of a TMG cap (trimethylguanosine cap) at the 5′ end (Singh and Reddy, 1989), 3) the interaction with Lsm proteins instead of Sm proteins (Achsel et al., 1999; Mayes et al., 1999), and a 2′,3′-cyclic phosphate in the mature form instead of a 3′ hydroxyl group (Lund and Dahlberg, 1992).

The spliceosome is assembled in a stepwise manner onto the pre-mRNA and performs two consecutive transesterification reactions. The initial identification of the consensus elements in a pre-mRNA is achieved by U1 snRNP, which recognizes the 5′SS, the splicing factor 1 (SF1), which recognizes the branch point, and the U2 auxiliary factor (U2AF), which recognizes the polypyrimidine tract and the 3′SS. In a next step, U2 snRNP is recruited and its snRNA base-pairs with the BP which leads to displacement of SF1. Subsequently, U4, U5, and U6 engage as a preassembled U4/U6.U5 tri-snRNP. At this point all spliceosomal snRNPs are sitting on the pre-mRNA, however, major conformational changes are now required in order for the spliceosome to gain catalytic activity. Particularly, snRNA-snRNA and snRNA-pre-mRNA interactions need to be rearranged. This is most impressively exemplified for the U6 snRNA which appears to be part of the catalytic site of the spliceosome. The U6 snRNA extensively base-pairs with the U4 snRNA. This tight interaction prohibits U6 snRNA to immediately trigger catalysis upon binding to the spliceosome. In order to form a catalytically active site, the U6/U4 snRNA bonding needs to be disrupted and novel interactions of U6 snRNA with the U2 snRNA as well as the pre-mRNA need to be formed. Additionally, in the course of U6 snRNA rearrangements, an intramolecular stem loop is formed that coordinates a metal-ion contributing to the catalysis (Yean et al., 2000). After each splicing event the spliceosome gets disassembled into the individual snRNPs and in order for another splicing event to take place it needs to be reassembled. Factors that have been implicated in the reassembly of the spliceosome include the yeast protein Prp24 and the human protein SART3 (see next sections).

The yeast protein Prp24

Prp24 is a spliceosomal recycling factor annealing the U4 and U6 snRNAs

Prp24 is a yeast RNA-binding protein that has homologs up to humans (Fig. 1A of result part). Prp24 has originally been isolated by Vijayraghavan *et al.* in a screen for temperature-sensitive mutants that affect pre-mRNA splicing in the budding yeast *S. cerevisiae* (Vijayraghavan et al., 1989). Alleles from 11 different complementation groups have been isolated showing impaired splicing ability at the repressive temperature and were termed pre-RNA processing (prp) mutants (*prp17-prp27*) in agreement with previously identified splicing-related proteins in yeast (*prp2-prp11*) (Vijayraghavan et al., 1989). Although Vijayraghavan *et al.* could show that loss of Prp24 leads to accumulation of pre-mRNA, the precise stage at which Prp24 acts during splicing as well as its mode of action remained elusive.

Later work, again carried out in *S. cerevisiae*, revealed a function of Prp24 as an snRNP recycling factor, reannealing the U4 and U6 snRNAs (Jandrositz and Guthrie, 1995; Raghunathan and Guthrie, 1998; Shannon and Guthrie, 1991; Vidaver et al., 1999). The U4 snRNA and the U6 snRNA interact extensively through base-pairing forming two intermolecular stems (stem I and stem II) separated by an intramolecular stem in the U4 snRNA (Fig. 2) (Bindereif et al., 1990; Brow and Guthrie, 1988; Rinke et al., 1985; Vankan et al., 1990). Due to the high sequence complementarity between the U4 and U6 snRNAs, the U4/U6 di-snRNP complex is highly stable *in vitro* (Brow and Guthrie, 1988). This high stability suggests that there might be an active mechanism required to disrupt the U4/U6 interaction during the extensive structural rearrangements that occur within the spliceosome in order to acquire catalytic activity. It is also conceivable that *trans*-acting factors might be needed to stabilize the U4 and U6 single complexes to prevent or regulate the formation of the energetically favored U4/U6 di-complex.

In *S. cerevisiae*, *trans*-acting factors that affect the stability of the U4/U6 complex were identified by screening for mutations that suppress the cold-sensitive phenotype of a destabilized U4/U6 complex obtained by introducing a single-base mutation (G14C) in U4 snRNA (Fig. 2 and (Shannon and Guthrie, 1991)). Apart from a mutation in U6 (C67G) compensating for the G14C in U4, two classes of mutations were able to rescue the cold-sensitive phenotype: mutations in Prp24, residing in the conserved RNA binding motif RRM3, and mutations in U6, which lie in a region outside the region that base-pairs with U4 (T38C, A40G, C43G). The latter have been shown to constitute the Prp24 binding site by chemical footprinting experiments (Jandrositz and Guthrie, 1995). Moreover, it was found that Prp24 co-immunoprecipitates U6 snRNA but not U1,U2,U4, U5 snRNAs from wild-type extracts (Shannon and Guthrie, 1991). Furthermore, separation of splicing particles using glycerol gradients revealed three different U6-containing snRNP complexes, U6 snRNP, U4/U6 di-snRNP, and U4/U6.U5 tri-snRNP. In a wild-type strain, Prp24 only interacted with U6 snRNP but not with the other two U6-containing complexes. However, in the strain carrying the destabilized U4(G14C)/U6 complex, Prp24 was found to interact with U4(G14C)/U6 di-snRNP at the expenses of the interaction with free U6 snRNP. From these data a model was derived whereby the Prp24/U6 complex is in equilibrium with the U4/U6 complex. Upon binding of U4 to U6/Prp24, base-pairing between U4 and U6 snRNAs occurs, which in turn leads to a displacement of Prp24. Thus the Prp24/U4/U6 complex exists only transiently and appears to require a sensitized back-ground in order to be observed (Shannon and Guthrie, 1991).

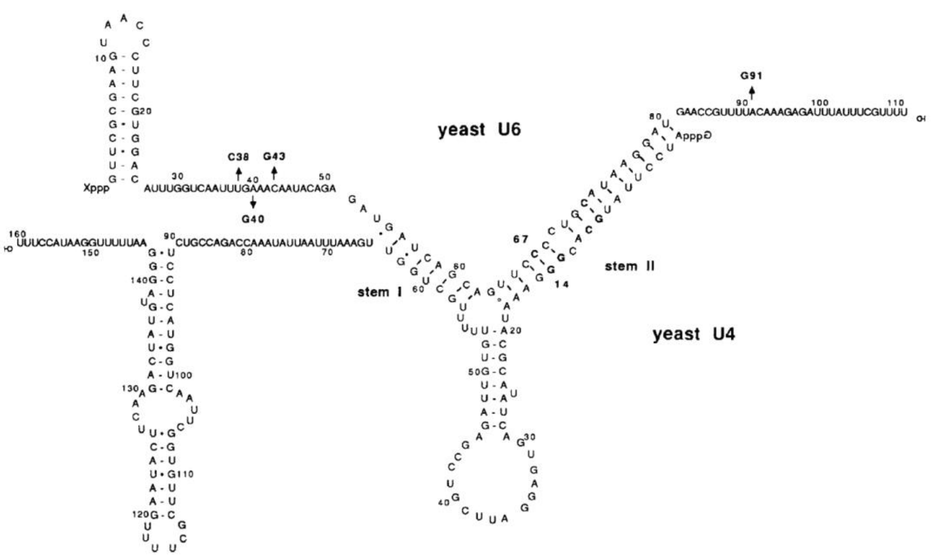
yeast U6
yeast U4
stem I
stem II
C38
G43
G40
G91
67
14
Xppp
Apppᴳ
AUUUGGUCAAUUUGAAACAAUACAGA
CUGCCAGACCAAAUAUUAAUUUAAAGU
UUUCCAUAAGGUUUUUAA
GAACCGUUUUACAAAGAGAUUUAUUUCGUUUU

Fig. 2. Secondary structure of the yeast U4/U6 snRNA complex (as proposed by (Brow and Guthrie, 1988)). Modified with permission from doi: 10.1101/gad.5.5.773.

Controversies about Prp24

Further studies have been conducted in yeast refining the initial model but at the same time bringing about some controversy on the function of Prp24 (Ghetti et al., 1995; Raghunathan and Guthrie, 1998; Vidaver et al., 1999). Vidaver *et al.* suggested a dual, U4/U6-stabilizing and -destabilizing, function for Prp24 (Vidaver et al., 1999). They proposed the existence of a novel intramolecular stem in U6 (telestem) that is able to bind Prp24 and that counteracts U4/U6 base-pairing. How Prp24 would possibly switch between the two opposing activities of associating U4 and U6 and dissociating U4/U6 remained unclear. Conversely, using an *in vitro* splicing assay it was found that Prp24 is not required for the ATP-dependent release of U4 from the spliceosome and the subsequent splicing catalysis but only for converting free U4 and U6 in an ATP-independent process to U4/U6 and U4/U6.U5 (Raghunathan and Guthrie, 1998).

Finally, in contrast to studies using yeast extracts (Jandrositz and Guthrie, 1995; Shannon and Guthrie, 1991), in an *in vitro* binding assay using recombinant Prp24 and *in vitro* transcribed U4 and U6 RNA, a preferential binding of Prp24 to the U4/U6 hybrid over free U6 was observed (Ghetti et al., 1995). It was hypothesized that the discrepancy between the findings obtained for extracts and the recombinant protein is due to the presence of an additional factor in extracts that triggers immediate leaving of Prp24 after the latter has assembled U4/U6. Further evidence that Prp24 activity *in vivo* might be supported by additional factors comes from the observation that immuno-purified Prp24 catalyzed the reannealing of U4 and U6 more efficiently with whole immuo-purified snRNPs than with similarly obtained but deproteinized snRNAs (Raghunathan and Guthrie, 1998). In search of co-factors for Prp24 that facilitate U4/U6 formation, Lsm proteins have been rediscovered (Rader and Guthrie, 2002; Ryan et al., 2002).

Lsm proteins enhance the recruitment of Prp24 to U6 snRNA

Like-Sm proteins (Lsm) belong to a large family of proteins that have been named after their first identified members, the Sm proteins (Tan and Kunkel, 1966). Lsm proteins are found from prokaryotes to humans and form hexa- or heptameric rings that are involved in various RNA-related processes such as mRNA decay, histone mRNA 3’ end processing, and pre-mRNA splicing (Tharun, 2009). The pathway in which a particular Lsm ring acts depends on the composition of its individual members. The Lsm2-8 ring has been implicated in splicing (He and Parker, 2000). Specifically, Lsm2-8 were found to co-immunoprecipitate with U6 snRNA from U6 snRNP, U4/U6 snRNP, and U4/U6.U5 snRNP in yeast (Mayes et al., 1999) and from U4/U6.U5 snRNP in HeLa cells (Achsel et al., 1999). In the latter case, the 3’-terminal U-stretch in the U6 snRNA was required for complex formation (Achsel et al., 1999). Moreover, the Lsm proteins facilitated annealing of U4 and U6 snRNA *in vitro* (Achsel et al., 1999). Subsequently, a yeast two-hybrid assay revealed an interaction between Lsm proteins and Prp24 (Rader and Guthrie, 2002). The interaction was mediated through a conserved motif of 10 amino acids at the very C-terminal end of Prp24, the Lsm interaction domain (LID). Deletion of LID led to reduced U4/U6 levels *in vivo* as well as a cold-sensitive growth phenotype reminiscent of the one observed for U4 snRNA mutations that destabilize the U4/U6 complex (Shannon and Guthrie, 1991). Finally, recombinant Prp24 lacking the LID exhibited slowed-down U4/U6 annealing kinetics *in vitro* compared to wild-type protein (Rader and

Guthrie, 2002). Ryan *et al.* came to a similar conclusion finding that the 3'-terminal U-stretch in the U6 snRNA is important for Lsm binding and that the Lsm-U6 interaction greatly enhances recruitment of Prp24 to U6 snRNA (Ryan et al., 2002). Taken together, it is likely that a combined effort of Prp24 and Lsm2-8 enables efficient assembly of the U4/U6 snRNP *in vivo*.

SART3 - the human homolog of Prp24

The role of SART3 in splicing

Homologs of Prp24 exist in several eukaryotes including humans where it previously has been described as p110 or SART3 (Bell et al., 2002; Gu et al., 1998). Despite an overall low sequence homology between different species, certain domains and their relative positions are highly conserved (Fig. 1A of result part). All homologs contain the Lsm interaction domain (LID) at the outermost C-terminal end. Between one and four RNA recognition motifs (RRMs) are localized in the C-terminal part. The two RRMs in SART3 correspond to RRM2 and RRM3 in Prp24 (Bell et al., 2002), which, when mutated, lead to defective U4/U6 assembly *in vivo* (Shannon and Guthrie, 1991; Vidaver et al., 1999). The N-terminal part (except for *S. cerevisiae*) contains several HAT repeats (half a TPR), which are thought to mediate protein-protein interactions in RNA processing pathways (Blatch and Lassle, 1999; Preker and Keller, 1998). Of note, Prp24 lacks the HAT repeats making it considerably smaller than its homologs (444 amino acids in Prp24 compared to 963 amino acids in SART3). The HAT-functionality might reside in a separate protein in *S. cerevisiae*. Generally, the primary role for Prp24 as a U4/U6 snRNP recycling factor could be largely confirmed for SART3 in humans (Bell et al., 2002; Licht et al., 2008; Medenbach et al., 2004). Co-immunoprecipitations of recombinant SART3 added to HeLa cell-extracted RNA or *in vitro* transcribed U6 RNA showed a specific interaction with U6 snRNA but not with the other spliceosomal RNAs in accordance with the results from yeast (Bell et al., 2002; Shannon and Guthrie, 1991). SART3 binding within U6 was mapped to an internal region (G38-U57) encompassing the analogous residues that have been shown to be crucial for the Prp24-U6 interaction in yeast (T38-C43) (Jandrositz and Guthrie, 1995; Shannon and Guthrie, 1991). Mutational analysis of SART3 demonstrated that RRM1 and RRM2 plus some of the neighboring sequence is sufficient for U6 snRNA binding but that neither the HAT repeats nor the LID are required (Medenbach et al., 2004). Whereas Prp24 has been shown to interact exclusively with U6 snRNP (Shannon and Guthrie, 1991), SART3 was found to be associated with U6 snRNP and the U4/U6 di-snRNP (though, again fitting yeast data, not with the U4/U6.U5 tri-snRNP or higher-order complexes) (Bell et al., 2002). Despite this discrepancy, Bell and colleagues observed that HeLa cell extracts under SART3-immunodepleted conditions largely fail to recyle the U4/U6 snRNP complex following splicing catalysis (Bell et al., 2002). This recycling activity was dependent on both the HAT repeats and the RRMs but not the LID (Medenbach et al., 2004). Finally, similar to Prp24, SART3 was found to be more efficiently recruited to Lsm-bound U6 snRNP compared to naked U6 snRNA in a LID-dependent manner (Licht et al., 2008).

In sum, there is intriguing agreement on the molecular function of Prp24/SART3 as a U4/U6 snRNP annealing factor in yeast and human cell culture. However, insights into the developmental function of SART3 are sparse. To date, the system wide role of SART3 has only been investigated in zebrafish where it was found that a loss-of-function mutant of SART3 leads to embryonic lethality (Trede et al., 2007).

Splicing-unrelated functions of SART3

Besides the vast amount of studies that suggest an essential role for SART3 in splicing, there are a few reports that place SART3 in other pathways. SART3 has been implicated to function as transcriptional activator (Liu et al., 2002) and repressor (Liu et al., 2004). Liu *et al.* showed that in HEK293T cells, SART3 directly binds the HIV-1 retroviral protein Tat, which is a transcriptional activator of the HIV-1 long terminal repeat (LTR) promoter element (Liu et al., 2002). Tat recognizes a stem-loop structure called transactivating response element (TAR), which is located immediately 3' to the LTR transcription start site (Cullen, 1998). Co-transfection of HEK293T cells with Tat and different amounts of SART3 amplified the expression of a LTR promoter-driven reporter gene in a dose-dependent manner. This synergistic response was lost upon deletion of the TAR element (Liu et al., 2002). Of note, it cannot be excluded that the effects observed by Liu and his colleagues on reporter genes arise due to an involvement of the SART3/TAT complex in splicing. A repressive activity of SART3 on transcription has been reported for androgen receptor (AR)-mediated gene expression (Liu et al., 2004). AR is a transcription factor that, upon binding of the steroid hormone androgen, regulates expression of target genes, most of which are implicated in the development and maintenance of the male sexual phenotype (Mooradian et al., 1987). Co-immunoprecipitation experiments from HEK293T cell lysates revealed an interaction of SART3 with AR. It appears that binding of SART3 to AR prevents binding of the latter to AREs (AR-responsive elements) in target gene promoters (Liu et al., 2004). Details concerning the mechanism of action remain unknown.

Additionally, SART3 has been shown to be required for maintenance of the pluripotency factors NANOG, OCT4, and SOX2 in human embryonic stem cells (hESCs) (Liu et al., 2012). SART3 is expressed in hESCs but its levels are strongly decreased (by 77%) upon differentiation of hESCs concomitantly with a reduction in NANOG, OCT4, and SOX2 levels. Knock-down of SART3 in hESCs, kept under undifferentiation conditions, led to diminished levels of pluripotency factors but increased levels of differentiation markers. Conversely, overexpression of SART3 in hESCs that have been allowed to differentiate for 5 days led to, although slightly, increased levels of NANOG, OCT4, and SOX2 but reduced levels of differentiation markers (Liu et al., 2012). Whether the modulation of levels of pluripotency factors by SART3 is direct or indirect, and if direct, transcriptional, co- or post-transcriptional, remained an open question. At least in the case of OCT4 it appears that SART3 regulates its alternative splicing into isoforms OCT4A and OCT4B (Liu et al., 2013). Overexpression of SART3 increased the OCT4A splicing form and knock-down of SART3 decreased the OCT4A splicing form, respectively, meanwhile levels of the OCT4B splicing form remained unaffected under both conditions.

Furthermore, co-immunoprecipitation experiments in HEK293 cells revealed an RNA-independent interaction of SART3 and Argonaute (AGO) protein family members, AGO1 and AGO2, essential components of the RNA silencing pathway (Hock et al., 2007). However, a potential function of SART3 in the RNA silencing pathway remains yet to be established. Finally, in the cancer immunology field, SART3 has been described as a surface tumor-rejection antigen recognized by HLA-A24-restricted cytotoxic T-lymphocytes in a multitude of cancers (Murayama et al., 2000; Suefuji et al., 2001; Tsuda et al., 2001; Yang et al., 1999). Therefore, SART3-derived peptides might be appropriate molecules for immunotherapy in patients with HLA-A24-positive tumors. It is the cancer field that gave SART3 its name, squamous-cell carcinoma antigen recognized by T cells-3.

Terminal uridylyl transferases (TUTases) and a connection to splicing

Terminal nucleotidyl transferases (TNTases) are enzymes that covalently add templated or non-templated nucleotides to the 3' end of target RNAs (Rissland and Norbury, 2008). The large and diverse protein family of TNTases is characterized by a nucleotidyltransferase domain (NTD) that contains two aspartic acids (in a DXD motif) essential for catalysis and a poly(A) polymerase-associated domain (PAD) (Fig. 3A of result part and (Hagan et al., 2009; Holm and Sander, 1995; Schmid et al., 2009)). Many TNTases such as Cid1 from *S. pombe*, unlike canonical poly(A) polymerase, do not contain an RNA recognition motif and therefore likely require interacting proteins that direct them to target RNAs (Rissland et al., 2007). TNTases possess either uridyl- or adenyl-transferase activity (correspondingly referred to as TUTase and TATase) but rarely cytidyl- or guanyl-transferase activity (Scott and Norbury, 2013). It appears difficult to predict the nucleotide specificity of a given transferase from the sequence (Rissland and Norbury, 2008). To distinguish TUTases from TATases, *in vitro* or, preferably, *in vivo* assays are required and ultimately structures need to be solved in order to understand the biochemical basis for nucleotide specificity such as for RET2 from *Trypansoma brucei* (Deng et al., 2005). Moreover, oftentimes a TNTase does not show exclusive specificity towards a particular nucleotide but allows, although usually at significantly lower frequency, the incorporation of different NTPs (Rissland et al., 2007). In the following, I focus on TUTases.

In HEK293T cells, the RNA-binding protein Lin28 recruits TUT4/ZCCHC11 to the precursor form of the *let-7* miRNA, pre-*let-7*, and a couple of other pre-miRNAs that contain the tetra-nucleotide sequence motif GGAG (miR-107, mir-143, and mir-200c) (Heo et al., 2008; Heo et al., 2009). TUT4/ZCCHC11 adds a 3'-terminal oligouridine-tail of 10-30 nucleotides to pre-miRNAs which makes them resistant to Dicer-mediated processing into the mature form and promotes their degradation. Interestingly, non-canonical group II pre-miRNAs that contain only a 1-nucleotide 3' overhang after Drosha processing (compared to the 2-nucleotide overhang of canonical group I pre-miRNAs) acquire a monouridylation through the action of TUT7/ZCCHC6, TUT4/ ZCCHC11, and TUT2/GLD2 (Heo et al., 2012). Addition of a single uridyl residue by these TUTases restores the canonical 2-nucleotide 3' overhang of group I pre-miRNAs and thus allows their subsequent processing into the mature form. In sum, pre-*let-7* mono- and oligouridylation demonstrates functional duality of uridylation.

In *S. pombe*, Cid1 has been reported to add poly(U) tails of hundreds of U residues to polyadenlyated mRNAs (Rissland et al., 2007; Rissland and Norbury, 2009). Initially suggested to be a TATase (Read et al., 2002), Cid1 was later found to possess TUTase activity that outcompetes its TATase activity *in vitro* and *in vivo* (Rissland et al., 2007). The same study demonstrated similar activity for TUT7/ZCCHC6, a human ortholog of Cid1. It was proposed that uridylation of polyadenylated mRNAs triggers an alternative, deadenylation-independent mRNA decay pathway acting in parallel with the classical deadenylation-dependent pathway (Rissland and Norbury, 2009). Furthermore, several TUTases have been identified in *A. thaliana*, *S. pombe*, *C. elegans*, and *H. sapiens* by injecting mRNA encoding candidate proteins fused to MS2 together with synthetic, radiolabeled RNA substrates harboring MS2 binding sites into *X. laevis* oocytes (Kwak and Wickens, 2007). To date, identification of the natural RNA substrates for some of these TUTases (At2g45620 in *A. thaliana* and PUP-3 in *C. elegans*) is still missing (Scott and Norbury, 2013). Finally, a human U6 snRNA-specific TUTase (HsTUT1) has been reported (Trippe et al., 1998).

Although the substrate requirements for HsTUT1 have been characterized *in vitro* (Trippe et al., 2003) the functional role of a U-tail on U6 snRNA in splicing remains largely speculative. The 3' end of U6 snRNA is not only uridylated but subject to several modifying activities. U6 snRNA is transcribed by RNA pol III (Reddy et al., 1987) and similar to other RNA pol III products, including 5S rRNA and tRNAs (Rinke and Steitz, 1982), its precursor form interacts with the La protein in yeast (Pannone et al., 2001) and metazoans (Rinke and Steitz, 1985). The La protein binds nascent RNA pol III transcripts through their characteristic 3'-terminal U-stretch (usually 4-5 Us) and protects them from exonucleolytic degradation (reviewed in (Wolin and Cedervall, 2002)). Not only the 3' U-tract has been shown to be pivotal for La protein binding but similarly the 3' OH-group. Substituting the 3' OH by a phosphate significantly reduced the interaction of La protein purified from HeLa cells with synthetic tRNA (Stefano, 1984) and of La protein purified from *D. melanogaster* and *S. cevervisiae* with *in vitro* transcribed U6 snRNA (Yoo and Wolin, 1994). Of note, in HeLa cells only 10% of U6 snRNA is available with a 3' OH, whereas 90% possess a cyclic 2',3'-phosphate (>p), though this ratio varies depending on the organism (100% >p in Soybean, 0% >p *Trypanosoma brucei rhodesiense*) or developmental stage (Lund and Dahlberg, 1992; Rinke and Steitz, 1985; Terns et al., 1992). The current model suggests that HsTUT1 is required to restore the four template uridines found in newly transcribed U6 snRNA thus counteracting exonucleolytic activity (Trippe et al., 2003; Trippe et al., 1998). Lack of an intact U-tail might prohibit the formation of >p and therefore interfere with Lsm protein recruitment (Licht et al., 2008).

4.3 Results

SART-3 interacts with LSM/SNR proteins and with USIP-1

Prp24 from *S. cerevisiae* and its human homolog SART3 function in the recycling of the U4/U6 snRNP, a transient complex that is crucial for spliceosome assembly (Bell et al., 2002; Shannon and Guthrie, 1991). In *C. elegans*, the protein most closely related to Prp24/SART3 is encoded by *B0035.12* (henceforth the gene is referred to as *sart-3* and the protein as SART-3) sharing 26% and 45% identity and similarity, respectively, with SART3 and 9% and 17% with Prp24 in the amino acid sequence. The domain organization of SART-3 is conserved from yeast to humans, with the notable absence of HAT repeats in Prp24 of *S. cerevisiae* (Fig. 1A). Given the lack of previous studies on SART-3 and the fact that multicellular *in vivo* models for this protein are largely missing, we aimed at a developmental and molecular characterization of SART-3 in *C. elegans*. In order to find interaction partners of SART-3 we carried out co-immunoprecipitations (co-IPs) with lysates from worms expressing transgenic, N-terminally FLAG-tagged SART-3 (Fig. 1B, lanes 1-3) and control worms expressing the triple GFP/His/FLAG-tag (Fig. 1B, lanes 4-6). Complete eluates from such IPs were subjected to mass spectrometry (MS) and the proteins identified with SART-3 but not with the GFP/His/FLAG control construct are presented in Figure 1C and S1A. To confirm the initial MS results (IP1 in Fig. 1C) the IP was repeated, this time, however, with a different protein extraction method to obtain lysates as well as a different approach to concentrate eluates prior to MS (see legend of Figure 1 for details) (IP2 in Fig. 1C). Despite deviating in crucial parameters, the outcome of IP1 and IP2 is virtually identical, strengthening the credibility of the result. Two main groups of proteins are found in complex with SART-3, namely LSM and SNR proteins, the latter being the *C. elegans* Sm proteins. The heptameric Lsm2-8 ring is known to bind exclusively to the U6 snRNA, whereas the Sm ring binds to the U1, U2, U4, and U5 snRNAs (He and Parker, 2000). Remarkably, in our co-IP we were able to recover the entire seven-membered Lsm ring and, with the exception of SNR-6, also the Sm ring. Considering that human SART3 has been shown to specifically bind to the U6 snRNP and the U4/U6 snRNP complex (Bell et al., 2002), our data is probably best explained by assuming a similar behavior for *C. elegans* SART-3. Interestingly, we find that RNase A treatment abolishes the interaction of SART-3 with LSM proteins, despite the presence of the Lsm interaction domain (LID) in SART-3 (Fig. 1A). The conserved C-terminal LID motif has previously been shown by a yeast two-hybrid assay to be required for Lsm binding in yeast (Rader and Guthrie, 2002) and by an *in vitro* binding assay to be important to recruit SART3 to the Lsm-bound U6 sRNA in HeLa cells (Licht et al., 2008). Here, we observe that binding of SART-3 to LSM proteins is RNA-dependent or at least enhanced by RNA.

Figure 1

(A)

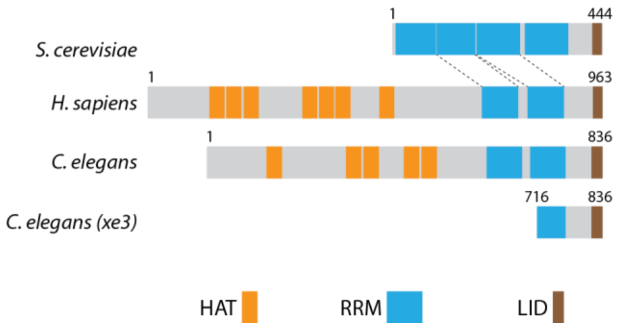

1
444
S. cerevisiae
1
963
H. sapiens
1
836
C. elegans
716
836
C. elegans (xe3)
HAT
RRM
LID

(B)

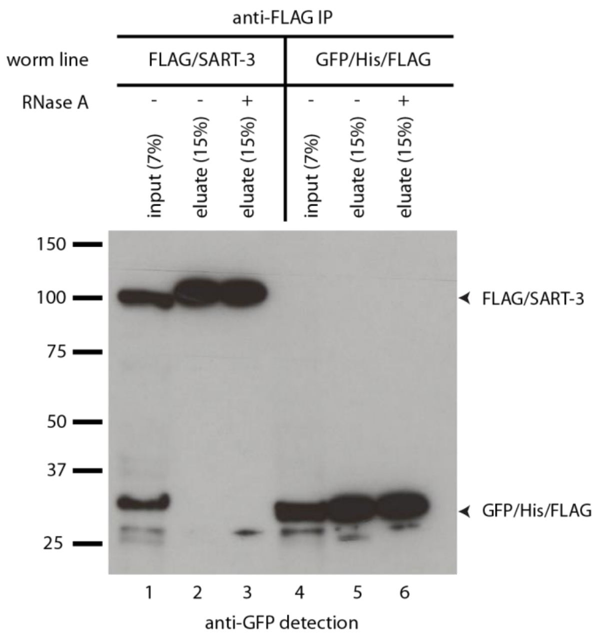

anti-FLAG IP
worm line
FLAG/SART-3
GFP/His/FLAG
RNase A
-
-
+
-
-
+
input (7%)
eluate (15%)
eluate (15%)
input (7%)
eluate (15%)
eluate (15%)
150
100
75
50
37
25
FLAG/SART-3
GFP/His/FLAG
1
2
3
4
5
6
anti-GFP detection

(C)

IP1

	FLAG/SART-3		GFP/His/FLAG	
RNase A	-	+	-	+
SART-3	304	238	0	0
GFP	0	0	29	24
GUT-2	22	0	0	0
LSM-3	45	0	0	0
LSM-4	21	0	0	0
LSM-5	11	0	0	0
LSM-6	19	0	0	0
LSM-7	12	0	0	0
LSM-8	20	0	0	0
SNR-1	27	0	0	0
SNR-2	18	0	0	0
SNR-3	15	0	0	0
SNR-4	30	0	0	0
SNR-5	11	0	0	0
SNR-7	15	0	0	0
USIP-1	16	0	0	0

IP2

	FLAG/SART-3		GFP/His/FLAG	
RNase A	-	+	-	+
SART-3	315	285	0	0
GFP	0	0	94	104
GUT-2	14	0	0	0
LSM-3	25	0	0	0
LSM-4	21	0	0	0
LSM-5	4	0	0	0
LSM-6	16	0	0	0
LSM-7	7	0	0	0
LSM-8	13	0	0	0
SNR-1	26	4	3	0
SNR-2	7	0	3	2
SNR-3	7	0	0	0
SNR-4	35	5	4	2
SNR-5	7	0	0	0
SNR-7	21	2	0	0
USIP-1	38	0	0	0

(D)

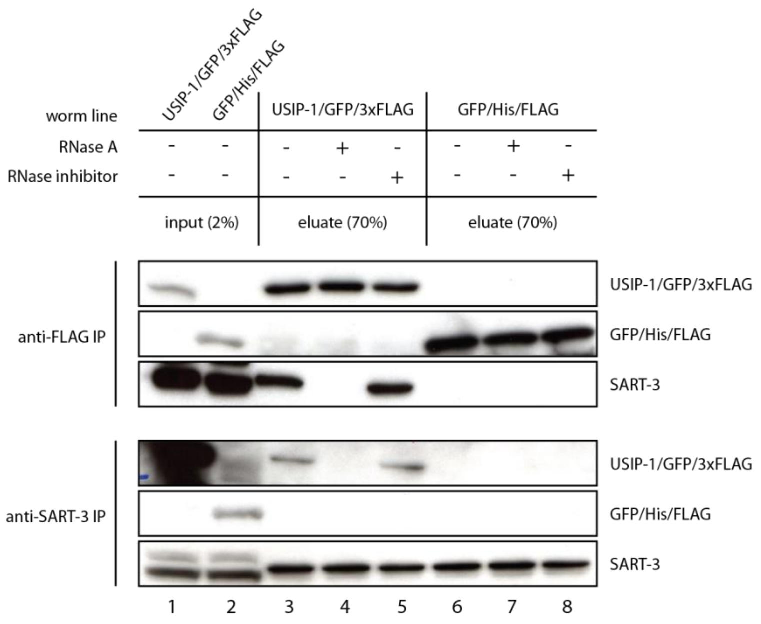

USIP-1/GFP/3xFLAG
GFP/His/FLAG
worm line
USIP-1/GFP/3xFLAG
GFP/His/FLAG
RNase A
- - - + - - + -
RNase inhibitor
- - - - + - - +
input (2%)
eluate (70%)
eluate (70%)
anti-FLAG IP
USIP-1/GFP/3xFLAG
GFP/His/FLAG
SART-3
anti-SART-3 IP
USIP-1/GFP/3xFLAG
GFP/His/FLAG
SART-3
1
2
3
4
5
6
7
8

Figure 1

(**A**) Schematic representation of the domain structure of Prp24 from *S. cevervisiae*, SART3 from *H. sapiens*, and SART-3 from *C. elegans*. *xe3* denotes an N-terminal truncation allele of SART-3. HAT = half a TPR, RRM = RNA recognition motif, LID = LSM interaction domain. (**B**) Western blot of anti-FLAG co-immunoprecipitation (co-IP) of N-terminally FLAG-tagged SART-3 (lanes 1-3) and a GFP/His/FLAG control construct (lanes 4-6). (**C**) Mass spectrometry results of co-IP shown in (B). IP1: Protein extraction using dounce homogenizer, RNase A treatment performed at room temperature, eluate concentration by TCA precipitation. IP2: Protein extraction using mortar and pestle, RNase A treatment performed at 4°C, eluate concentration by speed vac. GUT-2 is homologous to human Lsm2 and the SNR proteins to Sm proteins. Numbers indicate the exclusive spectrum count, i.e. number of spectra associated only with a given protein. (**D**) *Upper panel*: Western blot of anti-FLAG co-IP of C-terminally GFP/3xFLAG-tagged USIP-1 (lanes 1 and 3-5) and a C-terminally His/FLAG-tagged GFP control construct (lanes 2 and 6-8). *Lower panel*: Western blot of anti-SART-3 co-IP using the same samples as in the upper panel. USIP-1/GFP/3xFLAG and GFP/His/FLAG constructs were detected with anti-GFP. Endogenous SART-3 was detected with a polyclonal antibody produced in rabbit.

In addition to LSM and SNR proteins, we immunoprecipitated USIP-1 (U Six snRNA Interacting Protein, gene *usip-1/ZK863.4*) with SART-3 in an RNA-dependent manner (Fig. 1C). Domain prediction software (InterPro) revealed the existence of a PAP-associated domain (PAD) characteristic for terminal adenylyl- or uridylyltransferases, short TATases or TUTases (Fig. 3A). Besides, USIP-1 contains a conserved DXD motif that, in homologous proteins, is required for catalytic activity whereby D represents an aspartic acid and X represents any amino acid (Heo et al., 2009; Schmid et al., 2009). In light of the previous identification of a U6-specific TUTase, HsTUT1 (Trippe et al., 1998), USIP-1 caught our attention. Of note, there are TUTases in *C. elegans*, such as PUP-2 and CID-1, that are phylogenetically more closely related to HsTUT1 than USIP-1 (Schmid et al., 2009). In order to verify the interaction of SART-3 and USIP-1 found by MS, we created a worm line expressing C-terminally GFP/3xFLAG-tagged USIP-1 from a fosmid (Sarov et al., 2012). Transgenic USIP-1 was indeed able to co-IP endogenous SART-3, though, in agreement with the MS results, the interaction was lost by RNase A treatment (Fig. 1D, upper panel, lanes 1 and 3-5). A GFP/His/FLAG control construct did not bind to SART-3 (lanes 2 and 6-8). Similarly, performing the reverse IP, endogenous SART-3 was found to co-IP transgenic USIP-1, although inefficiently (Fig. 1D, lower panel). This low efficiency can be explained by the fact that the USIP-1/GFP/3xFLAG transgene forms an extrachromosomal array that is only transmitted to ~60% of the progeny. Thus, ~40% of the worms used in the IP do not contain the USIP-1/GFP/3xFLAG transgene but do contain endogenous USIP-1 competing for SART-3 binding. Of note, whereas in HEK293 cells SART3 has been found to interact with the Argonaute proteins AGO1 and AGO2 (Hock et al., 2007), we do not find any Argonaute proteins associated with SART-3 in *C. elegans* (data not shown). We conclude that SART-3 primarily interacts with the U4/U6 di-snRNP complex, however, a transient interaction with U6 single snRNP cannot be excluded, respectively, is even suggested by our model (see discussion).

SART-3 and USIP-1 are present in different spliceosomal sub-complexes

Our SART-3 co-IP data (Fig. 1) did not formally exclude an interaction of SART-3 with U1, U2, U4, or U5 snRNP complexes or combinations thereof. In order to more precisely define the sub-spliceosomal complex(es) in which SART-3 and USIP-1 reside, we conducted co-IPs with lysates from worms expressing FLAG/SART-3 and USIP-1/GFP/3xFLAG, respectively, and analyzed the bound RNA by northern blot (Fig. 2A). We find that SART-3 immunoprecipitates U6 and U4 but not U1, U2, or U5 snRNA. Given that purified Prp24 and recombinant SART3 only bind U6 snRNA but not U1, U2, U4, or U5 snRNAs (Bell et al., 2002; Shannon and Guthrie, 1991), we hypothesize that the U4 snRNA that we detect originates from the U4/U6 snRNP. USIP-1 exclusively interacts with the U6 snRNA (Fig. 2A). In line with this finding, USIP-1 does not interact with SNR proteins as assessed by MS results obtained from the same co-IP (Fig. 2B). However, despite an interaction of USIP-1 with U6 snRNA, USIP-1 does not interact with LSM proteins (Fig. 2B). This argues for an involvement of USIP-1 in the processing of LSM/SNR-unbound, possibly newly transcribed U6 snRNA into its mature form or in an early step during spliceosome assembly, prior to LSM and SNR participation. Several other proteins apart from LSM and SNR proteins co-immunoprecipitate with SART-3 and USIP-1 but are not further pursued in this study (Fig. S1B). Together, these results provide evidence for SART-3 and USIP-1 being present in distinctive complexes, although the fact that they precipitate each other suggests that they, at least transiently, engage in the same complex.

(A)

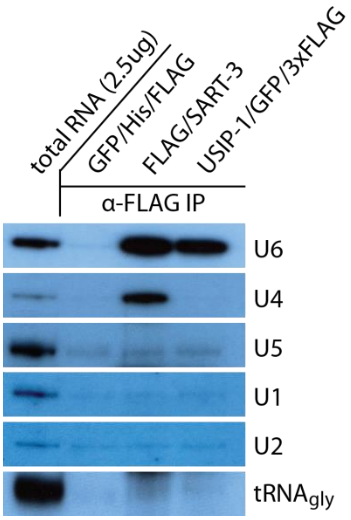

(B)

	GFP/His/FLAG	FLAG/SART-3	USIP-1/GFP/3xFLAG
USIP-1	0	33	233
SART-3	0	903	138
GFP	41	0	102
LSM-3	0	34	0
LSM-4	0	16	0
LSM-5	0	6	0
LSM-6	0	31	0
LSM-7	0	10	0
LSM-8	0	25	0
SNR-1	0	8	0
SNR-2	0	4	0
SNR-4	0	6	0
SNR-5	0	9	0
SNR-7	0	8	0

Figure 2

(**A**) Northern blot of RNA extracted from eluates obtained by an anti-FLAG co-IP on lysates from worms expressing the indicated transgene. (**B**) Proteins identified by mass spectrometry when in the co-IP shown in (A) protein instead of RNA was extracted (see additional proteins in Fig. S1B). Numbers indicate the exclusive spectrum count, i.e. number of spectra mapping uniquely to a given protein.

Physical interaction between SART-3 and USIP-1 predicts an overlapping expression pattern. We therefore set out to investigate in which tissues and developmental stages SART-3 and USIP-1 occur. We determined the spatio-temporal expression pattern of SART-3 and USIP-1 by fluorescence microscopy exploiting fosmids expressing *sart-3* and *usip-1* under their endogenous promoters and with a C-terminal GFP/3xFLAG-tag. The GFP signal was generally low and analysis was further complicated by mosaic expression due to the extrachromosomal nature of the fosmids. Nevertheless, analyzing multiple worms for each developmental stage led us to conclude that SART-3 as well as USIP-1 are expressed constitutively and ubiquitously across developmental stages and tissues, respectively. Exemplary pictures are shown in figure 3A and B. SART-3 and USIP-1 are dispersed throughout the nucleoplasm (arrows) but are depleted from the nucleolus (arrow heads). Sustained expression of SART-3 over the entire *C. elegans* life cycle was further validated by western blotting of lysates extracted at different time points during development using an antibody against endogenous SART-3 (Fig. 3C).

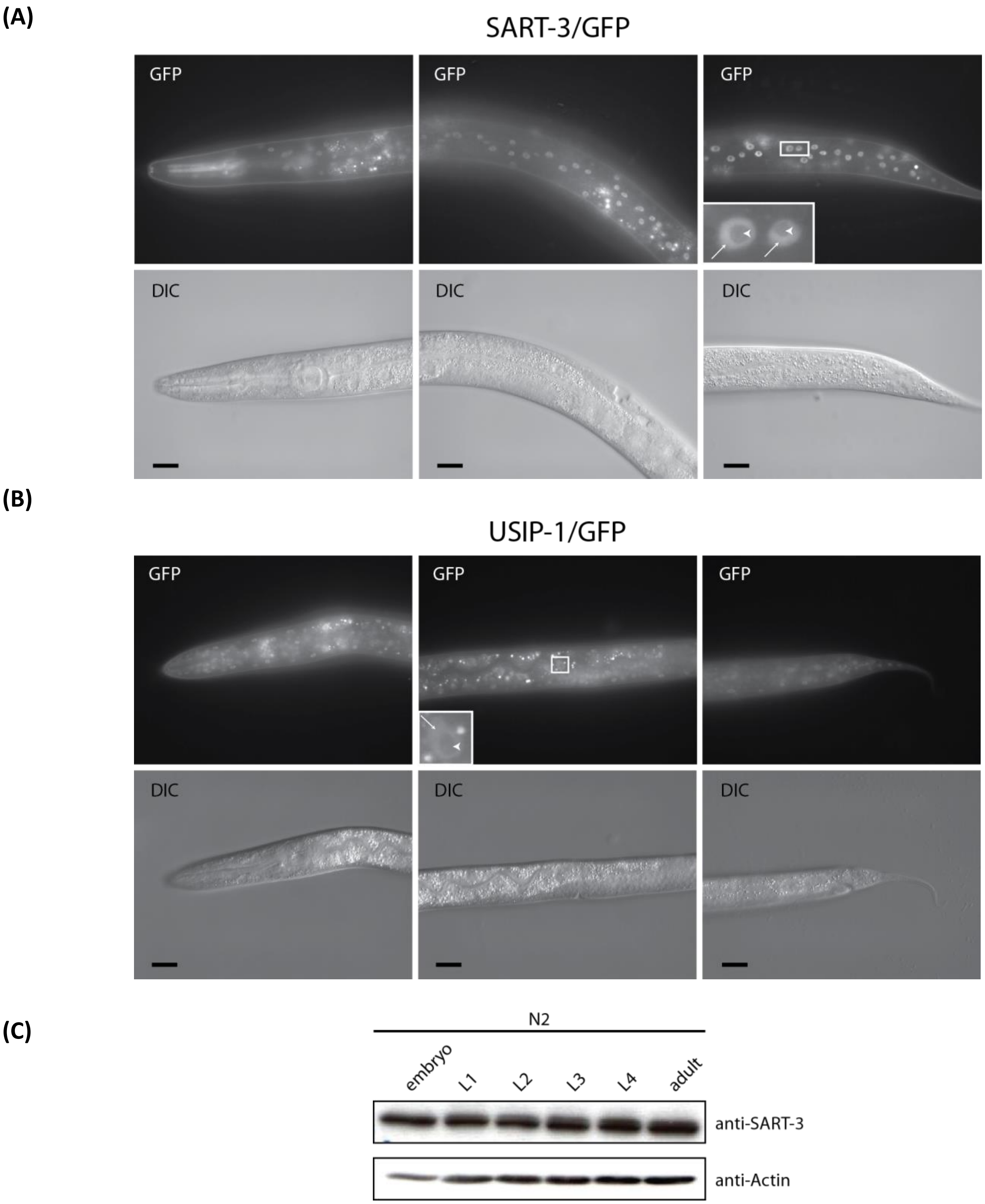
(A)
SART-3/GFP
GFP
GFP
GFP
DIC
DIC
DIC
(B)
USIP-1/GFP
GFP
GFP
GFP
DIC
DIC
DIC
(C)
N2
embryo
L1
L2
L3
L4
adult
anti-SART-3
anti-Actin

Figure 3

(**A-B**) Fluorescence microscopy of L4 stage worms expressing C-terminally GFP/3xFLAG-tagged SART-3 (A) or USIP-1 (B) from a fosmid. Pharynx signal in (A), top left panel, arises from an RFP co-injection marker leaking into the GFP channel. Arrows point to nucleoplasm, arrow heads point to nucleolus. Scale bar, 20 µm. (**C**) Western blot with lysates from wild-type worms (N2) extracted at different time points during development. Detection with SART-3 antibody Q5635.

sart-3 and *usip-1* interact genetically

Since we have demonstrated an RNA-mediated physical interaction between SART-3 and USIP-1, we next wanted to know whether they functionally interact. In order to look for genetic interaction, we made use of a putative null mutant of *usip-1*, *usip-1(tm1897)*, kindly provided by Dr. Shohei Mitani. The *tm1897* allele is a deletion of 542 bases that leads to a frame shift at amino acid position 233 (I233T) and to a premature termination codon shortly thereafter (S276Stop) (Fig. 4A). Thus, the mRNA transcript of *usip-1(tm1897)* is presumably degraded by nonsense-mediated decay (Baker and Parker, 2004). RNA extracted from worms homozygous for *tm1897* was subjected to semi-quantitative RT-PCR in order to test two regions of *usip-1*, one before and one after the deletion, for their ability to produce mRNA (Fig. S2A). The region in front of the *tm1897* deletion, which includes the catalytic DXD motif (Fig. 4A), did not reveal any band, whereas a strong band arose for wild-type worms (Fig. S2B). The region after the deletion showed mRNA levels similar to wild-type worms. However, it is unlikely that this C-terminal fragment, even if properly translated, would be functional given the loss of the DXD motif. Worms homozygous for *tm1897* are viable but developmentally slightly delayed (data not shown) and display moderately reduced brood size (data not shown). The same weak phenotype was observed when wild-type worms were exposed to *sart-3* RNAi (data not shown).

We analyzed whether combined diminishment of SART-3 and USIP-1 functionality would elicit a synthetic phenotype by subjecting L1 worms, either wild-type (N2) or *usip-1(tm1897)* mutant, to *sart-3* and mock RNAi. Efficient knock-down of SART-3 was confirmed by western blot (Fig S3A, upper panel). After 48h at 25°C wild-type worms under mock RNAi conditions had laid many embryos (Fig. S3B). Meanwhile, wild-type worms under *sart-3* RNAi conditions and *usip-1(tm1897)* worms under mock RNAi conditions had fewer progeny, and *usip-1(tm1897)* worms under *sart-3* RNAi conditions did not have any progeny (Fig. S3B). After 96 h at 25°C the conditions N2/mock RNAi, N2/*sart-3* RNAi, and *usip-1(tm1897)*/mock RNAi revealed hatched progeny that had exhausted the food, whereas the concerted depletion of *sart-3* and *usip-1* displayed mainly arrested embryos with only a few hatched worms (Fig. 4B). In a similar but quantitative experiment the number of hatched progeny after 60 h at 25°C was assessed and revealed a sharp drop for *usip-1(tm1897)*/*sart-3* RNAi but only a slight drop for N2/*sart-3* RNAi and *usip-1(tm1897)*/mock RNAi compared to N2/mock RNAi (Fig. 4C). Additionally, when L4 worms were exposed to *sart-3* or mock RNAi, the F1-progeny of *usip-1(tm1897)*/*sart-3* RNAi arrested at the L3 stage, whereas the other conditions led to fertile F1-progeny (data not shown). Expressing C-terminally FLAG-tagged *usip-1* in a *usip-1(tm1897)*/*sart-3* RNAi background rescued the embryonic arrest confirming that the synthetic phenotype is due to the deletion of *usip-1* (Fig. 4C).

To test whether catalytic activity of USIP-1 was required for its genetic interaction with SART-3, we generated a worm line expressing a supposedly catalytically inactive version of USIP-1, in which the aspartic acids in the DXD motif had been mutated to alanines. USIP-1(D183A/D185A)/FLAG was not able to rescue the embryonic arrest of *usip-1(tm1897)*/*sart-3* RNAi, highlighting the importance of TUTase activity for the physiological function of USIP-1 (Fig. 4C). Inability of the USIP-1(D183A/D185A)/FLAG protein to rescue is not due to destabilization in consequence of the point mutations, as it is expressed at similar levels as the wild-type USIP-1/FLAG transgene (Fig. S3C). In order to test whether the observation of a genetic interaction between *sart-3* and *usip-1* is due to altered U6 snRNA levels, we carried out a northern blot with RNA from N2 and *usip-1(tm1897)* worms grown under normal or mock RNAi conditions as well as with RNA from *usip-1(tm1897)* worms exposed to *sart-3* RNAi (Fig. S3A, lower panel). None of the conditions assayed revealed significantly changed U6 snRNA levels. In sum, we demonstrate a genetic interaction between *sart-3* and *usip-1* specified by a terminal phenotype, which, however, is not attributed to modified U6 snRNA levels.

Figure 4

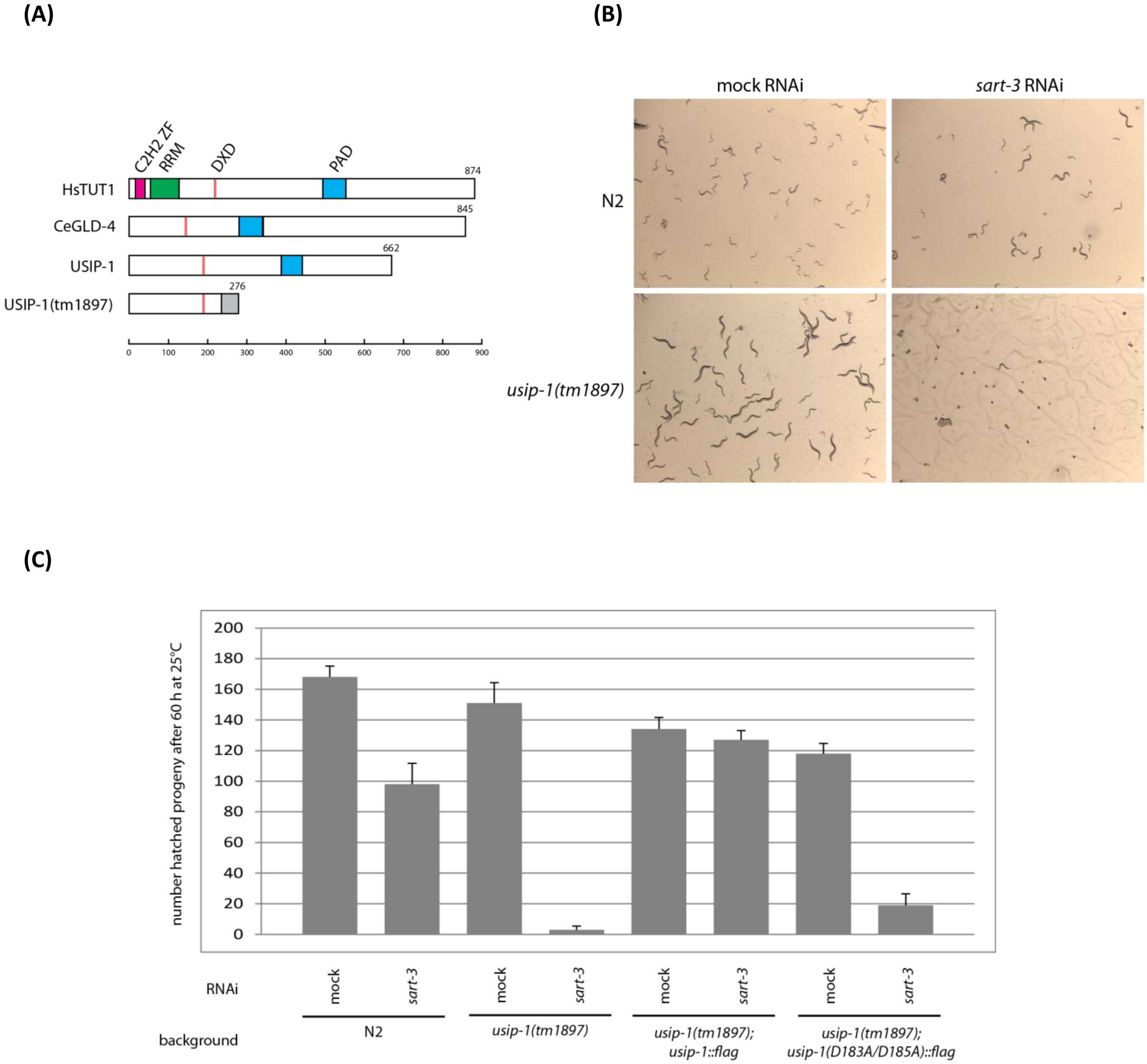

Figure 4

(**A**) Schematic representation of the domain structure of TUT1 from *H. sapiens* (UniProt: STPAP_HUMAN), and the *C. elegans* proteins GLD-4 (GLD4_CAEEL) and USIP-1 (Q23652_CAEEL). *tm1897* denotes a deletion allele of USIP-1 that leads to a frame shift (grayed out) and premature termination codon at position 276. C2H2 ZF = C2H2-type (classical) zinc finger (ZF), RRM = RNA recognition motif, PAD = PAP-associated domain, DXD: catalytically active site whereby D = aspartic acid and X = any amino acid. (**B**) Wild-type worms (N2) or worms homozygous for the *tm1897* allele were exposed to mock or *sart-3* RNAi at the L1 stage (P0 generation) and cultured at 25°C. Pictures of the next generation (F1 generation) were taken after 96 h revealing hatched F1s (that were arrested due to lack of food though) for N2/mock RNAi, N2/*sart-3* RNAi, and *usip-1*/mock RNAi but arrested embryos for *usip-1*/*sart-3* RNAi. (**C**) Quantification of hatched F1s after 60 h at 25°C in an experiment with a similar set-up as in (B). n = 3, error bars indicate SEM.

sart-3 null mutant worms die as adults

Knock-down of genes by RNAi is usually incomplete, leaving residual levels of the targeted mRNA, which are potentially able to maintain a vital function. In order to exclude this possibility for *sart-3* we generated a *bona fide* null allele making use of the MosDEL (*Mos1*-mediated deletion) technique allowing for targeted gene deletion (Frokjaer-Jensen et al., 2010). Exploiting the *ttTi5820 Mos1* transposon insertion within *sart-3*, we deleted a portion of the gene corresponding to amino acids 1-715 and termed the allele *xe3* (Fig. 1A). An affinity-purified polyclonal antibody against SART-3 failed to detect a band for full-length SART-3 in a western blot with lysates from worms homozygous for the *xe3* allele (Fig. 5A, lane 3 and 6). The status of the C-terminal fragment not targeted by MosDEL (amino acids 716-836) remained unclear as it does not cover the epitope region for our antibody. At any rate, translation of the C-terminal fragment is improbable considering the absence of the AUG start codon. RNA sequencing confirmed absence of reads in the region targeted by MosDEL (Fig. S4A). Worms homozygous for the *xe3* allele displayed a protruding vulva once reaching adulthood and eventually burst, a phenotype that was 100% penetrant (Fig. 5B, i). Furthermore, *sart-3*-deleted worms failed to produce oocytes (Fig. 5B, iv). We note, that until reaching adulthood there was no apparent phenotype apart from a developmental delay (*xe3/+* worms reaching early L4 stage after 28h at 25° and *xe3/xe3* worms after 31h) (Fig. S4B). Lack of more detrimental phenotypes in embryos and the subsequent larval stages of *xe3/xe3* worms might be due to wild-type mRNA or protein contributed by the heterozygous mothers (*xe3/+*). The vulval bursting as well as the sterility was fully rescued by transgenic, C-terminally GFP/His/FLAG-tagged SART-3 (Fig. 5B, ii and v) as well as N-terminally FLAG-tagged SART (data not shown). Wild-type worms are shown as a control (Fig. 5B, iii and vi). This confirms that the observed phenotypes indeed originate from a loss of SART-3 activity. Levels of the SART-3/GFP/His/FLAG transgene were shown to be similar to endogenous SART-3 levels by Western blot (Fig. 5A, compare lane 2 with 3 and 5 with 6). Taken together, the *xe3* allele leads to absence of the *sart-3* gene product (RNA and protein) and thus presents a genuine null allele by means of molecular criteria. *sart-3* loss-of-function causes a penetrant adult lethal phenotype.

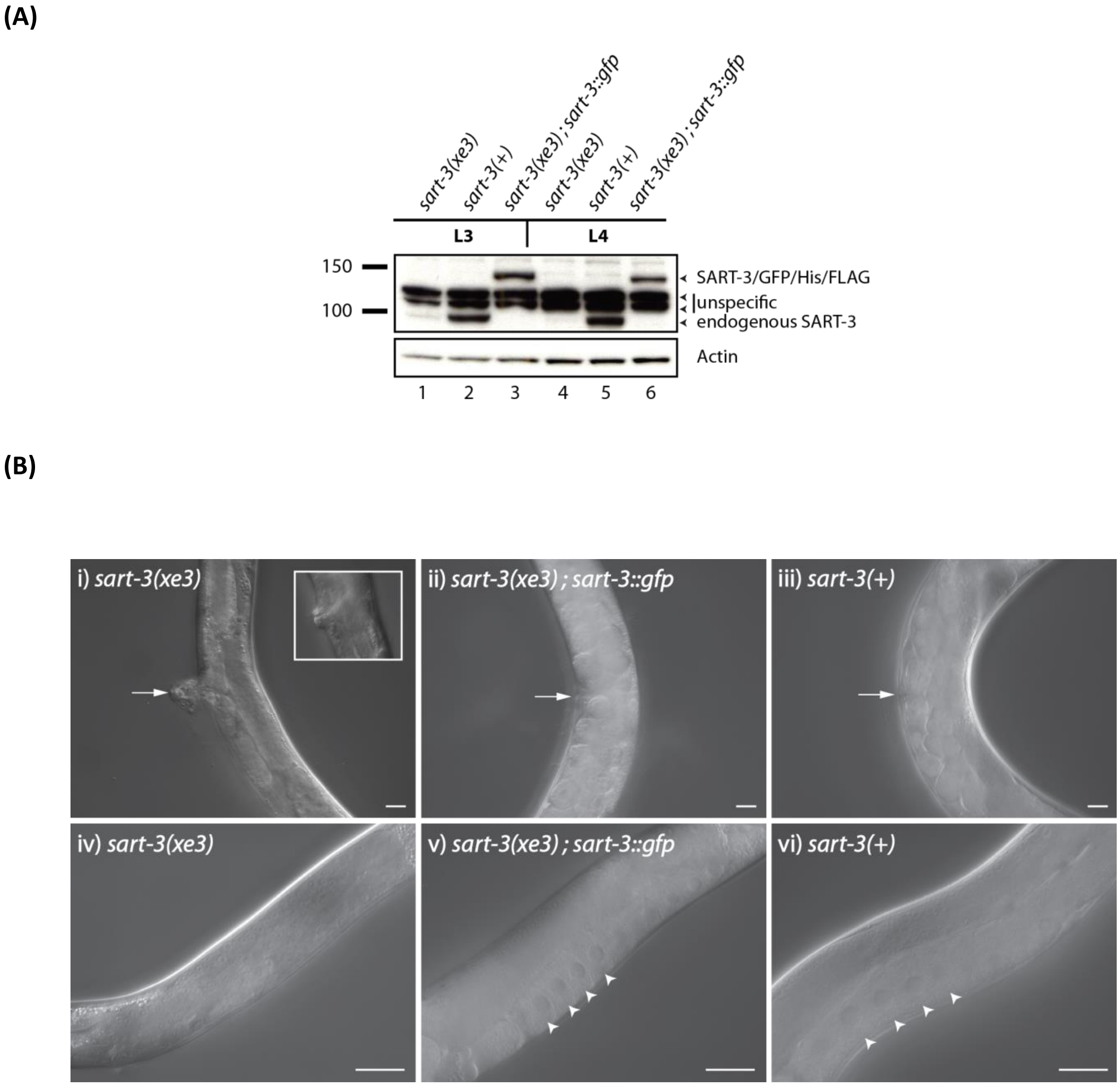
(A)
sart-3(xe3)
sart-3(+)
sart-3(xe3) ; sart-3::gfp
sart-3(xe3)
sart-3(+)
sart-3(xe3) ; sart-3::gfp
L3
L4
150
100
SART-3/GFP/His/FLAG
unspecific
endogenous SART-3
Actin
1
2
3
4
5
6
(B)
i) sart-3(xe3)
ii) sart-3(xe3) ; sart-3::gfp
iii) sart-3(+)
iv) sart-3(xe3)
v) sart-3(xe3) ; sart-3::gfp
vi) sart-3(+)

Figure 5

(**A**) Western blot of lysates extracted from L3 (lane 1-3) or L4 stage worms (lane 4-6). Lane 2 and 5 show protein from wild-type (N2) worms. Lane 1 and 4 show protein from worms homozygous for the *xe3* allele obtained by sorting. Lane 3 and 6 show protein from worms homozygous for the *xe3* allele, rescued by transgenic *sart-3* containing a C-terminal GFP/His/FLAG-tag. Transgenic and endogenous SART-3 were detected by anti-SART-3 (Q5635). (**B**) DIC microscopy pictures. Worms homozygous for *xe3* display a protruding vulva (inset in i) and eventually burst (i) and do not produce oocytes (iv). The bursting phenotype (ii) as well as the sterility (v) in *xe3* worms is rescued by transgenic *sart-3*::*gfp*::*his*::*flag*. Arrows point to the vulva and arrow heads point to oocytes. iii and vi show wild-type N2 control worms. Scale bar, 20 µm.

In Figure 2A we show an interaction between USIP-1 and U6 snRNA. Due to the fact that USIP-1 comprises a conserved PAD and DXD motif characteristic of a terminal transferase (Fig. 3A), it is tempting to speculate that USIP-1 modifies the 3'-terminal poly(U)-tail on U6 snRNA. We employed 3'-RACE to compare the 3' heterogeneity on U6 snRNA in wild-type worms and worms lacking either SART-3 or USIP-1 (Fig. 6). As a consequence of the lethal phenotype of worms homozygous for the *xe3* allele (*xe3/xe3*), worms were maintained as heterozygotes (*xe3/+*) utilizing the nT1[qls51] balancer containing a fluorescent marker (pharyngeal GFP) (Table S1). This allows to differentiate between *xe3/xe3* worms, which lack pharyngeal GFP, and *xe3/+* and *+/+* worms, which have pharyngeal GFP. Clean populations of *xe3/xe3* worms were obtained by sorting out GFP-containing worms from a mixed population on a COPAS BIOSORT device (Fig. 5A (compare lane 1 with 2 and 4 with 5) and Fig. S4A)). Northern blotting of RNA extracted from worms thus obtained did not reveal altered U6 snRNA levels compared to wild-type worms (Fig. S4C). In agreement with previous studies in HeLa cells (Gu et al., 1997; Rinke and Steitz, 1985), the 3' end of U6 snRNA in wild-type worms (N2) is heterogeneous in size ranging from 4-7 U-residues, thus exhibiting U-tails that are shorter as well as longer relative to the five templated uridines (Fig. 6). Similarly, worms deleted for *sart-3* or *usip-1* show variable U-stretches, however, abolishment of these proteins does not extend the scope of 4-7 U-residues observed in wild-type worms. Lack of an effect for *usip-1(tm1897)* is probably surprising but might be explained by TUTases acting redundantly *in vivo*. Of note, fractionation of HeLa cell extracts revealed U6-specific but also unspecific TUTase activity (Trippe et al., 1998). Alternatively, as our analysis considers only U6 molecules that have a 3'-hydroxyl group (see methods) corresponding to just ~5% of total U6, we may miss an effect of USIP-1 on ~95% of U6 molecules containing an unidentified 3' end group (Lund and Dahlberg, 1992), which might, or might not, be amenable to terminal transferase activity.

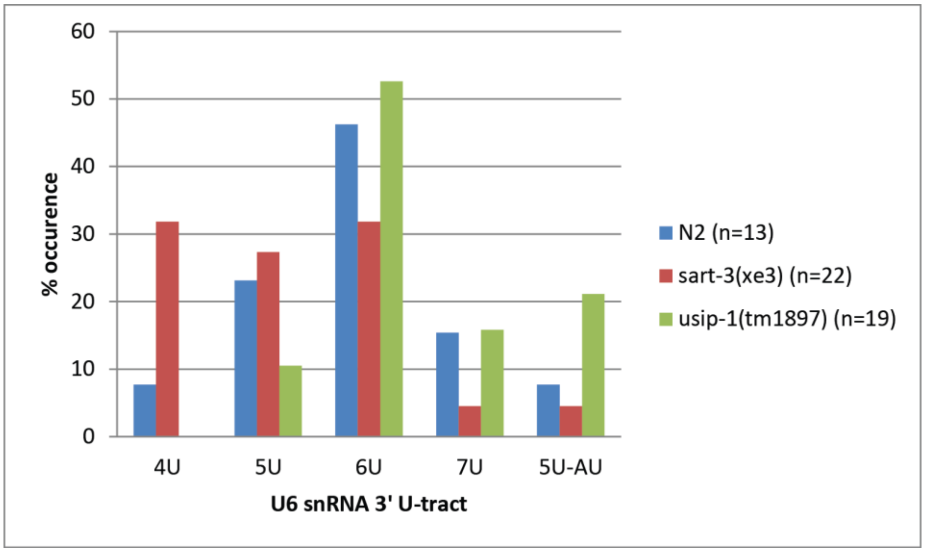

Figure 6

3' RACE on U6 snRNA extracted from wild-type worms (N2), worms homozygous for *xe3*, and worms homozygous for *tm1897*. In all three cases L4 stage worms were analyzed. U-tails between 4 and 7 residues are observed as well as UUUUUAU (5U-AU).

4.4 Discussion

In this study we analyzed the molecular function of SART-3 in *C. elegans* and characterized the phenotypes arising from its targeted deletion. We performed co-IPs on transgenic SART-3 and found an interaction with the splicing-related LSM and SNR proteins (Fig 1C). This is in agreement with findings for homologous proteins in yeast (Prp24) and mammals (SART3) which have been shown to be required for the assembly of the U4/U6 snRNP from individual U4 and U6 snRNPs (Bell et al., 2002; Shannon and Guthrie, 1991). However, whereas Prp24 appears to be part of the U6 mono-snRNP, SART3 is found in the U6 mono-snRNP and the U4/U6 di-snRNP. When we assessed the spliceosomal snRNAs that immunoprecipitate with SART-3 from whole worm lysates, we were able to detect U6 and U4 but not U1, U2, or U5 (Fig. 2A). U4 snRNA is most likely detected through its interaction with U6 snRNA and not directly bound by SART-3 (Bell et al., 2002). We thus conclude that SART-3 binds to U4/U6 di-snRNP but not to U4/U6.U5 tri-snRNP and the spliceosome, though our data does not allow to conclusively answer the question if and to what extent SART-3 interacts with the singular U6 snRNP complex. Besides, we show that the Lsm interaction domain (LID) at the C-terminal end of SART-3 is not sufficient to bind to LSM proteins in the absence of RNA (Fig. 1C). This might be equally true for human SART3. Whereas for Prp24 there is a clear consensus on a role of the LID in mediating an interaction with Lsm proteins and formation of the U4/U6 snRNP (Rader and Guthrie, 2002; Ryan et al., 2002), the LID of SART3 in HeLa cells appears to be largely dispensable for U6 snRNA binding and *in vitro* U4/U6 snRNP recycling (Medenbach et al., 2004). The reason for this discrepancy between yeast and mammals is currently unclear.

As expected for a spliceosome assembly factor, SART-3 and similarly USIP-1 are constitutively and ubiquitously expressed (Fig. 4). Immunofluorescent labeling as well as EGFP-tagging of SART3 in HeLa cells and human primary fibroblasts revealed an exclusive nuclear localization (Stanek and Neugebauer, 2004; Stanek et al., 2003). SART3 is found throughout the nucleoplasm but is highly enriched in Cajal bodies (CB), where U4/U6 snRNP recycling takes place (Stanek and Neugebauer, 2004). Localization of SART3 to CBs was dependent on the CB-specific protein coilin (Stanek and Neugebauer, 2004). Of note, neither CBs nor an ortholog of the coilin protein have yet been identified in *C. elegans*. Consistently, fluorescence microscopy reveals a diffuse signal for SART-3 throughout the nucleoplasm lacking any focal spots (Fig. 4A). How maturation of U6 snRNA and assembly of U6-containing snRNPs are temporally coordinated without spatial separation of these events in *C. elegans* remains to be investigated in future studies.

Although the molecular function of SART3/Prp24 has been investigated in sufficient detail in yeast and HeLa cells its role in development remains elusive. In *C. elegans*, loss of SART-3 leads to sterility (lack of oocytes) and eventually to death through vulval bursting (Fig 5B). A lethal phenotype has also been described for SART3 in zebrafish at 7-8 days postfertilization (Trede et al., 2007). However, whereas steady-state levels of U6 snRNA are reduced in zebrafish upon deletion of SART3, they remain unaffected in *C. elegans* (Fig. S4C). Whether the fatal phenotypes observed upon SART-3 deletion are linked to its role in splicing or another, possibly yet unrevealed function, remains to be investigated.

Taking into account the predominant interaction of SART-3 with LSM and SNR proteins under our conditions we speculate that spliceosome assembly is the main function of SART-3.

U6 snRNA undergoes a series of post-transcriptional modifications affecting internal residues, which include the conversion of certain uridines to pseudouridines and 2'-O-methylation of some backbone sugars (Tycowski et al., 1998). Besides multiple internal residues, the 3' end of U6 snRNA is subjected to major processing. U6 snRNA is transcribed by RNA pol III and accordingly its primary transcript ends in a series of uridine (U) residues that serve as a termination signal (4-5 Us in higher eukaryotes) and contains a 3' hydroxyl (OH) group (Gunnery et al., 1999). Intriguingly, the 3' poly(U) stretch in U6 snRNA has been found to be highly variable in length through post-transcriptional removal and addition of Us in murine tumor cells (Hirai et al., 1988) and HeLa cells (Gu et al., 1997; Lund and Dahlberg, 1992; Reddy et al., 1987; Tazi et al., 1993). What are the enzymes mediating the tailing and trimming of U6 snRNA? Here we describe USIP-1 from *C. elegans*, which we find to bind to U6 snRNA but not to the other spliceosomal snRNAs (Fig. 2A). Moreover, whereas USIP-1 binds to U6 snRNA, it does not bind to LSM or SNR proteins, which are components of the U6-containing snRNP complexes (e.g. U6 snRNP, U4/U6 snRNP). This result suggests that USIP-1 is involved in U6 snRNA maturation rather than snRNP assembly. However, although we find that USIP-1 does only interact with U6 among the spliceosomal snRNAs, it remains to be determined whether or not USIP-1 targets splicing-unrelated RNA substrates. Also, a formal demonstration of uridylyl-transferase activity for USIP-1 is still lacking. Though, the fact that a supposedly catalytically inactive version of USIP-1 is not able to rescue the terminal phenotype of *usip-1(tm1897)* in a *sart-3* RNAi background, strongly suggest that transferase activity of USIP-1 is crucial to its physiological function (Fig. 3C). Trippe *et al.* previously identified a U6-specific TUTase in Hela cells, HsTUT1 (Trippe et al., 1998), biochemically characterized it (Trippe et al., 2003) and eventually sequenced and cloned it (Trippe et al., 2006). Addition of purified HsTUT1 to *in vitro* transcribed U6 snRNA substrates varying in their U-tail length revealed a preference for HsTUT1 to restore the four 3' end template Us whereas incorporation of additional, non-templated Us might be mediated by an unspecific TUTase (Trippe et al., 2003; Trippe et al., 1998). Nevertheless, USIP-1 is phylogenetically only distantly related to HsTUT1 (Schmid et al., 2009) and thus further experimental evidence is required to bring to light whether USIP-1 functions in an analogous manner to HsTUT1. Trimming of the U6 snRNA 3' U-tail is supposedly mediated by exonuclease activity. Indeed, recently, the 3'-to-5' exonuclease MPN1 has been identified in yeast and humans to trim U6 oligo(U)-tails (Shchepachev and Azzalin, 2013). However, a homolog of MPN1 does not exist in *C. elegans*.

Consolidating our data with previous studies, we propose the following model (Fig. 7). Both the 3'-terminal U stretch and the 3' OH group of newly transcribed U6 snRNA are bound by the La protein which stabilizes the RNA (reviewed in (Wolin and Cedervall, 2002)). U6 snRNA with a free 3' hydroxyl group is amenable to tailing and trimming of the U-tail leading to a steady-state population of U6 snRNAs heterogeneous in size (Gu et al., 1997; Hirai et al., 1988; Lund and Dahlberg, 1992; Reddy et al., 1987; Tazi et al., 1993). In humans, tailing is mediated by the above mentioned enzyme HsTUT1 (Trippe et al., 1998). We speculate that a similar function might be carried out by USIP-1 in *C. elegans*. Trimming activity counteracting HsTUT1/USIP-1-mediated tailing is brought about by the conserved 3'-to-5' exonuclease MNP1 (Shchepachev and Azzalin, 2013). Importantly, MNP1 generates U6 molecules that terminate with a cyclic 2’,3’-phosphate (>p). Formation of a >p reduces the affinity to La protein and increases the affinity for Lsm proteins (Licht et al., 2008; Yoo and Wolin, 1994). At the same time, formation of >p and recruitment of Lsm proteins appears to replace HsTUT1/USIP-1 at the 3’ end of U6 as USIP-1 only binds to U6 snRNA not bound by Lsm proteins (Fig. 2). In HeLa cells, formation of >p even takes place upon targeted degradation of U1 and U2 snRNA suggesting that its generation is not dependent on the formation of the spliceosome or splicing for that matter (Gu et al., 1997). Moreover, >p is detected on U6 snRNAs with U-tails longer than the four templated Us (Gu et al., 1997) and these heterogeneously sized U6 snRNAs are incorporated into U4/U6 snRNP, U4/U6.U5 snRNP, and the spliceosome (Tazi et al., 1993). Formation of the U4/U6 snRNP from the individual U4 and U6 snRNPs requires the action of Prp24/SART3/SART-3 (this study and (Bell et al., 2002; Shannon and Guthrie, 1991)). Notably, we find that SART-3 and USIP-1 precipitate each other in an RNA-dependent manner (Fig. 2B) suggesting their presence in a common complex. Presumably, based on the finding that recombinant human SART3 can bind to *in vitro* transcribed U6 snRNA lacking >p (Bell et al., 2002), USIP-1 and SART-3 both bind to newly transcribed U6 snRNA but upon formation of >p and binding of Lsm proteins the interaction with USIP-1 is weakened whereas the interaction with SART-3 is reinforced. Association of U5 snRNP with the U4/U6 di-snRNP to form U4/U6.U5 tri-snRNP as well as subsequent spliceosome assembly steps are reviewed by Nagai and colleagues (Nagai et al., 2001). Whether >p is converted back to OH following splicing catalysis and thus releasing the Lsm proteins from U6 snRNA is unknown (Fourmann et al., 2013).

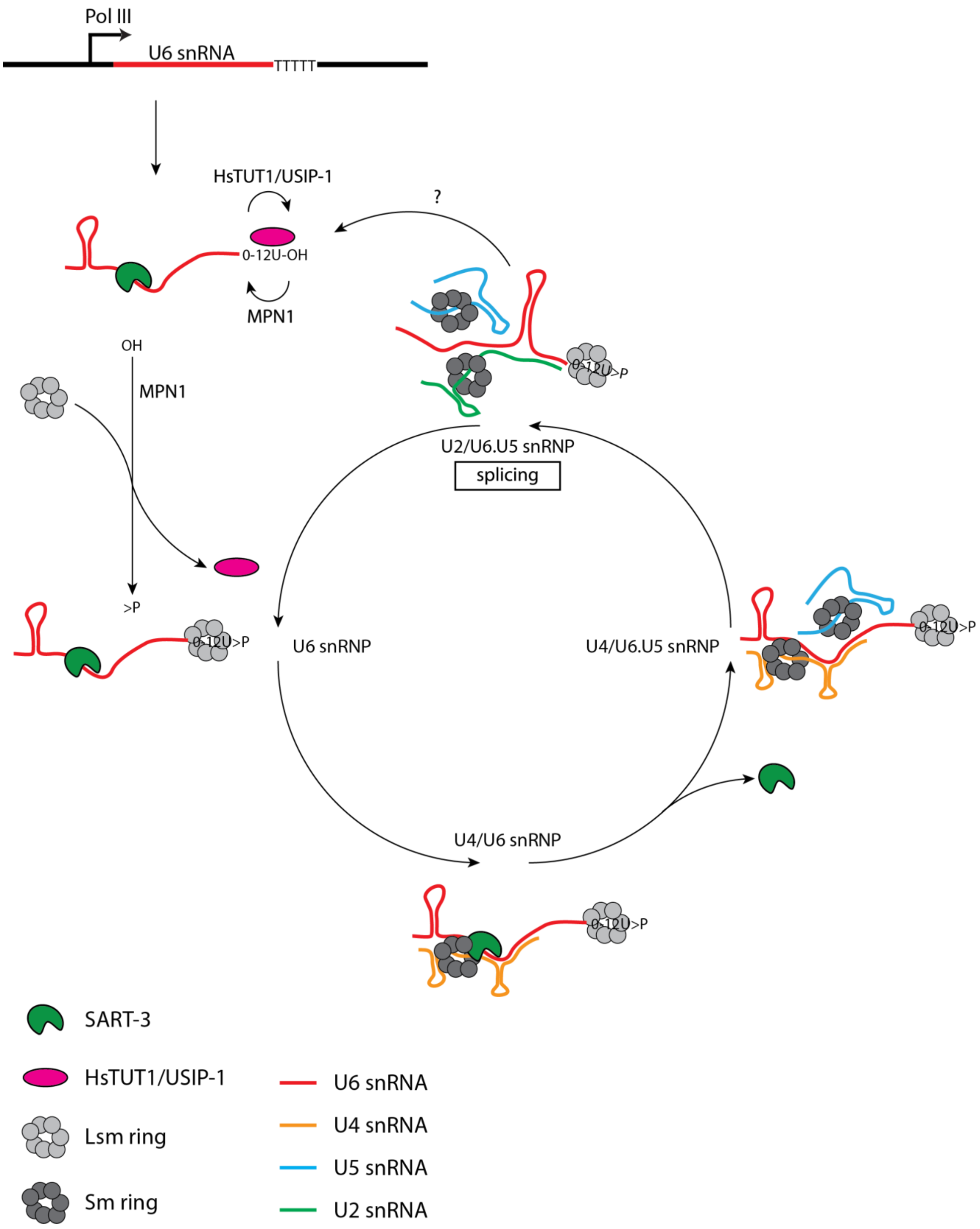
Pol III
U6 snRNA
TTTTT
HsTUT1/USIP-1
?
0-12U-OH
MPN1
OH
MPN1
>P
0-12U>P
U6 snRNP
U2/U6.U5 snRNP
splicing
0-12U>P
U4/U6.U5 snRNP
0-12U>P
U4/U6 snRNP
0-12U>P
SART-3
HsTUT1/USIP-1
Lsm ring
Sm ring
U6 snRNA
U4 snRNA
U5 snRNA
U2 snRNA

Figure 7

Model of the U6 snRNA life cycle (see text for details). The La protein and U1 snRNP are omitted for the sake of simplicity as well as many snRNP-specific splicing factors (e.g. hPrp3, hPrp4, hPrp31 are U4/U6 snRNP-specific, see (Wahl et al., 2009) for detailed composition of spliceosomal complexes).

4.5 Supplementary figures

(A)

IP1

	FLAG/SART-3		GFP/His/FLAG	
RNase A	no	yes	no	yes
SART-3	57	50	0	0
GFP	0	0	58	46
GUT-2	80	0	0	0
LSM-3	75	0	0	0
LSM-4	28	0	0	0
LSM-5	87	0	0	0
LSM-6	36	0	0	0
LSM-7	33	0	0	0
LSM-8	84	0	0	0
SNR-1	50	0	0	0
SNR-2	33	0	0	0
SNR-3	25	0	0	0
SNR-4	59	0	0	0
SNR-5	42	0	0	0
SNR-7	61	0	0	0
USIP-1	19	0	0	0

IP2

	FLAG/SART-3		GFP/His/FLAG	
RNase A	no	yes	no	yes
SART-3	53	53	0	0
GFP	0	0	78	75
GUT-2	60	0	0	0
LSM-3	71	0	0	0
LSM-4	41	0	0	0
LSM-5	21	0	0	0
LSM-6	60	0	0	0
LSM-7	19	0	0	0
LSM-8	72	0	0	0
SNR-1	51	0	0	0
SNR-2	0	0	0	0
SNR-3	42	0	0	0
SNR-4	56	0	0	26
SNR-5	48	0	0	0
SNR-7	53	40	0	0
USIP-1	33	0	0	0

	IP1		IP2	
	LSM	SNR	LSM	SNR
average % coverage	60.4	45	49.1	41.7

(B)

	GFP/His/FLAG	CeTUT-1/GFP/3xFLAG	FLAG/SART-3	CeTUT-1 to GFP ratio	SART-3 to GFP ratio
swsn-1	0	28	8	28	8
atp-2	0	25	8	25	8
pde-6	0	24	6	24	6
hsp-6	0	21	9	21	9
rpl-34	0	18	11	18	11
rpn-2	0	18	5	18	5
rpl-9	0	17	11	17	11
rpn-3	0	16	9	16	9
sip-1	0	16	0	16	0
rpl-26	0	14	11	14	11
rpl-19	0	14	5	14	5
rpl-32	0	13	9	13	9
atp-4	0	12	8	12	8
cct-5	0	12	5	12	5
F38E11.5	0	12	0	12	0
eef-2	0	11	6	11	6
nap-1	0	11	5	11	5
dlst-1	0	11	5	11	5
rpn-8	0	11	5	11	5
F18C12.3	0	11	4	11	4
cpsf-1	0	11	2	11	2
Y71F9AL.17	0	11	0	11	0
rpl-28	0	10	8	10	8
pas-4	0	10	5	10	5
cgh-1	0	10	3	10	3
cey-1	0	6	10	6	10

Figure S1

(A) % coverage of IP1 and IP2 shown in figure 1C. **(B)** Additional proteins identified by mass spectrometry in the co-IP shown in figure 2B enriched by ≥ 10-fold in either the USIP-1 or SART-3 IP over the GFP-control. Table is ranked according to the USIP-1/GFP ratio. Numbers indicate the exclusive spectrum count, i.e. number of spectra mapping uniquely to a given protein.

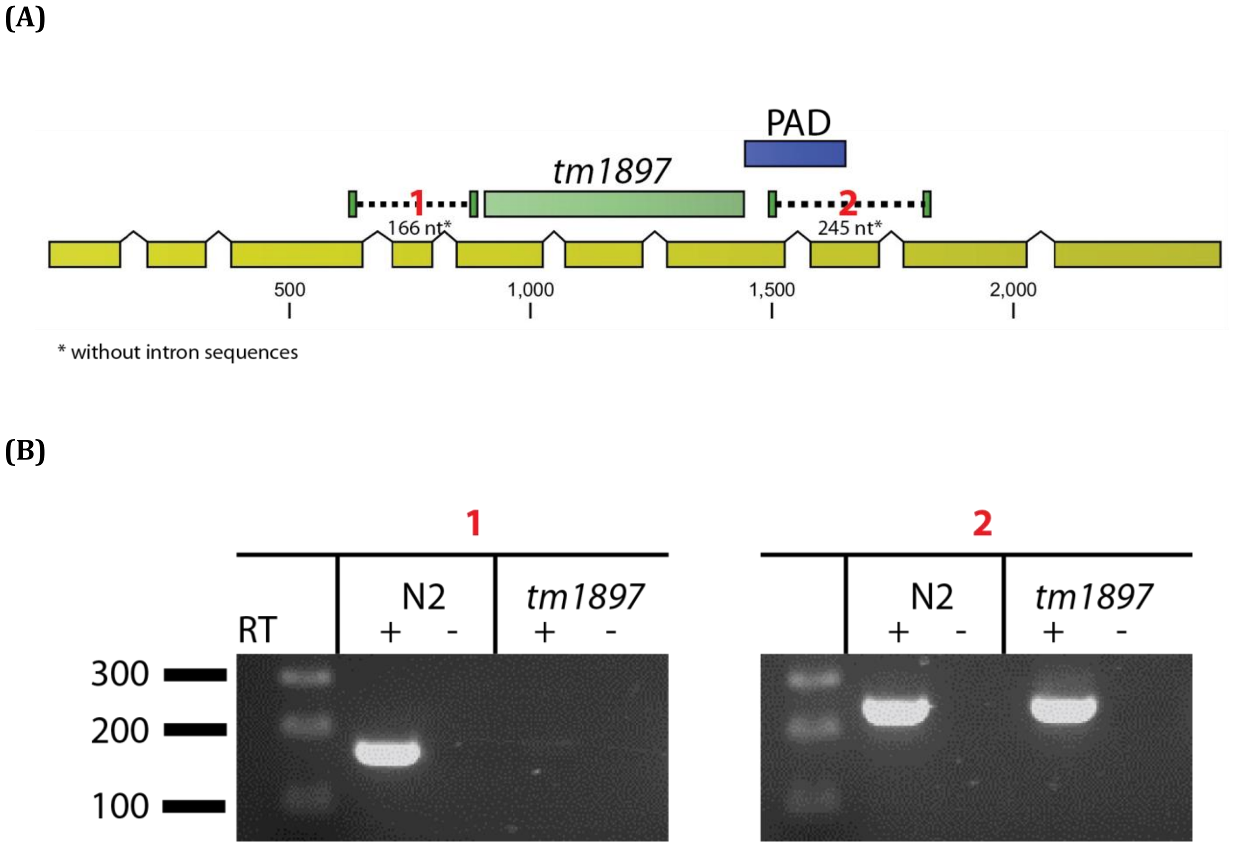
(A)
PAD
tm1897
1
2
166 nt*
245 nt*
500
1,000
1,500
2,000
* without intron sequences
(B)
1
2
RT
N2
tm1897
+
-
300
200
100

Figure S2

(A) *usip-1*/*ZK863.4* genomic locus indicating the region of the deletion *tm1897*, the PAP-associated domain (PAD), and the two regions amplified in (B) (dashed lines). **(B)** Semi-quantitative RT-PCR on *usip-1* with oligo(dT) primers amplifying the regions indicated in (A). RT = reverse transcriptase.

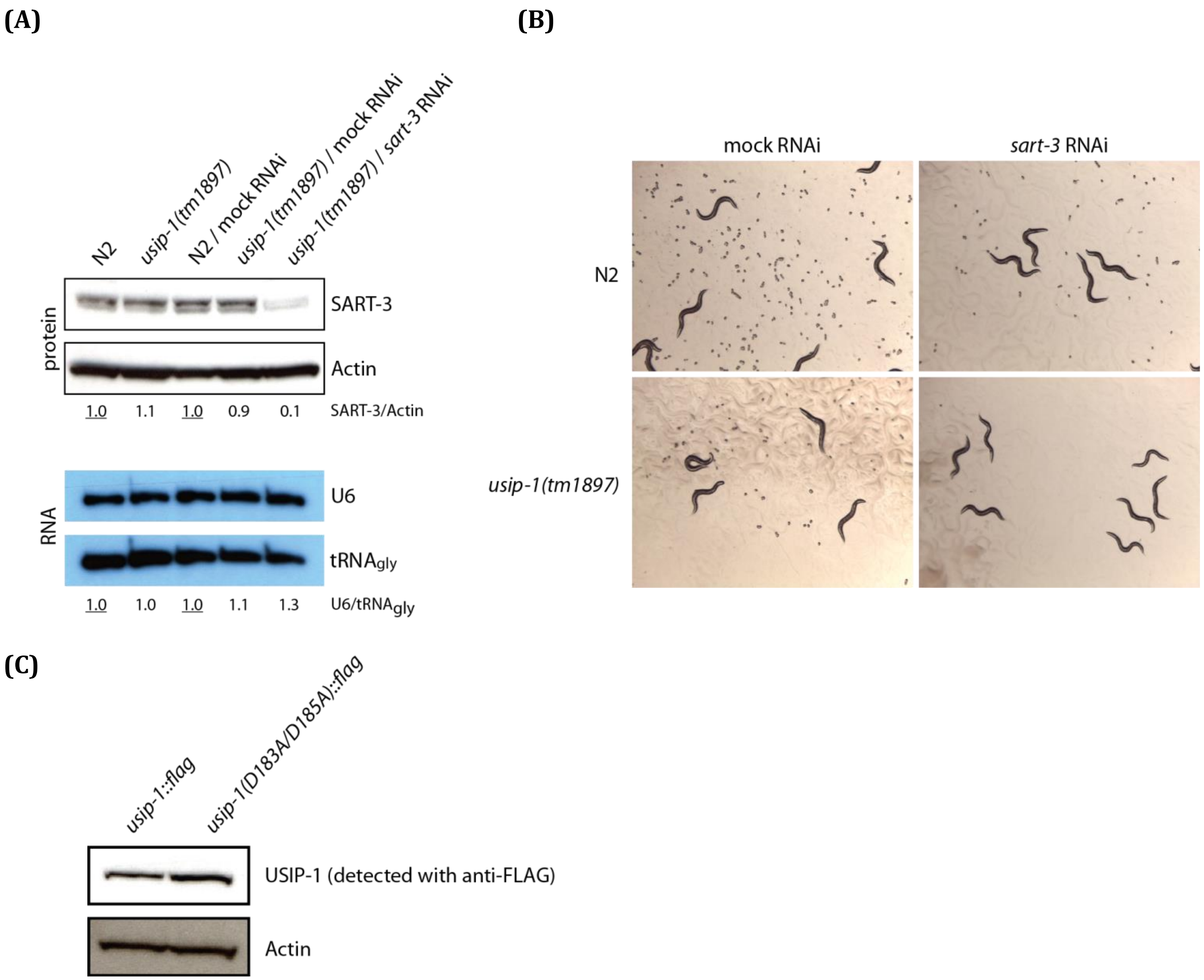
(A)
N2
usip-1(tm1897)
N2 / mock RNAi
usip-1(tm1897) / mock RNAi
usip-1(tm1897) / sart-3 RNAi
protein
SART-3
Actin
1.0 1.1 1.0 0.9 0.1 SART-3/Actin
RNA
U6
tRNAgly
1.0 1.0 1.0 1.1 1.3 U6/tRNAgly
(B)
mock RNAi
sart-3 RNAi
N2
usip-1(tm1897)
(C)
usip-1::flag
usip-1(D183A/D185A)::flag
USIP-1 (detected with anti-FLAG)
Actin

Figure S3

(A) *Upper panel*: Western blot of lysates extracted from wild-type (N2) worms or worms homozygous for the *tm1897* allele (*usip-1*) exposed to no RNAi (lane 1-2), mock RNAi (lane 3-4), or *sart-3* RNAi (lane 5). Deletion of *usip-1* does not affect SART-3 levels (compare lane 1 with 2). Knock-down of *sart-3* by RNAi reduces its levels by about 80% (compare lane 1 with 5). *Lower panel*: Northern blot for U6 snRNA using RNA extracted from worms treated as described for the upper panel. Quantification of bands is relative to the underlined value, which has been set to 1. **(B)** N2 or *usip-1(tm1897)* worms were exposed to mock or *sart-3* RNAi at the L1 stage (P0 generation) and cultured at 25°C. Pictures were taken after 48h showing P0 adults and F1 embryos. The number of laid embryos was reduced for N2/*sart-3* RNAi and *usip-1(tm1897)*/mock RNAi relative N2/mock RNAi. No embryos were observed after 48h for *usip-1(tm1897)/sart-3* RNAi. **(C)** Western blot showing similar protein levels for transgenic, FLAG-tagged wild-type USIP-1 or mutant USIP-1(D183A/D185A). Both transgenes are expressed in a *usip-1(tm1897)* background and were detected through their FLAG-tag.

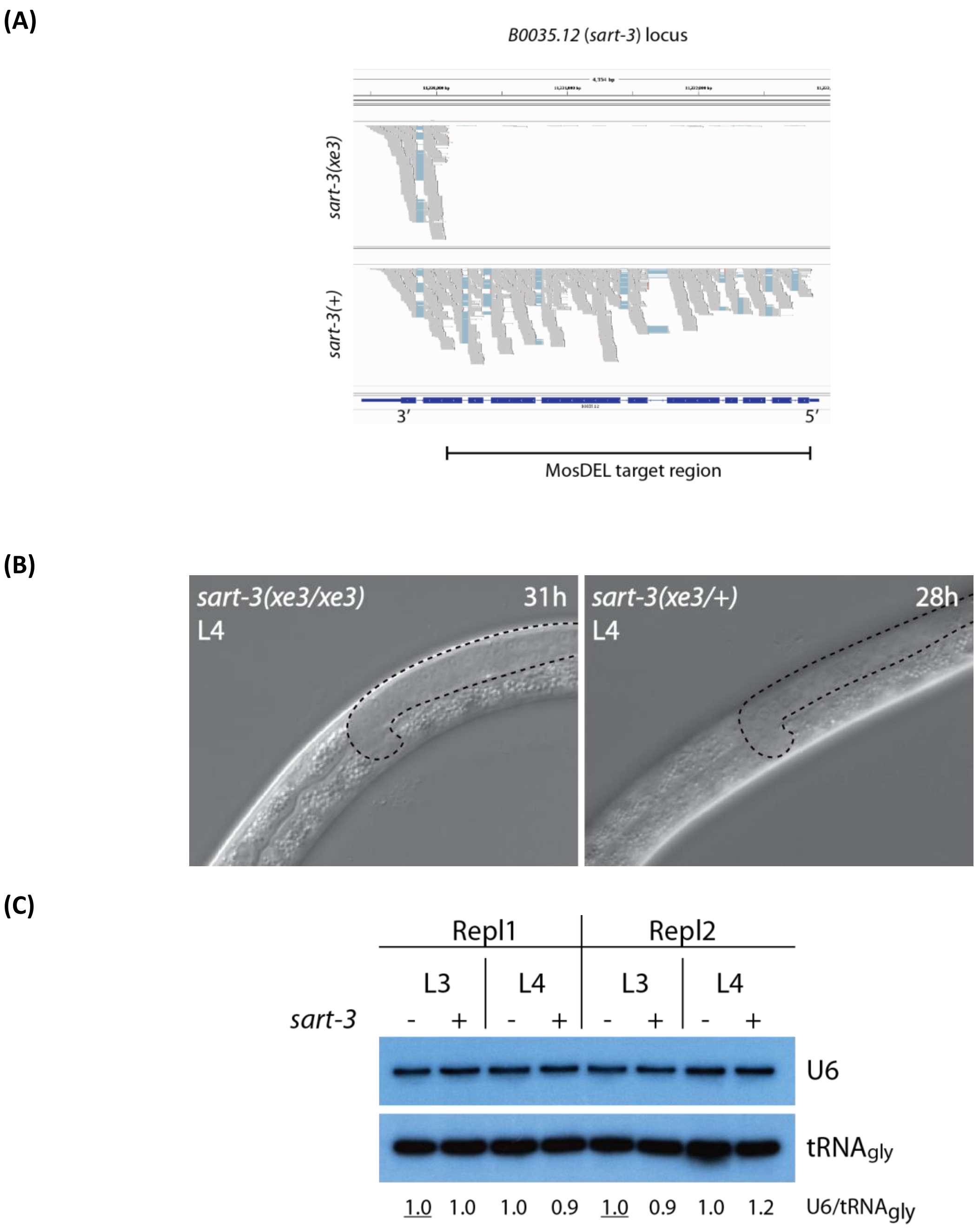
(A)
B0035.12 (sart-3) locus
sart-3(xe3)
sart-3(+)
3'
5'
MosDEL target region
(B)
sart-3(xe3/xe3)
L4
31h
sart-3(xe3/+)
L4
28h
(C)
Repl1
Repl2
L3
L4
L3
L4
sart-3
- + - + - + - +
U6
tRNAgly
1.0 1.0 1.0 0.9 1.0 0.9 1.0 1.2
U6/tRNAgly

Figure S4

(A) Snapshot of genome browser showing absence of mapping reads in the MosDEL-targeted region of *sart-3(xe3)* compared to wild-type N2 worms (*sart-3(+)*) in a poly(A)+ RNA deep sequencing experiment. **(B)** DIC microscopy pictures. Worms homozygous for the *xe3* allele need 31h at 25°C to reach early L4 stage (left panel) whereas worms heterozygous for *xe3* only need 28h (right panel). **(C)** Northern blot for U6 snRNA using RNA from wild-type (N2) worms (denoted '+' in the figure) and worms homozygous the *xe3* allele (denoted '-' in the figure) at two different developmental stages (L3 and L4). The experiment was performed in duplicates (Repl1 and Repl2). Quantification of bands is relative to the underlined value, which has been set to 1.

4.6 Methods

Strains

Strains were cultured using standard methods on OP50 seeded NGM plates (Stiernagle, 2006). The Bristol N2 strain was used as wild-type. Mutant and transgenic strains generated for this study are listed in Table S1. Except for HW1340 and HW1342, which express an extrachromosomal array, transgenic lines were obtained by Mos1-mediated Single-Copy transgene Insertion as previously described (MosSCI; (Frokjaer-Jensen et al., 2012; Frokjaer-Jensen et al., 2008). All strains have been backcrossed two times, unless indicated otherwise. *usip-1(tm1897)* animals were obtained from Dr. Shohei Mitani and backcrossed two times. The resulting strain was called HW1251.

RNAi

The RNAi clone against *sart-3* was obtained from (Kamath and Ahringer, 2003). RNAi was carried out by feeding worms with HT115 bacteria expressing dsRNA of *sart-3* or an insertless plasmid (L4440) as negative control according to (Timmons and Fire, 1998).

Single-copy transgene insertion

DNA fragments were inserted into pCFJ210 (for chromosome I), pCFJ150 (for chromosome II) or pCFJ201 (for chromosome IV) vectors by Multisite Gateway Technology (Life Technologies, Carlsbad, CA, USA) according to the supplier’s protocol and as detailed in Table S1. *Mos1*-mediated Single-Copy transgene Insertion (MosSCI) was performed according to previous reports (Frokjaer-Jensen et al., 2012; Frokjaer-Jensen et al., 2008). Successful insertion of transgenes was verified by PCR.

Semi-quantitative RT-PCR

For mRNA quantification, cDNA was generated from total RNA using the ImProm-II Reverse Transcription System (Promega, Fitchburg, WI, USA) and oligo(dT) primers according to the supplier’s protocol. cDNA was diluted 1:10 and amplified using Taq DNA polymerase (New England Biolabs, Ipswich, MA, USA) and gene-specific primers (Table S2).

Site-directed mutagenesis

Site-directed mutagenesis was performed by PfuUltra II Fusion HS DNA Polymerase (Agilent Technologies, Santa Clara, CA, USA) according to the supplier’s protocol using specific primers (Table S2).

Antibodies and Western blotting

Polyclonal, affinity purified anti-SART-3 was generated by SDIX (Newark, DE, USA) using DNA immunization of rabbits against a polypeptide (amino acids 1-163). Antibodies were used at the following dilutions: rabbit anti-*C. elegans* SART-3 (Q5635) 1:2’000, mouse anti-Actin (clone C4, MAB1501, Millipore, Billerica, MA, USA) 1:10’000, mouse anti-GFP (Roche, Penzberg, Germany) 1:2’000, mouse anti-FLAG (clone M2, F1804, Sigma-Aldrich, St. Louis, MI, USA) 1:2’000. Western blotting was performed as previously described (Miki et al., 2014). Band intensities were quantified using ImageJ software (NIH, Bethesda, MD, USA).

RNA isolation and Northern blotting

Worms were mixed with TRI Reagent (Molecular Research Center, Cincinnati, OH, USA) and freeze-thawed as described previously (Bethke et al., 2009). The RNA was extracted according to the manufacturer’s instructions. Total RNA or RNA from IP’s (see immunoprecipitation) was separated on a 10% urea-PAGE gel and transferred to a Hybond-NX membrane (GE Healthcare, Little Chalfont, UK) by semi-dry blotting. Cross-linking was carried out by UV irradiation using a UV Stratalinker 1800 (Stratagene, La Jolla, CA, USA) followed by baking (1 h at 80°C) (or by chemical cross-linking as described previously (Pall and Hamilton, 2008) in the case of Fig. S3A and S4C). Single-stranded DNA probes were designed with Unique Probe Selector (http://array.iis.sinica.edu.tw/ups/index.php). Sequences of probes are given in Table S2. Probes were 5’ end-labelled with ATP-γ-[32P] and polynucleotide kinase according to standard protocols. Hybridization was carried out overnight in 4x SSPE (0.6 M NaCl, 40 mM NaH2PO4, 4 mM EDTA), 7% SDS, 40% formamide at 37°C.

Immunoprecipitation

Mixed stage worms were lysed with a Dounce Tissue Grinder (BC Scientific, Miami, FL, USA) in 30 mM HEPES/KOH pH 7.4, 100 mM KCl, 1.5 mM MgCl2, 0.1% Triton X-100, and protease inhibitors (Protease Inhibitor Cocktail Tablets, EDTA-free, Roche). Lysates were cleared at 16,000xg for 15 min. RNase A-treated samples were additionally incubated with 0.1 mg/ml RNase A (Sigma-Aldrich) for 1 h at 4°C. Anti-FLAG IP: lysates were incubated with anti-FLAG M2 magnetic beads (Sigma-Aldrich) for 2 h. Washes were performed in lysis buffer. Elution was achieved by incubation with 1 mg/ml FLAG peptide (Sigma-Aldrich). For RNA extractions, TRI Reagent (Molecular Research Center) was directly added to the magnetics beads. Anti-SART-3 IP: Lysates were incubated with 5 µg purified antibody (anti-SART-3) for 1 h. Protein A sepharose beads (Roche) were added for 2 h. Washes were performed in lysis buffer. Complexes were eluted by heating the beads in sample loading buffer containing reducing agent for 10 min at 70°C.

Mass-spectrometry

TCA precipitated and acetone washed protein pellets were dissolved in 0.5 M Tris, pH 8.6, 6 M guanidinium hydrochloride, reduced in 16 mM TCEP for 30 min, and alkylated in 35 mM iodoacetamide for 30 min in the dark. The proteins were digested at 37°C with trypsin (Promega, Madison, USA) after 6x dilution in 50 mM Tris, 5 mM CaCl2 (pH 7.4) overnight. The generated peptides were separated on a 75µm x 10cm Magic C18 column (Michrom, Bioresources, Auburn, USA) with an Agilent 1100 Nanoflow LC System (Agilent, Palo Alto, California). The LC was connected to a LTQ Orbitrap Velos (Thermo Scientific). Mascot (Matrix Science, London, UK) searching UniProt data base version 2012_09 was used to identify the peptides.

Microscopy

DIC and fluorescent images were obtained using an Axio Observer Z1 microscope and AxioVision SE64 (release 4.8) software (Carl Zeiss, Oberkochen, Germany). Stereoscopic images were obtained by a M205 A stereo microscope (Leica, Solms, Germany).

MosDEL

The *xe3* allele was obtained by following the protocol established by (Frokjaer-Jensen et al., 2010). A targeting plasmid was created using the Multisite Gateway Technology (Life Technologies). Specific primers (Table S2) were used to amplify the left (2039 bp) and right (2988 bp) homology regions from genomic DNA and amplicons were cloned into pDONRP4-P1R and pDONRP2R-P3, respectively. Together with pENTR221 containing and *unc-119* rescue gene a pDESTR4-R3 targeting plasmid was created. The targeting plasmid was injected at 50 ng/ul into strain HW1350, a *Mos1*-engineered strain (IE5820 containing the ttTi5820 allele) obtained from the NemaGENETAG consortium (Bazopoulou and Tavernarakis, 2009) which we crossed into an *unc-119(ed3)* mutant background. Following injection, wild-type moving worms were screened for successful integration of the transgene by PCR (see Table S2 for primer sequences).

3’ RACE

U6 does not contain a poly(A) tail and therefore we ligated an RNA oligonucleotide to the 3’ end of U6 to serve as a primer binding site for reverse transcription. The 3’ RNA adapter from the TruSeq Small RNA Sample Preparation Kit (Illumina, San Diego, CA, USA) was ligated onto 1ug total RNA according to the supplier’s protocol. This adapter only ligates to RNA molecules with a 3'-hydroxyl group but not to U6 molecules with a 2’- or 3’-monophosphate (or a 2’,3’-cyclic phosphate) at the 3’ end. For reverse transcription, components of the TruSeq Small RNA Sample Preparation Kit (Illumina) were used. Reverse transcription was performed 30 min at 42°C followed by 1 h at 50°C using a primer that introduces a primer binding site for subsequent amplification (Table S2). The reverse transcriptase was inactivated by putting samples to 70°C for 15 min. Subsequently, the RNA template was degraded by RNase H for 20 min at 37°C. The cDNA was diluted 1:10 and U6 was amplified using a U6-specific primer and a primer complementary to the region introduced by reverse transcription (Table S2) by PfuUltra II Fusion HS DNA Polymerase (Agilent Technologies). PCR amplicons were cloned into the pCR8 vector according to the supplier’s protocol (pCR8/GW/TOPO TA Cloning Kit, Life Technologies) and sequenced.

Table S1 (Strains)

Strain name	genotype	comment
gfp control		
HW781	EG5003, xeSi17[Pxrn-2::gfp::his::flag::xrn-2 3', unc-119(+)] IV	
sart-3 lines		
HW1008	EG6701, xeSi55[Pdpy-30::sart-3::gfp::his::flag::xrn-2 3', unc-119(+)] I	
HW1337	sart-3(xe3)/nT1[qIs51] IV	
HW1338	HW1008 ; sart-3(xe3) IV	
HW1339	EG6699, xeSi126[Pdpy-30::flag::sart-3::gpd-operon::gfp::his-58::tbb-2 3', unc-119(+)] II	
HW1340	EG6699, xeEx386(WRM0622D_C09::gfp::3xflag;Pmyo-2::mCherry)	gfp::3xflag tagged B0035.12 (sart-3) on fosmid
HW1341	HW1339 ; sart-3(xe3)/nT1[qIs51] IV	
HW1350	unc-119(ed3) III; ttTi5820 IV	
usip-1 lines		
HW1251	ZK863.4(tm1897) V	
HW1342	EG6699, xeEx387(WRM0610A_C05::gfp::3xflag)	gfp::3xflag tagged ZK863.4 (usip-1) on fosmid
HW1343	EG6699, xeSi127[Pdpy-30::ZK863.4::flag::gpd-operon::gfp::his-58::tbb-2 3'), unc-119(+)] II	
HW1344	EG6699, xeSi128[Pdpy-30::ZK863.4(D183A/D185A)::flag::gpd-operon::gfp::his-58::tbb-2 3'), unc-119(+)] II	
HW1345	HW1343 ; ZK863.4(tm1897) V	

Table S2 (Primer and northern probes)

Cloning	**Forward (5'-->3')**	**Reverse (5'-->3')**
sart-3 (genomic DNA)	ggggacaagtttgtacaaaaaagcaggcttgATGTCCGATGTGGATATGG	ggggaccactttgtacaagaaagctgggtgATTTTTCATAAACATTTTACGG
flag::sart-3 (genomic DNA)	ggggacaagtttgtacaaaaaagcaggctgcATG GATTATAAAGATGATGATGACAAGTCCGATGTGGATATG	ggggaccactttgtacaagaaagctgggtgTTAATTTTTCATAAACATTTTAC
usip-1 (genomic DNA)	ggggacaagtttgtacaaaaaagcaggcttgATGTCTTCAAACTTGCAACTGG	ggggaccactttgtacaagaaagctgggtgTTATGGCCAAGTTGGGGCTGC
Genotyping		
tm1897	CGCCTCCGTGCGCACTTGAG	GTTATGCTGTGAAAACAAGC
Site-directed mutagenesis		
usip-1(D183A)	GGCGAAATGGTTACTCAGCGATTGTAAGTTGTTAG	CTAACAACTTACAATCGCTGAGTAACCATTTCGCC
usip-1(D185A)	CAATAATGTTTTTAGGCGATTAACGTGGAATCAG	CTGATTCCACGTTAATCGCCTAAAAACATTATTG
Semi-quantitative RT-PCR		
usip-1 amplicon 1	CACCGGTGCGGCGAAATGG	GGGTATGTCTCAAGCTCCG
usip-1 amplicon 2	CGAACAAAGCGATTTACGG	CATAGTAGCCATCGTGTTG
MosDEL		
left homology region	ggggacaactttgtatagaaaagttggcCGAACCATCTGAGTACGTCG	ggggactgctttttttgtacaaacttgcGCTCAAAAATGTGTTGCTTCTGG
right homology region	ggggacagctttcttgtacaaagtggcgCTTGCAGAATTTTGATGGAAAC	ggggacaactttgtataataaagttgcGAAGCTTTCCTACAAAGAGC
xe3 5' end insertion	CGTCCTCACTTTCTGAGCTG	CCAATTCATCCCGGTTTCTG
xe3 3' end insertion	CCAATTACTCTTCAACATCC	CGACATTATTGATGTAACACC
3' RACE		
RT primer	GACCGAGTGTAGCAAGCGAGGACTCGAGCTCAAGCCAAGCAGAAGACGGCATACGA	
U6 amplification	GACCGAGTGTAGCAAGCG	GTTCTTCCGAGAACATATAC
Probes for Nothern blotting		
U1	GCACGCAGCCCCGATACGCA	
U2	CGATAAGAACAGATACTACAC	
U4	CGCACCTCGGCAAAGCCTCA	
U5	GGTTAAATGCAGAGGAACCAGAGT	
U6	ATTTGCGTGTCATCCTTGCGCAGG	
tRNA(gly)	GCTTGGAAGGCATCCATGCTGACCATT	

Lower case letters = gateway recombination sites

5 Conclusion

This study aimed at a better understanding of the developmental and molecular function of two proteins involved in ncRNA metabolism, XRN2 and SART-3. XRN2 is the major 5’-to-3’ exonuclease in the nucleus and had been implicated in the processing or degradation of many non-coding RNA species including rRNAs, snoRNAs, tRNAs, and miRNAs. Whereas XNR2 comprises a broad spectrum of substrates, SART-3, according to my findings and published literature, appears to be specifically involved in U6 snRNA metabolism where it mediates the recruitment of the U4 snRNP to the U6 snRNP. For both, XRN2 and SART-3, knowledge of their systemic role had been scarce and *C. elegans* provided an excellent model to investigate their function in a multicellular context. Moreover, once phenotypes for mutants of these proteins had been characterized, they allowed looking for functionally linked factors by testing candidate proteins for genetic interaction with XRN2 and SART-3. Indeed, genetic interaction as well as biochemical approaches led me to the identification of novel physical and functional interaction partners for XRN2 and SART-3, which we termed PAXT-1 and USIP-1, respectively. PAXT-1 binds to XRN2 through a conserved XRN2-binding domain (XTBD) and modulates its stability. Importantly, by showing that human proteins possessing an XTB-domain are also able to bind to XRN2, we could nicely extend our initial findings in *C. elegans* to humans. It remains to be investigated whether XTBD-containing proteins in organisms other than *C. elegans* similarly function in XRN2 stabilization. Whereas we know how PAXT-1 modulates XRN2 activity, we only have a preliminary understanding of how the synthetic lethal phenotype of SART-3 and USIP-1 arises. Future enquiries are needed to establish the functional implications of the putative uridylyl-transferase activity of USIP-1 for splicing. Aberrant levels of XRN2 as well as SART-3 have been correlated with cancer. Thus, a precise understanding of their mode of action might eventually pave the way for therapeutic approaches.

6 Publication: "PAXT-1 promotes XRN2 activity by stabilizing it through a conserved domain"

Please cite this article in press as: Miki et al., PAXT-1 Promotes XRN2 Activity by Stabilizing It through a Conserved Domain, Molecular Cell (2014), http://dx.doi.org/10.1016/j.molcel.2014.01.001

Molecular Cell
Short Article

PAXT-1 Promotes XRN2 Activity by Stabilizing It through a Conserved Domain

Takashi S. Miki,[1] Hannes Richter,[1,2,3] Stefan Rüegger,[1,2,3] and Helge Großhans[1,*]
[1]Friedrich Miescher Institute for Biomedical Research, Maulbeerstrasse 66, 4058 Basel, Switzerland
[2]University of Basel, Petersplatz 1, 4003 Basel, Switzerland
[3]These authors contributed equally to this work
*Correspondence: helge.grosshans@fmi.ch
http://dx.doi.org/10.1016/j.molcel.2014.01.001

SUMMARY

XRN2 is an essential eukaryotic exoribonuclease that processes and degrades various substrates. Here we identify the previously uncharacterized protein R05D11.6/PAXT-1 as a subunit of an XRN2 complex in *C. elegans*. Targeted *paxt-1* inactivation through TALEN-mediated genome editing reduces XRN2 levels, decreases miRNA turnover activity, and results in worm death, which can be averted by overexpressing *xrn-2*. Hence, stabilization of XRN2 is a major function of PAXT-1. A truncated PAXT-1 protein retaining a predicted domain of unknown function (DUF3469) suffices to restore viability to *paxt-1* mutant animals, elevates XRN2 levels, and binds to XRN2. This domain occurs in additional metazoan proteins and mediates interaction of human CDKN2AIP/CARF and NKRF with XRN2. Thus, we have identified a bona fide XRN2-binding domain (XTBD) that can link different proteins, and possibly functionalities, to XRN2.

INTRODUCTION

Ribonucleases (RNases) play important roles in various aspects of gene expression through their functions in RNA processing, surveillance, and decay. Although some RNases may specialize in only a subset of these functions, others seem to function more broadly in diverse processes. This is particularly true for the processive eukaryotic 5′-to-3′ exoribonuclease XRN2 (Miki and Großhans, 2013; Nagarajan et al., 2013). Its major substrate requirements in vitro are the presence of a 5′ monophosphate and the absence of strong secondary structures (Kenna et al., 1993). In cells, its nuclear steady-state localization may restrict substrate availability, but XRN2 was nonetheless shown to act on various types of RNAs. Among its substrates are pre-rRNA (Amberg et al., 1992; Henry et al., 1994) and snoRNAs (Petfalski et al., 1998; Qu et al., 1999), which XRN2 processes, as well as pre-mRNAs (Bousquet-Antonelli et al., 2000; Davidson et al., 2012) and aberrant tRNAs (Chernyakov et al., 2008), which XRN2 degrades. In *C. elegans*, XRN2, encoded by the *xrn-2* gene, degrades functional, mature miRNAs (Chatterjee and Grosshans, 2009).

Consistent with its diverse and extensive functions in cellular RNA metabolism, XRN2 is essential for growth of *S. cerevisiae* (Amberg et al., 1992) and for development of *C. elegans*. Specifically, RNAi-mediated depletion of *C. elegans* XRN2 causes growth delay, sterility, and larval molting defects (Chatterjee and Grosshans, 2009; Frand et al., 2005).

A number of different proteins have been shown to interact with XRN2 in various systems or organisms (Nagarajan et al., 2013), which may be a prerequisite for the diversity of functions that it executes. However, it is frequently unclear whether interactions reflect direct binding and hence what the immediate functional consequences of interactions are. A notable exception is yeast Rai1p, which was shown to bind XRN2/Rat1p and promote its exoribonuclease activity (Xiang et al., 2009). Rai1p also exhibits pyrophosphohydrolase activity for 5′ triphosphorylated RNA, which is resistant to XRN2, raising a possibility that Rai1p preprocesses these substrates into 5′ monophosphorylated RNA for XRN2 (Xiang et al., 2009). However, Dom3Z/DXO, the metazoan ortholog of Rai1p, does not bind to XRN2 (Xiang et al., 2009), but instead functions as a decapping enzyme, pyrophosphohydrolase, and distributive 5′-to-3′ exoribonuclease (Jiao et al., 2013; Xiang et al., 2009).

A second protein whose interaction with XRN2 is well characterized is the Argonaute/Piwi protein Twi12 in the ciliate *Tetrahymena thermophila*. Twi12 can bind to small fragments of tRNAs, and this enables it to bind XRN2, localize it to the nucleus, and stimulate RNase activity (Couvillion et al., 2012). Twi-associated novel 1 (Tan1) is an additional protein subunit of this XRN2 complex, whose function is, however, currently unknown. Since Piwi proteins in other organisms are preferentially or exclusively expressed in the germline and since Twi12 is rather divergent in sequence from other Piwi proteins, it is unknown if similar complexes function outside *Tetrahymena.*

Whereas Rai1p and Twi12 appear to be constitutive subunits of functional XRN2 complexes in yeast and *Tetrahymena*, respectively, additional XRN2 interacting partners may function in more specific processes. For instance, TTF2 and some decapping factors such as Dcp1a coimmunoprecipitate with XRN2 from human HeLa cell nuclear extract, and complex formation may allow these proteins to terminate RNA polymerase II transcription prematurely (Brannan et al., 2012). Conversely, recruitment of XRN2 to 3′ RNA fragments downstream of poly(A) cleavage sites facilitates their degradation and transcriptional termination in yeast and mammals and is promoted by Rtt103p (Kim et al., 2004) and p54nrb/PSF (Kaneko et al., 2007). Whether

Please cite this article in press as: Miki et al., PAXT-1 Promotes XRN2 Activity by Stabilizing It through a Conserved Domain, Molecular Cell (2014), http://dx.doi.org/10.1016/j.molcel.2014.01.001

these interactions with more specific factors are direct remains largely unexplored.

Here we report a complex formed by XRN2 and the previously uncharacterized protein R05D11.6/PAXT-1 in *C. elegans*. PAXT-1 binds and stabilizes XRN2, and this activity is required for efficient degradation of miRNAs by XRN2. Generation of *paxt-1* null mutant animals reveals that an essential function of PAXT-1 in *C. elegans* development can be compensated for by an increased *xrn-2* gene dosage. PAXT-1 binds XRN2 through a predicted domain of unknown function, DUF3469, and expression of this domain in *paxt-1* mutant animals suffices for XRN2 stabilization and worm development. Although PAXT-1 has overall little homology to other sequences, DUF3469 occurs in human CDKN2AIP/CARF and NKRF/NRF and mediates their interaction with XRN2. Thus, DUF3469 constitutes an XRN2-binding module that is employed by different metazoan proteins to link to XRN2.

RESULTS

PAXT-1 Is in a Complex with XRN2

In order to gain insight into XRN2 function, we purified XRN2 complexes by immunoprecipitation from whole lysates of worms expressing XRN2 fused to GFP/FLAG at the C terminus (XRN2/GFP/FLAG). One band migrating between the 50 and 37 kDa markers was present specifically in XRN2/GFP/FLAG but not in GFP/FLAG precipitates (Figure S1A). Mass spectrometry analysis of the XRN2 immunoprecipitates identified a 38 kDa uncharacterized protein, R05D11.6 (Figure 1A). Interaction of endogenous XRN2 and R05D11.6 was confirmed by coimmunoprecipitation from whole wild-type worm lysate, whereas XRN1, a paralog of XRN2, did not coprecipitate with R05D11.6 (Figure 1B). Based on these and additional data presented below, we named R05D11.6 Partner of Xrn-Two, or PAXT-1 for short.

The interaction between XRN2 and PAXT-1 was resistant to RNase treatment (Figure 1B), suggesting that it was not mediated by RNA. To test directly whether XRN2 and PAXT-1 were capable of binding to one another, we sought to produce recombinant proteins in *E. coli*. To facilitate expression, we utilized an XRN2 construct comprising amino acids 1–821, which lacks the glycine-rich C terminus that is not found in orthologous proteins from other organisms and that is not required for enzymatic activity (data not shown). Whereas PAXT-1 alone was poorly expressed, it could be produced at good yields when XRN2 was coexpressed in the same cells (data not shown). This suggested that the recombinant proteins bound to one another. We confirmed this by size-exclusion chromatography (SEC), which revealed a shift in protein migration when assaying the complex relative to XRN2 alone (Figures 1C and 1D). We conclude that PAXT-1 is a direct binding partner of XRN2. Furthermore, considering that SEC assays complexes at high dilutions and that the complex resisted dissociation by salt concentration of up to 2 M NaCl (data not shown), binding appears very stable.

PAXT-1 Is a Nuclear Protein that Is Present throughout *C. elegans* Development

xrn-2 is expressed ubiquitously throughout *C. elegans* development, and XRN2 protein localizes predominantly to the nucleus (Miki et al., 2014). To examine the expression of *paxt-1*, we generated a strain that produced GFP-tagged full-length PAXT-1 (GFP/PAXT-1) by *Mos1*-mediated single-copy transgene insertion (MosSCI) (Frøkjær-Jensen et al., 2012; Frøkjaer-Jensen et al., 2008). Since *paxt-1* is expressed in an operon (CEOP1484; http://www.wormbase.org), we used the sequence 5′ of *ran-4*, the most upstream gene of the operon, as a promoter (Figure S1B). GFP/PAXT-1 was observed ubiquitously and throughout worm development and predominantly located in the nucleus (Figure 1E). In the nucleus of adult hypodermal cells, GFP/PAXT-1 was localized both in the nucleolus and in the nucleoplasm.

GFP/PAXT-1 was functional as demonstrated by the fact that it rescued developmental defects associated with a *paxt-1* null mutation (see below). However, fertility was only partially restored in rescued animals, presumably because the transgene is cDNA based and may thus express at reduced levels. Hence, to examine the accumulation of endogenous PAXT-1, we raised a polyclonal antibody that detects two specific bands in western blots, of which the bottom band appears close to an additional, nonspecific band (Figure S2B). Consistent with the GFP/PAXT-1 data, we find that PAXT-1 is present in all stages at similar levels (Figure S1C). Thus, PAXT-1 and XRN2 share a similar expression pattern and subcellular localization.

PAXT-1 Depletion Enhances *xrn-2* Mutant Phenotypes

Whereas depletion of XRN2 by RNAi leads to various developmental defects (Chatterjee and Grosshans, 2009; Frand et al., 2005), we failed to observe any gross developmental phenotypes when exposing wild-type N2 animals to RNAi against *paxt-1* (Figures 2A and 2B). To test whether PAXT-1 function would become more readily detectable when XRN2 function was impaired, we utilized an *xrn-2* temperature-sensitive (*xrn-2ts*) strain that we recently generated (Miki et al., 2014). This strain displays various defects such as embryonic lethality, larval arrest, and sterility at high temperature (≥23°C), but is viable, albeit slow-growing, at 20°C. Remarkably, when *xrn-2ts* worms were grown at the permissive temperature, depletion of PAXT-1 was fatal: *xrn-2ts* worms fed with *paxt-1(RNAi)* bacteria from L3 stage laid eggs, but the eggs failed to hatch (Figure 2A). By contrast, embryos from *xrn-2ts* animals exposed to mock RNAi or from wild-type animals exposed to *paxt-1(RNAi)* hatched normally (Figure 2A).

To see effects of PAXT-1 depletion in early larval development, we fed *xrn-2ts* worms with *paxt-1(RNAi)* bacteria from L1 stage. Most of the worms developed into adults, but they were all sterile, and half showed a molting defect (Figure 2B). These phenotypes have also been observed in *xrn-2ts* worms at restrictive temperature (Miki et al., 2014) as well as wild-type worms subjected to RNAi against *xrn-2* (Chatterjee and Grosshans, 2009; Frand et al., 2005), suggesting that *paxt-1* is a genetic enhancer of *xrn-2*. Thus, PAXT-1 interacts with XRN2 both physically and genetically.

A Complete PAXT-1 Knockout Causes Larval Arrest

Using RNAi, we were unable to deplete PAXT-1 by more than half (Figure S4C), suggesting that residual PAXT-1 would prevent us from observing mutant phenotypes in wild-type animals

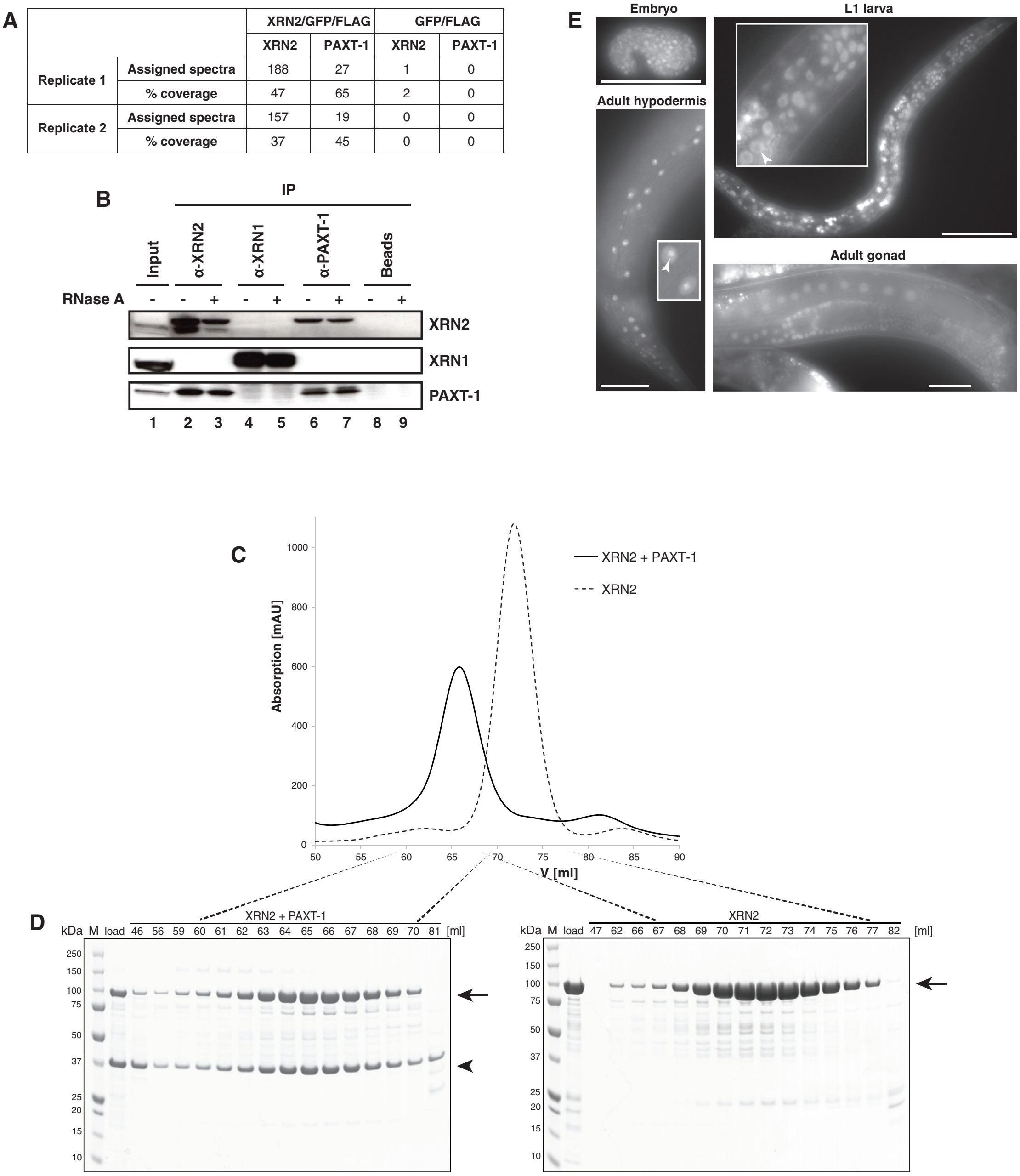

		XRN2/GFP/FLAG		GFP/FLAG	
		XRN2	PAXT-1	XRN2	PAXT-1
Replicate 1	Assigned spectra	188	27	1	0
	% coverage	47	65	2	0
Replicate 2	Assigned spectra	157	19	0	0
	% coverage	37	45	0	0

Figure 1. PAXT-1 and XRN2 Form a Complex

(A) Two replicates of mass spectrometry following IP of transgenic, FLAG-tagged XRN2 detect R05D11.6/PAXT-1 above the background (i.e., GFP/FLAG control) in total eluates.

(B) Western blot analysis of IPs against endogenous XRN1, XRN2, and R05D11.6/PAXT-1. R05D11.6/PAXT-1 is detected in the XRN2 IP (lane 2 and 3) and vice versa (lane 6 and 7). R05D11.6/PAXT-1 does not interact with XRN1 (lanes 4–7). RNase A treatment does not abolish the R05D11.6-XRN2 interaction. 10% of input and 100% of eluate was loaded. Note that in this and similar figures below, differences in salt concentrations cause high molecular weight proteins (XRN1, XRN2) to migrate slightly differently in input versus eluate samples.

(C) Preparative size-exclusion chromatography elution profiles of XRN2 (dashed line) alone and a PAXT-1 XRN2 complex (solid line). mAU, milliabsorption unit.

(D) SDS-PAGE analysis of aliquots of the indicated fractions collected from the individual elutions. XRN2 and PAXT-1 are indicated by an arrow and an arrowhead, respectively.

(E) Worms expressing GFP/PAXT-1 on chromosome II from the *paxt-1* operon promoter were observed by epifluorescence microscopy. Scale bar, 50 μm. Arrowheads point to nucleoli. See also Figure S1.

Please cite this article in press as: Miki et al., PAXT-1 Promotes XRN2 Activity by Stabilizing It through a Conserved Domain, Molecular Cell (2014), http://dx.doi.org/10.1016/j.molcel.2014.01.001

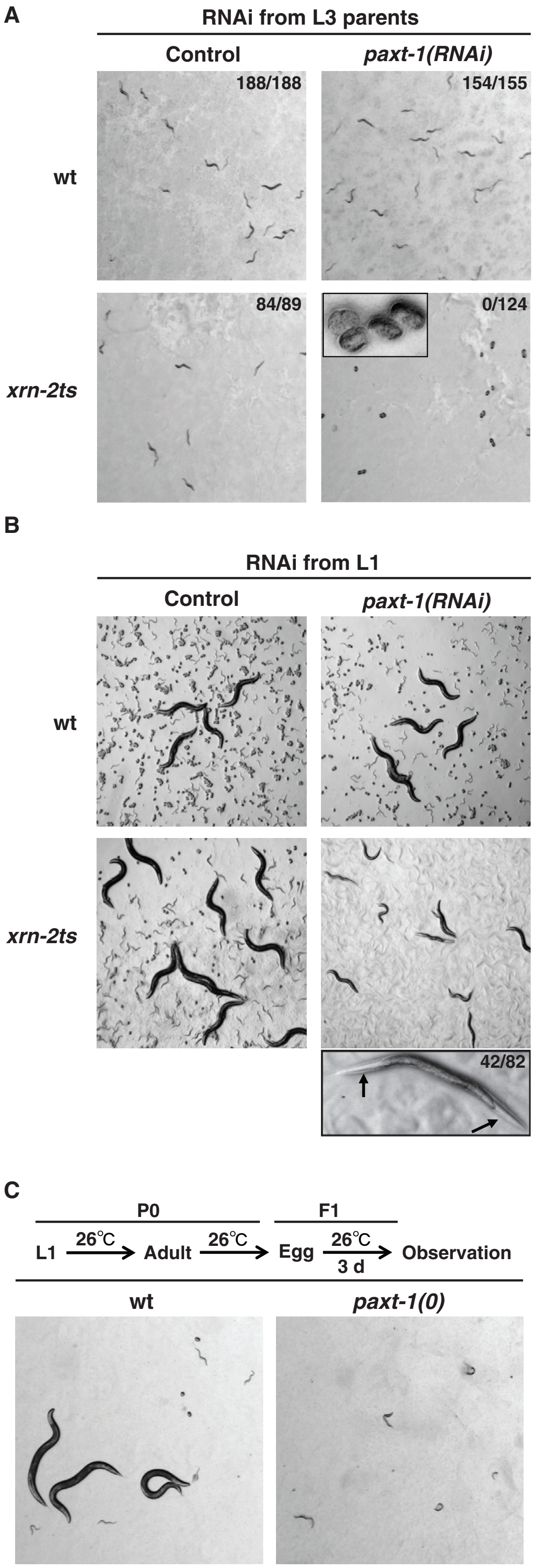

Figure 2. *paxt-1* Is Essential for Larval Development at Elevated Temperature

(A) Wild-type (WT) or *xrn-2ts* worms were cultured on a control or a *paxt-1(RNAi)* plate from L3 stage at 20°C, and hatching rates of their eggs were examined. Numbers of hatched eggs/total numbers are shown.

(B) WT or *xrn-2ts* worms were cultured on a control or an *paxt-1(RNAi)* plate from L1 stage at 20°C. All *xrn-2ts* worms on an *paxt-1(RNAi)* plate were sterile, with 42 out of 82 showing a molting defect. Arrows indicate unshed cuticles.

(C) WT or *paxt-1(0)* animals were cultured from L1 until laying eggs. After 3 days, hatched progeny were observed by stereo microscopy at the same magnification. See also Figure S2.

exposed to *paxt-1(RNAi)*. To circumvent this limitation, we generated *paxt-1* knockout strains by genome engineering using transcription activator-like effector nucleases (TALENs) (Wood et al., 2011). We recovered two *paxt-1* null alleles (Figure S2A) and confirmed lack of PAXT-1 in these strains by western blotting (Figure S2B). We used the *paxt-1(xe5)* strain for further experiments. At 20°C, these animals were viable, with growth rates comparable to wild-type animals and no obvious differences in fertility (data not shown). Similarly, when shifted to 26°C during larval stage 1 (L1), *paxt-1(0)* worms developed into adults without obvious defects and segregated F1 progeny. However, > 80% of F1 progeny arrested at the L1 stage, while wild-type F1 progeny developed into fertile adults (Figure 2C and see below). Thus, *C. elegans* requires PAXT-1 for larval development at elevated temperature.

PAXT-1 Is Required for Efficient RNA Degradation by XRN2

The genetic data revealed that PAXT-1 is important for XRN2 function. To test the effect of PAXT-1 on XRN2 enzymatic activity, we compared RNA degradation by recombinant XRN2 and XRN2-PAXT-1 complexes (Figures 1C and 1D) utilizing an assay previously used for yeast Xrn1p and Rat1p (Sinturel et al., 2009). This assay is particularly suitable for processive enzymes, as it measures full degradation of substrate molecules (Supplemental Experimental Procedures). Using a 5′ monophosphorylated RNA substrate of 30 nucleotides, we made two observations. First, the initial velocity of RNA degradation remained unaffected by PAXT-1, suggesting that PAXT-1 does not modulate XRN2 enzymatic kinetics (Figures 3A and S3A, insets). Second, when assaying activity over extended times at enzyme or complex concentrations exceeding 10 nM, more substrate was turned over by the complex than by XRN2 alone (Figure 3A and data not shown). For instance, under the conditions shown in Figure 3A, the complex consumes 42.7% (±1.0% SEM; mean of three replicate measurements) of substrate compared to 32.4% (±1.2%) for XRN2 alone within 1,800 s and 58.2% (±0.3%) versus 44.5% (±1.9%) after 3,600 s, the endpoint of the assay. This presumably reflects increased stability of the complex relative to XRN2 alone. However, the experiments are performed in a > 50-fold excess of substrate, and the later phase is thus driven by multiple turnover activity (Liu et al., 2011). Hence, beyond stabilizing XRN2, PAXT-1 might enhance multiple substrate turnover.

To examine whether PAXT-1 affected XRN2 activity in vivo, we examined degradation of endogenous miR-51 and miR-87, two known XRN2 substrates (Miki et al., 2014) in synchronized

Please cite this article in press as: Miki et al., PAXT-1 Promotes XRN2 Activity by Stabilizing It through a Conserved Domain, Molecular Cell (2014), http://dx.doi.org/10.1016/j.molcel.2014.01.001

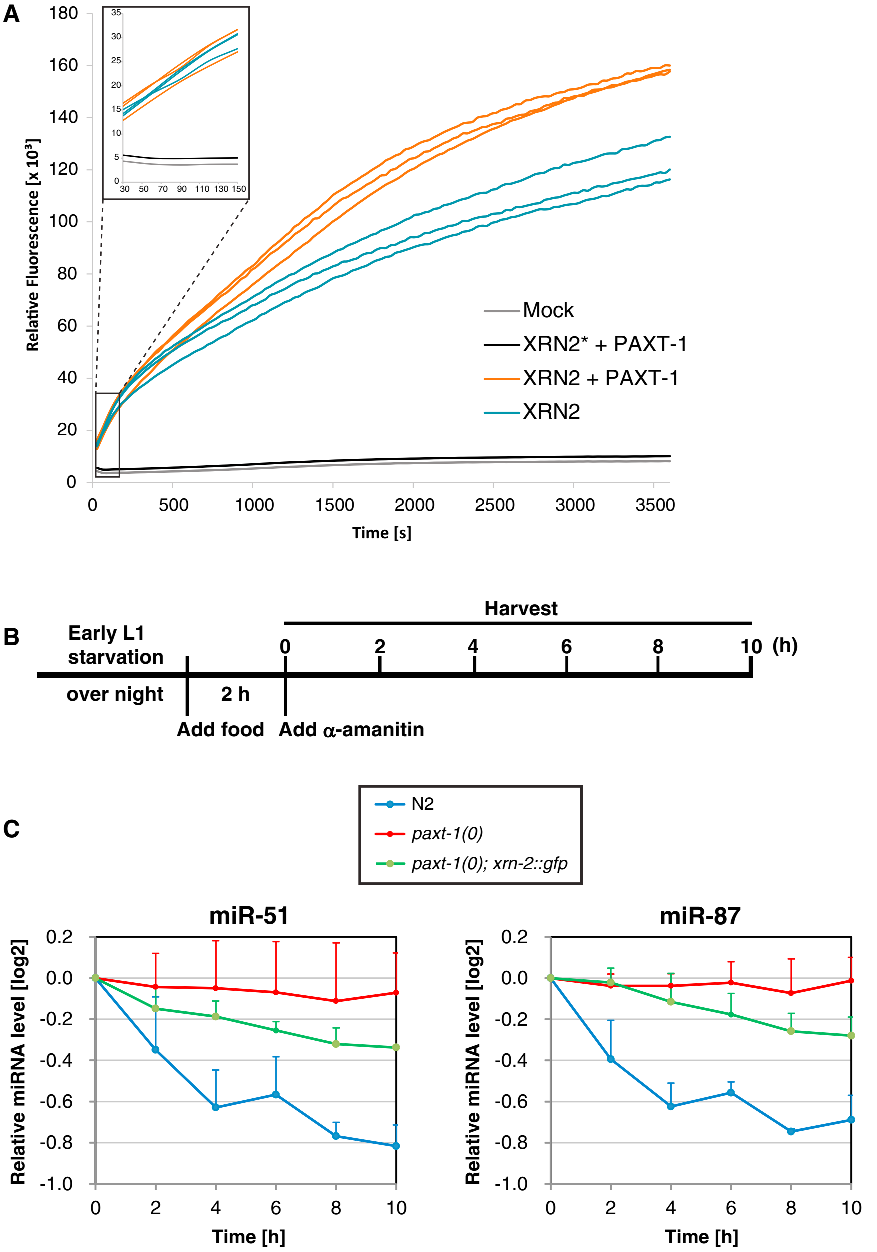

Figure 3. PAXT-1 Is Required for RNA Degradation by XRN2 In Vivo

(A) Comparison of nucleolytic activity over time of XRN2 (blue), PAXT-1 XRN2 complex (orange), PAXT-1 XRN2* (catalytic dead) complex (black), and mock control (gray) at 10 nM of protein or complex and 500 nM of RNA substrate. Lines of the same color indicate individual replicates. Inset, initial velocity of the reaction.

(B) Experimental design for miRNA decay analysis in vivo. Eggs were hatched overnight, and the resulting synchronized L1 larvae were cultured with food for 2 hr prior to addition of α-amanitin. Samples were harvested at the indicated times. All processes were done at 26°C.

(D) Levels of miR-51 and miR-87 were examined by RT-qPCR. The levels relative to the time point 0 hr are shown (n = 2 for WT and *paxt-1(0); xrn-2::gfp* and 3 for *paxt-1(0)*; means ± SD). See also Figure S3.

wild-type and *paxt-1(0)* L1-stage worms. The animals were treated with α-amanitin to block de novo production of miRNAs, and the levels of miR-51 and miR-87 were followed over time (Figure 3C). Under these conditions, the *paxt-1(0)* developmental arrest phenotype will not influence the measured decay rates, because α-amanitin equally arrests the development of wild-type animals (Miki et al., 2014). Whereas the levels of both miRNAs substantially decreased in wild-type animals, they remained essentially unchanged in *paxt-1(0)* animals throughout the entire time course. Figure S3B shows this to be true for miR-56, a third XRN2 target miRNA, but not for miR-87*, the passenger strand of miR-87, which is not a target of XRN2 either (Miki et al., 2014). Thus, PAXT-1 is important for in vivo degradation of the same miRNAs that are also substrates of XRN2.

Stabilization of XRN2 Is an Essential Function of PAXT-1

Although it remained formally possible that PAXT-1 promoted miRNA degradation independently of XRN2, this seemed unlikely given the physical interaction of the two proteins. Moreover, we noticed that in the *xrn-2ts* strain, where GFP is appended to the C terminus of the temperature-sensitive XRN2 protein, *paxt-1 (RNAi)* caused a decrease in GFP levels relative to mock RNAi (Figures S4A and S4B), providing a possible mechanism by which PAXT-1 would stimulate XRN2. To confirm that PAXT-1 promotes endogenous, wild-type XRN2 accumulation, we quantified XRN2 protein levels by western blotting in wild-type worms exposed to *paxt-1(RNAi)* and found a reduction by 50% relative to mock RNAi-treated animals in L4-stage worms (Figure S4C). This effect was specific, as XRN2 levels also declined in *paxt-1(0)* animals (Figure 4A). Reciprocally, depletion of XRN2 by RNAi in wild-type worms (Figure S4D) or by temperature shift of *xrn-2ts* worms (Figure 4B) reduced PAXT-1 protein levels. Notably, depletion was specific to proteins; the corresponding mRNAs continued to accumulate (Figures 4A and 4B, Figures S4C and S4D). We conclude that PAXT-1 and XRN2 proteins stabilize one another through formation of a complex.

When we examined XRN2 levels in *paxt-1(0)* animals, we found that the timing of developmental defects were mirrored by the observed decline in XRN2 levels. Whereas XRN2 levels were reduced by about 60% in L4 stage *paxt-1(0)* animals from the P0 generation relative to wild-type animals, XRN2 was nearly

Please cite this article in press as: Miki et al., PAXT-1 Promotes XRN2 Activity by Stabilizing It through a Conserved Domain, Molecular Cell (2014), http://dx.doi.org/10.1016/j.molcel.2014.01.001

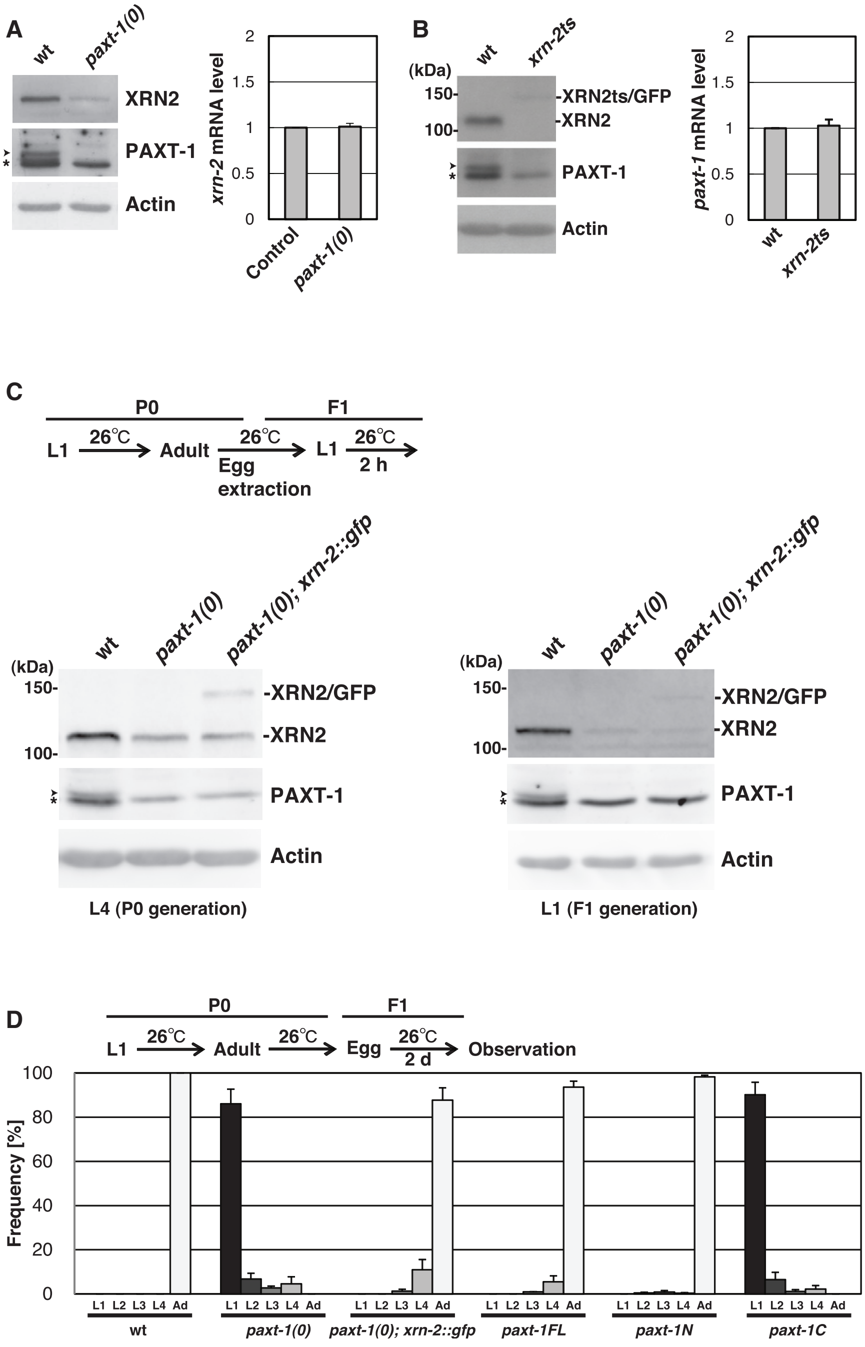

Figure 4. XRN2 and PAXT-1 Stabilize One Another

(A) WT or *paxt-1(0)* worms were cultured from L1 to L4 at 26°C. Levels of XRN2, PAXT-1, and Actin were examined by western blot. An arrowhead indicates PAXT-1, an asterisk a mixture of PAXT-1 and a cross-reacting protein. *xrn-2* mRNA levels were quantified by RT-qPCR and normalized to *act-1* mRNA levels with control values defined as 1 (n = 2, means ± SD).

(B) WT or *xrn-2ts* worms were cultured from L3 to L4 at 26°C. Levels of the indicated proteins and mRNAs were analyzed as in (A).

(C) The indicated worms were cultured from L1 at 26°C, and protein was extracted at the L4 stage of the same generation (P0, left panel). Alternatively, following continued growth to adult stage, eggs were extracted and hatched in medium without food, and the resulting synchronized larvae of the next generation (F1) were cultured with food for 2 hr prior to harvesting (right panel). Levels of XRN2, PAXT-1, and Actin at L4 were examined by western blot. An arrowhead indicates PAXT-1, an asterisk a mixture of PAXT-1 and a crossreacting protein.

(D) Worms of the indicated genotypes were cultured from L1 at 26°C until laying eggs. After 2 days, hatched progeny were scored on their developmental stages (n = 2, means ± SD; ≥ 40 worms were scored per experiment and genotype). Whereas *paxt-1(0)* animals arrest at the L1 stage, expression of full-length *paxt-1*, *paxt-1N*, or *xrn-2::gfp* from transgenes restores larval development; expression of *paxt-1C* does not. See also Figure S4.

undetectable in lysates from newly arrested *paxt-1(0)* F1 worms (Figure 4C). It is possible that these differences in levels reflect gradual depletion of XRN2 during the entire developmental period. However, we favor an alternative model where PAXT-1 function would be particularly important during the adult or embryonic stages because shifting *paxt-1(0)* animals to 26°C at the late L4 stage sufficed to induce an L1 stage arrest in their progeny (data not shown).

The fact that *paxt-1* mutant phenotypes correlated with the extent of XRN2 depletion suggested that loss of XRN2 activity could be causal to the developmental arrest of *paxt-1(0)* animals. We tested this possibility by expressing *xrn-2::gfp* in addition to endogenous *xrn-2* in *paxt-1(0)* worms. Although even the combined levels of both XRN2/GFP and endogenous XRN2 in *paxt-1(0)* animals were significantly lower than those of endogenous XRN2 in wild-type animals (Figure 4C), more than 80% of the F1 from *paxt-1(0)*; *xrn-2::gfp* animals developed to adult (Figures 4D and S4E), and 40% of those segregated F2 progeny (data not shown). The presence of XRN2/GFP also enhanced decay of miR-51 and miR-87 in *paxt-1(0)* animals (Figure 3C). As anticipated from the low levels of XRN2/GFP that can be achieved in the absence of PAXT-1, this enhancement was modest. Collectively, these results reveal that stabilization of XRN2 is a major function of PAXT-1 and essential for worm development at elevated temperature.

The Essential DUF3469 Domain of PAXT-1 Mediates Complex Formation with and Stabilization of XRN2

To determine which part of PAXT-1 is responsible for stabilization of XRN2 in vivo, we expressed truncated proteins

Please cite this article in press as: Miki et al., PAXT-1 Promotes XRN2 Activity by Stabilizing It through a Conserved Domain, Molecular Cell (2014), http://dx.doi.org/10.1016/j.molcel.2014.01.001

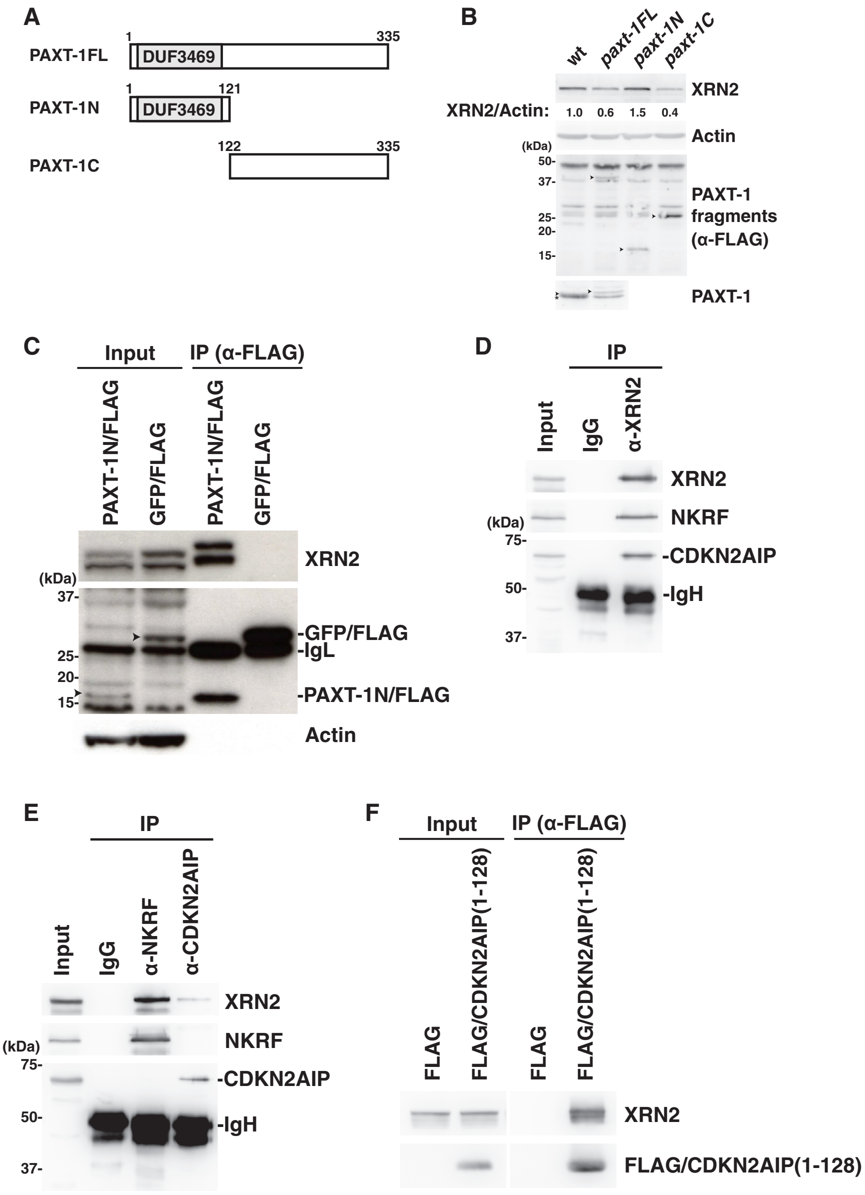

Figure 5. DUF3469 Is a Bona Fide XRN2-Binding Domain

(A) Schematic drawings of full-length (PAXT-1FL) and truncation muntants (PAXT-1N and PAXT-1C) of PAXT-1. Amino acid numbers relative to the first methionin of PAXT-1 are indicated.

(B) Wild-type and *paxt-1(0)* worms expressing FLAG-tagged PAXT-1FL, PAXT-1N, or PAXT-1C were cultured from L1 to L4 at 26°C. Levels of XRN2, PAXT-1, and Actin were examined by western blot. Levels of XRN2 are normalized to actin levels and shown with values of WT defined as 1. Arrowheads indicate PAXT-1FL, PAXT-1N, and PAXT-1C. An asterisk indicates a mixture of PAXT-1 and a crossreacting protein.

(C) PAXT-1N/FLAG coimmunoprecipitates XRN2 whereas GFP/FLAG does not. 5% of input and 15% of eluate was loaded. Note that GFP/FLAG is overloaded. Arrowheads indicate PAXT-1N/GFP and GFP/FLAG. IgL, immunoglobulin light chain.

(D–F) Coimmunoprecipitation of human XRN2 with NKRF and CDKN2AIP. Endogenous XRN2 (D), NKRF or CDKN2AIP (E), or FLAG/CDKN2AIP_DUF3649 (F) was immunoprecipitated from RNase A-treated HEK293T cell lysate. 1% of input and 20% of immunoprecipitate (IP) fractions were analyzed by western blot. IgH, immunoglobulin heavy chain. In (F), nonadjacent lanes from a single scan were spliced together. See also Figure S5.

bearing a C-terminal FLAG-tag in *paxt-1(0)* animals. The N-terminal part of PAXT-1, PAXT-1N, comprises a domain of unknown function, DUF3649, whereas no domains or motifs are discernable within the C-terminal part, PAXT-1C (Figure 5A). As a control, full-length PAXT-1 (PAXT-1FL) could rescue the *paxt-1(0)* worms from L1 stage arrest so that more than 90% of *paxt-1(0)*; PAXT-1FL worms became adult (Figure 4D), although half of them did not segregate progeny (data not shown). Incomplete rescue may result from reduced levels relative to endogenous PAXT-1, as would be expected for a cDNA-based transgene. Similar to PAXT-1FL, PAXT-1N permitted development of *paxt-1(0)* animals into adults (Figure 4D), more than 80% of which segregated progeny (data not shown). On the other hand, PAXT-1C failed to rescue *paxt-1(0)* worms (Figure 4D).

Consistent with PAXT-1N being key to stabilization of XRN2, XRN2 levels were restored in PAXT-1N-producing worms to wild-type levels or above, while PAXT-1C-producing worms showed XRN2 levels approximating 40% of those in wild-type worms (Figure 5B), similar to the *paxt-1(0)* worms (Figures 4A and 4C). The presence of PAXT-1FL restored XRN2 levels less efficiently than that of PAXT-1N (Figure 5B), consistent also with less complete rescue of the developmental phenotypes in the F2 generation.

The fact that PAXT-1N sufficed for restoration of both XRN2 levels and larval development of *paxt-1(0)* animals suggested that it was sufficient for binding to XRN2. Indeed, XRN2 coprecipitated when we immunoprecipitated PAXT-1N/FLAG with anti-FLAG antibodies, whereas it did not precipitate with a FLAG-tagged control protein (Figure 5C). For unknown reasons, we were unable to precipitate PAXT-1FL/FLAG or PAXT-1C/FLAG with anti-FLAG antibodies so that we cannot rule out that the PAXT-1 C terminus may supply additional XRN2-binding activity. Nonetheless, these data clearly demonstrate that PAXT-1N, comprising DUF3469, is sufficient for XRN2 binding.

Binding of DUF3469-Containing Proteins to XRN2 Is Conserved in Humans

Given that PAXT-1 binds and stabilizes XRN2 through DUF3469, we were intrigued by the existence of additional

Please cite this article in press as: Miki et al., PAXT-1 Promotes XRN2 Activity by Stabilizing It through a Conserved Domain, Molecular Cell (2014), http://dx.doi.org/10.1016/j.molcel.2014.01.001

DUF3469-containing proteins in metazoa (Figure S5). We tested if the three human proteins predicted to contain this domain, CDKN2AIP/CARF, CDKN2AIPNL/C2AIL, and NKRF/NRF, bound to XRN2. We were unable to detect CDKN2AIPNL/C2AIL in HEK293T cells using a commercially available antibody (data not shown). However, both CDKN2AIP and NKRF were not only present in the cell lysates, but also readily detectable in XRN2 immunoprecipitates that had been treated with RNase (Figure 5D). Conversely, immunoprecipitation of CDKN2AIP or NKRF, respectively, coprecipitated XRN2 from RNase-treated lysates (Figure 5E). To see if the two proteins bind XRN2 through DUF3469, we transfected HEK293T cells with expression vectors for FLAG-tagged CDKN2AIP(1-128) and NKRF(1-94), i.e., the respective DUF3469. Although we failed to express FLAG/NKRF(1-94) for unknown reasons (data not shown), we detected XRN2 in FLAG/CDKN2AIP(1-128) immunoprecipitates (Figure 5F). These data indicate that DUF3469 represents a conserved XRN2-binding domain. Moreover, since CDKN2AIP and and NKRF did not coimmunoprecipitate one another, they appear to form distinct complexes with XRN2. It seems likely that this may be a consequence of mutually exclusive binding.

DISCUSSION

XRN2 Stabilization Is a Major Function of PAXT-1

We report here identification of a protein complex in *C. elegans* consisting of XRN2 and PAXT-1. The extensive destabilization that we observe for either subunit upon loss of the other suggests that a large fraction of each protein is contained within the XRN2-PAXT-1 complex. Genetic data strongly support this notion for PAXT-1 in that its essential function for development at elevated temperature can be bypassed by an increased *xrn-2* gene dosage.

At this point, it is not known why PAXT-1 becomes essential for larval development only at temperatures of 26°C and above. In principle, this fact could reflect an increased demand for XRN2 activity at the elevated temperature. However, we favor an alternative, although not necessarily mutually exclusive, explanation, namely that XRN2 alone is sufficiently stable at the lower temperatures but exceedingly destabilized at temperatures at or above 26°C. This notion is not only consistent with the differences in XRN2 accumulation that we observed in *paxt-1* mutant animals grown under different conditions, but also with the synthetic lethality of *xrn-2ts* and *paxt-1(RNAi)*, which occurs already at reduced temperature.

Since our data establish that stabilization of XRN2 is a key function of PAXT-1 in the context of larval development, an intriguing question for future work will be whether this relates to a specific activity of XRN2 on a specific substrate. Alternatively, *paxt-1(0)* animals may arrest development because of impaired XRN2 function in diverse processes and on a diverse set of substrates. Addressing this point will require a deeper understanding of the identity and function of XRN2 substrates in *C. elegans*, extending beyond miRNAs as the only currently known substrate.

DUF3469/XTBD Constitutes a Bona Fide XRN2-Binding Domain in Metazoa

A PAXT-1 fragment consisting of DUF3469 suffices for binding and stabilization of XRN2. Metazoan genomes typically contain a small number of proteins with this domain of unknown function (Figure S5). Strikingly, we found that CDKN2AIP/CARF and NKRF/NRF, the two human proteins with this domain that are expressed in HEK293T cells, also coimmunoprecipitated XRN2, as did a FLAG-tagged fragment comprising the CDKN2AIP DUF3469 only. Similarly, XRN2 complexes obtained by Brannan et al. (2012) by immunoprecipitation from HeLa cell nuclear extracts contain CDKN2AIP and NKRF as shown by mass spectrometry. Mass spectrometry also revealed the presence of XRN2, CDKN2AIP, and NKRF in hnRNP A1-containing, chromatin-associated mRNPs that Close et al. (2012) purified. Finally, Couvillion et al. (2012) identified Tan1, another DUF3469-containing protein, as a component of an XRN2-containing ternary complex in *Tetrahymena*. Thus, we consider DUF3469 a bona fide XRN2 binding domain and propose to name it XTBD (Xrn-Two-Binding Domain).

Whereas XTBD-containing proteins are readily identifiable in metazoa, they appear not to exist in fungi (http://pfam.sanger.ac.uk/family/duf3469#tabview=tab7). By contrast, homologs of Rai1p, which binds to XRN2/Rat1p in yeast and promotes its RNase activity (Stevens and Poole, 1995; Xue et al., 2000), are present in metazoa but do not bind to XRN2 (Xiang et al., 2009). Thus, Rai1p and XTBD-containing proteins such as PAXT-1 may represent two solutions to the problem of ensuring optimal XRN2 activity. Although we do not know why distinct proteins would serve this function in different organisms, we note that Rai1p also exhibits enzymatic activities that are independent of its function with XRN2, namely decapping and pyrophosphohydrolase activities (Xiang et al., 2009; Jiao et al., 2010). The presence of multiple activities within a single protein may facilitate their coordinated regulation, but in turn make the task of regulating them independently more difficult. Interestingly, although the mammalian Rai1p homolog DOM3Z/DXO does not bind XRN2, it shares the two enzymatic activities with Rai1p (Jiao et al., 2013). Thus, we speculate that a need to coordinately or separately regulate the enzymatic and the XRN2-binding activities may have been a driving force for this evolutionary development. Understanding if and how XRN2-dependent and -independent functions of Rai1p/DOM3Z/DXO1-type proteins, including the yeast Rai1p paralogue Dxo1p (Chang et al., 2012), and XTBD-containing proteins are regulated in different organisms may then shed light on this issue.

Implications for XTBD-Containing Proteins beyond *C. elegans*

Although ours and the published data demonstrate that CDKN2AIP, NKRF, and Tan1, like PAXT-1, occur in complexes with XRN2, unlike PAXT-1, no functional links with XRN2 have been established for these three proteins. Based on the fact that the PAXT-1 XTBD can supply much of the function of the full-length protein in vivo, we might speculate that these proteins similarly function in XRN2 stabilization. However, given that PAXT-1 is, at 335 amino acids (aa), considerably shorter than CDKN2AIP (580 aa) or NKRF (690 aa), it is equally possible that the latter proteins provide additional functionality that is then recruited to XRN2 via XTBD. For instance, NKRF and other XTBD-containing proteins also have domain(s) implicated in

RNA binding, e.g., single- and double-stranded (ds) RNA binding or a G-patch domain, and dsRNA-binding activity has been confirmed for NKRF (Niedick et al., 2004). It may be interesting to examine whether these domains serve to regulate target RNA recognition and/or processing by XRN2.

Whereas *C. elegans* XRN2 requires PAXT-1 for function, we note that a reverse scenario is also possible, i.e., XTBD-containing proteins may require XRN2 to execute specific functions. We are particularly intrigued by the NF-κB repressing factor (NKRF), which antagonizes NF-κB-mediated activation of transcription (Nourbakhsh and Hauser, 1999). While this function involves binding of NKRF to specific DNA sequences, NKRF does not appear to act through steric hindrance of DNA binding by NF-κB but through active repression of transcription by an unknown mechanism (Nourbakhsh and Hauser, 1999). Given the recent discovery that XRN2 may oppose transcription by inducing premature termination (Brannan et al., 2012), we propose that a role for XRN2 in NKRF's function in repression of transcription could be considered. A second example that may be worth investigating is the *Drosophila melanogaster* protein CG31301, which binds to siRNAs and functions, by an unknown mechanism, in RNAi (Gerbasi et al., 2010). Since this protein contains a readily detectable XTB domain, a connection to XRN2-dependent RNA decay may be a possibility.

To conclude, although it is currently unknown whether XTBD-containing proteins beyond PAXT-1 will function by modulating XRN2 activity or whether, conversely, XRN2 will contribute to the functions of these proteins, or both, we expect that identification of DUF3469 as a bona fide XRN2-binding domain will open up new avenues of research to understand the functions of these proteins.

EXPERIMENTAL PROCEDURES

Strains

The Bristol N2 wild-type, mutant, and transgenic strains generated for this study (Table S1) were cultured by standard methods (Brenner, 1974). Transgenic lines were obtained by *Mos1*-mediated single-copy transgene insertion (MosSCI) (Frøkjær-Jensen et al., 2012; Frøkjaer-Jensen et al., 2008).

Antibodies, Immunoprecipitation, and Western Blotting

Affinity-purified rabbit anti-PAXT-1 and anti-XRN1 antibodies were generated by SDIX (Newark, DE) using DNA immunization. IP and western blotting were performed as described in the Supplemental Experimental Procedures.

RNAi

RNAi clones against *xrn-2* and *paxt-1* were obtained from the libraries by Fraser et al. (2000) and Kamath and Ahringer (2003) and by Rual et al. (2004), respectively. RNAi was performed by the feeding method (Timmons and Fire, 1998); bacteria carrying the insertless L4440 RNAi vector were used as a negative control.

Microscopy

DIC and fluorescent images were obtained using a Zeiss Axio Observer Z1 microscope. Stereoscopic images were obtained with a Leica M205 A stereo microscope.

TALEN-Mediated Gene Targeting

TALEN-mediated *paxt-1* gene targeting was performed according to a previous report (Wood et al., 2011) and as detailed in the Supplemental Experimental Procedures.

miRNA Decay Analysis

Eggs from animals cultured at 26°C were extracted with bleach and hatched overnight in M9 medium at 26°C. The resulting synchronized L1 larvae were cultured with food at 26°C for 2 hr before α-amanitin was added. Aliquots of worms were harvested at each sampling time point and RNA was extracted and purified. Individual miRNAs were quantified by RT-qPCR (see Supplemental Experimental Procedures for details).

In Vitro Turnover Assay

In vitro RNA turnover was assayed as described (Sinturel et al., 2009). Briefly, a 17-mer DNA oligonucleotide bearing a fluorescence quencher was annealed to a 30 nt 5′ monophosphorylated, 3′ fluorescently labeled RNA substrate. Increase of fluorescence due to degradation of the RNA and thus release of the quencher was measured using a real-time PCR machine.

Recombinant Protein Expression and Preparative Size Exclusion Chromatography

C. elegans XRN2 (aa 1–821) was cloned into pOPINE (C-terminal hexa-histidine tag). PAXT-1 with XRN2 or XRN2* (D234A,D236A double mutant; catalytic dead) were cloned into a bicistronic vector at positions one and two, respectively. The vector is a modified pCOLADuet-1 with an N-terminal hexa-histidine tag plus TEV protease cleavage site at the first position and no affinity tag at the second position. *E. coli* was used for expression, followed by Ni-NTA (QIAGEN) and size-exclusion chromatography (Superdex 200 pg, 16/600) purification. Fractions of 1 ml were collected and 12 μl taken to analyze eluted proteins by SDS-PAGE.

SUPPLEMENTAL INFORMATION

Supplemental Information includes five figures, two tables, and Supplemental Experimental Procedures and can be found with this article online at http://dx.doi.org/10.1016/j.molcel.2014.01.001.

AUTHOR CONTRIBUTIONS

S.R. performed co-IP experiments in *C. elegans*, H.R. protein purification and enzymatic assays, and T.S.M. all other experiments.

ACKNOWLEDGMENTS

We thank Monika Fasler, Mirela Vitanescu, and Jeremy Keusch for technical support and Daniel Hess for performing expert mass spectrometry analysis. We are particularly grateful to Iskra Katic for establishing TALEN-mediated genome editing at FMI and technical support and Christopher Horst Lillig for insightful discussions. We thank Iskra Katic and Witold Filipowicz for a critical reading of the manuscript. The research leading to these results has received funding from the European Union Seventh Framework Programme (FP7/2007-2013) under grant agreement number 241985 (European Research Council "miRTurn"). Additional funding was provided by the Novartis Research Foundation through the FMI, and the Swiss National Science Foundation (SNF 31003A_127052 and SNF 31003A_143313). S.R. was supported by a Boehringer Ingelheim Fonds PhD Fellowship. Some *C. elegans* strains were provided by the CGC, which is funded by NIH Office of Research Infrastructure Programs (P40 OD010440).

Received: June 20, 2013
Revised: November 1, 2013
Accepted: December 10, 2013
Published: January 23, 2014

REFERENCES

Amberg, D.C., Goldstein, A.L., and Cole, C.N. (1992). Isolation and characterization of RAT1: an essential gene of Saccharomyces cerevisiae required for the efficient nucleocytoplasmic trafficking of mRNA. Genes Dev. *6*, 1173–1189.

Please cite this article in press as: Miki et al., PAXT-1 Promotes XRN2 Activity by Stabilizing It through a Conserved Domain, Molecular Cell (2014), http://dx.doi.org/10.1016/j.molcel.2014.01.001

Bousquet-Antonelli, C., Presutti, C., and Tollervey, D. (2000). Identification of a regulated pathway for nuclear pre-mRNA turnover. Cell *102*, 765–775.

Brannan, K., Kim, H., Erickson, B., Glover-Cutter, K., Kim, S., Fong, N., Kiemele, L., Hansen, K., Davis, R., Lykke-Andersen, J., and Bentley, D.L. (2012). mRNA decapping factors and the exonuclease Xrn2 function in widespread premature termination of RNA polymerase II transcription. Mol. Cell *46*, 311–324.

Brenner, S. (1974). The genetics of Caenorhabditis elegans. Genetics *77*, 71–94.

Chang, J.H., Jiao, X., Chiba, K., Oh, C., Martin, C.E., Kiledjian, M., and Tong, L. (2012). Dxo1 is a new type of eukaryotic enzyme with both decapping and 5′-3′ exoribonuclease activity. Nat. Struct. Mol. Biol. *19*, 1011–1017.

Chatterjee, S., and Grosshans, H. (2009). Active turnover modulates mature microRNA activity in Caenorhabditis elegans. Nature *461*, 546–549.

Chernyakov, I., Whipple, J.M., Kotelawala, L., Grayhack, E.J., and Phizicky, E.M. (2008). Degradation of several hypomodified mature tRNA species in Saccharomyces cerevisiae is mediated by Met22 and the 5′-3′ exonucleases Rat1 and Xrn1. Genes Dev. *22*, 1369–1380.

Close, P., East, P., Dirac-Svejstrup, A.B., Hartmann, H., Heron, M., Maslen, S., Chariot, A., Söding, J., Skehel, M., and Svejstrup, J.Q. (2012). DBIRD complex integrates alternative mRNA splicing with RNA polymerase II transcript elongation. Nature *484*, 386–389.

Couvillion, M.T., Bounova, G., Purdom, E., Speed, T.P., and Collins, K. (2012). A Tetrahymena Piwi bound to mature tRNA 3′ fragments activates the exonuclease Xrn2 for RNA processing in the nucleus. Mol. Cell *48*, 509–520.

Davidson, L., Kerr, A., and West, S. (2012). Co-transcriptional degradation of aberrant pre-mRNA by Xrn2. EMBO J. *31*, 2566–2578.

Frand, A.R., Russel, S., and Ruvkun, G. (2005). Functional genomic analysis of C. elegans molting. PLoS Biol. *3*, e312.

Fraser, A.G., Kamath, R.S., Zipperlen, P., Martinez-Campos, M., Sohrmann, M., and Ahringer, J. (2000). Functional genomic analysis of C. elegans chromosome I by systematic RNA interference. Nature *408*, 325–330.

Frøkjaer-Jensen, C., Davis, M.W., Hopkins, C.E., Newman, B.J., Thummel, J.M., Olesen, S.P., Grunnet, M., and Jorgensen, E.M. (2008). Single-copy insertion of transgenes in Caenorhabditis elegans. Nat. Genet. *40*, 1375–1383.

Frøkjær-Jensen, C., Davis, M.W., Ailion, M., and Jorgensen, E.M. (2012). Improved Mos1-mediated transgenesis in C. elegans. Nat. Methods *9*, 117–118.

Gerbasi, V.R., Golden, D.E., Hurtado, S.B., and Sontheimer, E.J. (2010). Proteomics identification of Drosophila small interfering RNA-associated factors. Mol. Cell. Proteomics *9*, 1866–1872.

Henry, Y., Wood, H., Morrissey, J.P., Petfalski, E., Kearsey, S., and Tollervey, D. (1994). The 5′ end of yeast 5.8S rRNA is generated by exonucleases from an upstream cleavage site. EMBO J. *13*, 2452–2463.

Jiao, X., Xiang, S., Oh, C., Martin, C.E., Tong, L., and Kiledjian, M. (2010). Identification of a quality-control mechanism for mRNA 5’-end capping. Nature *467*, 608–611.

Jiao, X., Chang, J.H., Kilic, T., Tong, L., and Kiledjian, M. (2013). A mammalian pre-mRNA 5′ end capping quality control mechanism and an unexpected link of capping to pre-mRNA processing. Mol. Cell *50*, 104–115.

Kamath, R.S., and Ahringer, J. (2003). Genome-wide RNAi screening in Caenorhabditis elegans. Methods *30*, 313–321.

Kaneko, S., Rozenblatt-Rosen, O., Meyerson, M., and Manley, J.L. (2007). The multifunctional protein p54nrb/PSF recruits the exonuclease XRN2 to facilitate pre-mRNA 3′ processing and transcription termination. Genes Dev. *21*, 1779–1789.

Kenna, M., Stevens, A., McCammon, M., and Douglas, M.G. (1993). An essential yeast gene with homology to the exonuclease-encoding XRN1/KEM1 gene also encodes a protein with exoribonuclease activity. Mol. Cell. Biol. *13*, 341–350.

Kim, M., Krogan, N.J., Vasiljeva, L., Rando, O.J., Nedea, E., Greenblatt, J.F., and Buratowski, S. (2004). The yeast Rat1 exonuclease promotes transcription termination by RNA polymerase II. Nature *432*, 517–522.

Liu, Y., Tan, H., Tian, H., Liang, C., Chen, S., and Liu, Q. (2011). Autoantigen La promotes efficient RNAi, antiviral response, and transposon silencing by facilitating multiple-turnover RISC catalysis. Mol. Cell *44*, 502–508.

Miki, T.S., and Großhans, H. (2013). The multifunctional RNase XRN2. Biochem. Soc. Trans. *41*, 825–830.

Miki, T.S., Rüegger, S., Gaidatzis, D., Stadler, M.B., and Großhans, H. (2014). Engineering of a conditional allele reveals multiple roles of XRN2 in Caenorhabditis elegans development and substrate specificity in microRNA turnover. Nucleic Acids Res., in press. Published online January ■■, 2014. http://dx.doi.org/10.1093/nar/gkt1418.

Nagarajan, V.K., Jones, C.I., Newbury, S.F., and Green, P.J. (2013). XRN 5′→3′ exoribonucleases: structure, mechanisms and functions. Biochim. Biophys. Acta *1829*, 590–603.

Niedick, I., Froese, N., Oumard, A., Mueller, P.P., Nourbakhsh, M., Hauser, H., and Köster, M. (2004). Nucleolar localization and mobility analysis of the NF-kappaB repressing factor NRF. J. Cell Sci. *117*, 3447–3458.

Nourbakhsh, M., and Hauser, H. (1999). Constitutive silencing of IFN-beta promoter is mediated by NRF (NF-kappaB-repressing factor), a nuclear inhibitor of NF-kappaB. EMBO J. *18*, 6415–6425.

Petfalski, E., Dandekar, T., Henry, Y., and Tollervey, D. (1998). Processing of the precursors to small nucleolar RNAs and rRNAs requires common components. Mol. Cell. Biol. *18*, 1181–1189.

Qu, L.H., Henras, A., Lu, Y.J., Zhou, H., Zhou, W.X., Zhu, Y.Q., Zhao, J., Henry, Y., Caizergues-Ferrer, M., and Bachellerie, J.P. (1999). Seven novel methylation guide small nucleolar RNAs are processed from a common polycistronic transcript by Rat1p and RNase III in yeast. Mol. Cell. Biol. *19*, 1144–1158.

Rual, J.F., Ceron, J., Koreth, J., Hao, T., Nicot, A.S., Hirozane-Kishikawa, T., Vandenhaute, J., Orkin, S.H., Hill, D.E., van den Heuvel, S., and Vidal, M. (2004). Toward improving Caenorhabditis elegans phenome mapping with an ORFeome-based RNAi library. Genome Res. *14* (10B), 2162–2168.

Sinturel, F., Pellegrini, O., Xiang, S., Tong, L., Condon, C., and Bénard, L. (2009). Real-time fluorescence detection of exoribonucleases. RNA *15*, 2057–2062.

Stevens, A., and Poole, T.L. (1995). 5′-exonuclease-2 of Saccharomyces cerevisiae. Purification and features of ribonuclease activity with comparison to 5′-exonuclease-1. J. Biol. Chem. *270*, 16063–16069.

Timmons, L., and Fire, A. (1998). Specific interference by ingested dsRNA. Nature *395*, 854.

Wood, A.J., Lo, T.W., Zeitler, B., Pickle, C.S., Ralston, E.J., Lee, A.H., Amora, R., Miller, J.C., Leung, E., Meng, X., et al. (2011). Targeted genome editing across species using ZFNs and TALENs. Science *333*, 307.

Xiang, S., Cooper-Morgan, A., Jiao, X., Kiledjian, M., Manley, J.L., and Tong, L. (2009). Structure and function of the 5′—>3′ exoribonuclease Rat1 and its activating partner Rai1. Nature *458*, 784–788.

Xue, Y., Bai, X., Lee, I., Kallstrom, G., Ho, J., Brown, J., Stevens, A., and Johnson, A.W. (2000). Saccharomyces cerevisiae RAI1 (YGL246c) is homologous to human DOM3Z and encodes a protein that binds the nuclear exoribonuclease Rat1p. Mol. Cell. Biol. *20*, 4006–4015.

7 Publication: “The Decapping Scavenger Enzyme DCS-1 Controls MicroRNA Levels in *Caenorhabditis elegans*”

Molecular Cell
Short Article

The Decapping Scavenger Enzyme DCS-1 Controls MicroRNA Levels in *Caenorhabditis elegans*

Gabriel D. Bossé,[1] Stefan Rüegger,[2,3] Maria C. Ow,[4] Alejandro Vasquez-Rifo,[1] Evelyne L. Rondeau,[1] Victor R. Ambros,[4] Helge Großhans,[2] and Martin J. Simard[1,*]
[1]Laval University Cancer Research Centre, Hôtel-Dieu de Québec (Centre Hospitalier Universitaire de Québec), Quebec City, QC G1R 2J6, Canada
[2]Friedrich Miescher Institute for Biomedical Research, Maulbeerstrasse 66, 4058 Basel, Switzerland
[3]University of Basel, Petersplatz 1, 4003 Basel, Switzerland
[4]Program in Molecular Medicine, University of Massachusetts Medical School, Worcester, MA 01605, USA
*Correspondence: martin.simard@crhdq.ulaval.ca
http://dx.doi.org/10.1016/j.molcel.2013.02.023

SUMMARY

In metazoans, microRNAs play a critical role in the posttranscriptional regulation of genes required for cell proliferation and differentiation. MicroRNAs themselves are regulated by a multitude of mechanisms influencing their transcription and posttranscriptional maturation. However, there is only sparse knowledge on pathways regulating the mature, functional form of microRNA. Here, we uncover the implication of the decapping scavenger protein DCS-1 in the control of microRNA turnover. In *Caenorhabditis elegans*, mutations in *dcs-1* increase the levels of functional microRNAs. We demonstrate that DCS-1 interacts with the exonuclease XRN-1 to promote microRNA degradation in an independent manner from its known decapping scavenger activity, establishing two molecular functions for DCS-1. Our findings thus indicate that DCS-1 is part of a degradation complex that performs microRNA turnover in animals.

INTRODUCTION

MicroRNAs (miRNAs) are ~22 nt long noncoding RNAs that regulate gene expression at the posttranscriptional level by binding to partially complementary sequences of target messenger RNAs (mRNAs) (reviewed in Ebert and Sharp, 2012). miRNA genes are mostly transcribed by RNA polymerase II to yield a primary miRNA transcript (pri-miRNA). The pri-miRNA undergoes processing by a multiprotein complex known as the microprocessor to produce an intermediate called the precursor miRNA (pre-miRNA). After nuclear export, the pre-miRNA is cleaved by Dicer, resulting in the mature miRNA. Subsequently, mature miRNAs are bound by an Argonaute protein to form the core of a multisubunit effector complex termed miRISC (miRNA-induced silencing complex) (reviewed in Krol et al., 2010; Kim et al., 2009). miRISC binds to partially complementary sequences found typically in the 3′ untranslated region (3′ UTR) of mRNAs, leading to their translational repression and/or degradation (reviewed in Huntzinger and Izaurralde, 2011; Pasquinelli, 2012).

miRNA-mediated gene regulation is involved in diverse biological functions, including the control of development in metazoans (reviewed in Ebert and Sharp, 2012) as well as cellular pathways such as DNA damage and stress responses (reviewed in Hu and Gatti, 2011; Leung and Sharp, 2010). Notably, miRNAs are dysregulated in many diseases, such as cancer (reviewed in Esteller, 2011; Mendell and Olson, 2012). Thus, it is essential for a cell to tightly control miRNA biogenesis and turnover.

Like other RNA polymerase II-transcribed genes, miRNA loci are subject to widespread transcriptional regulation. Additionally, the different biogenesis steps are controlled by cellular factors that either modulate the activity of processing factors or bind miRNA precursor molecules to interfere with the processing of a subset of miRNAs (reviewed in Bajan and Hutvagner, 2011; Krol et al., 2010; Newman et al., 2011). More recently, evidence has emerged that miRNA decay pathways contribute to the control of miRNA levels (for details see Kai and Pasquinelli, 2010; Rüegger and Großhans, 2012). In particular, the small RNA degrading nucleases (SDNs) mediate 3′ to 5′ turnover of miRNAs in plants (Ramachandran and Chen, 2008), and the exoribonucleases XRN-1 and XRN-2 function in 5′ to 3′ miRNA degradation in *C. elegans* (Chatterjee et al., 2011; Chatterjee and Grosshans, 2009).

In this study, we identify the decapping scavenger enzyme 1 (DCS-1, also known as DcpS) as a player in the *C. elegans* miRNA turnover pathway. Our data reveal that DCS-1 stimulates XRN-1-mediated miRNA degradation through a physical interaction and that this process is independent of the decapping scavenger activity previously assigned to DCS-1.

RESULTS

Mutations in *dcs-1* Lead to Precocious Adult Fate and Enhanced Repression of miRNA Targets

In order to discover factors implicated in the miRNA pathway, we performed a genetic screen to identify genes that interact synthetically with *alg-2*, one of the two *C. elegans* Argonautes that functions in the miRNA pathway (Grishok et al., 2001). The rationale of the screen was based on the observation that an *alg-2* mutant, *alg-2(ok304)*, is viable, whereas the combined

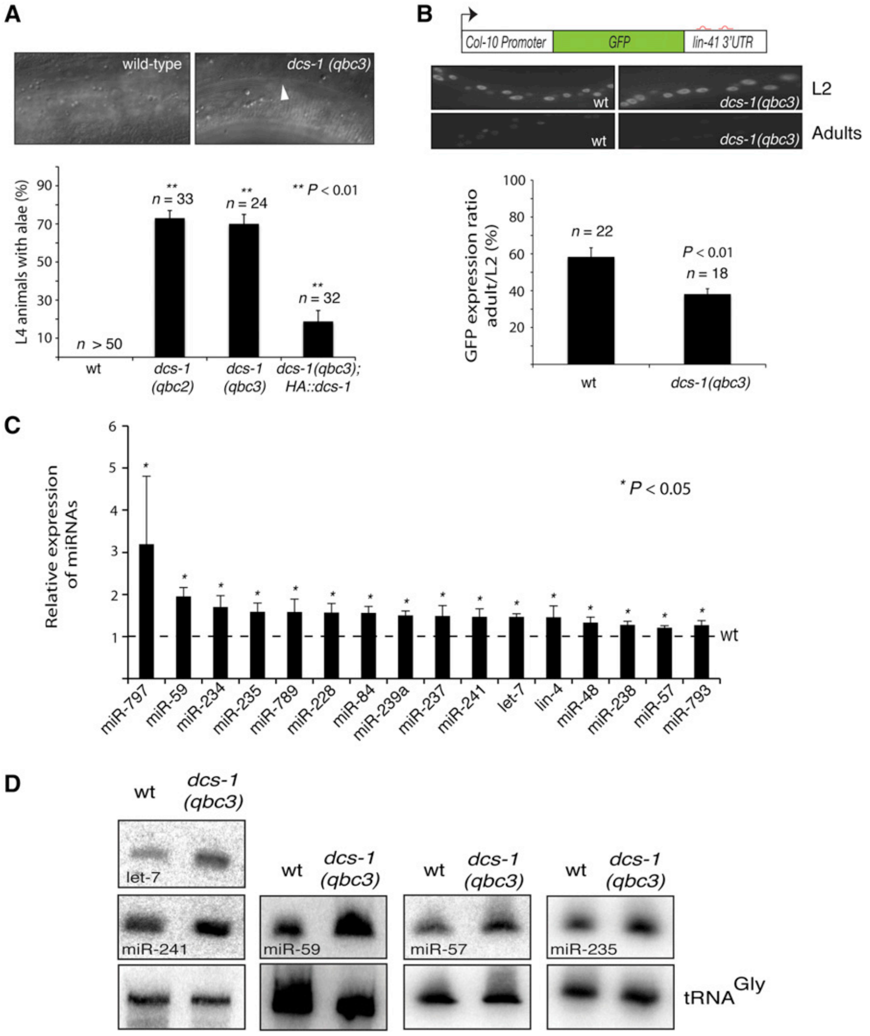

Figure 1. The Loss of *dcs-1* Affects miRNA-Mediated Gene Regulation and miRNA Levels

(A) Alae are produced precociously in *dcs-1* animals. L4 animals were precisely staged by observing vulval and gonad formation by Nomarski optics (Figure S2A), and the percentage (%) of animals with precocious alae (white arrow; right picture) was scored. Magnification is 1,000×. The number of animals scored (n) is indicated.

(B) To study *lin-41* regulation in vivo, we monitored the expression of green fluorescent protein (GFP) under the control of a hypodermis-specific *col-10* promoter and the *lin-41* 3′ UTR containing the *let-7* miRNA binding sites (red; diagram). GFP is expressed during early larvae stages (L2) and downregulated when animals reach young adulthood (Adults). Young adult *dcs-1(qbc3)* animals repressed the miRNA-sensitive reporter more strongly than wild-type animals. Quantification of GFP in adults relative to L2 stage animals. The quantification of the GFP signal was performed by measuring the mean of the GFP detected in five different cells for each animal (below). The magnification of all pictures is 1,000×. The number of animals scored (n) is indicated.

(C) The levels of miRNA found in *dcs-1(qbc3)* young adult animals were measured by quantitative RT-PCR (TaqMan assay) and compared with the levels found in wild-type animals (wt; 1). TaqMan assay for the small nucleolar RNA (snoRNA) sn2343 was used as the normalization control. The error bars represent the 95% confidence interval of three independent experiments. p values were obtained using normalized delta delta C_t values. Normalized delta delta C_t values were obtained by subtracting the mean of delta delta C_t from all experiments.

(D) The levels of significantly increased miRNAs (*let-7*, *miR-57*, *miR-59*, *miR-235*, and *miR-241*) in *dcs-1* mutant were detected by northern blot hybridization of RNA samples purified from young adult animals. $tRNA^{Gly}$ (transfer RNA-glycine) was used as loading control.

loss of *alg-2* and its paralog *alg-1* results in lethality (Grishok et al., 2001; Vasquez-Rifo et al., 2012). We generated an *alg-2(ok304)* strain that carries an extrachromosomal array expressing wild-type *alg-2* and a green fluorescent protein (GFP) marker. Since *alg-2* is not required for viability, the array is lost stochastically from this strain. Following chemical mutagenesis, we screened for animals that remained GFP positive, indicating a potential requirement for the array, and thus *alg-2*, for survival. Among the six complementation groups isolated from this screen, we characterize here one group of two mutant alleles, *qbc2* and *qbc3*, that were lesions in the *dcs-1* gene (Figure S1).

The *dcs-1* gene encodes the decapping scavenger enzyme, which has been shown to hydrolyze the residual cap structure that results from 3′ to 5′ decay of mRNAs by the exosome (Cohen et al., 2004; Liu et al., 2002). Whereas *alg-2(ok304); dcs-1(qbc3)* double-mutant animals arrested in development as early as embryos postfertilization (data not shown), *dcs-1(qbc3)* single-mutant embryos developed normally. However, in contrast to wild-type animals, animals carrying lesions in the *dcs-1* gene displayed alae structures at the larval L4 stage, one developmental stage earlier than wild-type (Figure 1A); the developmental stage was confirmed by examining the vulval and gonad morphology (Figure S2A). Re-establishing the expression of wild-type *dcs-1* using a transgenic array rescued the precocious formation of the alae (Figure 1A), confirming that this developmental phenotype is caused by the mutation in the *dcs-1* gene.

LIN-41 is an important regulator of the L4-to-adult developmental transition in *C. elegans*. During the L4 stage, *lin-41* mRNA levels are repressed by the *let-7* miRNA allowing developmental progression (Reinhart et al., 2000; Slack et al., 2000). Similar to what we observe for *dcs-1*, *lin-41* loss-of-function alleles cause precocious formation of alae (Slack et al., 2000). To test whether *dcs-1(qbc3)* leads to misregulation of *lin-41*, a GFP reporter under the control of the *lin-41* 3′ UTR was used. Consistent with the fact that the *let-7* miRNA is only expressed during late larval stages (Reinhart et al., 2000; Slack et al., 2000), we found that, in wild-type worms, the GFP signal was present in the L2 stage but decreased in adult animals.

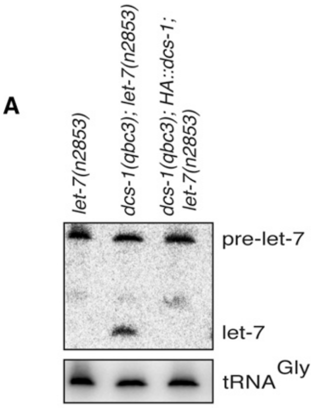

B

Genotype	Percentage of animals (number scored) Viability	Alae
let-7(n2853)	20 (30)	0 (30)
lin-28; let-7(n2853)	84 (34)	100 (31)
dcs-1(qbc3); let-7(n2853)	83 (38)	100 (32)
dcs-1(qbc3); HA::dcs-1; let-7(n2853)	18 (53)	5 (22)

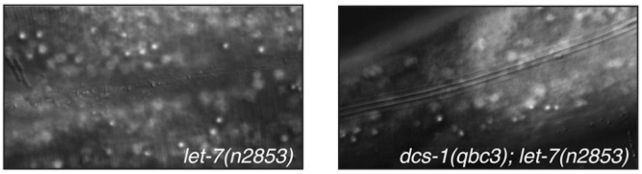

Figure 2. The Loss of *dcs-1* Function Rescues *let-7* Mutant Developmental Defects by Increasing Mature *let-7* miRNA Levels

(A) Detection by northern blotting of *let-7* molecules in various genetic backgrounds of young adult animals. The detection of $tRNA^{Gly}$ by northern hybridization acted as loading control.

(B) Viability and complete adult alae were scored at 20°C on young adult animals in the genetic background listed. The number of animals scored is indicated in parentheses.

Although the signal was comparable for wild-type and *dcs-1(qbc3)* animals at the L2 stage, repression appeared enhanced in adult *dcs-1* mutant animals relative to wild-type (Figure 1B). This effect was accompanied by significantly decreased endogenous *lin-41* mRNA levels in *dcs-1(qbc3)* relative to wild-type adult animals (Figure S2B). Notably, the effect on the *lin-41* mRNA level also suggests that the role of *dcs-1* in this process does not involve the decapping scavenger activity since its loss lead to an increase of overall mRNA levels (Liu and Kiledjian, 2005). Thus, our data indicate that the precocious alae observed in *dcs-1* mutant animals are a consequence of precocious downregulation of *lin-41*.

Mutations in *dcs-1* Lead to an Increase of Functional miRNA Levels

A possible explanation for the robust repression of a miRNA-targeted gene such as *lin-41* in *dcs-1* mutants is that the loss of *dcs-1* increases the levels of functional miRISC. To test this hypothesis, we monitored the level of two core constituents of miRISC, namely, miRNAs and the Argonaute protein ALG-1 (Hutvagner et al., 2004). Whereas *alg-1* mRNA and protein levels were unaltered in *dcs-1(qbc3)* (Figures S2C and S2D), the levels of 16 out of 97 tested miRNAs, including *let-7*, were significantly increased relative to wild-type (Figures 1C and 1D). It remains to be shown what the common feature is that qualifies the miRNAs that change as DCS-1 targets since many miRNAs are not affected by the loss of *dcs-1* (Table S1).

To determine whether the elevated miRNA levels are due to enhanced miRNA transcription or processing, we examined the levels of *let-7* miRNA-related RNA species and did not detect any significant change in the levels of pre-*let-7* and pri-*let-7* molecules between wild-type and *dcs-1(qbc3)* animals (Figures S3A and S3B). We conclude that the increase in mature *let-7* is not a consequence of increased transcription, enhanced stability of the pri- or pre-miRNA molecules, or enhanced processing, which is consistent with a function for *dcs-1* that is not related to the decapping scavenger activity, but instead reflects an effect on the stability of mature miRNA molecules.

To obtain further evidence that the miRNAs that accumulate in *dcs-1* animals are functional, we investigated *let-7(n2853)* mutant animals. This point mutation in the mature *let-7* miRNA causes reduced *let-7* levels as well as temperature-sensitive alae defects and lethality due to vulval bursting (Reinhart et al., 2000). Similar to wild-type, the *let-7* RNA was significantly increased during the development of *dcs-1(qbc3); let-7(n2853)* animals (Figure S3C), with no significant changes in the pre-*let-7* RNA levels (Figure 2A). Moreover, this increase in *let-7* levels coincided with suppression of both the lethality and alae defects of *let-7(n2853)* animals to an extent comparable to that seen with *lin-28* knockout, a conserved negative regulator of *let-7* production (Figure 2B; Lehrbach et al., 2009). We conclude that the loss of *dcs-1* leads to the accumulation of functional miRNAs in animals.

DCS-1 Is Required for the Degradation of miRNAs that Are Released from miRISC

Because our observations argue against a role of DCS-1 in miRNA transcription or biogenesis, we next sought to evaluate a potential role of DCS-1 in miRNA degradation. To this end, we performed miRNA degradation assays by incubating radiolabeled synthetic miRNA molecules with total worm lysates as described previously (Chatterjee and Grosshans, 2009). While we observed complete degradation of synthetic *let-7* after incubation with lysates prepared from wild-type animals, degradation was severely impaired in lysates prepared from *dcs-1(qbc3)* mutant animals (Figures 3A and S3D). This effect was specific because lysate from *dcs-1(qbc3)* animals that expressed a *dcs-1* transgene restored decay (Figure 3A). We conclude that DCS-1 is required for efficient miRNA degradation in vitro.

To further characterize the function of DCS-1 in miRNA degradation, we performed a miRNA release assay. In this assay, miRISC is purified by immunoprecipitation of endogenous ALG-1 and then incubated with a miRNA-depleted worm lysate (by treating the extract with micrococcal nuclease). Subsequently, the miRNA molecules that remain associated with, or are released from, miRISC are quantified (Figure 3B; Chatterjee

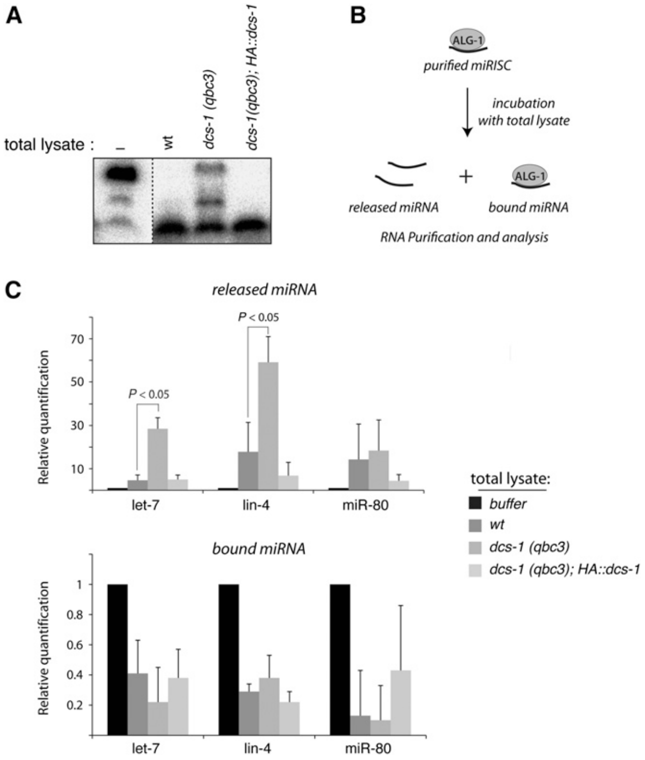

Figure 3. DCS-1 Is Required for miRNA Degradation

(A) Degradation assays of a $5'$-^{32}P-labeled, 21 nt long RNA incubated for 15 min with total worm lysates produced from wild-type (wt), *dcs-1(qbc3)* mutant, and *dcs-1(qbc3)* rescued with an HA::*dcs-1* transgene (*HA::dcs-1*) animals. Dashed lines indicate that unrelated lanes have been removed between samples.

(B) Schematic of the miRNA release assay.

(C) The miRISC purified by immunoprecipitation of endogenous ALG-1 was incubated with micrococcal nuclease-treated worm lysate, and the *let-7*, *lin-4*, and *miR-80* miRNAs that are released into the supernatant (top panel) or the remains associated with ALG-1 complexes (bottom panel) were quantified by quantitative RT-PCR (TaqMan assay). The error bars represent the 95% confidence interval of three independent experiments. p values were obtained using a two-sided Student's t test with the normalized C_t values.

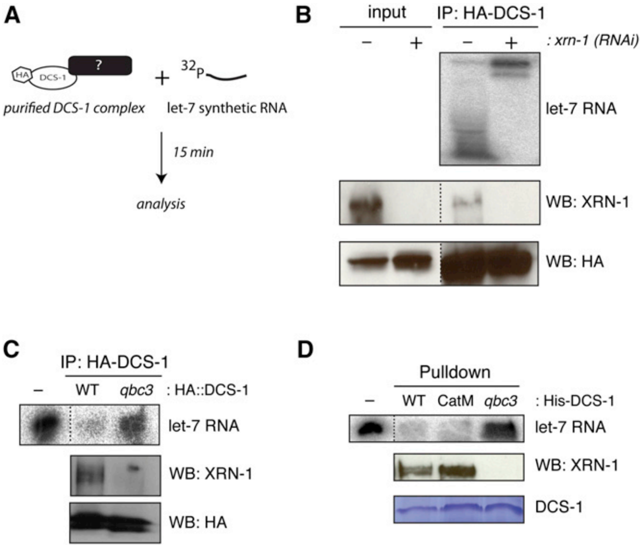

Figure 4. DCS-1 and XRN-1 Form a miRNA Degradation Complex

(A) Schematic of the immunoprecipitation assay.

(B) Transgenic animals are first exposed to either control (–) or *xrn-1* (+) double-stranded RNA (dsRNA)-expressing bacteria for 38 hr followed by total protein extraction and HA::DCS-1 complex purification with beads coupled with anti-HA monoclonal antibody. Inputs represent 10% of the total protein lysate used for the immunoprecipitation (bottom panels). Dashed lines indicate that unrelated lanes have been removed between samples.

(C) Same as (B), with transgenic lines expressing either wild-type (WT) HA-tagged DCS-1 or HA-DCS-1 with the point mutation found in the *dcs-1* mutant allele *qbc3*. In both cases, the detection of HA::DCS-1 and XRN-1 was achieved by western blotting. The minus (–) lane represents the amount of $5'$-^{32}P-labeled *let-7* RNA used for the assay.

(D) The point mutation in DCS-1 abrogates the XRN-1 interaction and exonuclease activity. Beads coupled with histidine (His)-tagged recombinant wild-type (WT), mutated in the catalytic histidine triad (CatM), or mutated at the leucine residue 32 to the proline (L32P; *qbc3*) DCS-1 protein were incubated with worm total protein extracts. Each purified DCS-1 complex was then incubated with the $5'$-^{32}P-labeled, 21 nt long *let-7* RNA for 15 min. The minus (–) lane represents the amount of radiolabeled *let-7* RNA used for the assay. Coomassie blue staining monitored His-DCS-1 proteins, and western blotting was used to detect XRN-1 association.

and Grosshans, 2009). Incubation of miRISC with wild-type lysate led to efficient release of miRNAs; this was unchanged when *dcs-1* mutant lysate was used (Figure 3C). However, whereas wild-type lysate caused substantial degradation of the released miRNAs, which thus was detectable in only small amounts in the supernatant, *dcs-1(qbc3)* lysate caused a significant accumulation in the supernatant of *let-7* and *lin-4* (Figure 3C). By contrast, *miR-80*, a miRNA that is not affected by the loss of *dcs-1* (Table S1), did not accumulate in the supernatant (Figure 3C). These data suggest that DCS-1 is important for the degradation of some miRNAs released from the miRISC.

DCS-1 Interacts with XRN-1 to Form a miRNA Degradation Complex

Since our previous results did not rule out the possibility that DCS-1 affected miRNA turnover indirectly, we immunoprecipitated hemagglutinin (HA)-tagged DCS-1 complexes from rescued *dcs-1(qbc3)* animals and performed a miRNA degradation assay (Figure 4A). As previously observed with total lysates, the purified DCS-1 complex efficiently degraded exogenously supplied radiolabeled miRNA (Figure 4B). This confirms that miRNA degrading activity is associated with DCS-1.

The DCS-1 protein has dinucleoside triphosphate hydrolase activity, which allows it to remove the m7G cap from capped oligonucleotides, but is not known to degrade oligoribonucleotides themselves (Cohen et al., 2004). Hence, we hypothesized that a copurifying RNase could endow DCS-1 immunoprecipitates with miRNA degrading activity. XRN-1 and XRN-2 appeared to be suitable candidates, as these two 5′ to 3′ exonucleases are associated with miRNA degradation in *C. elegans* (Chatterjee et al., 2011; Chatterjee and Grosshans, 2009). Because DCS-1 (Lall et al., 2005) and GFP-tagged XRN-1, but not XRN-2, are localized in the cytoplasm (Figures S4A and S4B), we investigated whether the purified DCS-1 complex contained the XRN-1 protein. Using an antibody specific to endogenous XRN-1 (S.R. and H.G., unpublished data), we found that the functional HA::DCS-1 fusion protein did contain endogenous XRN-1 (Figure 4B).

To confirm that this interaction was functionally relevant for decay, we purified DCS-1 complexes from animals depleted for XRN-1 by RNA interference (RNAi) and observed that miRNA degradation was lost (Figure 4B). Moreover, when we introduced an HA::*dcs-1* transgene carrying the L32P missense mutation found in *dcs-1(qbc3)* animals (Figure S1), both the interaction with XRN-1 as well as the miRNA degrading activity of the immunopurified DCS-1 was lost (Figure 4C). We conclude that XRN-1 is the catalytic engine driving miRNA turnover in the DCS-1 complex.

Finally, to determine whether the decapping scavenger activity of DCS-1 participates in miRNA degradation and to verify that the *qbc3* mutation affects binding to XRN-1, we performed pull-down experiments with recombinant wild-type, catalytically inactive (CatM), and *qbc3* mutant DCS-1 proteins (Figure S1). Whereas the wild-type and catalytically inactive DCS-1 interacted with XRN-1 and retained the degradation activity in the complex, the interaction as well as the degradation activity was lost with DCS-1 *qbc3* protein (Figure 4D). We therefore conclude that the implication of DCS-1 in miRNA turnover is uncoupled from its decapping scavenger activity. Because we did not observe any changes in *xrn-1* mRNA or protein levels in *dcs-1(qbc3)* animals (Figures S4C and S4D), our data support the notion that an interaction with DCS-1 promotes the enzymatic activity of, rather than stabilizes, XRN-1. Altogether, we conclude that DCS-1 and XRN-1 form an enzymatic complex that performs miRNA degradation in *C. elegans*.

DISCUSSION

Overall, our observations demonstrate that the interaction between DCS-1 and XRN-1 promotes the degradation of miRNAs. Consistent with this notion, the orthologous *S. cerevisiae* proteins Dcs1p and Xrn1p have recently been shown to interact, and Dcs1p is essential for Xrn1p enzymatic activity in vitro and, at least in the presence of a nonfermentable carbon source, in vivo (Sinturel et al., 2012). Strikingly, Sinturel et al. (2012) further observed that the stimulation of Xrn1p by Dcs1p did not require Dcs1p catalytic activity. Similarly, our in vitro results indicate that the catalytic activity of *C. elegans* DCS-1 is dispensable for XRN-1 interaction and stimulation. Therefore, our data demonstrate that in addition to its previously characterized role in the degradation of the cap structure of mRNAs (Cohen et al., 2004; Liu et al., 2002; Wang and Kiledjian, 2001), DCS-1 contributes to miRNA turnover in animals by promoting the exonuclease activity of XRN-1 on miRNAs.

Currently, it is unknown how miRNAs are released from the miRISC for degradation by the DCS-1/XRN-1 complex. Recent crystal structures of yeast and human Argonautes showed that the 5′ end of the small RNA is embedded within the Mid domain of the protein (Elkayam et al., 2012; Nakanishi et al., 2012; Schirle and MacRae, 2012) and thus most likely not accessible to the 5′ to 3′ exonuclease complex. Our observation that DCS-1 does not promote miRNA release in vitro but facilitates degradation of the released miRNA is indeed consistent with the notion that DCS-1 and XRN-1 act after the release step, once the miRNA 5′ end has become available. In vivo, our analysis clearly indicates that not only miRNA levels, but also miRNA activity, are increased in *dcs-1* mutant animals, which suggests that miRNA will, at least in part, be retained on Argonaute. It therefore seems possible that the release of the miRNA from the Argonaute protein is driven by a dedicated factor that itself needs to unload the miRNA onto the DCS-1/XRN-1 complex to promote further rounds of release.

Our finding that *dcs-1* loss-of-function mutations are embryonic lethal when combined with loss of the Argonaute *alg-2* in embryos but promote miRNA accumulation in the presence of *alg-2* is puzzling, since this finding suggests that DCS-1 can have both positive and negative effects on miRNA activity. However, it seems possible that impaired miRNA decay alone might account for both phenotypes. In our recent effort to characterize *alg-1* and *alg-2*, we observed that while nearly all *C. elegans* miRNAs are associated with both Argonaute proteins, a small subset of miRNAs remains specifically interacting with ALG-1 or ALG-2 (Vasquez-Rifo et al., 2012). Therefore, if loss of ALG-2 leads to increased competition among miRNAs for access to ALG-1, overaccumulation of selected miRNAs by loss of DCS-1 could further compromise Argonaute loading of a subset of miRNAs. If these include miRNAs essential for embryonic viability, synthetic lethality might result. Future work on the function of DCS-1 during embryogenesis may help us to confirm or refute this idea.

Our data, along with previous observations, support that the level of miRNAs in *C. elegans* must be carefully controlled to enable precisely timed developmental transitions in animal development. Loss or excess of miRNAs can severely impair developmental timing, leading to heterochronic phenotypes (e.g., animals that adopt adult cell fates prematurely or not at all) (Resnick et al., 2010). The fact that DCS-1 expression is developmentally regulated in *C. elegans* (Kwasnicka et al., 2003; Figure S4E) suggests that modulating DCS-1 levels may represent an efficient way to regulate XRN-1 activity, thus rapidly turning over miRNAs at a specific point during development. This timely controlled expression of DCS-1 may also explain why some miRNAs are less sensitive to the loss of *dcs-1* function in animals. We speculate that the role of DCS-1 in miRNA turnover would be more prominent during important developmental switches during which animals undergo significant changes in gene expression, such as the initial steps of embryogenesis and at the larvae-adult transition (Kaufman and Miska, 2010).

EXPERIMENTAL PROCEDURES

Nematode Methods

C. elegans strains were grown under standard conditions (Brenner, 1974). Animal transgenic lines were produced by microinjections as described in (Mello and Fire, 1995). All worm cultures were performed at 20°C unless otherwise noted.

Synthetic Lethal Forward Screen

A population of 500,000 *alg-2(ok304)*Ex[*alg-2*;*sur-5::GFP*] animals was mutagenized with 50 mM ethyl methanesulfonate (EMS) for 4 hr. A total of four GFP-positive F2 animals per F1 were isolated from 1,000 GFP-positive F1. We screened the F3 population from 1,556 F2 to obtain six unlinked mutations.

Total Worm Lysate Preparation

Populations of synchronized animals were harvested at the adult stage. Harvested animals were homogenized in ice-cold lysis buffer (100 mM potassium acetate, 30 mM HEPES-KOH [pH 7.4], 2 mM magnesium acetate, 1 mM dichlorodiphenyltrichloroethane [DDT], 0.5% [v/v] Triton X-100, 2% [v/v] SUPERase•In [Ambion], and cOmplete, Mini, EDTA-free Protease Inhibitor Cocktail [1 tablet/10 ml solution; Roche]). The homogenized extract was clarified by centrifugation at 13,817 × *g* for 10 min at 4°C, and the protein concentrations of the different samples were normalized using DC protein assay (Bio-Rad).

DCS-1 Protein Purification

HA-tagged DCS-1 wild-type and mutant proteins were expressed and purified as reported in (Cohen et al., 2004).

Pull-Down Assays

Purified recombinant DCS-1 proteins were first incubated with total worm protein lysate for 1 hr at 4°C, followed by purification on a TALON Affinity Column (Clontech). Purified DCS-1 complexes were washed three times with lysis buffer, and proteins associated with DCS-1 were identified by western blotting.

MicroRNA Degradation Assays

Assays were performed as described previously in (Chatterjee and Grosshans, 2009).

SUPPLEMENTAL INFORMATION

Supplemental Information includes four figures, one table, and Supplemental Experimental Procedures and can be found with this article online at http://dx.doi.org/10.1016/j.molcel.2013.02.023.

ACKNOWLEDGMENTS

We thank Dr. Julie Claycomb, Dr. Gyorgy Hutvagner, and members of our laboratories for comments on the manuscript. We also thank Eric Paquet for statistical support and Dr. Martin Bisaillon for reagents and advices. Some nematode strains were provided by the *Caenorhabditis* Genetics Center, which is funded by the NIH National Center for Research Resources (NCRR). G.D.B. was a recipient of a Fonds de la recherche en santé du Québec Scholarship and is a Natural Sciences and Engineering Research Council of Canada Graham Bell Scholar. S.R. gratefully acknowledges his Boehringer Ingelheim Fonds PhD fellowship. Work in the lab of M.J.S. has been funded by the Canadian Institutes of Health Research (CIHR). Work in the lab of H.G. is funded by grants from the European Research Council (miRTurn; ERC 2419845), the Swiss National Science Foundation (SNF 31003A_127052), and the Friedrich Miescher Institute, which is supported by the Novartis Research Foundation. Contributions from V.A. and M.C.O. were supported by funding from the US NIH grant (R01 GM24028). M.J.S. is a Junior 2 Scholar from Fonds de la recherche en santé du Québec.

G.D.B. and M.J.S. conceived and designed nearly all experiments. S.R. and H.G. conceived and designed the XRN-1/XRN-2 localization experiments and contributed tools. M.C.O. and V.R.A. conceived and designed the TaqMan miRNA profiling. E.L.R. performed the screen. A.V.-R. contributed to the identification of mutant alleles from the screen. G.D.B., S.R., and M.C.O. performed the experiments. G.D.B., S.R., M.C.O., V.R.A., H.G., and M.J.S. analyzed the data and wrote the paper.

Received: July 23, 2012
Revised: January 18, 2013
Accepted: February 15, 2013
Published: March 28, 2013

REFERENCES

Bajan, S., and Hutvagner, G. (2011). Another "loophole" in miRNA processing. Mol. Cell *44*, 345–347.

Brenner, S. (1974). The genetics of *Caenorhabditis elegans*. Genetics *77*, 71–94.

Chatterjee, S., and Grosshans, H. (2009). Active turnover modulates mature microRNA activity in *Caenorhabditis elegans*. Nature *461*, 546–549.

Chatterjee, S., Fasler, M., Büssing, I., and Grosshans, H. (2011). Target-mediated protection of endogenous microRNAs in *C. elegans*. Dev. Cell *20*, 388–396.

Cohen, L.S., Mikhli, C., Friedman, C., Jankowska-Anyszka, M., Stepinski, J., Darzynkiewicz, E., and Davis, R.E. (2004). Nematode m7GpppG and m3(2,2,7)GpppG decapping: activities in Ascaris embryos and characterization of *C. elegans* scavenger DcpS. RNA *10*, 1609–1624.

Ebert, M.S., and Sharp, P.A. (2012). Roles for microRNAs in conferring robustness to biological processes. Cell *149*, 515–524.

Elkayam, E., Kuhn, C.D., Tocilj, A., Haase, A.D., Greene, E.M., Hannon, G.J., and Joshua-Tor, L. (2012). The structure of human argonaute-2 in complex with miR-20a. Cell *150*, 100–110.

Esteller, M. (2011). Non-coding RNAs in human disease. Nat. Rev. Genet. *12*, 861–874.

Grishok, A., Pasquinelli, A.E., Conte, D., Li, N., Parrish, S., Ha, I., Baillie, D.L., Fire, A., Ruvkun, G., and Mello, C.C. (2001). Genes and mechanisms related to RNA interference regulate expression of the small temporal RNAs that control *C. elegans* developmental timing. Cell *106*, 23–34.

Hu, H., and Gatti, R.A. (2011). MicroRNAs: new players in the DNA damage response. J Mol Cell Biol *3*, 151–158.

Huntzinger, E., and Izaurralde, E. (2011). Gene silencing by microRNAs: contributions of translational repression and mRNA decay. Nat. Rev. Genet. *12*, 99–110.

Hutvagner, G., Simard, M.J., Mello, C.C., and Zamore, P.D. (2004). Sequence-specific inhibition of small RNA function. PLoS Biol. *2*, E98.

Kai, Z.S., and Pasquinelli, A.E. (2010). MicroRNA assassins: factors that regulate the disappearance of miRNAs. Nat. Struct. Mol. Biol. *17*, 5–10.

Kaufman, E.J., and Miska, E.A. (2010). The microRNAs of *Caenorhabditis elegans*. Semin. Cell Dev. Biol. *21*, 728–737.

Kim, V.N., Han, J., and Siomi, M.C. (2009). Biogenesis of small RNAs in animals. Nat. Rev. Mol. Cell Biol. *10*, 126–139.

Krol, J., Loedige, I., and Filipowicz, W. (2010). The widespread regulation of microRNA biogenesis, function and decay. Nat. Rev. Genet. *11*, 597–610.

Kwasnicka, D.A., Krakowiak, A., Thacker, C., Brenner, C., and Vincent, S.R. (2003). Coordinate expression of NADPH-dependent flavin reductase, Fre-1, and Hint-related 7meGMP-directed hydrolase, DCS-1. J. Biol. Chem. *278*, 39051–39058.

Lall, S., Piano, F., and Davis, R.E. (2005). *Caenorhabditis elegans* decapping proteins: localization and functional analysis of Dcp1, Dcp2, and DcpS during embryogenesis. Mol. Biol. Cell *16*, 5880–5890.

Lehrbach, N.J., Armisen, J., Lightfoot, H.L., Murfitt, K.J., Bugaut, A., Balasubramanian, S., and Miska, E.A. (2009). LIN-28 and the poly(U) polymerase PUP-2 regulate let-7 microRNA processing in *Caenorhabditis elegans*. Nat. Struct. Mol. Biol. *16*, 1016–1020.

Leung, A.K., and Sharp, P.A. (2010). MicroRNA functions in stress responses. Mol. Cell *40*, 205–215.

Liu, H., and Kiledjian, M. (2005). Scavenger decapping activity facilitates 5′ to 3′ mRNA decay. Mol. Cell. Biol. *25*, 9764–9772.

Liu, H., Rodgers, N.D., Jiao, X., and Kiledjian, M. (2002). The scavenger mRNA decapping enzyme DcpS is a member of the HIT family of pyrophosphatases. EMBO J. *21*, 4699–4708.

Mello, C., and Fire, A. (1995). DNA transformation. Methods Cell Biol. *48*, 451–482.

Mendell, J.T., and Olson, E.N. (2012). MicroRNAs in stress signaling and human disease. Cell *148*, 1172–1187.

Nakanishi, K., Weinberg, D.E., Bartel, D.P., and Patel, D.J. (2012). Structure of yeast Argonaute with guide RNA. Nature *486*, 368–374.

Newman, M.A., Mani, V., and Hammond, S.M. (2011). Deep sequencing of microRNA precursors reveals extensive 3′ end modification. RNA *17*, 1795–1803.

Pasquinelli, A.E. (2012). MicroRNAs and their targets: recognition, regulation and an emerging reciprocal relationship. Nat. Rev. Genet. *13*, 271–282.

Ramachandran, V., and Chen, X. (2008). Degradation of microRNAs by a family of exoribonucleases in *Arabidopsis*. Science *321*, 1490–1492.

Reinhart, B.J., Slack, F.J., Basson, M., Pasquinelli, A.E., Bettinger, J.C., Rougvie, A.E., Horvitz, H.R., and Ruvkun, G. (2000). The 21-nucleotide let-7 RNA regulates developmental timing in *Caenorhabditis elegans*. Nature *403*, 901–906.

Resnick, T.D., McCulloch, K.A., and Rougvie, A.E. (2010). miRNAs give worms the time of their lives: small RNAs and temporal control in *Caenorhabditis elegans*. Dev. Dyn. *239*, 1477–1489.

Rüegger, S., and Großhans, H. (2012). MicroRNA turnover: when, how, and why. Trends Biochem. Sci. *37*, 436–446.

Schirle, N.T., and MacRae, I.J. (2012). The crystal structure of human Argonaute2. Science *336*, 1037–1040.

Sinturel, F., Bréchemier-Baey, D., Kiledjian, M., Condon, C., and Bénard, L. (2012). Activation of 5′-3′ exoribonuclease Xrn1 by cofactor Dcs1 is essential for mitochondrial function in yeast. Proc. Natl. Acad. Sci. USA *109*, 8264–8269.

Slack, F.J., Basson, M., Liu, Z., Ambros, V., Horvitz, H.R., and Ruvkun, G. (2000). The *lin-41* RBCC gene acts in the *C. elegans* heterochronic pathway between the let-7 regulatory RNA and the LIN-29 transcription factor. Mol. Cell *5*, 659–669.

Vasquez-Rifo, A., Jannot, G., Armisen, J., Labouesse, M., Bukhari, S.I., Rondeau, E.L., Miska, E.A., and Simard, M.J. (2012). Developmental characterization of the microRNA-specific *C. elegans* Argonautes *alg-1* and *alg-2*. PLoS ONE *7*, e33750.

Wang, Z., and Kiledjian, M. (2001). Functional link between the mammalian exosome and mRNA decapping. Cell *107*, 751–762.

8 References

Aalto, A.P., and Pasquinelli, A.E. (2012). Small non-coding RNAs mount a silent revolution in gene expression. Curr Opin Cell Biol *24*, 333-340.

Achsel, T., Brahms, H., Kastner, B., Bachi, A., Wilm, M., and Luhrmann, R. (1999). A doughnut-shaped heteromer of human Sm-like proteins binds to the 3'-end of U6 snRNA, thereby facilitating U4/U6 duplex formation in vitro. EMBO J *18*, 5789-5802.

Alekseyenko, A.V., Kim, N., and Lee, C.J. (2007). Global analysis of exon creation versus loss and the role of alternative splicing in 17 vertebrate genomes. RNA *13*, 661-670.

Alvarez-Saavedra, E., and Horvitz, H.R. (2010). Many families of C. elegans microRNAs are not essential for development or viability. Curr Biol *20*, 367-373.

Amberg, D.C., Goldstein, A.L., and Cole, C.N. (1992). Isolation and characterization of RAT1: an essential gene of Saccharomyces cerevisiae required for the efficient nucleocytoplasmic trafficking of mRNA. Genes Dev *6*, 1173-1189.

An, H.S., Lee, K.H., and Kim, J. (2004). Identification of an exoribonuclease homolog, CaKEM1/CaXRN1, in Candida albicans and its characterization in filamentous growth. FEMS microbiology letters *235*, 297-303.

Aravind, L., and Koonin, E.V. (2001). A natural classification of ribonucleases. Methods in enzymology *341*, 3-28.

Arraiano, C.M., Mauxion, F., Viegas, S.C., Matos, R.G., and Seraphin, B. (2013). Intracellular ribonucleases involved in transcript processing and decay: precision tools for RNA. Biochim Biophys Acta *1829*, 491-513.

Arribas-Layton, M., Wu, D., Lykke-Andersen, J., and Song, H. (2013). Structural and functional control of the eukaryotic mRNA decapping machinery. Biochim Biophys Acta *1829*, 580-589.

Artamonova, II, and Gelfand, M.S. (2007). Comparative genomics and evolution of alternative splicing: the pessimists' science. Chemical reviews *107*, 3407-3430.

Azzalin, C.M., Reichenbach, P., Khoriauli, L., Giulotto, E., and Lingner, J. (2007). Telomeric repeat containing RNA and RNA surveillance factors at mammalian chromosome ends. Science *318*, 798-801.

Baker, K.E., and Parker, R. (2004). Nonsense-mediated mRNA decay: terminating erroneous gene expression. Curr Opin Cell Biol *16*, 293-299.

Bazopoulou, D., and Tavernarakis, N. (2009). The NemaGENETAG initiative: large scale transposon insertion gene-tagging in Caenorhabditis elegans. Genetica *137*, 39-46.

Bell, M., Schreiner, S., Damianov, A., Reddy, R., and Bindereif, A. (2002). p110, a novel human U6 snRNP protein and U4/U6 snRNP recycling factor. EMBO J *21*, 2724-2735.

Bethke, A., Fielenbach, N., Wang, Z., Mangelsdorf, D.J., and Antebi, A. (2009). Nuclear hormone receptor regulation of microRNAs controls developmental progression. Science *324*, 95-98.

Beyer, A.L., and Osheim, Y.N. (1988). Splice site selection, rate of splicing, and alternative splicing on nascent transcripts. Genes Dev *2*, 754-765.

Bindereif, A., Wolff, T., and Green, M.R. (1990). Discrete domains of human U6 snRNA required for the assembly of U4/U6 snRNP and splicing complexes. EMBO J *9*, 251-255.

Blatch, G.L., and Lassle, M. (1999). The tetratricopeptide repeat: a structural motif mediating protein-protein interactions. BioEssays : news and reviews in molecular, cellular and developmental biology *21*, 932-939.

Bosse, G.D., Ruegger, S., Ow, M.C., Vasquez-Rifo, A., Rondeau, E.L., Ambros, V.R., Grosshans, H., and Simard, M.J. (2013). The Decapping Scavenger Enzyme DCS-1 Controls MicroRNA Levels in Caenorhabditis elegans. Mol Cell.

Bousquet-Antonelli, C., Presutti, C., and Tollervey, D. (2000). Identification of a regulated pathway for nuclear pre-mRNA turnover. Cell *102*, 765-775.

Bouveret, E., Rigaut, G., Shevchenko, A., Wilm, M., and Seraphin, B. (2000). A Sm-like protein complex that participates in mRNA degradation. EMBO J *19*, 1661-1671.

Brannan, K., Kim, H., Erickson, B., Glover-Cutter, K., Kim, S., Fong, N., Kiemele, L., Hansen, K., Davis, R., Lykke-Andersen, J*., et al.* (2012). mRNA decapping factors and the exonuclease Xrn2 function in widespread premature termination of RNA polymerase II transcription. Mol Cell *46*, 311-324.

Braun, J.E., Truffault, V., Boland, A., Huntzinger, E., Chang, C.T., Haas, G., Weichenrieder, O., Coles, M., and Izaurralde, E. (2012). A direct interaction between DCP1 and XRN1 couples mRNA decapping to 5' exonucleolytic degradation. Nat Struct Mol Biol *19*, 1324-1331.

Brow, D.A., and Guthrie, C. (1988). Spliceosomal RNA U6 is remarkably conserved from yeast to mammals. Nature *334*, 213-218.

Buratowski, S. (2009). Progression through the RNA polymerase II CTD cycle. Mol Cell *36*, 541-546.

Cartegni, L., and Krainer, A.R. (2002). Disruption of an SF2/ASF-dependent exonic splicing enhancer in SMN2 causes spinal muscular atrophy in the absence of SMN1. Nat Genet *30*, 377-384.

Carthew, R.W., and Sontheimer, E.J. (2009). Origins and Mechanisms of miRNAs and siRNAs. Cell *136*, 642--655.

Cech, T.R. (2000). Structural biology. The ribosome is a ribozyme. Science *289*, 878-879.

Chang, J.H., Xiang, S., and Tong, L. (2011a). 5'-3' Exoribonucleases. In Ribonucleases, A. Nicholson, ed. (Springer-Verlag Berlin Heidelberg), pp. 167-192.

Chang, J.H., Xiang, S., Xiang, K., Manley, J.L., and Tong, L. (2011b). Structural and biochemical studies of the 5'-->3' exoribonuclease Xrn1. Nat Struct Mol Biol *18*, 270-276.

Chatterjee, S., and Grosshans, H. (2009). Active turnover modulates mature microRNA activity in Caenorhabditis elegans. Nature *461*, 546-549.

Chen, Y., Pane, A., and Schupbach, T. (2007). Cutoff and aubergine mutations result in retrotransposon upregulation and checkpoint activation in Drosophila. Curr Biol *17*, 637-642.

Chernyakov, I., Whipple, J.M., Kotelawala, L., Grayhack, E.J., and Phizicky, E.M. (2008). Degradation of several hypomodified mature tRNA species in Saccharomyces cerevisiae is mediated by Met22 and the 5'-3' exonucleases Rat1 and Xrn1. Genes Dev *22*, 1369-1380.

Chiba, K., Yamamoto, J., Yamaguchi, Y., and Handa, H. (2010). Promoter-proximal pausing and its release: molecular mechanisms and physiological functions. Experimental cell research *316*, 2723-2730.

Chlebowski, A., Lubas, M., Jensen, T.H., and Dziembowski, A. (2013). RNA decay machines: the exosome. Biochim Biophys Acta *1829*, 552-560.

Cho, E.J., Kobor, M.S., Kim, M., Greenblatt, J., and Buratowski, S. (2001). Opposing effects of Ctk1 kinase and Fcp1 phosphatase at Ser 2 of the RNA polymerase II C-terminal domain. Genes Dev *15*, 3319-3329.

Chorev, M., and Carmel, L. (2012). The function of introns. Frontiers in genetics *3*, 55.

Coller, J., and Parker, R. (2004). Eukaryotic mRNA decapping. Annual review of biochemistry *73*, 861-890.

Conti, E., and Izaurralde, E. (2005). Nonsense-mediated mRNA decay: molecular insights and mechanistic variations across species. Curr Opin Cell Biol *17*, 316-325.

Cooper, T.A., Wan, L., and Dreyfuss, G. (2009). RNA and disease. Cell *136*, 777-793.

Couvillion, M.T., Bounova, G., Purdom, E., Speed, T.P., and Collins, K. (2012). A Tetrahymena Piwi bound to mature tRNA 3' fragments activates the exonuclease Xrn2 for RNA processing in the nucleus. Mol Cell *48*, 509-520.

Cullen, B.R. (1998). HIV-1 auxiliary proteins: making connections in a dying cell. Cell *93*, 685-692.

Dahmus, M.E. (1996). Reversible phosphorylation of the C-terminal domain of RNA polymerase II. J Biol Chem *271*, 19009-19012.

Danin-Kreiselman, M., Lee, C.Y., and Chanfreau, G. (2003). RNAse III-mediated degradation of unspliced pre-mRNAs and lariat introns. Mol Cell *11*, 1279-1289.
Davidson, L., Kerr, A., and West, S. (2012). Co-transcriptional degradation of aberrant pre-mRNA by Xrn2. EMBO J *31*, 2566-2578.
Deng, J., Ernst, N.L., Turley, S., Stuart, K.D., and Hol, W.G. (2005). Structural basis for UTP specificity of RNA editing TUTases from Trypanosoma brucei. EMBO J *24*, 4007-4017.
Dieci, G., Preti, M., and Montanini, B. (2009). Eukaryotic snoRNAs: a paradigm for gene expression flexibility. Genomics *94*, 83-88.
Djebali, S., Davis, C.A., Merkel, A., Dobin, A., Lassmann, T., Mortazavi, A., Tanzer, A., Lagarde, J., Lin, W., Schlesinger, F.*, et al.* (2012). Landscape of transcription in human cells. Nature *489*, 101-108.
Djuranovic, S., Nahvi, A., and Green, R. (2011). A parsimonious model for gene regulation by miRNAs. Science *331*, 550-553.
Dodson, R.E., and Shapiro, D.J. (2002). Regulation of pathways of mRNA destabilization and stabilization. Progress in nucleic acid research and molecular biology *72*, 129-164.
Edgell, D.R., Belfort, M., and Shub, D.A. (2000). Barriers to intron promiscuity in bacteria. Journal of bacteriology *182*, 5281-5289.
El Hage, A., Koper, M., Kufel, J., and Tollervey, D. (2008). Efficient termination of transcription by RNA polymerase I requires the 5' exonuclease Rat1 in yeast. Genes Dev *22*, 1069-1081.
Fang, F., Hoskins, J., and Butler, J.S. (2004). 5-fluorouracil enhances exosome-dependent accumulation of polyadenylated rRNAs. Mol Cell Biol *24*, 10766-10776.
Fang, F., Phillips, S., and Butler, J.S. (2005). Rat1p and Rai1p function with the nuclear exosome in the processing and degradation of rRNA precursors. RNA *11*, 1571-1578.
Fatica, A., and Bozzoni, I. (2014). Long non-coding RNAs: new players in cell differentiation and development. Nat Rev Genet *15*, 7-21.
Fourmann, J.B., Schmitzova, J., Christian, H., Urlaub, H., Ficner, R., Boon, K.L., Fabrizio, P., and Luhrmann, R. (2013). Dissection of the factor requirements for spliceosome disassembly and the elucidation of its dissociation products using a purified splicing system. Genes Dev *27*, 413-428.
Frand, A.R., Russel, S., and Ruvkun, G. (2005). Functional genomic analysis of C. elegans molting. PLoS Biol *3*, e312.
Frith, M.C., Pheasant, M., and Mattick, J.S. (2005). The amazing complexity of the human transcriptome. European journal of human genetics : EJHG *13*, 894-897.
Frokjaer-Jensen, C., Davis, M.W., Ailion, M., and Jorgensen, E.M. (2012). Improved Mos1-mediated transgenesis in C. elegans. Nat Methods *9*, 117-118.
Frokjaer-Jensen, C., Davis, M.W., Hollopeter, G., Taylor, J., Harris, T.W., Nix, P., Lofgren, R., Prestgard-Duke, M., Bastiani, M., Moerman, D.G.*, et al.* (2010). Targeted gene deletions in C. elegans using transposon excision. Nat Methods *7*, 451-453.
Frokjaer-Jensen, C., Davis, M.W., Hopkins, C.E., Newman, B.J., Thummel, J.M., Olesen, S.P., Grunnet, M., and Jorgensen, E.M. (2008). Single-copy insertion of transgenes in Caenorhabditis elegans. Nat Genet *40*, 1375-1383.
Fujinaga, K., Irwin, D., Huang, Y., Taube, R., Kurosu, T., and Peterlin, B.M. (2004). Dynamics of human immunodeficiency virus transcription: P-TEFb phosphorylates RD and dissociates negative effectors from the transactivation response element. Mol Cell Biol *24*, 787-795.
Gatfield, D., and Izaurralde, E. (2004). Nonsense-mediated messenger RNA decay is initiated by endonucleolytic cleavage in Drosophila. Nature *429*, 575-578.
Geerlings, T.H., Vos, J.C., and Raue, H.A. (2000). The final step in the formation of 25S rRNA in Saccharomyces cerevisiae is performed by 5'-->3' exonucleases. RNA *6*, 1698-1703.
Geisler, S., Lojek, L., Khalil, A.M., Baker, K.E., and Coller, J. (2012). Decapping of long noncoding RNAs regulates inducible genes. Mol Cell *45*, 279-291.

Geraldo, N., Baurle, I., Kidou, S., Hu, X., and Dean, C. (2009). FRIGIDA delays flowering in Arabidopsis via a cotranscriptional mechanism involving direct interaction with the nuclear cap-binding complex. Plant physiology *150*, 1611-1618.

Ghetti, A., Company, M., and Abelson, J. (1995). Specificity of Prp24 binding to RNA: a role for Prp24 in the dynamic interaction of U4 and U6 snRNAs. RNA *1*, 132-145.

Gregory, B.D., O'Malley, R.C., Lister, R., Urich, M.A., Tonti-Filippini, J., Chen, H., Millar, A.H., and Ecker, J.R. (2008). A link between RNA metabolism and silencing affecting Arabidopsis development. Dev Cell *14*, 854-866.

Grima, D.P., Sullivan, M., Zabolotskaya, M.V., Browne, C., Seago, J., Wan, K.C., Okada, Y., and Newbury, S.F. (2008). The 5'-3' exoribonuclease pacman is required for epithelial sheet sealing in Drosophila and genetically interacts with the phosphatase puckered. Biology of the cell / under the auspices of the European Cell Biology Organization *100*, 687-701.

Gu, J., Shimba, S., Nomura, N., and Reddy, R. (1998). Isolation and characterization of a new 110 kDa human nuclear RNA-binding protein (p110nrb). Biochim Biophys Acta *1399*, 1-9.

Gu, J., Shumyatsky, G., Makan, N., and Reddy, R. (1997). Formation of 2',3'-cyclic phosphates at the 3' end of human U6 small nuclear RNA in vitro. Identification of 2',3'-cyclic phosphates at the 3' ends of human signal recognition particle and mitochondrial RNA processing RNAs. J Biol Chem *272*, 21989-21993.

Gudipati, R.K., Xu, Z., Lebreton, A., Seraphin, B., Steinmetz, L.M., Jacquier, A., and Libri, D. (2012). Extensive degradation of RNA precursors by the exosome in wild-type cells. Mol Cell *48*, 409-421.

Gunnery, S., Ma, Y., and Mathews, M.B. (1999). Termination sequence requirements vary among genes transcribed by RNA polymerase III. Journal of molecular biology *286*, 745-757.

Guo, J., and Price, D.H. (2013). RNA polymerase II transcription elongation control. Chemical reviews *113*, 8583-8603.

Guthrie, C., and Patterson, B. (1988). Spliceosomal snRNAs. Annual review of genetics *22*, 387-419.

Hagan, J.P., Piskounova, E., and Gregory, R.I. (2009). Lin28 recruits the TUTase Zcchc11 to inhibit let-7 maturation in mouse embryonic stem cells. Nat Struct Mol Biol *16*, 1021-1025.

Hahn, S. (2004). Structure and mechanism of the RNA polymerase II transcription machinery. Nat Struct Mol Biol *11*, 394-403.

Hansen, T.B., Wiklund, E.D., Bramsen, J.B., Villadsen, S.B., Statham, A.L., Clark, S.J., and Kjems, J. (2011). miRNA-dependent gene silencing involving Ago2-mediated cleavage of a circular antisense RNA. EMBO J *30*, 4414-4422.

He, W., and Parker, R. (2000). Functions of Lsm proteins in mRNA degradation and splicing. Curr Opin Cell Biol *12*, 346-350.

Henry, Y., Wood, H., Morrissey, J.P., Petfalski, E., Kearsey, S., and Tollervey, D. (1994). The 5' end of yeast 5.8S rRNA is generated by exonucleases from an upstream cleavage site. EMBO J *13*, 2452-2463.

Heo, I., Ha, M., Lim, J., Yoon, M.J., Park, J.E., Kwon, S.C., Chang, H., and Kim, V.N. (2012). Mono-uridylation of pre-microRNA as a key step in the biogenesis of group II let-7 microRNAs. Cell *151*, 521-532.

Heo, I., Joo, C., Cho, J., Ha, M., Han, J., and Kim, V.N. (2008). Lin28 mediates the terminal uridylation of let-7 precursor MicroRNA. Mol Cell *32*, 276-284.

Heo, I., Joo, C., Kim, Y.-K., Ha, M., Yoon, M.-J., Cho, J., Yeom, K.-H., Han, J., and Kim, V.N. (2009). TUT4 in concert with Lin28 suppresses microRNA biogenesis through pre-microRNA uridylation. Cell *138*, 696--708.

Hilleren, P.J., and Parker, R. (2003). Cytoplasmic degradation of splice-defective pre-mRNAs and intermediates. Mol Cell *12*, 1453-1465.

Hirai, H., Lee, D.I., Natori, S., and Sekimizu, K. (1988). Uridylation of U6 RNA in a nuclear extract in Ehrlich ascites tumor cells. Journal of biochemistry *104*, 991-994.

Hock, J., Weinmann, L., Ender, C., Rudel, S., Kremmer, E., Raabe, M., Urlaub, H., and Meister, G. (2007). Proteomic and functional analysis of Argonaute-containing mRNA-protein complexes in human cells. EMBO Rep *8*, 1052-1060.
Holm, L., and Sander, C. (1995). DNA polymerase beta belongs to an ancient nucleotidyltransferase superfamily. Trends in biochemical sciences *20*, 345-347.
Hug, N., and Lingner, J. (2006). Telomere length homeostasis. Chromosoma *115*, 413-425.
Isken, O., and Maquat, L.E. (2007). Quality control of eukaryotic mRNA: safeguarding cells from abnormal mRNA function. Genes Dev *21*, 1833-1856.
Jackson, R.J., Hellen, C.U., and Pestova, T.V. (2010). The mechanism of eukaryotic translation initiation and principles of its regulation. Nat Rev Mol Cell Biol *11*, 113-127.
Jandrositz, A., and Guthrie, C. (1995). Evidence for a Prp24 binding site in U6 snRNA and in a putative intermediate in the annealing of U6 and U4 snRNAs. EMBO J *14*, 820-832.
Jeffries, C.D., Fried, H.M., and Perkins, D.O. (2011). Nuclear and cytoplasmic localization of neural stem cell microRNAs. RNA *17*, 675-686.
Jiao, X., Chang, J.H., Kilic, T., Tong, L., and Kiledjian, M. (2013). A Mammalian Pre-mRNA 5' End Capping Quality Control Mechanism and an Unexpected Link of Capping to Pre-mRNA Processing. Mol Cell *50*, 104-115.
Jiao, X., Xiang, S., Oh, C., Martin, C.E., Tong, L., and Kiledjian, M. (2010). Identification of a quality-control mechanism for mRNA 5'-end capping. Nature *467*, 608-611.
Jinek, M., Coyle, S.M., and Doudna, J.A. (2011). Coupled 5' nucleotide recognition and processivity in Xrn1-mediated mRNA decay. Mol Cell *41*, 600-608.
Johnson, A.W. (1997). Rat1p and Xrn1p are functionally interchangeable exoribonucleases that are restricted to and required in the nucleus and cytoplasm, respectively. Mol Cell Biol *17*, 6122-6130.
Jones, C.I., Zabolotskaya, M.V., and Newbury, S.F. (2012). The 5' --> 3' exoribonuclease XRN1/Pacman and its functions in cellular processes and development. Wiley interdisciplinary reviews. RNA *3*, 455-468.
Kamath, R.S., and Ahringer, J. (2003). Genome-wide RNAi screening in Caenorhabditis elegans. Methods *30*, 313-321.
Kaneko, S., Rozenblatt-Rosen, O., Meyerson, M., and Manley, J.L. (2007). The multifunctional protein p54nrb/PSF recruits the exonuclease XRN2 to facilitate pre-mRNA 3' processing and transcription termination. Genes Dev *21*, 1779-1789.
Kastenmayer, J.P., and Green, P.J. (2000). Novel features of the XRN-family in Arabidopsis: evidence that AtXRN4, one of several orthologs of nuclear Xrn2p/Rat1p, functions in the cytoplasm. Proc Natl Acad Sci U S A *97*, 13985-13990.
Keren, H., Lev-Maor, G., and Ast, G. (2010). Alternative splicing and evolution: diversification, exon definition and function. Nat Rev Genet *11*, 345-355.
Kim, H., Klein, R., Majewski, J., and Ott, J. (2004a). Estimating rates of alternative splicing in mammals and invertebrates. Nat Genet *36*, 915-916; author reply 916-917.
Kim, J., and Kim, J. (2002). KEM1 is involved in filamentous growth of Saccharomyces cerevisiae. FEMS microbiology letters *216*, 33-38.
Kim, J., Ljungdahl, P.O., and Fink, G.R. (1990). kem mutations affect nuclear fusion in Saccharomyces cerevisiae. Genetics *126*, 799-812.
Kim, M., Krogan, N.J., Vasiljeva, L., Rando, O.J., Nedea, E., Greenblatt, J.F., and Buratowski, S. (2004b). The yeast Rat1 exonuclease promotes transcription termination by RNA polymerase II. Nature *432*, 517-522.
Kornblihtt, A.R., Schor, I.E., Allo, M., Dujardin, G., Petrillo, E., and Munoz, M.J. (2013). Alternative splicing: a pivotal step between eukaryotic transcription and translation. Nat Rev Mol Cell Biol *14*, 153-165.

Krol, J., Loedige, I., and Filipowicz, W. (2010). The widespread regulation of microRNA biogenesis, function and decay. Nat Rev Genet *11*, 597-610.
Krueger, B.J., Varzavand, K., Cooper, J.J., and Price, D.H. (2010). The mechanism of release of P-TEFb and HEXIM1 from the 7SK snRNP by viral and cellular activators includes a conformational change in 7SK. PLoS One *5*, e12335.
Kuai, L., Fang, F., Butler, J.S., and Sherman, F. (2004). Polyadenylation of rRNA in Saccharomyces cerevisiae. Proc Natl Acad Sci U S A *101*, 8581-8586.
Kwak, J.E., and Wickens, M. (2007). A family of poly(U) polymerases. RNA *13*, 860-867.
Larimer, F.W., and Stevens, A. (1990). Disruption of the gene XRN1, coding for a 5'----3' exoribonuclease, restricts yeast cell growth. Gene *95*, 85-90.
Lee, C.Y., Lee, A., and Chanfreau, G. (2003). The roles of endonucleolytic cleavage and exonucleolytic digestion in the 5'-end processing of S. cerevisiae box C/D snoRNAs. RNA *9*, 1362-1370.
Lejeune, F., Li, X., and Maquat, L.E. (2003). Nonsense-mediated mRNA decay in mammalian cells involves decapping, deadenylating, and exonucleolytic activities. Mol Cell *12*, 675-687.
Li, C.H., Irmer, H., Gudjonsdottir-Planck, D., Freese, S., Salm, H., Haile, S., Estevez, A.M., and Clayton, C. (2006). Roles of a Trypanosoma brucei 5'->3' exoribonuclease homolog in mRNA degradation. RNA *12*, 2171-2186.
Liao, J.Y., Ma, L.M., Guo, Y.H., Zhang, Y.C., Zhou, H., Shao, P., Chen, Y.Q., and Qu, L.H. (2010). Deep sequencing of human nuclear and cytoplasmic small RNAs reveals an unexpectedly complex subcellular distribution of miRNAs and tRNA 3' trailers. PLoS One *5*, e10563.
Licht, K., Medenbach, J., Luhrmann, R., Kambach, C., and Bindereif, A. (2008). 3'-cyclic phosphorylation of U6 snRNA leads to recruitment of recycling factor p110 through LSm proteins. RNA *14*, 1532-1538.
Lin, M.D., Jiao, X., Grima, D., Newbury, S.F., Kiledjian, M., and Chou, T.B. (2008). Drosophila processing bodies in oogenesis. Dev Biol *322*, 276-288.
Liu, Y., Kim, B.O., Kao, C., Jung, C., Dalton, J.T., and He, J.J. (2004). Tip110, the human immunodeficiency virus type 1 (HIV-1) Tat-interacting protein of 110 kDa as a negative regulator of androgen receptor (AR) transcriptional activation. J Biol Chem *279*, 21766-21773.
Liu, Y., Lee, M.R., Timani, K., He, J.J., and Broxmeyer, H.E. (2012). Tip110 maintains expression of pluripotent factors in and pluripotency of human embryonic stem cells. Stem cells and development *21*, 829-833.
Liu, Y., Li, J., Kim, B.O., Pace, B.S., and He, J.J. (2002). HIV-1 Tat protein-mediated transactivation of the HIV-1 long terminal repeat promoter is potentiated by a novel nuclear Tat-interacting protein of 110 kDa, Tip110. J Biol Chem *277*, 23854-23863.
Liu, Y., Timani, K., Ou, X., Broxmeyer, H.E., and He, J.J. (2013). C-MYC controlled TIP110 protein expression regulates OCT4 mRNA splicing in human embryonic stem cells. Stem cells and development *22*, 689-694.
Lu, Y., Liu, P., James, M., Vikis, H.G., Liu, H., Wen, W., Franklin, A., and You, M. (2010). Genetic variants cis-regulating Xrn2 expression contribute to the risk of spontaneous lung tumor. Oncogene *29*, 1041-1049.
Luke, B., Panza, A., Redon, S., Iglesias, N., Li, Z., and Lingner, J. (2008). The Rat1p 5' to 3' exonuclease degrades telomeric repeat-containing RNA and promotes telomere elongation in Saccharomyces cerevisiae. Mol Cell *32*, 465-477.
Lund, E., and Dahlberg, J.E. (1992). Cyclic 2',3'-phosphates and nontemplated nucleotides at the 3' end of spliceosomal U6 small nuclear RNA's. Science *255*, 327-330.
Luo, W., Johnson, A.W., and Bentley, D.L. (2006). The role of Rat1 in coupling mRNA 3'-end processing to transcription termination: implications for a unified allosteric-torpedo model. Genes Dev *20*, 954-965.
Mandel, C.R., Kaneko, S., Zhang, H., Gebauer, D., Vethantham, V., Manley, J.L., and Tong, L. (2006). Polyadenylation factor CPSF-73 is the pre-mRNA 3'-end-processing endonuclease. Nature *444*, 953-956.

Maniatis, T., and Reed, R. (2002). An extensive network of coupling among gene expression machines. Nature *416*, 499-506.

Marshall, N.F., Peng, J., Xie, Z., and Price, D.H. (1996). Control of RNA polymerase II elongation potential by a novel carboxyl-terminal domain kinase. J Biol Chem *271*, 27176-27183.

Mayes, A.E., Verdone, L., Legrain, P., and Beggs, J.D. (1999). Characterization of Sm-like proteins in yeast and their association with U6 snRNA. EMBO J *18*, 4321-4331.

Medenbach, J., Schreiner, S., Liu, S., Luhrmann, R., and Bindereif, A. (2004). Human U4/U6 snRNP recycling factor p110: mutational analysis reveals the function of the tetratricopeptide repeat domain in recycling. Mol Cell Biol *24*, 7392-7401.

Miki, T.S., and Grosshans, H. (2013). The multifunctional RNase XRN2. Biochem Soc Trans *41*, 825-830.

Miki, T.S., Richter, H., Rüegger, S., and Grosshans, H. (2014). PAXT-1 promotes XRN2 activity by stabilizing it through a conserved domain. Mol Cell, in press.

Modrek, B., and Lee, C. (2002). A genomic view of alternative splicing. Nat Genet *30*, 13-19.

Mooradian, A.D., Morley, J.E., and Korenman, S.G. (1987). Biological actions of androgens. Endocrine reviews *8*, 1-28.

Murayama, K., Kobayashi, T., Imaizumi, T., Matsunaga, K., Kuramoto, T., Shigemori, M., Shichijo, S., and Itoh, K. (2000). Expression of the SART3 tumor-rejection antigen in brain tumors and induction of cytotoxic T lymphocytes by its peptides. Journal of immunotherapy *23*, 511-518.

Nagai, K., Muto, Y., Pomeranz Krummel, D.A., Kambach, C., Ignjatovic, T., Walke, S., and Kuglstatter, A. (2001). Structure and assembly of the spliceosomal snRNPs. Novartis Medal Lecture. Biochem Soc Trans *29*, 15-26.

Nagarajan, V.K., Jones, C.I., Newbury, S.F., and Green, P.J. (2013). XRN 5'-->3' exoribonucleases: structure, mechanisms and functions. Biochim Biophys Acta *1829*, 590-603.

Newbury, S., and Woollard, A. (2004). The 5'-3' exoribonuclease xrn-1 is essential for ventral epithelial enclosure during C. elegans embryogenesis. RNA *10*, 59-65.

Nissan, T., Rajyaguru, P., She, M., Song, H., and Parker, R. (2010). Decapping activators in Saccharomyces cerevisiae act by multiple mechanisms. Mol Cell *39*, 773-783.

O'Sullivan, R.J., and Karlseder, J. (2010). Telomeres: protecting chromosomes against genome instability. Nat Rev Mol Cell Biol *11*, 171-181.

Orban, T.I., and Izaurralde, E. (2005). Decay of mRNAs targeted by RISC requires XRN1, the Ski complex, and the exosome. RNA *11*, 459-469.

Page, A.M., Davis, K., Molineux, C., Kolodner, R.D., and Johnson, A.W. (1998). Mutational analysis of exoribonuclease I from Saccharomyces cerevisiae. Nucleic Acids Res *26*, 3707-3716.

Pall, G.S., and Hamilton, A.J. (2008). Improved northern blot method for enhanced detection of small RNA. Nature protocols *3*, 1077-1084.

Pannone, B.K., Kim, S.D., Noe, D.A., and Wolin, S.L. (2001). Multiple functional interactions between components of the Lsm2-Lsm8 complex, U6 snRNA, and the yeast La protein. Genetics *158*, 187-196.

Parker, R., and Song, H. (2004). The enzymes and control of eukaryotic mRNA turnover. Nat Struct Mol Biol *11*, 121-127.

Pelechano, V., and Steinmetz, L.M. (2013). Gene regulation by antisense transcription. Nat Rev Genet *14*, 880-893.

Petfalski, E., Dandekar, T., Henry, Y., and Tollervey, D. (1998). Processing of the precursors to small nucleolar RNAs and rRNAs requires common components. Mol Cell Biol *18*, 1181-1189.

Porrua, O., and Libri, D. (2013). RNA quality control in the nucleus: the Angels' share of RNA. Biochim Biophys Acta *1829*, 604-611.

Potuschak, T., Vansiri, A., Binder, B.M., Lechner, E., Vierstra, R.D., and Genschik, P. (2006). The exoribonuclease XRN4 is a component of the ethylene response pathway in Arabidopsis. The Plant cell *18*, 3047-3057.

Preker, P.J., and Keller, W. (1998). The HAT helix, a repetitive motif implicated in RNA processing. Trends in biochemical sciences *23*, 15-16.
Proudfoot, N.J. (2011). Ending the message: poly(A) signals then and now. Genes Dev *25*, 1770-1782.
Qu, L.H., Henras, A., Lu, Y.J., Zhou, H., Zhou, W.X., Zhu, Y.Q., Zhao, J., Henry, Y., Caizergues-Ferrer, M., and Bachellerie, J.P. (1999). Seven novel methylation guide small nucleolar RNAs are processed from a common polycistronic transcript by Rat1p and RNase III in yeast. Mol Cell Biol *19*, 1144-1158.
Rader, S.D., and Guthrie, C. (2002). A conserved Lsm-interaction motif in Prp24 required for efficient U4/U6 di-snRNP formation. RNA *8*, 1378-1392.
Raghunathan, P.L., and Guthrie, C. (1998). A spliceosomal recycling factor that reanneals U4 and U6 small nuclear ribonucleoprotein particles. Science *279*, 857-860.
Read, R.L., Martinho, R.G., Wang, S.W., Carr, A.M., and Norbury, C.J. (2002). Cytoplasmic poly(A) polymerases mediate cellular responses to S phase arrest. Proc Natl Acad Sci U S A *99*, 12079-12084.
Reddy, R., Henning, D., Das, G., Harless, M., and Wright, D. (1987). The capped U6 small nuclear RNA is transcribed by RNA polymerase III. J Biol Chem *262*, 75-81.
Rinke, J., Appel, B., Digweed, M., and Luhrmann, R. (1985). Localization of a base-paired interaction between small nuclear RNAs U4 and U6 in intact U4/U6 ribonucleoprotein particles by psoralen cross-linking. Journal of molecular biology *185*, 721-731.
Rinke, J., and Steitz, J.A. (1982). Precursor molecules of both human 5S ribosomal RNA and transfer RNAs are bound by a cellular protein reactive with anti-La lupus antibodies. Cell *29*, 149-159.
Rinke, J., and Steitz, J.A. (1985). Association of the lupus antigen La with a subset of U6 snRNA molecules. Nucleic Acids Res *13*, 2617-2629.
Rissland, O.S., Mikulasova, A., and Norbury, C.J. (2007). Efficient RNA polyuridylation by noncanonical poly(A) polymerases. Mol Cell Biol *27*, 3612-3624.
Rissland, O.S., and Norbury, C.J. (2008). The Cid1 poly(U) polymerase. Biochim Biophys Acta *1779*, 286-294.
Rissland, O.S., and Norbury, C.J. (2009). Decapping is preceded by 3' uridylation in a novel pathway of bulk mRNA turnover. Nat Struct Mol Biol *16*, 616-623.
Ruegger, S., and Grosshans, H. (2012). MicroRNA turnover: when, how, and why. Trends in biochemical sciences *37*, 436-446.
Ryan, D.E., Stevens, S.W., and Abelson, J. (2002). The 5' and 3' domains of yeast U6 snRNA: Lsm proteins facilitate binding of Prp24 protein to the U6 telestem region. RNA *8*, 1011-1033.
Sarov, M., Murray, J.I., Schanze, K., Pozniakovski, A., Niu, W., Angermann, K., Hasse, S., Rupprecht, M., Vinis, E., Tinney, M.*, et al.* (2012). A genome-scale resource for in vivo tag-based protein function exploration in C. elegans. Cell *150*, 855-866.
Schimmel, P., Giege, R., Moras, D., and Yokoyama, S. (1993). An operational RNA code for amino acids and possible relationship to genetic code. Proc Natl Acad Sci U S A *90*, 8763-8768.
Schmid, M., Kuchler, B., and Eckmann, C.R. (2009). Two conserved regulatory cytoplasmic poly(A) polymerases, GLD-4 and GLD-2, regulate meiotic progression in C. elegans. Genes Dev *23*, 824-836.
Scott, D.D., and Norbury, C.J. (2013). RNA decay via 3' uridylation. Biochim Biophys Acta *1829*, 654-665.
Sedore, S.C., Byers, S.A., Biglione, S., Price, J.P., Maury, W.J., and Price, D.H. (2007). Manipulation of P-TEFb control machinery by HIV: recruitment of P-TEFb from the large form by Tat and binding of HEXIM1 to TAR. Nucleic Acids Res *35*, 4347-4358.
Shannon, K.W., and Guthrie, C. (1991). Suppressors of a U4 snRNA mutation define a novel U6 snRNP protein with RNA-binding motifs. Genes Dev *5*, 773-785.
Sharp, P.A. (2005). The discovery of split genes and RNA splicing. Trends in biochemical sciences *30*, 279-281.
Shatkin, A.J., and Manley, J.L. (2000). The ends of the affair: capping and polyadenylation. Nature structural biology *7*, 838-842.

Shchepachev, V., and Azzalin, C.M. (2013). The Mpn1 RNA exonuclease: cellular functions and implication in disease. FEBS letters *587*, 1858-1862.

Shi, Y., Di Giammartino, D.C., Taylor, D., Sarkeshik, A., Rice, W.J., Yates, J.R., 3rd, Frank, J., and Manley, J.L. (2009). Molecular architecture of the human pre-mRNA 3' processing complex. Mol Cell *33*, 365-376.

Singh, R., and Reddy, R. (1989). Gamma-monomethyl phosphate: a cap structure in spliceosomal U6 small nuclear RNA. Proc Natl Acad Sci U S A *86*, 8280-8283.

Singh, R., and Valcarcel, J. (2005). Building specificity with nonspecific RNA-binding proteins. Nat Struct Mol Biol *12*, 645-653.

Sinturel, F., Pellegrini, O., Xiang, S., Tong, L., Condon, C., and Benard, L. (2009). Real-time fluorescence detection of exoribonucleases. RNA *15*, 2057-2062.

Solinger, J.A., Pascolini, D., and Heyer, W.D. (1999). Active-site mutations in the Xrn1p exoribonuclease of Saccharomyces cerevisiae reveal a specific role in meiosis. Mol Cell Biol *19*, 5930-5942.

Song, M.G., Li, Y., and Kiledjian, M. (2010). Multiple mRNA decapping enzymes in mammalian cells. Mol Cell *40*, 423-432.

Souret, F.F., Kastenmayer, J.P., and Green, P.J. (2004). AtXRN4 degrades mRNA in Arabidopsis and its substrates include selected miRNA targets. Mol Cell *15*, 173-183.

Srebrow, A., and Kornblihtt, A.R. (2006). The connection between splicing and cancer. Journal of cell science *119*, 2635-2641.

Stanek, D., and Neugebauer, K.M. (2004). Detection of snRNP assembly intermediates in Cajal bodies by fluorescence resonance energy transfer. The Journal of cell biology *166*, 1015-1025.

Stanek, D., Rader, S.D., Klingauf, M., and Neugebauer, K.M. (2003). Targeting of U4/U6 small nuclear RNP assembly factor SART3/p110 to Cajal bodies. The Journal of cell biology *160*, 505-516.

Stefano, J.E. (1984). Purified lupus antigen La recognizes an oligouridylate stretch common to the 3' termini of RNA polymerase III transcripts. Cell *36*, 145-154.

Stevens, A., and Poole, T.L. (1995). 5'-exonuclease-2 of Saccharomyces cerevisiae. Purification and features of ribonuclease activity with comparison to 5'-exonuclease-1. J Biol Chem *270*, 16063-16069.

Stiernagle, T. (2006). Maintenance of C. elegans. WormBook : the online review of C. elegans biology, 1-11.

Suefuji, Y., Sasatomi, T., Shichijo, S., Nakagawa, S., Deguchi, H., Koga, T., Kameyama, T., and Itoh, K. (2001). Expression of SART3 antigen and induction of CTLs by SART3-derived peptides in breast cancer patients. British journal of cancer *84*, 915-919.

Sugano, S., Shobuike, T., Takeda, T., Sugino, A., and Ikeda, H. (1994). Molecular analysis of the dhp1+ gene of Schizosaccharomyces pombe: an essential gene that has homology to the DST2 and RAT1 genes of Saccharomyces cerevisiae. Molecular & general genetics : MGG *243*, 1-8.

Tan, E.M., and Kunkel, H.G. (1966). Characteristics of a soluble nuclear antigen precipitating with sera of patients with systemic lupus erythematosus. Journal of immunology *96*, 464-471.

Tang, R., Li, L., Zhu, D., Hou, D., Cao, T., Gu, H., Zhang, J., Chen, J., Zhang, C.Y., and Zen, K. (2012). Mouse miRNA-709 directly regulates miRNA-15a/16-1 biogenesis at the posttranscriptional level in the nucleus: evidence for a microRNA hierarchy system. Cell research *22*, 504-515.

Tazi, J., Bakkour, N., and Stamm, S. (2009). Alternative splicing and disease. Biochim Biophys Acta *1792*, 14-26.

Tazi, J., Forne, T., Jeanteur, P., Cathala, G., and Brunel, C. (1993). Mammalian U6 small nuclear RNA undergoes 3' end modifications within the spliceosome. Mol Cell Biol *13*, 1641-1650.

Terns, M.P., Lund, E., and Dahlberg, J.E. (1992). 3'-end-dependent formation of U6 small nuclear ribonucleoprotein particles in Xenopus laevis oocyte nuclei. Mol Cell Biol *12*, 3032-3040.

Tharun, S. (2009). Roles of eukaryotic Lsm proteins in the regulation of mRNA function. International review of cell and molecular biology *272*, 149-189.

Timmons, L., and Fire, A. (1998). Specific interference by ingested dsRNA. Nature *395*, 854.

Tollervey, D. (2004). Molecular biology: termination by torpedo. Nature *432*, 456-457.

Trede, N.S., Medenbach, J., Damianov, A., Hung, L.H., Weber, G.J., Paw, B.H., Zhou, Y., Hersey, C., Zapata, A., Keefe, M.*, et al.* (2007). Network of coregulated spliceosome components revealed by zebrafish mutant in recycling factor p110. Proc Natl Acad Sci U S A *104*, 6608-6613.

Trippe, R., Guschina, E., Hossbach, M., Urlaub, H., Luhrmann, R., and Benecke, B.J. (2006). Identification, cloning, and functional analysis of the human U6 snRNA-specific terminal uridylyl transferase. RNA *12*, 1494-1504.

Trippe, R., Richly, H., and Benecke, B.J. (2003). Biochemical characterization of a U6 small nuclear RNA-specific terminal uridylyltransferase. European journal of biochemistry / FEBS *270*, 971-980.

Trippe, R., Sandrock, B., and Benecke, B.J. (1998). A highly specific terminal uridylyl transferase modifies the 3'-end of U6 small nuclear RNA. Nucleic Acids Res *26*, 3119-3126.

Tsuda, N., Murayama, K., Ishida, H., Matsunaga, K., Komiya, S., Itoh, K., and Yamada, A. (2001). Expression of a newly defined tumor-rejection antigen SART3 in musculoskeletal tumors and induction of HLA class I-restricted cytotoxic T lymphocytes by SART3-derived peptides. Journal of orthopaedic research : official publication of the Orthopaedic Research Society *19*, 346-351.

Tycowski, K.T., You, Z.H., Graham, P.J., and Steitz, J.A. (1998). Modification of U6 spliceosomal RNA is guided by other small RNAs. Mol Cell *2*, 629-638.

Valadkhan, S. (2010). Role of the snRNAs in spliceosomal active site. RNA biology *7*, 345-353.

Valadkhan, S., and Gunawardane, L.S. (2013). Role of small nuclear RNAs in eukaryotic gene expression. Essays in biochemistry *54*, 79-90.

van Dijk, E.L., Chen, C.L., d'Aubenton-Carafa, Y., Gourvennec, S., Kwapisz, M., Roche, V., Bertrand, C., Silvain, M., Legoix-Ne, P., Loeillet, S.*, et al.* (2011). XUTs are a class of Xrn1-sensitive antisense regulatory non-coding RNA in yeast. Nature *475*, 114-117.

Vankan, P., McGuigan, C., and Mattaj, I.W. (1990). Domains of U4 and U6 snRNAs required for snRNP assembly and splicing complementation in Xenopus oocytes. EMBO J *9*, 3397-3404.

Vidaver, R.M., Fortner, D.M., Loos-Austin, L.S., and Brow, D.A. (1999). Multiple functions of Saccharomyces cerevisiae splicing protein Prp24 in U6 RNA structural rearrangements. Genetics *153*, 1205-1218.

Vijayraghavan, U., Company, M., and Abelson, J. (1989). Isolation and characterization of pre-mRNA splicing mutants of Saccharomyces cerevisiae. Genes Dev *3*, 1206-1216.

Wagschal, A., Rousset, E., Basavarajaiah, P., Contreras, X., Harwig, A., Laurent-Chabalier, S., Nakamura, M., Chen, X., Zhang, K., Meziane, O.*, et al.* (2012). Microprocessor, Setx, Xrn2, and Rrp6 co-operate to induce premature termination of transcription by RNAPII. Cell *150*, 1147-1157.

Wahl, M.C., Will, C.L., and Luhrmann, R. (2009). The spliceosome: design principles of a dynamic RNP machine. Cell *136*, 701-718.

Wahle, E., and Winkler, G.S. (2013). RNA decay machines: deadenylation by the Ccr4-not and Pan2-Pan3 complexes. Biochim Biophys Acta *1829*, 561-570.

Wang, E.T., Sandberg, R., Luo, S., Khrebtukova, I., Zhang, L., Mayr, C., Kingsmore, S.F., Schroth, G.P., and Burge, C.B. (2008). Alternative isoform regulation in human tissue transcriptomes. Nature *456*, 470-476.

Wang, M., and Pestov, D.G. (2011). 5'-end surveillance by Xrn2 acts as a shared mechanism for mammalian pre-rRNA maturation and decay. Nucleic Acids Res *39*, 1811-1822.

Watanabe, Y., Yokobori, S., Inaba, T., Yamagishi, A., Oshima, T., Kawarabayasi, Y., Kikuchi, H., and Kita, K. (2002). Introns in protein-coding genes in Archaea. FEBS letters *510*, 27-30.

Weinmann, L., Hock, J., Ivacevic, T., Ohrt, T., Mutze, J., Schwille, P., Kremmer, E., Benes, V., Urlaub, H., and Meister, G. (2009). Importin 8 is a gene silencing factor that targets argonaute proteins to distinct mRNAs. Cell *136*, 496-507.

West, S., Gromak, N., and Proudfoot, N.J. (2004). Human 5' --> 3' exonuclease Xrn2 promotes transcription termination at co-transcriptional cleavage sites. Nature *432*, 522-525.

Wolin, S.L., and Cedervall, T. (2002). The La protein. Annual review of biochemistry *71*, 375-403.
Wyers, F., Rougemaille, M., Badis, G., Rousselle, J.C., Dufour, M.E., Boulay, J., Regnault, B., Devaux, F., Namane, A., Seraphin, B.*, et al.* (2005). Cryptic pol II transcripts are degraded by a nuclear quality control pathway involving a new poly(A) polymerase. Cell *121*, 725-737.
Xiang, S., Cooper-Morgan, A., Jiao, X., Kiledjian, M., Manley, J.L., and Tong, L. (2009). Structure and function of the 5'-->3' exoribonuclease Rat1 and its activating partner Rai1. Nature *458*, 784-788.
Xue, Y., Bai, X., Lee, I., Kallstrom, G., Ho, J., Brown, J., Stevens, A., and Johnson, A.W. (2000). Saccharomyces cerevisiae RAI1 (YGL246c) is homologous to human DOM3Z and encodes a protein that binds the nuclear exoribonuclease Rat1p. Mol Cell Biol *20*, 4006-4015.
Yang, D., Nakao, M., Shichijo, S., Sasatomi, T., Takasu, H., Matsumoto, H., Mori, K., Hayashi, A., Yamana, H., Shirouzu, K.*, et al.* (1999). Identification of a gene coding for a protein possessing shared tumor epitopes capable of inducing HLA-A24-restricted cytotoxic T lymphocytes in cancer patients. Cancer research *59*, 4056-4063.
Yean, S.L., Wuenschell, G., Termini, J., and Lin, R.J. (2000). Metal-ion coordination by U6 small nuclear RNA contributes to catalysis in the spliceosome. Nature *408*, 881-884.
Yik, J.H., Chen, R., Nishimura, R., Jennings, J.L., Link, A.J., and Zhou, Q. (2003). Inhibition of P-TEFb (CDK9/Cyclin T) kinase and RNA polymerase II transcription by the coordinated actions of HEXIM1 and 7SK snRNA. Mol Cell *12*, 971-982.
Yokobori, S., Itoh, T., Yoshinari, S., Nomura, N., Sako, Y., Yamagishi, A., Oshima, T., Kita, K., and Watanabe, Y. (2009). Gain and loss of an intron in a protein-coding gene in Archaea: the case of an archaeal RNA pseudouridine synthase gene. BMC Evol Biol *9*, 198.
Yoo, C.J., and Wolin, S.L. (1994). La proteins from Drosophila melanogaster and Saccharomyces cerevisiae: a yeast homolog of the La autoantigen is dispensable for growth. Mol Cell Biol *14*, 5412-5424.
Zabolotskaya, M.V., Grima, D.P., Lin, M.D., Chou, T.B., and Newbury, S.F. (2008). The 5'-3' exoribonuclease Pacman is required for normal male fertility and is dynamically localized in cytoplasmic particles in Drosophila testis cells. The Biochemical journal *416*, 327-335.
Zhang, K., Dion, N., Fuchs, B., Damron, T., Gitelis, S., Irwin, R., O'Connor, M., Schwartz, H., Scully, S.P., Rock, M.G.*, et al.* (2002). The human homolog of yeast SEP1 is a novel candidate tumor suppressor gene in osteogenic sarcoma. Gene *298*, 121-127.
Zisoulis, D.G., Kai, Z.S., Chang, R.K., and Pasquinelli, A.E. (2012). Autoregulation of microRNA biogenesis by let-7 and Argonaute. Nature *486*, 541-544.

9 Curriculum vitae

Stefan Rüegger *Curriculum Vitae*

Address:
Wattstrasse 16
4056 Basel
Switzerland

Contact:
Telephone: +41 61 697 66 84
Cell phone: +41 79 748 77 40
E-mail: stefan.rueegger@fmi.ch

Personal data:
Date of birth: February 3, 1984
Place of birth: Zurich, Switzerland
Nationality: Swiss

Education

04/2009 - present	PhD thesis in the laboratory of Dr. Helge Grosshans at the Friedrich Miescher Institute for Biomedical Research (FMI), Basel, Switzerland
10/2007 - 01/2009	MSc in Biochemistry, University of Zurich, Zurich, Switzerland (Master thesis under supervision of Prof. Dr. Benjamin Schuler)
10/2004 - 10/2007	BSc in Biochemistry, University of Zurich, Zurich, Switzerland

Fellowships

04/2010 - 04/2012	Boehringer Ingelheim Fonds PhD Fellowship

Voluntary activities

09/2010 - 12/2010	Giving tutorials in Biology for advanced students in sport science at the University of Basel
05/2011	Attendence of a one-week communication training given by experts at the Cold Spring Harbor Laboratories, New York, USA (organized by Boehringer Ingelheim Fonds) on writing papers, designing figures for papers , and giving oral presentations

Language skills

German	native
English	fluent
French	intermediate

Rüegger, S., and H. Großhans. 'USIP-1 is a terminal transferase acting upstream of SART-3 in spliceosome assembly.' manuscript in preparation

Miki, T.S., H. Richter*, **S. Rüegger***, and H. Großhans. 'PAXT-1 promotes XRN2 activity by stabilizing it through a conserved domain.' ***Mol Cell***, in press.

Miki, T.S.*, **Rüegger, S.***, D. Gaidatzis, M.B. Stadler, and H. Großhans. 'Engineering of a conditional allele reveals multiple roles of XRN2 in Caenorhabditis elegans development and substrate specificity in microRNA turnover.' ***Nucleic Acids Res***, in press.

Bossé, G., **S. Rüegger**, M. Ow, A. Vasquez-Rifo, E. Rondeau, V. Ambros, H. Großhans, and M. Simard. 'The decapping scavenger enzyme DCS-1 controls microRNA levels in *Caenorhabditis elegans*.' ***Mol Cell***, 50(2):281-7. 2013.

Rüegger, S. and Großhans, H. 'MicroRNA turnover: when, how, and why'. ***Trends Biochem Sci***, 37(10):436-46. 2012 (Review)

Müller-Späth, S., A. Soranno, V. Hirschfeld, H. Hofmann, **S. Rüegger**, L. Reymond, D. Nettels, and B. Schuler. 'Charge interactions can dominate the dimensions of intrinsically disordered proteins'. ***PNAS***, 107(33):14609-14. 2010.

Nettels, D., S. Müller-Späth, F. Küster, H. Hofmann, D. Haenni, **S. Rüegger**, L. Reymond, A. Hoffmann, J. Kubelka, B. Heinz, K. Gast, R.B. Best, and B. Schuler. 'Single-molecule spectroscopy of the temperature-induced collapse of unfolded proteins'. ***PNAS***, 106(49):20740-45. 2009.

* equal contribution